Seismological Applications of Lattice Theory

Thesis by

Charles George Sammis

In Partial Fulfillment of the Requirements

For the Degree of

Doctor of Philosophy

California Institute of Technology

Pasadena, California

1971

(Submitted May 14, 1971)

ACKNOWLEDGMENTS

The author gratefully acknowledges the guidance and support of Dr. Don L. Anderson throughout this study, and the many hours of advice and encouragement from Dr. Charles Archambeau.

To Dr. Hartmut Spetzler and Dr. Richard O'Connell for access to their data prior to publication, to Tom Jordan for invaluable assistance in fitting the finite strain theory to earth-inversion models, and to my colleagues, Dr. E. K. "Buzz" Graham, Dr. Taro Takahashi, Ed Gaffney, Dr. Leon Thomsen, Dr. Robert Liebermann, and Dr. Thomas Ahrens, for their many helpful comments and stimulating discussions, the author is deeply indebted.

The author would also like to thank Dr. Orson Anderson for his encouragement, Dr. Francis Birch for helpful comments on isotropic finite strain theory, and Dr. Gerhard Barsch for pointing out the distinction between effective and thermodynamic elastic constants.

Special thanks are due Laszlo Lenches for preparation of the figures and Sally Henyey for the difficult task of typing the manuscript.

During a period of this research the author held a NDEA fellowship. This work was supported by NASA Contract NGL 05-002-069 and NSF Grant GA-12703.

ABSTRACT

Lattice models based upon empirical two-body potential functions are used to predict the elastic constants of "mantle-candidate" minerals at high pressures for direct comparison with seismic velocity profiles. The method of long waves, originally formulated by Born and his co-workers, has been applied to solids in the rock salt, spinel, and rutile structures. Calculations for NaCl (rock salt), MgO (rock salt), Al_2MgO_4 (spinel), and TiO_2 (rutile) are compared with recent high-precision ultrasonic data. The effect of van der Waals forces and second-neighbor anion-anion interactions is shown to be small. The NaCl and MgO data are best fit with an exponential cation-anion repulsive potential. The elastic constants of MgO cannot be well fit unless the ionicity (valence product) is lowered to 0.7 of its full ionic value. For NaCl this is not required. The shear instability ($C_{44} = 0$) is predicted for both NaCl and MgO, but the exact pressure is sensitive to the details of the potential.

Using the Mg—O two-body potential found for periclase, Al_2MgO_4 spinel was investigated using only two pieces of input datum, $\tilde{K}$ and $\tilde{\rho}$. Although the predicted elastic constants were in good agreement with the data, the pressure derivatives were not. The discrepancy is caused by a large contribution from the internal deformations which occur in all non-centrosymmetric structures. The same result was found for TiO_2. A relaxation of the rigid-ion and central-force approximations may correct this discrepancy.

Using the Mg—O bond parameters found for periclase and the Si—O bond parameters found from $\tilde{K}$ and $\tilde{\rho}$ of stishovite, the elastic properties of the high-pressure polymorph γ-Mg_2SiO_4 spinel were predicted. The predicted equilibrium density was in agreement with previous experimental extrapolations; the predicted u parameter was in agreement with prior estimates based on bond-length arguments, and the predicted bulk modulus was in agreement with prior systematics estimates. However, the internal deformation contribution again dominated the pressure derivatives and caused both the predicted V_p and V_s to be lower than the corresponding seismic velocities in the "spinel region" of the mantle. A comparison of MgO (rock salt) and SiO_2 (stishovite) with the seismic profiles for the "post-spinel" lower mantle shows a discrepancy in both absolute value and gradient. Unlike the silicate spinel, this is not obviously caused by the internal deformations. The lattice models predict that both TiO_2 and stishovite will become unstable in shear ($1/2\,(C_{11} - C_{12}) = 0$) at high pressure.

Other methods of using laboratory data to interpret seismic profiles are reviewed. Birch's formulation of isotropic finite strain theory is corrected and used to test the homogeneity and adiabaticity of the lower mantle of recent earth-inversion models. Systematics are shown to be insufficient to treat the shear properties. Although lattice models are limited by empirical approximations to the complex bonding forces, the empiricism is on a more basic level than that of velocity density systematics previously used to interpret seismic profiles. By using lattice models, one gains the natural dependence of both the compressional and shear properties on the crystal structure.

TABLE OF CONTENTS

	Page
I. INTRODUCTION	1
II. SOME PREVIOUS ATTEMPTS TO USE LABORATORY DATA TO INTERPRET SEISMIC VELOCITY AND DENSITY PROFILES	6
1. ISOTROPIC FINITE STRAIN THEORIES	6
2. THE SYSTEMATICS APPROACH	15
III. THE DEFINITION AND MEANING OF ELASTIC CONSTANTS AND METHODS FOR THEIR CALCULATION	30
1. EFFECTIVE VS. THERMODYNAMIC ELASTIC CONSTANTS	30
Reference States	32
Measures of Strain	32
Elastic Constants	33
Elastic Waves in a Prestressed Crystal	37
Hydrostatic Prestress	39
2. CALCULATION OF THE ELASTIC CONSTANTS - FINITE STRAIN AND INTERATOMIC POTENTIAL MODELS	41
The Finite Strain Approach	42
Atomistic Approach Based on Two-Body Interatomic Potentials	47
3. THE METHOD OF LONG WAVES	47
Analogy between Vibration Equation and the Electric Field in a Dipole Lattice	54
Ewald's Theta Function Transformation	55
Long Wave Expansion	63
The Zero-Order Equation	66
The First-Order Equation	67
The Second-Order Equation	71
Symmetry Properties of the Round and Square Brackets	72

TABLE OF CONTENTS (continued)

	Page
Continuum Equation for the Propagation of Small Amplitude Waves in a Prestressed, Piezoelectric Medium	73
Central Forces	75
IV. THE INTERATOMIC POTENTIAL	80
1. QUANTUM MECHANICAL CALCULATIONS FOR IONIC SOLIDS	82
2. THE BORN APPROXIMATION	86
Electrostatic Potential	86
The van der Waals Potential	88
The Empirical Repulsive Potential	92
The Cohesive Energy and Evaluation of the Empirical Parameters	94
3. OBTAINING THE BULK MODULUS AND DENSITY APPROPRIATE TO THE STATIC LATTICE	96
V. SPECIALIZATION OF THE INTERATOMIC POTENTIAL MODEL TO SPECIFIC STRUCTURES OF GEOPHYSICAL INTEREST	106
1. THE SODIUM CHLORIDE STRUCTURE	106
Specialization to the NaCl Structure	107
Evaluation of the Empirical Parameters in V_{AB} and Expressions for the Bulk Modulus	111
Expressions for the First and Second Pressure Derivatives of the Elastic Constants at P = 0	119
Numerical Predictions for NaCl and MgO	125
Discussion and Conclusions	126
2. THE SPINEL STRUCTURE	
The Consistent Pair-Potential Assumption	161
Specialization to the Spinel Structure	163
Evaluation of the Empirical Parameters in V_{AO} and V_{BO}	168

TABLE OF CONTENTS (continued)

	Page
The Volume Dependence of the Bulk Modulus and the Pressure	172
Numerical Predictions for Al_2MgO_4 and Discussion	174
3. THE RUTILE STRUCTURE	191
Specialization to the Rutile Structure	193
Evaluation of the Empirical Parameters in V_{BO}	197
Computational Results and Discussion for Rutile and Stishovite	200
Taylor Series Potential	202
VI. APPLICATIONS TO THE EARTH	214
1. Mg_2SiO_4 SPINEL	214
2. POST-SPINEL PHASES	218
VII. SUMMARY AND CONCLUSIONS	228
REFERENCES	233
APPENDIX 1	244
APPENDIX 2	247
APPENDIX 3	256
APPENDIX 4	258

I. INTRODUCTION

One of the primary objectives of solid earth geophysics is the determination of the pressure, temperature, composition, and crystal structure of the earth as a function of depth. The solution of this problem requires input from a wide range of disciplines. The seismologist provides the most direct data. By fitting the observed travel time of compressional waves, dispersion of surface waves, free oscillation spectrum, mass, and moment of inertia of the earth, he attempts to find the best distribution of compressional wave velocity V_p, shear wave velocity V_s, and density ρ as a function of depth. The interpretation of these material constants in terms of temperature, pressure, composition, and phase requires the skills of a materials scientist.

The ultimate experiment which such a materials scientist could perform would be to reproduce the temperature and pressure conditions of the earth's interior in his laboratory. If he could, at the same time, measure the compressional and shear wave velocities and density of "mantle-candidate" mineral assemblages, he could effect a direct comparison with the seismically determined profiles.

Unfortunately, such an approach is not yet technologically feasible. The only experimental methods capable of reproducing the temperature and pressure conditions throughout the entire earth are the shock-wave techniques. Although the shock-wave method has yielded the only pressure-volume information available for many of the high-pressure polymorphs of oxides and silicates (Ahrens, Anderson, and Ringwood,

1969), the pressure-volume information is neither adiabatic nor isothermal, but follows a thermodynamic path known as a Hugoniot. Even if one knew how to accurately correct these data to an adiabat or an isotherm, which one doesn't, this method is presently capable of yielding only the volume dependence of the free energy, i.e., the pressure, the bulk modulus, and the pressure derivatives of the bulk modulus to all orders. No technique has yet been perfected to measure the elastic wave velocities behind a shock front in solids. Until this is achieved, only the density and the combination $\Phi = V_p^2 - (4/3)V_s^2 = K/\rho$ can be compared to the seismic velocity profiles. Although this method has been successfully pursued by Anderson (1967), it does not make full use of the seismic data since V_p and V_s and ρ all carry information about the physical constitution of the mantle.

Static compression experiments are similarly limited in that they yield only the volume dependence of the internal energy and not the elastic constants. Although the compression in such cells is isothermal, these experiments have presently been limited to room temperature and pressure to $\sim$ 200 kbar, which corresponds to an approximate depth of 500 km.

Of all the techniques presently used, only ultrasonics gives all the information necessary for a direct comparison with seismically determined velocities and density, but unfortunately these experiments have been limited to pressures of 10-15 kbar or depths of about 50 km. For the upper mantle, above the 400 km discontinuity, such information is very useful. The theory of finite strain,

which will be discussed in Chapter III, can be used to extrapolate these data from the relatively low-pressure laboratory regime to the high pressures of the earth's upper mantle.

Below 400 km, the situation is quite different. The seismic velocity profiles show two major discontinuities, one at about 400 km and one at about 600 km, which are presumably evidence of solid-solid phase changes of the olivines, pyroxenes, and garnets to more close-packed, high-pressure forms. Even though the olivine-spinel phase change has been directly studied in the x-ray cells, and the spinel - post-spinel change has been observed for germanate analogs and the fayalite end member of the olivine series, no elasticity data are available for these high-pressure silicate modifications, and finite strain theory is therefore of no use.

What is needed is some method which is capable of not only extrapolating elastic constants, but also of predicting them. Previous prediction methods have involved the scaling of V_p, V_s, or some combination like the seismic parameter $\Phi = V_p^2 - (4/3)V_s^2$ as a function of density. These scaling laws will be reviewed in the next chapter. Besides being purely empirical, they contain the assumption that pressure changes the elastic constants in the same way as composition, that is, through the density.

It is the purpose of this thesis to develop a more physically sound method of predicting and extrapolating the elastic velocities and density of mantle-candidate minerals for comparison with the seismically determined profiles in the mantle. No claim of originality is made for

the method; it is the well-known method of long waves pioneered by Born and his co-workers in the 1920's and improved upon ever since. What is new is its application to complex crystals and to the problem of the constitution of the earth's mantle.

Basically, the approach is to use all the data available for a given mineral, plus data on similar minerals, to determine the two-body interatomic potentials for each of the various bonds. Once these two-body potentials are fixed, the density and all the elastic constants may be calculated as a function of pressure.

The exact nature of these interatomic forces are extremely complicated and are only partially understood on the quantum mechanical level. They are many bodied in nature and thus depend on the angles between atoms as well as on their separation. The claim in this work is not to make any exact calculation of these interactions, but only to find the most physically reasonable empirical approximation to them. It is important to point out that although the lattice models are limited by empirical approximations to the complex bonding forces, the empiricism is on a more basic level than in velocity-density systematics previously used to interpret seismic profiles. By using lattice models one gains the natural dependence of both compressional and shear properties on the crystal structure. One is no longer constrained to the bulk modulus, but can make full use of both the compressional and shear velocities.

Following a brief discussion of the definition and meaning of elastic constants, the method of long waves is developed in detail in

Chapter III. In Chapter IV the interatomic potential is discussed. Chapter V applies the method to the rock salt, spinel, and rutile structures. The objective is to use the precise ultrasonic data to see if the input of only two parameters, $\tilde{K}$ and $\tilde{\rho}$, are enough to predict the elastic constants and their pressure derivatives. The assumption that the bond parameters found for these compounds which are stable at P = 0 also describe the bonds in high-pressure modifications allows one to predict the elastic constants and density of these high-pressure structures. γ-Mg_2SiO_4 spinel is treated as an example in Chapter VI.

The two assumptions of the model developed here which most severely limit its geophysical usefulness are seen to be the central force approximation and the rigid-ion approximation. While relaxation of the former assumption requires a deeper quantum mechanical understanding and may require more input parameters, the latter assumption can be relaxed knowing only the dipolarizability and quadrupolarizability of the anions and should be the next improvement.

In lieu of direct high-temperature, high-pressure data, these lattice models represent the most physically reasonable framework through which available laboratory data may be used to predict V_p, V_s, and ρ of mantle-candidate minerals for comparison with the seismic profiles.

II. SOME PREVIOUS ATTEMPTS TO USE LABORATORY DATA TO INTERPRET SEISMIC VELOCITY AND DENSITY PROFILES

2-1. Isotropic Finite Strain Theories

Birch (1938) applied Murnaghan's (1937) finite strain theory to the case of an isotropic solid under hydrostatic pressure arriving at the following expressions for the velocities and density as a function of compression at constant temperature (or along an adiabat).

$$V_p = \left\{ \frac{(1-2\epsilon)^{5/2}}{\rho_o} \left[\lambda_o + 2\mu_o - \epsilon(11\lambda_o + 10\mu_o) \right] \right\}^{1/2} \qquad (2\text{-}1\text{-}1)$$

$$V_s = \left\{ \frac{(1-2\epsilon)^{5/2}}{\rho_o} \left[\mu_o + \epsilon(3\lambda_o + 4\mu_o) \right] \right\}^{1/2} \qquad (2\text{-}1\text{-}2)$$

$$P = -\left\{ (1-2\epsilon)^{5/2} \epsilon (3\lambda_o + 2\mu_o) \right\} \qquad (2\text{-}1\text{-}3)$$

In these expressions ϵ is the Eulerian measure of the hydrostatic strain and is related to the density by $\rho/\rho_o = (1 - 2\epsilon)^{3/2}$.

In a following paper, Birch (1939) used these equations to make the first interpretation of the seismic velocity and density profiles in terms of composition. Assuming a two layer mantle with a discontinuity at 474 km, he found that V_p, V_s, and ρ in the upper layer were in excellent agreement with Jeffrey's (1937) observed values for input parameters $\lambda_o = 6.81 \times 10^{11}$ dynes/cm^2, $\mu_o = 6.065 \times 10^{11}$ dynes/cm^2, and $\rho_o = 3.28$ gm/cm^3. In the region beginning at 474 km, Birch's fit gave $\lambda_o = 12.12 \times 10^{11}$ dynes/cm^2, $\mu_o = 8.91 \times 10^{11}$ dynes/cm^2, and $\rho_o = 3.91$ gm/cm^3, but the agreement with Jeffrey's observed profile was

not as good.

This failure to fit the lower mantle was partly a result of poor seismological data (the 600 km discontinuity had not been discovered) and partly a result of Birch's incomplete formulation of the finite strain theory. Sammis, et al., (1970) pointed out that Birch's equations (2-1-1) and (2-1-2) should be written

$$V_p = \left\{ \frac{(1-2\epsilon)^{5/2}}{\rho_o} \left[\lambda_o + 2\mu_o - \epsilon(11\lambda_o + 10\mu_o - 18\ell - 4m) \right] \right\}^{1/2} \qquad (2\text{-}1\text{-}4)$$

$$V_s = \left\{ \frac{(1-2\epsilon)^{5/2}}{2\rho_o} \left[2\mu_o - \epsilon(6\lambda_o + 8\mu_o + 3m + n) \right] \right\}^{1/2} . \qquad (2\text{-}1\text{-}5)$$

The coefficients ℓ, m, and n are third-order coefficients in the expansion of the elastic energy density in powers of the strain invarients.

$$\rho_o \phi = \frac{\lambda_o + 2\mu_o}{2} I_1^2 - 2\mu_o I_2 + \ell I_1^3 + m I_1 I_2 + n I_3 + O(\epsilon^4) \qquad (2\text{-}1\text{-}6)$$

The three invarients of the Eulerian strain tensor are given by

$$I_1 = \epsilon_{ii}$$

$$I_2 = \tfrac{1}{2}(\epsilon_{ii}\epsilon_{jj} - \epsilon_{ij}\epsilon_{ji}) \qquad (2\text{-}1\text{-}7)$$

$$I_3 = \tfrac{1}{6}(\epsilon_{ii}\epsilon_{jj}\epsilon_{kk} - 3\epsilon_{ij}\epsilon_{ji}\epsilon_{kk} + 2\epsilon_{ij}\epsilon_{jk}\epsilon_{ki}) .$$

The derivation of equations (2-1-4) and (2-1-5) is identical to Birch's (1938) derivation of (2-1-1) and (2-1-2) in every detail except one: the expansion of the strain energy density is not truncated after the second-order terms, but is retained to third-order in ϵ as written.

Following Birch, the compressional and shear velocities in an isotropic material subjected to a finite hydrostatic strain are

$$V_p^2 = A(1-\alpha)^2/\rho_o$$

$$V_s^2 = C(1-\alpha)^2/2\rho_o \qquad (2\text{-}1\text{-}8)$$

where

$$A=\rho\left[(1-2\epsilon)\left(\frac{\partial^2\phi}{\partial I_1^2} + 4\epsilon\frac{\partial^2\phi}{\partial I_1\partial I_2} + 2\epsilon^2\frac{\partial^2\phi}{\partial I_1\partial I_3} + 4\epsilon^2\frac{\partial^2\phi}{\partial I_2^2} + 4\epsilon^3\frac{\partial^2\phi}{\partial I_2\partial I_3} + \right.\right.$$

$$\left.\left. + \epsilon^4\frac{\partial^2\phi}{\partial I_3^2}\right) - 3\left(\frac{\partial\phi}{\partial I_1} + 2\epsilon\frac{\partial\phi}{\partial I_2} + \epsilon^2\frac{\partial\phi}{\partial I_2}\right)\right] \qquad (2\text{-}1\text{-}9)$$

$$C = \rho\left[-2\frac{\partial\phi}{\partial I_1} - (1+2\epsilon)\frac{\partial\phi}{\partial I_2} - \epsilon\frac{\partial\phi}{\partial I_3}\right].$$

Here ϵ is the finite hydrostatic strain ($\epsilon = -\alpha - \alpha^2/2$, $\rho/\rho_o = (1-2\epsilon)^{3/2}$ and $1/(1+\alpha)$ is the factor by which each line in the crystal is hydrostatically shortened.

By taking the indicated partial derivatives of ϕ and arranging the terms in ascending powers of ϵ, we get

$$V_p^2 = (1-2\epsilon)^{5/2}\left[\lambda_o + 2\mu_o - \epsilon(11\lambda_o + 10\mu_o - 18l - 4m)\right.$$
$$\left. - \epsilon^2(117l + 35m + 3n)\right]/\rho_o$$
$$V_s^2 = (1-2\epsilon)^{5/2}\left[2\mu_o - \epsilon(6\lambda_o + 8\mu_o + 3m + n)\right. \qquad (2\text{-}1\text{-}10)$$
$$\left. - \epsilon^2(54l + 12m)\right]/2\rho_o .$$

Because of the differentiation in the calculation of A and C, the third-order coefficients l, m, and n appear with λ_o and μ_o to the first order in ϵ. For the same reason, the coefficients of the ϵ^2 terms are incomplete. The complete terms would contain fourth-order constants ignored in the truncation of equation (2-1-6) after the ϵ^3 terms. For this reason, these equations should be used in the form given by equations (2-1-4) and (2-1-5). By truncating the free energy expansion after the

second-order terms, Birch got only the λ_o and μ_o contribution to the ϵ terms. Hughes and Kelly (1953) derived equations analogous to (2-1-10) in Lagrangian coordinates having the same form; i.e., the third-order coefficients appear to first order in the Lagrangian hydrostatic strain η.

Upon computing the bulk modulus $K/\rho = V_P^2 - (4/3)V_S^2$ by using (2-1-10), we obtain

$$K = (1-2\epsilon)^{5/2}\left[K_o - \epsilon(7K_o - 18l - 6m - \tfrac{2}{3}n) - \epsilon^2(81l + 27m + 3n)\right] \qquad (2\text{-}1\text{-}11)$$

which is identical to the expression given by Birch (1952):

$$K = K_o(1+2f)^{5/2}\left[1 + 7f - 2\xi f(2-9f)\right] \qquad (2\text{-}1\text{-}12)$$

where $f = -\epsilon$ and $\xi = (18l + 6m + 2/3n)/4K_o$. Note that the f^2 term in (2-1-12) is incomplete, being composed of the incomplete ϵ^2 terms in the velocities.

The third-order constants, l, m, and n, may be interpreted in terms of the pressure derivatives of the velocity. By using the expression for the pressure given by Birch (1952)

$$P = -3K_o\epsilon(1-2\epsilon)^{5/2}(1+2\epsilon\xi) \qquad (2\text{-}1\text{-}13)$$

and equations (2-1-10) for the velocities, the pressure derivatives may be expressed as

$$\left(\frac{1}{V_P}\frac{\partial V_P}{\partial P}\right)_o = \frac{1}{6K_o}\,\frac{13\lambda_o + 14\mu_o - 18l - 4m}{\lambda_o + 2\mu_o} \qquad (2\text{-}1\text{-}14)$$

$$\left(\frac{1}{V_S}\frac{\partial V_S}{\partial P}\right)_o = \frac{1}{6K_o}\,\frac{3\lambda_o + 6\mu_o + 3/2m + 1/2n}{\mu_o}\,. \qquad (2\text{-}1\text{-}15)$$

Given only a hydrostatic finite strain, it is not possible to determine ℓ, m, and n individually, but only the combinations

$$\begin{aligned} \zeta &= 18\ell + 4m \\ \eta &= \tfrac{1}{2}(3m+n) \end{aligned} \qquad (2\text{-}1\text{-}16)$$

which appear in the velocity derivatives. Since

$$\left(\frac{\partial K}{\partial P}\right)_0 = 4 - \frac{4}{3}\xi \qquad (2\text{-}1\text{-}17)$$

and

$$\xi = \frac{18\ell + 6m + {}^2\!/_3 n}{4K_0} = \frac{\zeta + {}^4\!/_3 \eta}{4K_0} \qquad (2\text{-}1\text{-}18)$$

equation (2-1-17) is linearly dependent on equations (2-1-3) and (2-1-4). For most geophysical purposes, however, ζ and η are sufficient. These parameters are given in Table 2-1-1 for a number of solids.

The most serious objection to finite strain theory is that one is never certain as to the convergence of the expressions for the velocities (2-1-10) or the bulk modulus (2-1-12). The coefficient of the ϵ term is typically an order of magnitude larger than the leading term, and the coefficient of the ϵ^2 term, although incomplete, appears to be an order of magnitude larger still. Therefore, these expressions are probably insufficient for $\epsilon > 0.1$, which is roughly the strain at the base of the mantle. For self-consistent analyses, the ϵ^2 terms, being incomplete, should not be retained. The expressions should be used in the form

$$V_P^2 = \frac{1}{\rho_o}(1-2\epsilon)^{5/2}\left[\lambda_o + 2\mu_o - \epsilon(11\lambda_o + 10\mu_o - \xi)\right]$$
$$V_S^2 = \frac{1}{\rho_o}(1-2\epsilon)^{5/2}\left[\mu_o - \epsilon(3\lambda_o + 4\mu_o + \eta)\right] \qquad (2\text{-}1\text{-}19)$$
$$K = (1-2\epsilon)^{5/2} K_o\left[1 - \epsilon(7 - 4\xi)\right]$$
$$P = -3K_o\epsilon(1-2\epsilon)^{5/2}(1+2\epsilon\xi).$$

By fitting equations (2-1-19) to the seismic velocity and density profiles, it is possible to evaluate λ_o, μ_o, ρ_o, ξ, and η for any homogeneous region of the earth having an adiabatic temperature gradient. Jordan, et al., (1971) have made this fit for the following velocity and density profiles (in the lower mantle)

(1) Birch I (1964)

(2) Birch II (1964)

(3) Pyrolite (Clark and Ringwood, 1964)

(4) Eclogite (Clark and Ringwood, 1964)

(5) CIT 435002 (Jordan and Anderson, 1971)

(6) CIT 435003 (Jordan and Anderson, 1971).

The Birch II model and the two CIT models have been superimposed in Figure 2-1-1. The major difference between these profiles is the low density gradient of the CIT models in the lower mantle.

In addition to equations (2-1-19), equations of the form

$$V_P^2 = \left(\frac{1}{\rho_o}\right)(1-2\epsilon)^{5/2}\left[\lambda_o + 2\mu_o - \epsilon(11\lambda_o - 10\mu_o - \xi) + \epsilon^2(\beta)\right]$$
$$V_S^2 = \left(\frac{1}{\rho_o}\right)(1-2\epsilon)^{5/2}\left[\mu_o - \epsilon(3\lambda_o + 4\mu_o + \eta) + \epsilon^2(\gamma)\right] \qquad (2\text{-}1\text{-}20)$$
$$P = -3K_o\epsilon(1-2\epsilon)^{5/2}\left[1 + 2\epsilon\xi + \epsilon^2(\alpha)\right]$$

were also fit to the above models and the parameters α, β, and γ found. Equations (2-1-20) are perfectly valid in form, but the α, β, and γ parameters cannot be interpreted in terms of zero pressure velocity derivatives unless the ϵ^4 terms are retained in the expansion of ϕ.

It is in fact possible to add any number of terms with increasing powers of ϵ. The important question is how many terms do we need to define the low order parameters; i.e., do the coefficients in the expansion become smaller at a faster rate than ϵ ? It is a basic problem of finite strain expansions that this question cannot be answered. The question we can answer in this type of analysis is how many orders are needed to fit a given V_p, V_s set of data within some acceptable r.m.s. limit.

In Figure 2-1-2 the total r.m.s. discrepancy between the Birch II model and finite strain fits is plotted as a function of the order of the finite strain theory. It can be seen that while the fit is significantly improved by going from the incomplete first-order formulation given by Birch, (2-1-1 through 2-1-3), to the complete first-order fit (2-1-19), it is not significantly improved by going to the complete second-order (2-1-20). This is true of all the models.

Table 2-1-2 gives the parameters for the six models fit. The Birch I and II, pyrolite, and eclogite models were well fit by the second-order theory and gave "physically reasonable" zero-order parameters. The inversion models CIT 435002 and CIT 435003 could be fit, but did not yield "reasonable" zero-pressure parameters as will be discussed

below.

It is not surprising that the two Birch models and the Clark-Ringwood eclogite and pyrolite models are well fit by the finite strain since the assumptions of homogeneity and adiabaticity are built into the Adams-Williamson inversion used to compute them. However, the recent inversion models CIT 435002 and CIT 435003 contain no implicit relations between V_p, V_s, and ρ. Both fit the seismic data equally well. Our inability to fit the lower mantle of these models with physically reasonable zero-pressure parameters implies that the region under study is either anisotropic, inhomogeneous, or non-adiabatic. These possibilities will now be investigated.

There is seismological evidence that the lower mantle is inhomogeneous. Johnson (1969) gives evidence for the following discontinuities

Depth	$\Delta V_p/V_p$
830	0.0045
1000	0.0079
1230	0.0059
1540	0.0065
1910	0.0032

Assuming $\Delta V_s/V_s \approx \Delta V_p/V_p$ as observed at the major discontinuities, it is possible to estimate the change in the seismic parameter $\Delta\Phi/\Phi$ at each discontinuity. Since $d\rho/dP = 1/\Phi$, each observed $\Delta\Phi$ has the effect of decreasing $d\rho/dP$ relative to the homogeneous case, as illustrated in Figure 2-1-3. Correcting for the approximate Φ change associated

with Johnson's observed V_p discontinuities increases the slope of $\rho(z)$ by ~ 0.07 gm/cm^3 in the region 800-3000 km. By assuming $\rho = A\Phi^{1/3}$, the density jumps associated with the Φ jumps, $\frac{\Delta\rho}{\rho} = \frac{1}{3}\frac{\Delta\Phi}{\Phi}$ may be removed. The net effect in the region 800-3000 km is to decrease the slope of $\rho(z)$ by ~ 0.09 gm/cm^3. Hence removal of the observed jumps has two cancelling effects on the density gradient which leave ρ (z) approximately unchanged.

The effect of a superadiabatic temperature gradient can be approximately estimated as outlined in Table 2-1-3. The effect of correcting the profile CIT 435002 for a superadiabatic gradient ranging from 0 to 0.5 °C/km is illustrated in Figure 2-1-4. In this figure the zero-pressure Φ and ρ found from the fit parameters (Table 2-1-2) are superimposed on the estimated ρ-Φ trajectories for olivines, pyroxenes, and garnets given by Anderson and Jordan (1970). It can be seen that for a superadiabatic gradient of 0.2-0.4°C/km the model CIT 435002 can be fit with "reasonable" parameters.

The conclusion is that while the two inversion models 435002 and 435003 cannot be fit by isotropic finite strain theory with "reasonable" zero-pressure parameters, the more nearly adiabatic of the two, 435002, yields reasonable parameters when corrected for a superadiabatic of $\sim$0.2-0.4°C/km. The effect of the observed inhomogeneity is minimal.

It should be pointed out that this type of a finite strain analysis is as far as one can go in an interpretation of the velocity and density profiles without assuming a compositional model. This analysis gives the velocities and their pressure derivates at P = 0 and some high T on the adiabat which can then be compared to lab data. In the more

sophisticated finite strain models (Leibfried and Ludwig, 1961) or the lattice model calculations presented in the following chapters, one must assume a compositional model, then predict its elastic properties at mantle T, P conditions for a direct comparison with the seismic profiles.

2-2. The Systematics Approach

The next step in the use of lab data to interpret seismic velocity profiles was initiated by Birch's (1961a) observation that the compressional-wave velocity was an approximate linear function of the density and mean atomic weight $\bar{M}$ for some 250 specimens of rock. He put this relation in the form

$$\rho = A(\bar{M}) + B V_p . \qquad (2\text{-}2\text{-}1)$$

Quoting Birch, "It is tempting to infer that if the density is changed by compression, for a given substance, the velocity varies in much the same way with the density as it does for these structural and compositional changes; in other words, that lines of constant $\bar{M}$ show the relation of velocity to density for compression of any material whose points fall on this line." Most of the early (pre-1965) geophysical ultrasonic measurements were made on rocks to 10 kilobars. The purpose of the pressure was not to allow the measurement of pressure derivatives, but rather to remove the effects of porosity. The motivation of the ultrasonic work was to define the constants A and B in equation (2-2-1).

If one succumbs to "Birch's temptation" and assumes that temperature and pressure have the same effect on V_p as the change in

composition, then equation (2-2-1) becomes very useful in the interpretation of seismic profiles. Birch (1961b) used relation (2-2-1) to show that many previous velocity and density profiles were not self-consistent in that assumed "homogeneous" regions corresponded to lines of changing $\bar{M}$ on the velocity-density Birch diagrams. Only Bullen's (1956) model A was self-consistent, and was very similar to an $\bar{M}$ = constant model throughout the mantle.

The first attempt to infer composition was made by Birch (1964). He used (2-2-1) to obtain the density from the velocities through the transition zone, but then used the Adams-Williamson procedure to obtain the density of the lower mantle. He could thus use equation (2-2-1) to infer $\bar{M}$ of the lower mantle.

Like all purely empirical relations, Birch's hypothesis has its exceptions. Simmons (1964a) pointed out that calcium-rich rocks did not seem to follow the trend for other rocks and suggested the following form for equation (2-2-1).

$$V_p = A + 4.60[CaO] + B\rho \qquad (2\text{-}2\text{-}2)$$

In this expression the bracketed quantity is the weight-fraction of CaO.

Simmons (1964b) measured the shear wave velocity in many of the rock specimens used by Birch (1960) in his compression wave study. Apparently this data could not be expressed in the form:

$$V_S = A(\bar{M}) + B\rho \qquad (2\text{-}2\text{-}3)$$

since no follow-up paper was published on the systematics.

The next major step in the evolution of systematics was Anderson's (1967a) "seismic equation of state", a simplified form of which may be written (for small compressions)

$$\rho = A \bar{M} \Phi^n \qquad (2\text{-}2\text{-}4)$$

In this equation A and n are constants and Φ is the seismic parameter $V_p^2 - \frac{4}{3} V_s^2$ which is also equal to K_s/ρ. Although equation (2-2-4) is essentially an empirical relationship in the spirit of Birch's hypothesis (2-2-1) regarding the compressional velocities, it has the following advantages:

(1) The functional form of (2-2-4) is consistent with an equation of state of the rather general form

$$P = (N-M)^{-1} K_o \left[\left(\frac{\rho}{\rho_o}\right)^N - \left(\frac{\rho}{\rho_o}\right)^M \right]$$

as is easily shown using the definition $\Phi = (dP/d\rho)_s$, in the limit of small compressions.

(2) Static compression and shock data can be used as well as ultrasonic data to determine the parameters in (2-2-4), thus significantly enlarging the relevant experimental pressure range.

In the case of the seismic equation of state (2-2-4) the temptation to infer that pressure and composition have the same effect in $\rho - \Phi$ space is thus even stronger since the relation has the functional form of an equation of state.

More recent refinements (Anderson, 1969) have attempted to isolate the effect on Φ of factors other than $\bar{M}$ and ρ. In specific,

the effects of cation-radius, crystal field effects, and anion-cation coordination were empirically investigated.

The seismic equation of state was first used by Anderson and Smith (1968) as a constraint on the inversion. They required that the density and Φ be related by $\rho = A\bar{M}\Phi^n$ but did not constrain $A\bar{M}$ or n. By fitting the free oscillations, group and phase velocity of surface waves, and travel times of body waves, they determined $A\bar{M}$ and n, and thus obtained some information about the composition. They concluded that $\bar{M}$, and hence the composition, changed through the transition zone.

The use of laboratory data to establish an empirical relation between the bulk modulus and the density has thus proved quite useful. However, this approach does not fully utilize the seismic data. As independent V_p and V_s profiles are being refined, one would like to be able to fully utilize this information, rather than just the combination $\Phi = V_p^2 - \frac{4}{3} V_s^2$. Toward this end the systematics approach is far less useful.

Figures 2-2-1 and 2-2-2 are Birch diagrams V_p vs. ρ and V_s vs. ρ based upon ultrasonic data. Each plot shows the effect of pressure as computed from equations (2-1-19). The effect of a 1000°C change in temperature is also shown. Note that for V_p, both the temperature and pressure effects are approximately parallel to the lines of $\bar{M}$ = constant. For V_s, not only is the data determining the lines of $\bar{M}$ = constant more scattered, but the effect of pressure for certain structures like rutile and spinel is not parallel to the $\bar{M}$ = constant line.

The remainder of this thesis deals with an alternate method of using laboratory data in the interpretation of seismic profiles. Rather than use the data to establish an empirical relation between velocity and density, it will be used to establish the empirical parameters in the two-body potential functions of a lattice model for each mineral. By thus putting the empiricism on a more fundamental level, one gains the natural dependence of elastic wave velocities on the cyrstal structure.

TABLE 2-1-1

Ultrasonic Data for the Velocity Derivatives, Bulk Modulus, and Shear Modulus

		$\frac{1}{V_P}\frac{dV_P}{dP}$ 10^{-12} cm²/dyne	$\frac{1}{V_S}\frac{dV_S}{dP}$ 10^{-12} cm²/dyne	K_S 10^{12} dynes/cm²	μ 10^{12} dynes/cm²	ζ 10^{12} dynes/cm²	η 10^{12} dynes/cm²
Forsterite[1]	Mg_2SiO_4	1.249	.714	1.286	.811	-1.8	-2.6
Olivine[1]	$Fo_{.93}Fa_{.07}$	1.211	.737	1.294	.791	-1.0	-2.5
Periclase	MgO	.862	.665	1.622	1.308	-0.2	-1.6
Lime*	CaO	1.309	.603	1.059	.761	0.6	-3.3
Bromelite*	BeO	.538	.0449	2.201	1.618	6.3	-12.1
Zincite*	ZnO	.613	-1.138	1.394	.442	10.3	-10.2
Corundum	Al_2O_3	.478	.347	2.521	1.613	7.6	-5.5
Hematite*	Fe_2O_3	.591	.151	2.066	.910	7.7	-8.1
Spinel	$MgO \cdot 2.6\ Al_2O_3$	.494	.0762	2.020	1.153	11.1	-9.6
Trevorite[2]*	$NiFe_2O_4$	.610	-.0082	1.823	.713	9.0	-8.4
Garnet	Al-Py	.919	.456	1.770	.943	-1.5	-4.5
Rutile[3]	TiO_2	.825	.101	2.155	1.124	-3.9	-9.3

Finite strain parameters ζ and η were computed according to equations (2-1-14), (2-1-15), and (2-1-16).

*polycrystalline

[1]Kumazawa, M., and Orson L. Anderson [1969]

[2]Liebermann [1969]

[3]Manghnani, M. [1969]

All others from Anderson, O. L., et al. [1968]

TABLE 2-1-2

Finite Strain Parameters for the Lower Mantles of Several Earth Models

Model and Interval fit	0^{th} Order			1^{st} Order		2^{nd} Order		
	ρ_o (gm/cm^3)	λ_o (kb)	μ_o (kb)	ϑ (kb)	$-\eta$ (kb)	$-\alpha$	$-\beta$ (kb)	$-\delta$ (kb)
Birch I (1000-3000 km.)	3.91	1155	1295	8254	5688	--	--	--
	3.91	1164	1237	4532	4225	2.47	4339	1165
Birch II (1000-3000 km)	3.96	1072	1308	5915	5380	--	--	--
	3.94	905	1257	-1850	4010	8.00	6941	540
Pyrolite (1000-3000 km.)	4.11	1327	1405	10,744	13,266	--	--	--
	4.13	1555	1279	9210	6693	-2.24	3681	3612
Eclogite (1000-3000 km.)	3.91	1221	1323	10,074	12,424	--	--	--
	3.92	1428	1189	7907	5782	-1.86	3740	3545
CIT 435002 (1035-2703 km)	3.93	923	1312	1844	5269	--	--	--
CIT 435003 (1035-2703 km)	3.74	-270	1193	-18,132	1430	--	--	--
	4.13	2402	1392	49,640	8008	-57	-52,077	4.5

Parameters of the Complete 1st Order Fit (P = 0, T 1600°C)

Model and depth range	ρ_o (gm/cm^3)	$(V_p)_o$ (km/sec)	$(V_s)_o$ (km/sec)	σ_o	K_o (kb)	Φ_o (km/sec)^2
Birch I	3.91	9.79	5.76	.24	2018	51.6
Birch II	3.96	9.65	5.75	.23	1944	49.1
Pyrolite	4.11	10.03	5.85	.24	2264	55.1
Eclogite	3.91	9.95	5.82	.24	2103	53.8
CIT 435002	3.93	9.50	5.78	.13	1798	39.3
CIT 435003	3.74	7.52	5.65	-.15	525	14.0

TABLE 2-1-3

Correcting Seismic Profiles for a

Superadiabatic Temperature Gradient

From ultrasonic data:

$$\left(\partial \ln V_p / \partial \ln \rho\right)_p \approx 2.0$$

$$\left(\partial \ln V_s / \partial \ln \rho\right)_p \approx 2.5$$

$$\partial V_p \approx -2.0\, \alpha\, V_p\, \partial T$$

$$\partial V_s \approx -2.5\, \alpha\, V_s\, \partial T$$

$$\partial \rho = -\alpha \rho\, \partial T$$

Following Birch(1968):

$$\frac{\alpha}{\alpha_o} \approx \frac{K_o}{K}$$

Let Δ deg/km. = superadiabatic temperature gradient

$$\delta\rho = -\frac{\alpha_o K_o}{K} \rho \Delta\, \delta z = \frac{\alpha_o K_o}{\Phi} \Delta\, \delta z$$

$$\delta V_p = 2.0\, \frac{\alpha_o K_o}{K}\, V_p \Delta\, \delta z$$

$$\delta V_s = 2.5\, \frac{\alpha_o K_o}{K}\, V_s \Delta\, \delta z$$

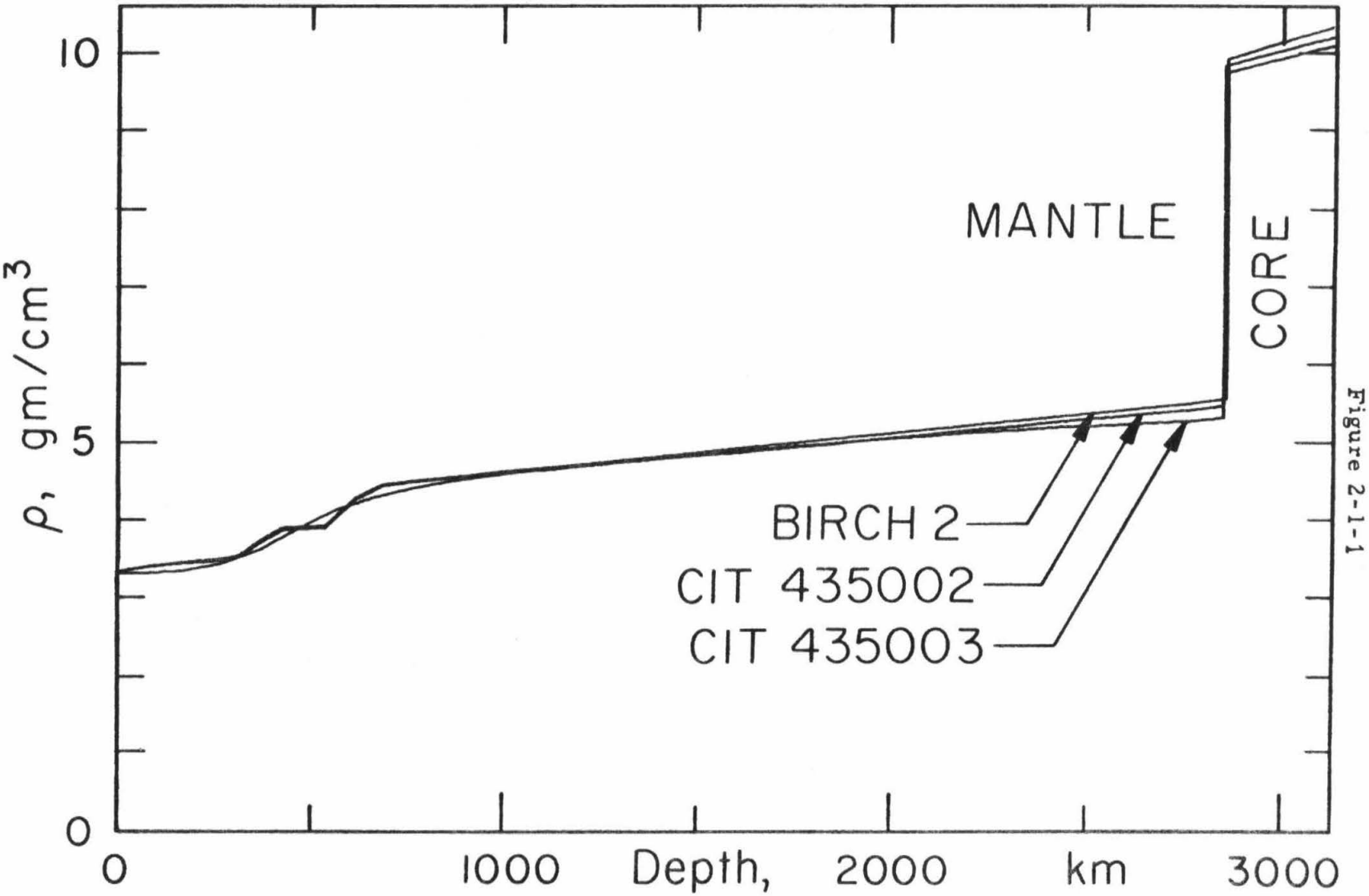

Figure 2-1-1

Comparison of lower mantle densities of three earth models

Figure 2-1-2

BIRCH II - FIT vs. ORDER

r.m.s. error

Order	V_p	V_s	ρ	Total
Incomplete 1st	.014	.032	.0013	.035
Complete 1st	.0055	.0027	.0010	.006
Complete 2nd	.0021	.0007	.0004	.002

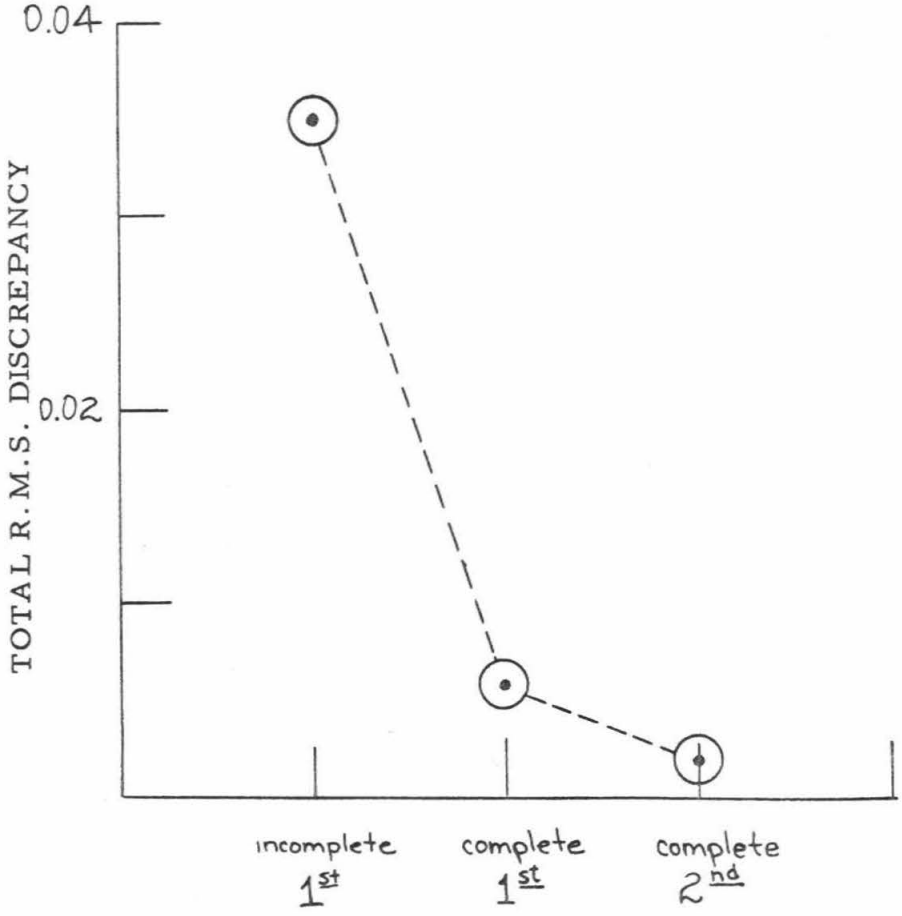

Figure 2-1-3

CORRECTING SEISMIC PROFILES

FOR OBSERVED INHOMOGENEITY

Johnson (1969) gives evidence of the following discontinuities:

Depth	$\Delta V_p/V_p$	Depth	$\Delta V_p/V_p$
830	0.0045	1540	0.0065
1000	0.0079	1910	0.0032
1230	0.0059		

Assume $\Delta V_s/V_s \approx \Delta V_p/V_p$ as observed at other discontinuities.
We can then estimate $(\Delta\Phi/\Phi)_i$

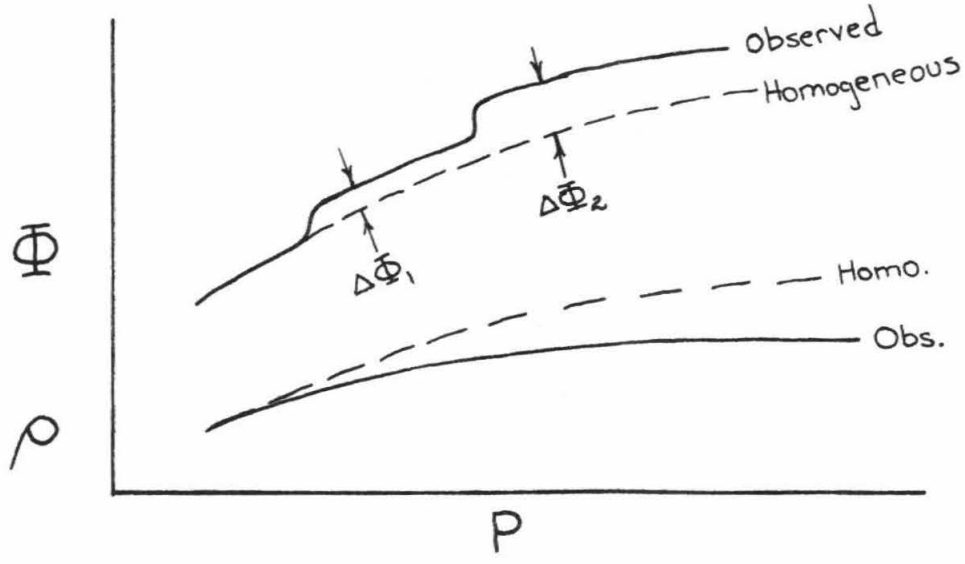

$(d\rho/dP) = 1/\Phi$ so each $\Delta\Phi_i$ has the effect of decreasing $(d\rho/dP)$ relative to the homogeneous case.

Correcting for Johnson's Φ increases the slope of ρ by ~ 0.07 gm/cm^3 in the region 800-3000 km.

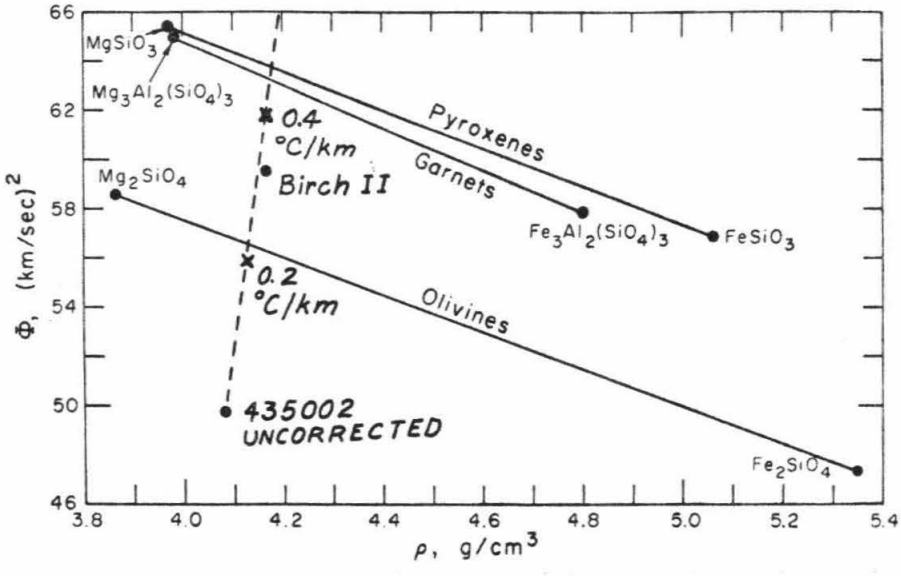

Figure 2-1-4. Seismic parameter versus density for olivines, pyroxenes, and garnets assuming both molar volumes and seismic ratios are molar averageable (after Anderson and Jordan, 1970). The effect of correcting seismic profile CIT 435002 for a superadiabatic temperature gradient according to Table 2-1-3 is shown by the dashed line.

Figure 2-2-1. (following page) Compressional velocity versus density for various oxides and silicates. The dark circles are minerals with mean atomic weight near 20. The light dashed lines are pressure trajectories calculated from finite strain theory and the parameters of Table 2-1-1. The solid lines with arrows show the effect of a 1000°C rise in temperature (after Anderson, et al., 1971).

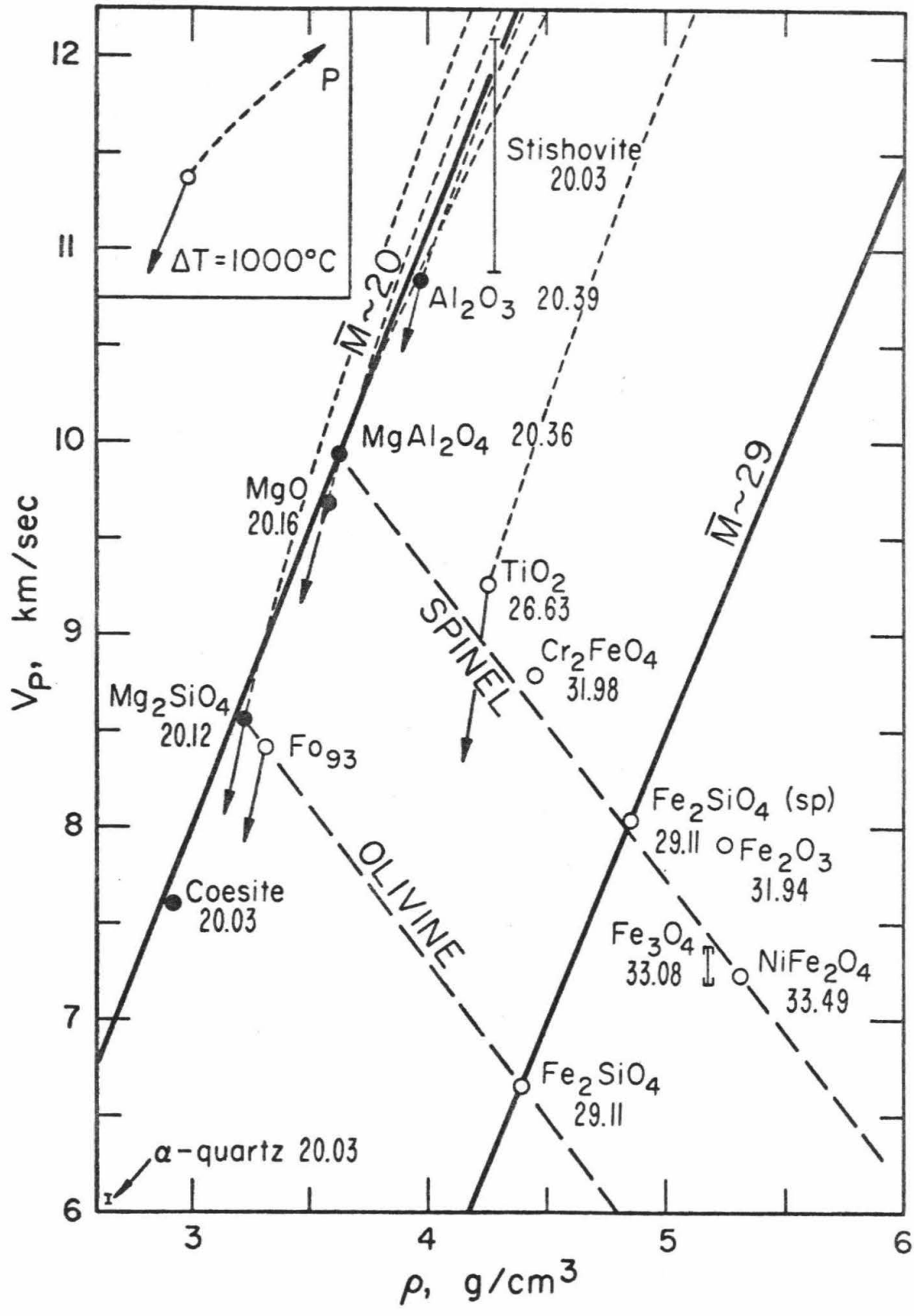
P
ΔT=1000°C
Stishovite
20.03
$\bar{M}$~20
Al_2O_3 20.39
$MgAl_2O_4$ 20.36
MgO
20.16
TiO_2
26.63
SPINEL
Cr_2FeO_4
31.98
$\bar{M}$~29
Mg_2SiO_4
20.12
Fo_{93}
Fe_2SiO_4 (sp)
29.11
Fe_2O_3
31.94
Coesite
20.03
OLIVINE
Fe_3O_4
33.08
$NiFe_2O_4$
33.49
Fe_2SiO_4
29.11
α-quartz 20.03
V_P, km/sec
ρ, g/cm³
12
11
10
9
8
7
6
3
4
5
6

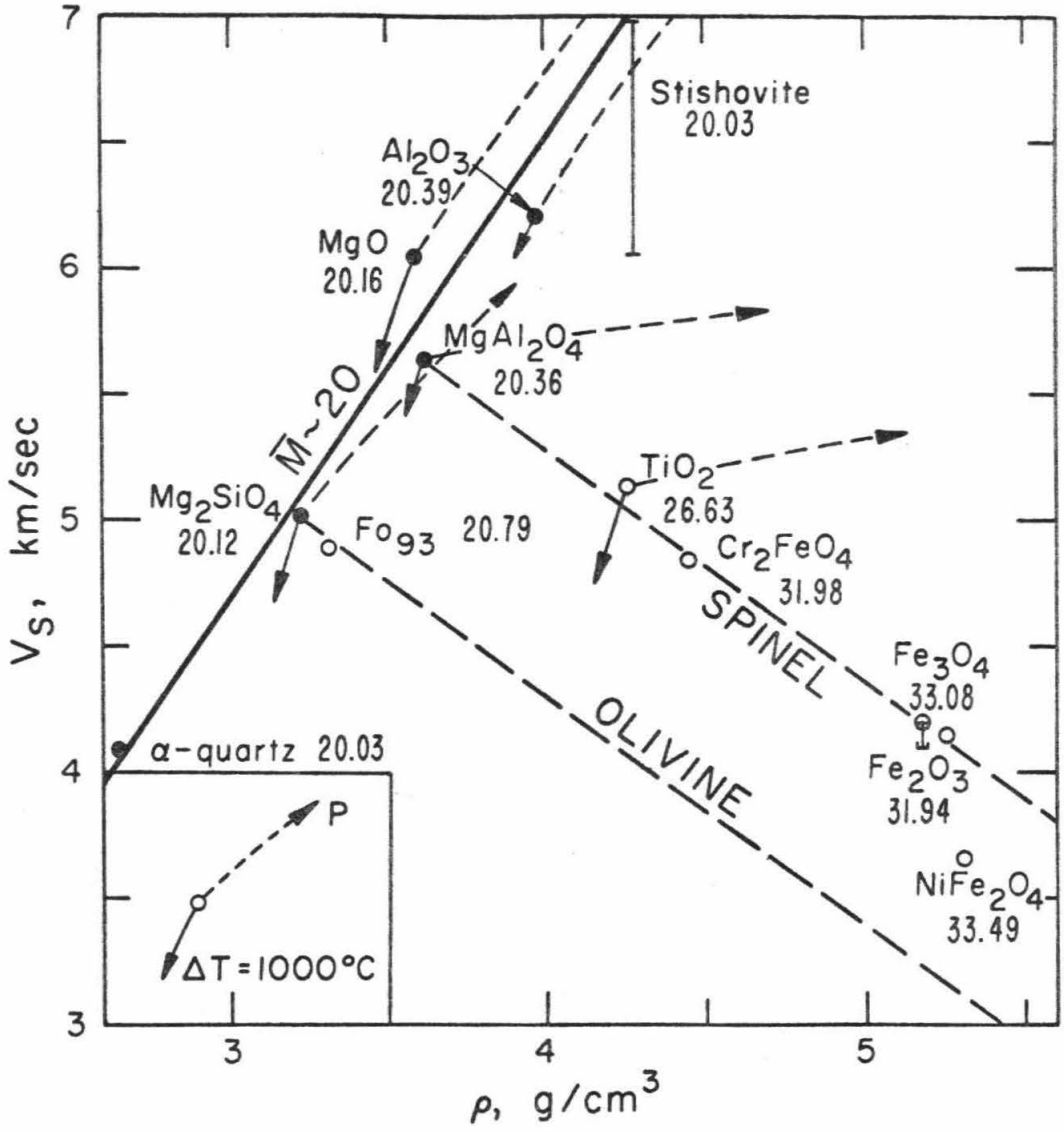

Figure 2-2-2. Shear velocity versus density for various oxides and silicates. The effect of pressure is shown by the light dashed lines; of temperature, by the solid lines with arrows (after Anderson, et al., 1971).

III. THE DEFINITION AND MEANING OF ELASTIC CONSTANTS AND METHODS FOR THEIR CALCULATION

This chapter has three objectives. The first is to establish the reference states, coordinate systems, and strain measures necessary to discuss elastic constants in a prestrained elastic medium. The second is to compare methods of calculation based upon finite strain expansions of the internal energy with those methods which assume a specific functional form for the two-body, central, interatomic forces. The third is to develop the interatomic potential model using Born's (1923) method of long waves, obtaining general expressions for the volume dependence of the elastic constants of ionic crystals.

This chapter develops the theoretical framework used to investigate the potential and predict the elastic properties of geophysically interesting structures in the following chapters.

3-1. Effective vs. Thermodynamic Elastic Constants

Before proceeding to an atomistic formulation of the elastic constants, it is important to review their definition in the context of continuum mechanics. There are as many different ways to define the elastic constants as there are different tensor measures of the strain, but only one definition gives the "effective" constants. The "effective" elastic constants are defined as those constants which control the propagation velocity of small amplitude waves in a medium which has undergone a finite homogeneous prestrain. It is these "effective" elastic constants

for the case of a hydrostatic prestrain which we wish to compute and average for comparison with the seismically determined velocity profiles in the earth.

There have been several recent papers dealing with the distinction between thermodynamic and effective elastic constants, most notably Thurston (1964, 1965) and Wallace (1965, 1967). The following discussion is a brief review of their work. It serves the dual purpose of comparing the various definitions of the elastic constants and establishing the notation to be used in the remainder of this thesis. Only the results are presented in the following text; the mathematical derivations have been relegated to Appendix 1.

As pointed out by Thurston (1965), the elastic constants may be defined in at least three different ways: "(1) as second derivatives of the internal energy with respect to some tensor measure of the deformation; (2) as first derivatives of the stress tensor with respect to some tensor measure of the deformation; (3) as coefficients in a linearized equation of motion or, equivalently, as coefficients in formulas for the propagation velocities of small amplitude waves." Further, the elastic constants defined by each of these methods depend upon the specific measure of the deformation. The coefficients of the stress-strain relation depend upon the choice of a reference state from which the strains are measured, the tensor measure of the deformation with respect to which the derivatives are taken, and the choice of a stress tensor. The coefficients of the linearized wave equation depend upon the coordinates used in the equation of motion.

Reference States

In order to sort out the various possibilities, consider the three states as diagrammed in Figure (3-1-1). Again following Thurston (1965) call these the "natural" unstressed state, the "initial" homogeneously deformed state, and the "present" or current state. Denote the density of the natural state by $\tilde{\rho}$ and the position of a material particle by a_i ($i = 1, 3$). Denote the density of the initial state by $\overline{\rho}$, the position of a material particle by X_i ($i = 1, 3$), and the associated stresses by $\overline{T}_{ij}$. Denote the density of the present state by ρ, the position of a material particle by x_i ($i = 1, 3$), and the stresses by T_{ij}. The coordinates a_i, X_i, and x_i are referenced to the same cartesian axes.

Measures of the Strain

The strain tensor may be referenced to either the natural state, the initial state, or the present state. If it is referenced to the natural state, we make the following definitions (Murnaghan, 1951)

$$u_i = x_i - a_i \qquad f_{ij} = \partial x_i / \partial a_j$$

$$u_{ij} = \partial u_i / \partial a_j \tag{3-1-1}$$

$$\eta_{ij} = \frac{1}{2}(f_{ki} f_{kj} - \delta_{ij}) = \frac{1}{2}(u_{ij} + u_{ji} + u_{ki} u_{kj})$$

The η_{ij} are called the Lagrangian or material strains. If the strain tensor is referenced to the present state we make the definitions

$$g_{ij} = \partial a_i / \partial x_j$$

$$\varepsilon_{ij} = \frac{1}{2}(\delta_{ij} - g_{ki} g_{kj}) \tag{3-1-2}$$

The ε_{ij} are called the Eulerian or spatial strains. If one wishes to express the internal energy as a Taylor series in the strains, the question naturally arises as to which tensor should be used. Since either expansion must be truncated, this decision should be based upon which is more rapidly convergent. Thomsen (1970a, b) considers the question in some detail and concludes that the Lagrangian expansion is to be preferred for two reasons. First, it gives a more accurate prediction of the observed shear instability ($C_{44} = 0$) in NaCl. Second, and more important, the Lagrangian formulation is consistent with the Mie-Grüneisen treatment of the vibrational energy. This point is discussed further in section 3-2. The distinction between Eulerian and Lagrangian strains is not important in the interatomic potential approach because the elastic constants are derived in closed form. They are defined by comparing the long-wave limit of the lattice vibrational equation with the continuum equation of motion for plane wave propagation in the initial (stressed) state. In this case, since we are dealing with small displacements from the initial state $U_\alpha = x_\alpha - X_\alpha$, the displacement gradient $U_{\alpha\beta} = \partial U_\alpha / \partial X_\beta$ is the natural measure of the strain as required by the Lagrangian. Also, it is most convenient to reference the atomistic expressions to the initial (equilibrium) state.

Elastic Constants

Limiting the discussion to Lagrangian strains, the following definitions are made :

$$t_{ij} = \tilde{\rho}\left(\frac{\partial E}{\partial \eta_{ij}}\right)_S = \tilde{\rho}\left(\frac{\partial F}{\partial \eta_{ij}}\right)_T$$

$$C^S_{ijkl} = \left(\frac{\partial t_{ij}}{\partial \eta_{kl}}\right)_S = \tilde{\rho}\left(\frac{\partial^2 E}{\partial \eta_{kl}\partial \eta_{ij}}\right)_S \qquad (3\text{-}1\text{-}3)$$

$$C^T_{ijkl} = \left(\frac{\partial t_{ij}}{\partial \eta_{kl}}\right)_T = \tilde{\rho}\left(\frac{\partial^2 F}{\partial \eta_{kl}\partial \eta_{ij}}\right)_T$$

where E = internal energy per unit mass

F = Helmholtz free energy per unit mass

S = entropy

T = temperature .

All derivatives are evaluated in the natural state.

The t_{ij} were named the thermodynamic tensions by Truesdell and Toupin (1960). They are introduced to remove the complications arising from the fact that the strains are usually referenced to the natural state while the stress is usually defined per unit area of the deformed body. By definition they are the conjugate variables to $\eta_{ij}/\tilde{\rho}$; i.e., $t_{ij}d\eta_{ij}$ is the differential of work per unit of original volume done by stretching the body. The expansion for E and F are therefore:

$$\tilde{\rho}E(\eta_{ij},S) = \tilde{\rho}E(0,S) + t_{ij}\eta_{ij} + \tfrac{1}{2}C^S_{ijkl}\eta_{ij}\eta_{kl} + \ldots \qquad (3\text{-}1\text{-}4)$$

$$\tilde{\rho}F(\eta_{ij},T) = \tilde{\rho}F(0,T) + t_{ij}\eta_{ij} + \tfrac{1}{2}C^T_{ijkl}\eta_{ij}\eta_{kl} + \ldots .$$

In the lattice calculation it will be shown that it is more convenient to reference the strain to the initial state. Working again with Lagrangian strains:

$$
\left.
\begin{aligned}
&U_i = x_i - X_i \qquad F_{ij} = \partial x_i / \partial X_j \\
&U_{ij} = \partial U_i / \partial X_j \\
&S_{ij} = \tfrac{1}{2}\left(F_{ki} F_{kj} - \delta_{ij}\right) = \tfrac{1}{2}\left(U_{ij} + U_{ji} + U_{ki} U_{kj}\right)
\end{aligned}
\right\} \qquad (3\text{-}1\text{-}5)
$$

$$
\left.
\begin{aligned}
&\bar{T}_{ij} = \bar{\rho}\left(\partial E / \partial S_{ij}\right)_S = \bar{\rho}\left(\partial F / \partial S_{ij}\right)_T \\
&C^S_{ijkl} = \left(\frac{\partial \bar{T}_{ij}}{\partial S_{kl}}\right)_S = \bar{\rho}\left(\frac{\partial^2 E}{\partial S_{kl}\partial S_{ij}}\right)_S \\
&C^T_{ijkl} = \left(\frac{\partial \bar{T}_{ij}}{\partial S_{kl}}\right)_T = \bar{\rho}\left(\frac{\partial^2 F}{\partial S_{kl}\partial S_{ij}}\right)_T
\end{aligned}
\right\} \qquad (3\text{-}1\text{-}6)
$$

In these expressions all derivatives are evaluated in the initial state. Expansions for E and F about the initial state have the form

$$
\begin{aligned}
&\bar{\rho} E(S_{ij}, S) = \bar{\rho} E(0, S) + \bar{T}_{ij} S_{ij} + \tfrac{1}{2} C^S_{ijkl} S_{ij} S_{kl} + \cdots \\
&\bar{\rho} F(S_{ij}, S) = \bar{\rho} F(0, T) + \bar{T}_{ij} S_{ij} + \tfrac{1}{2} C^T_{ijkl} S_{ij} S_{kl} + \cdots .
\end{aligned}
\qquad (3\text{-}1\text{-}7)
$$

The elastic constants c_{ijkl} and C_{ijkl} are called the thermodynamic elastic constants.

The energy density may also be expanded in powers of the displacement gradients U_{ij}

$$
\bar{\rho} E(X, U_i, S) = \bar{\rho} E(X, 0, S) + S_{ij} U_{ij} + \tfrac{1}{2} S_{ijkl} U_{ij} U_{kl} + \cdots . \qquad (3\text{-}1\text{-}8)
$$

Since this was the expansion originally used by Huang (1949), Wallace (1967) has named S_{ijkl} the Huang coefficients. By casting the Lagrangian expansion (3-1-7) in terms of the displacement gradients and identifying terms, one gets the following relation between the Huang coefficients and the thermodynamic elastic constants (see Appendix 1).

$$S^s_{ij} = C^s_{ij} = \overline{T}_{ij}$$

$$S^s_{ijkl} = \overline{T}_{jl}\,\delta_{ik} + C^s_{ijkl} \qquad (3\text{-}1\text{-}9)$$

The definition of the elastic constants as the second derivatives of the energy density has led to three sets of elastic constants c_{ijkl}, C_{ijkl} and S_{ijkl}, each corresponding to a different reference state or measure of the strain.

Consider now those constants which relate the stress to the strain. If the stress tensor in the present state is expanded in terms of the displacement gradients U_{kl}, one can define a set of elastic constants

$$A_{ijkl} \equiv \left(\partial T_{ij} / \partial U_{kl}\right)_{\mathcal{I}} . \qquad (3\text{-}1\text{-}10)$$

The associated Taylor series is:

$$T_{ij} = \overline{T}_{ij} + A_{ijkl}\,U_{kl} . \qquad (3\text{-}1\text{-}11)$$

The tensor U_{kl} may be decomposed into symmetric and antisymmetric parts

$$U_{kl} = \epsilon_{kl} + \omega_{kl}$$

$$\epsilon_{kl} = \tfrac{1}{2}\left(U_{kl} + U_{lk}\right) \qquad (3\text{-}1\text{-}12)$$

$$\omega_{kl} = \tfrac{1}{2}\left(U_{kl} - U_{lk}\right) .$$

Note that ϵ_{kl} is the infinitesimal of S_{kl} defined in equation (3-1-5). A new set of constants may be defined as the tensor elements relating stress in the present state to these infinitesimal strains. Wallace (1967) has named these the Birch coefficients defined as:

$$B_{ijkl} \equiv \left(\partial T_{ij} / \partial \epsilon_{kl} \right).$$

This is just the differential form of Hooke's Law. The associated Taylor series expansion for the stress is

$$T_{ij} = \overline{T}_{ij} + B_{ijkl}\, \epsilon_{kl} + \left(\partial T_{ij} / \partial \omega_{kl} \right) \omega_{kl} + \ldots . \tag{3-1-13}$$

The Birch coefficients are related to the thermodynamic elastic constants (proof given in Appendix 1) as

$$B_{ijkl} = \tfrac{1}{2} \left(\overline{T}_{ik}\, \delta_{jl} + \overline{T}_{il}\, \delta_{jk} + \overline{T}_{jk}\, \delta_{il} + \overline{T}_{jl}\, \delta_{ik} - 2\overline{T}_{ij}\, \delta_{kl} \right) + C_{ijkl} . \tag{3-1-14}$$

Elastic Waves in a Prestressed Crystal

We have now defined five different elastic constants c_{ijkl}, C_{ijkl}, S_{ijkl}, A_{ijkl}, B_{ijkl}, each corresponding to a specific reference state and strain measure. The question now is which, if any, of these elastic constants defines the propagation velocity of infinitesimal elastic waves in the initial (strained) state? It is these "effective elastic constants" which we ultimately wish to compute for the case of a finite hydrostatic prestress.

Following Huang (1950, Appendix 6) we form the Lagrangian density for the displacement field $U_i(X_j)$.

$$\mathcal{L}(X_i, U_i, U_{ij}) = \tfrac{1}{2}\bar{\rho}\,|\dot{\underline{U}}|^2 - E \quad . \tag{3-1-15}$$

Using the expansion in terms of the displacement gradients (3-1-8) for the potential energy density gives

$$\mathcal{L} = \tfrac{1}{2}\bar{\rho}\,|\dot{U}|^2 + \bar{\rho}\,E(X,0,S) - \sum_{ij} S_{ij}\frac{\partial U_i}{\partial X_j} - \tfrac{1}{2}\sum_{ijkl} S_{ijkl}\frac{\partial U_i}{\partial X_j}\frac{\partial U_k}{\partial X_l} - \cdots . \tag{3-1-16}$$

By the usual variational technique (i.e., see Moiseiwitsch, 1966, Chapter 3), the Euler field equations are obtained in the form

$$\frac{\partial \mathcal{L}}{\partial U_i} - \sum_{j=1}^{3}\frac{\partial}{\partial X_j}\frac{\partial \mathcal{L}}{\partial(\partial U_i/\partial X_j)} - \frac{\partial}{\partial t}\left(\frac{\partial \mathcal{L}}{\partial \dot{U}_i}\right) = 0 \qquad (i = 1,2,3) \tag{3-1-17}$$

Which, upon differentiating (3-1-16), become

$$\bar{\rho}\,\ddot{U}_i = \sum_j \frac{\partial}{\partial X_j}\left\{ S_{ij} + \tfrac{1}{2}\sum_{kl}\left(S_{ijkl} + S_{klij}\right)\frac{\partial U_k}{\partial X_l}\right\} .$$

In order that the strain energy function exists, we must have (see, i.e., Love (1944), §66) $S_{ijkl} = S_{klij}$. Upon differentiating, we get

$$\bar{\rho}\,\ddot{U}_i = \sum_k\left(\sum_{jl} S_{ijkl}\,\frac{\partial^2 U_k}{\partial X_j \partial X_l}\right) \qquad i = 1,2,3 \tag{3-1-18}$$

For a plane elastic wave

$$U_i = \bar{u}_i\, e^{2\pi i\, \underline{\gamma}\cdot\underline{X} - i\omega t} \tag{3-1-19}$$

equations (3-1-18) become

$$\bar{\rho}\,\omega^2\,\bar{u}_i = 4\pi^2 \sum_k\left\{\sum_{jl} S_{ijkl}\; \gamma_j \gamma_l\right\}\bar{u}_k \qquad i = 1,2,3 . \tag{3-1-20}$$

Hence it is the Huang coefficients which are the effective elastic constants. The sum over j and ℓ means that it is only the symmetric combination $(S_{ijkl} + S_{ilkj})$ which is observed in experiments. Note that the wave equation (3-1-20) has exactly the form of a wave equation in an unstressed medium; the only difference being that the S_{ijkl} are, in general, of lower symmetry than the corresponding elastic constants in a stress-free medium. By requiring rotational invariance, Huang (1950) derived the following symmetry relations for the elastic constants in a prestressed medium.

$$S_{ij} = S_{ji}$$

$$S_{i\ell}\,\delta_{jk} - S_{j\ell}\,\delta_{ik} + S_{ijk\ell} + S_{jik\ell} = 0 \qquad (3\text{-}1\text{-}21)$$

Note that in a stress-free medium, $S_{ij} = 0$ and equation (3-1-21) gives the familiar symmetry relation $S_{ijkl} = S_{jikl}$.

Hydrostatic Prestress

The various elastic constants and their interrelationships have been defined above for the case of an arbitrary finite prestress $\overline{T}_{ij} = S_{ij}$. In the application to the earth's interior, it is generally assumed that the pressure is hydrostatic.

$$\overline{T}_{ij} = -P\,\delta_{ij} \qquad (3\text{-}1\text{-}22)$$

In this case the symmetry relations (3-1-21) become

$$P(\delta_{j\ell}\,\delta_{ik} - \delta_{i\ell}\,\delta_{jk}) + S_{ijk\ell} - S_{jik\ell} = 0 \qquad (3\text{-}1\text{-}23)$$

and we see that even in the case of hydrostatic pressure the S_{ijkl} lack

the familiar symmetry. However, if we define new elastic constants $\mathcal{S}_{ijkl}$ such that

$$\mathcal{S}_{ijkl} \equiv P(\delta_{ij}\delta_{kl} - \delta_{il}\delta_{jk}) + S_{ijkl} \tag{3-1-24}$$

where it is easily seen that

$$\mathcal{S}_{ijkl} + \mathcal{S}_{ilkj} = S_{ijkl} + S_{ilkj} \tag{3-1-25}$$

then the $\mathcal{S}_{ijkl}$ can replace the S_{ijkl} in the equation of motion (3-1-20); the two are therefore equivalent. However, by using equation (3-1-24) in the symmetry relations (3-1-21), we see that for the case of a hydrostatic prestrain

$$\mathcal{S}_{ijkl} = \mathcal{S}_{jikl} \tag{3-1-26}$$

and the $\mathcal{S}_{ijkl}$ therefore have the full symmetry of the elastic constants. We henceforth call $\mathcal{S}_{ijkl}$ the effective elastic constants.

By using equation (3-1-9), the effective elastic constants may be related to the thermodynamic elastic constants.

$$\mathcal{S}_{ijkl} = P(\delta_{ij}\delta_{kl} - \delta_{il}\delta_{jk} - \delta_{jl}\delta_{ik}) + C_{ijkl} \tag{3-1-27}$$

Further, by specializing equation (3-1-14) to the case of hydrostatic prestress and comparing with (3-1-27), it is easily seen that

$$B_{ijkl} = \mathcal{S}_{ijkl}\,. \tag{3-1-28}$$

As mentioned in the introduction, most of the relations given in this section have previously been given by Thurston (1964, 1965) and Wallace (1965, 1967). To facilitate comparison with their work,

Table 3-1-1 compares the notation used here with the notation in their papers.

Having established notation and defined the various elastic constants, the next section reviews the various methods of actually calculating and extrapolating the effective elastic constants for comparison with the seismic profiles.

3-2. Calculation of the Elastic Constants -- Finite Strain and Interatomic Potential Models

It was shown in the previous section that the effective elastic constants may be calculated as the second derivatives of the free-energy density with respect to the strains. An expression for the free energy is now required such that it can be appropriately differentiated. This is usually handled in one of two ways.

(a) The free energy may be expanded as a Taylor series in the strains, the coefficients evaluated from the measured elastic constants and their pressure and temperature derivatives at the "natural" zero pressure state.

(b) The free energy may be expressed as the sum of atomic interactions of assumed functional form. Parameters in the potential are fixed by data in the natural state. The elastic constants may be computed either by direct differentiation (method of homogeneous static deformation) or by a direct comparison between the long-wave limit of the lattice vibration equation and the continuum wave equation (3-1-20) (method of long waves).

We will call (a) the finite strain approach and (b) the interatomic potential approach.

The Finite Strain Approach

The formulation presented here was first given by Leibfried and Ludwig (1961) and has more recently been applied by Thomsen (1970a, b) to the sodium chloride data. Since the approach will only be sketched here, the reader is referred to these works for a more detailed development.

The free energy is written

$$F = \phi_o + F_s \tag{3-2-1}$$

where ϕ_o is the potential energy of the static lattice and F_s is the vibrational energy.

$$F_s = \sum_j \left[\frac{\hbar\omega_j}{2} + kT \ln\left(1 - e^{-\hbar\omega_j/kT}\right) \right] \tag{3-2-2}$$

In this approach the potential energy of the static lattice is expanded to fourth-order in the Lagrangian strain η

$$\begin{aligned} \phi_o(\eta) = \tilde{\phi}_o &+ 1/2\, \tilde{V} \sum_{ijkl} \tilde{C}_{ijkl}\, \eta_{ij}\, \eta_{kl} + \\ &+ 1/3!\, \tilde{V} \sum_{i\ldots n} \tilde{C}_{ijklmn}\, \eta_{ij}\, \eta_{kl}\, \eta_{mn} + \\ &+ 1/4!\, \tilde{V} \sum_{i\ldots q} \tilde{C}_{ijklmnpq}\, \eta_{ij}\, \eta_{kl}\, \eta_{mn}\, \eta_{pq} + \cdots . \end{aligned} \tag{3-2-3}$$

The super-tilde denotes evaluation in the fixed reference state; this reference state is chosen such that ϕ_o is a minimum.

The thermal energy F_s is expanded to second-order in the strains

$$F_s(\eta,T) = \tilde{F}_s(0,T) + \sum_{ij}\left(\frac{\partial F_s}{\partial \eta_{ij}}\right)_{\sim}\eta_{ij} + \tfrac{1}{2}\sum_{ijkl}\left(\frac{\partial^2 F_s}{\partial \eta_{ij}\partial \eta_{kl}}\right)_{\sim}\eta_{ij}\eta_{kl} + \ldots \quad (3\text{-}2\text{-}4)$$

Applying the Grüneisen approximation that the strain derivatives of all frequencies are the same, allows equation (3-2-4) to be written

$$F_s(\eta,T) = \tilde{F}_s(T) + \tilde{U}_s\sum_{ij}\tilde{\gamma}_{ij}\eta_{ij} + \quad (3\text{-}2\text{-}5)$$
$$+ \tfrac{1}{2}\sum_{ijkl}\left[-\tilde{\lambda}_{ijkl}\tilde{U}_s + \tilde{\gamma}_{ij}\tilde{\gamma}_{kl}\left(\tilde{U}_s - T\tilde{C}_v\right)\right]\eta_{ij}\eta_{kl} + \ldots$$

where

$$\tilde{\gamma}_{ij} = -\tfrac{1}{2}\left(\frac{\partial \ln \overline{\omega^2}}{\partial \eta_{ij}}\right)_{\sim} \quad (3\text{-}2\text{-}6)$$

$$\tilde{\lambda}_{ijkl} = -\tfrac{1}{2}\left(\frac{\partial^2 \ln \overline{\omega^2}}{\partial \eta_{ij}\partial \eta_{kl}}\right)_{\sim} = \left(\frac{\partial \gamma_{ij}}{\partial \eta_{kl}}\right)_{\sim} \quad (3\text{-}2\text{-}7)$$

$$\tilde{U}_s = \sum_{\nu}\hbar\omega_\nu\left(\tfrac{1}{2} + \frac{1}{e^{\hbar\omega_\nu/kT}-1}\right) \quad (3\text{-}2\text{-}8)$$

$$\tilde{C}_v = \sum_{\nu} k\left(\frac{\hbar\omega_\nu}{kT}\right)^2\left(e^{\hbar\omega_\nu/kT}-1\right)^2 e^{\hbar\omega_\nu/kT} \quad (3\text{-}2\text{-}9)$$

Substituting equations (3-2-3) and (3-2-4) into (3-2-1), the free energy is given (in Voigt notation) by:

$$F(\eta,T) = F(0,T) + \tilde{V}\sum_{\alpha\beta} 1/2\,\tilde{C}_{\alpha\beta}\eta_\alpha\eta_\beta +$$

$$+ \tilde{V}\sum_{\alpha\beta\mu} 1/3!\,\tilde{C}_{\alpha\beta\mu}\eta_\alpha\eta_\beta\eta_\mu + \qquad (3\text{-}2\text{-}10)$$

$$+ \tilde{V}\sum_{\alpha\beta\mu\nu} 1/4!\,\tilde{C}_{\alpha\beta\mu\nu}\eta_\alpha\eta_\beta\eta_\mu\eta_\nu$$

$$- \tilde{U}_s(T)\sum_\alpha \tilde{\gamma}_\alpha\eta_\alpha +$$

$$+ 1/2\sum_{\alpha\beta}\left[-\tilde{\lambda}_{\alpha\beta}\tilde{U}_s(T) + \tilde{\gamma}_\alpha\tilde{\gamma}_\beta(\tilde{U}_s - T\tilde{C}_v)\right]\eta_\alpha\eta_\beta + \ldots .$$

Equation (3-1-27) defines the effective elastic constants under hydrostatic prestrain as

$$\mathcal{B}_{ijkm} = C_{ijkm} + P(\delta_{ij}\delta_{km} - \delta_{im}\delta_{jk} - \delta_{ik}\delta_{jm}) . \qquad (3\text{-}2\text{-}11)$$

Changing the coordinate system from the initial to the natural so that the free-energy expansion (3-2-10) may be used

$$\mathcal{B}_{ijkm} = \frac{1}{\bar{V}} f_{ir}f_{js}C_{rstu}f_{tk}f_{um} + P(\delta_{ij}\delta_{km} - \delta_{im}\delta_{jk} - \delta_{ik}\delta_{jm}) \qquad (3\text{-}2\text{-}12)$$

$$C_{rstu} = \frac{\partial^2 F(\eta,T)}{\partial\eta_{rs}\partial\eta_{tu}} .$$

Thomsen (1970b) has evaluated this expression for a cubic crystal. He gives (in Voigt notation) for hydrostatic stress:

$$\mathcal{B}_{\alpha\beta}(V,T) = \left(\frac{V}{\bar{V}}\right)^{1/3}\left\{\tilde{C}_{\alpha\beta} + \eta\sum_\mu \tilde{C}_{\alpha\beta\mu} + 1/2\,\eta^2\sum_{\mu\nu}\tilde{C}_{\alpha\beta\mu\nu} - \right.$$

$$\left. - \tilde{U}_s\lambda_{\alpha\beta} + \tilde{\gamma}_\alpha\tilde{\gamma}_\beta(\tilde{U}_s - T\tilde{C}_v)\right\} - P\,\delta_\alpha^\beta . \qquad (3\text{-}2\text{-}13)$$

where $$\delta_\alpha^\beta = \delta_{ij}^{kl} = -\delta_{ij}\delta_{kl} + \delta_{lj}\delta_{ik} + \delta_{il}\delta_{kj}$$

$$\eta = 1/2\left[\left(\frac{V}{\tilde{V}}\right)^{2/3} - 1\right].$$

He changes from isothermal to adiabatic constants using the relation

$$\beta_{\alpha\beta}^S - \beta_{\alpha\beta} = \frac{T\tilde{C}_v}{\tilde{V}}\tilde{\gamma}_\alpha\tilde{\gamma}_\beta\left(\frac{V}{\tilde{V}}\right)^{1/3}. \tag{3-2-14}$$

The expressions for the adiabatic constants are given by Thomsen as:

$$\beta_{\alpha\beta}^S(V,T) = \left(\frac{V}{\tilde{V}}\right)^{1/3}\left\{\tilde{\beta}_{\alpha\beta} - 3\tilde{K}\Gamma_{\alpha\beta}\eta + 9/2\,\tilde{K}\Lambda_{\alpha\beta}\eta^2 - \frac{\tilde{U}_s}{\tilde{V}}\left[\lambda_{\alpha\beta} - \tilde{\gamma}^2\delta_\alpha\delta_\beta\right]\right\} - P\delta_\alpha^\beta. \tag{3-2-15}$$

The pressure is given by:

$$P(V,T) = -3\tilde{K}\left(\frac{V}{\tilde{V}}\right)^{-1/3}\left\{\eta - \frac{3}{2}\Gamma\eta^2 + \frac{3}{2}\Lambda\eta^3 - \frac{\tilde{U}_s}{\tilde{V}\tilde{K}}\left[\frac{\tilde{\gamma}}{3} + \left(\lambda - \tilde{\gamma}^2\left(1 - \frac{T\tilde{C}_v}{\tilde{U}_s}\right)\right)\eta\right]\right\}. \tag{3-2-16}$$

The constants are defined as

$$\Gamma_{\alpha\beta} = -\frac{1}{3\tilde{K}}\sum_\mu \tilde{\beta}_{\alpha\beta\mu} \qquad \Gamma = \frac{1}{9}\sum_{\alpha\beta}\Gamma_{\alpha\beta}$$

$$\Lambda_{\alpha\beta} = \frac{1}{9\tilde{K}}\sum_{\mu\nu}\tilde{\beta}_{\alpha\beta\mu\nu} \qquad \Lambda = \frac{1}{9}\sum_{\alpha\beta}\Lambda_{\alpha\beta}. \tag{3-2-17}$$

These constants are evaluated from data near $T = T_o$, $P = 0$. Thomsen gives six simultaneous equations for the unknowns $\tilde{V}$, $\tilde{K}$, $\tilde{\gamma}$, λ, Γ, Λ in terms of six experimental quantities V_o, K_o^S, α_o, $(\partial K^S/\partial T)_{P=0}$, $(\partial K^S/\partial P)_{T_o}$, $(\partial^2 K^S/\partial P^2)_{T_o}$. An additional four

simultaneous equations give the unknowns $\tilde{\delta}_{\alpha\beta}$, $\lambda_{\alpha\beta}$, $\Gamma_{\alpha\beta}$, $\Lambda_{\alpha\beta}$ in terms of the measured quantities $\delta_{\alpha\beta}$, $(\partial \delta_{\alpha\beta} / \partial T)_{P=0}$, $(\partial \delta_{\alpha\beta} / \partial P)_{T_o}$, and $(\partial^2 \delta_{\alpha\beta} / \partial P^2)_{T_o}$.

In the finite strain approach as outlined above, all the relevant data is used to determine the coefficients in the Taylor series expansion of the free energy and to determine the Grüneisen parameters. The crucial question in using this approach to extrapolate elastic constants is how rapidly does the above expansion converge? Questions such as how large is $1/3! \, \eta^3 \sum_{\mu\nu\delta} \delta_{\alpha\beta\mu\nu\delta}$ relative to the other terms in equation (3-2-13) must be faced.

In a geophysical context, this theory provides the most straightforward means of extrapolating the elastic constants and density for those materials for which the 16+ pieces of data discussed above are available, and is thus limited to discussions of the upper mantle. For those materials in the transition region (400-700 km) and below, it has not been experimentally possible to measure the elastic properties required for such a finite strain approach. For these transition region and lower-mantle minerals, a theory with some ability to make predictions is required — the atomistic approach based upon two-body interatomic potentials is such a theory. By replacing the input data required by the finite strain approach with a physically-motivated interatomic potential, the elastic properties of the lower mantle oxides and silicates may be discussed.

Atomistic Approach Based on Two-Body Interatomic Potentials

Instead of expanding the free energy as a Taylor series in the strains, it may be written as the sum of interactions between the atoms. If the functional form of the two-body potential between each pair of atoms in the solid is known, the free energy may be expressed in closed form. Thus the convergence problem facing the finite strain approach does not arise; it is replaced by the problem that the functional form of the interatomic potential is poorly known.

The problem of formulating a physically reasonable potential with the minimum number of empirical parameters will be deferred to the next chapter. In the remainder of this chapter the method of long waves will be reviewed in considerable detail as it yields expressions for the volume dependence of the effective elastic constants in terms of the interatomic potentials.

3-3. The Method of Long Waves

In the method of long waves one uses a perturbation expansion to solve the vibration equation of the lattice in the limit of long wavelengths. The elastic constants are then identified by comparing the resultant vibration equations with wave equations of macroscopic elasticity theory (3-1-20). The method was first developed by Born (1923) and Begbie and Born (1947). Although in their formulation the method is not applicable to ionic crystals, since they are, in general, piezoelectric, Huang (1949) used Ewald's theta-function transformation to separate out the macroscopic electric field associated with the elastic wave, and was thus able

to formulate the method of long waves in convergent form for ionic solids.

In this section Huang's formulation (also given in Born and Huang, 1962) will be developed. There is no original work except for the extension to the case of hydrostatic prestress, which turns out to be trivial. The objective is rather to lay the theoretical framework for the geophysical applications to follow.

Since this development so closely parallels that given in Born and Huang, it is convenient to change to their notation, thus saving the reader the rather bothersome task of effecting the change. We shall drop the distinction between natural and initial states; henceforth all coordinates will be referenced to the initial state and, following Born and Huang, the coordinates in this state will be donated by x_i rather than X_i. Further, $\underset{\sim}{u}$ will be used to denote displacements from the initial state rather than $\underset{\sim}{U}$, and $\underset{\sim}{a}_i$ will now be used to denote the lattice basis vectors. It should be emphasized that the initial state is an equilibrium state but not necessarily a stress-free state, and that the assumption that it be stress-free will not be made in the following development.

Following the notation in Born and Huang (1962) let:

$\ell(\ell^1, \ell^2, \ell^3)$	=	lattice cell index
n	=	number of particles in basis
$k(0...n-1)$	=	base index
$\underset{\sim}{a}_1, \underset{\sim}{a}_2, \underset{\sim}{a}_3$	=	lattice basis vectors
$\underset{\sim}{b}^1, \underset{\sim}{b}^2, \underset{\sim}{b}^3$	=	basis vectors of reciprocal lattice
m_k	=	mass of particle k in the basis

V_a = volume of the lattice cell

$\underset{\sim}{x}\left(\begin{smallmatrix}\ell\\k\end{smallmatrix}\right) = \underset{\sim}{x}(\ell) + \underset{\sim}{x}(k)$ = lattice point occupied by particle $\left(\begin{smallmatrix}\ell\\k\end{smallmatrix}\right)$ in the initial state

$\underset{\sim}{x}(\ell) = \ell^1 \underset{\sim}{a}_1 + \ell^2 \underset{\sim}{a}_2 + \ell^3 \underset{\sim}{a}_3$ = lattice vector

$\underset{\sim}{x}\left(\begin{smallmatrix}\ell\ell'\\kk'\end{smallmatrix}\right) = \underset{\sim}{x}\left(\begin{smallmatrix}\ell\\k\end{smallmatrix}\right) - \underset{\sim}{x}\left(\begin{smallmatrix}\ell'\\k'\end{smallmatrix}\right)$ = vector connecting particle $\left(\begin{smallmatrix}\ell'\\k'\end{smallmatrix}\right)$ to particle $\left(\begin{smallmatrix}\ell\\k\end{smallmatrix}\right)$

$\underset{\sim}{u}\left(\begin{smallmatrix}\ell\\k\end{smallmatrix}\right)$ = small displacement vector of $\left(\begin{smallmatrix}\ell\\k\end{smallmatrix}\right)$

Φ = lattice energy of entire lattice to be normalized later (see B & H, p.219).

Expanding the lattice energy in terms of ion displacements from the initial state

$$\Phi = \Phi_0 + \sum_{\alpha \ell k} \Phi_\alpha\left(\begin{smallmatrix}\ell\\k\end{smallmatrix}\right) u_\alpha\left(\begin{smallmatrix}\ell\\k\end{smallmatrix}\right) + \frac{1}{2} \sum_{\substack{\alpha\beta\\ \ell\ell'\\ kk'}} \Phi_{\alpha\beta}\left(\begin{smallmatrix}\ell\ell'\\kk'\end{smallmatrix}\right) u_\alpha\left(\begin{smallmatrix}\ell\\k\end{smallmatrix}\right) u_\beta\left(\begin{smallmatrix}\ell'\\k'\end{smallmatrix}\right) + \tag{3-3-1}$$

$$+ \frac{1}{6} \sum_{\substack{\alpha\beta\gamma\\ \ell\ell'\ell''\\ kk'k''}} \Phi_{\alpha\beta\gamma}\left(\begin{smallmatrix}\ell\ell'\ell''\\kk'k''\end{smallmatrix}\right) u_\alpha\left(\begin{smallmatrix}\ell\\k\end{smallmatrix}\right) u_\beta\left(\begin{smallmatrix}\ell'\\k'\end{smallmatrix}\right) u_\gamma\left(\begin{smallmatrix}\ell''\\k''\end{smallmatrix}\right) + \cdots .$$

The coefficients are given by

$$\Phi_\alpha\left(\begin{smallmatrix}\ell\\k\end{smallmatrix}\right) = \left(\frac{\partial \Phi}{\partial u_\alpha\left(\begin{smallmatrix}\ell\\k\end{smallmatrix}\right)}\right)_0 = \Phi_\alpha(k)$$

$$\Phi_{\alpha\beta}\left(\begin{smallmatrix}\ell\ell'\\kk'\end{smallmatrix}\right) = \left(\frac{\partial^2 \Phi}{\partial u_\alpha\left(\begin{smallmatrix}\ell\\k\end{smallmatrix}\right) \partial u_\beta\left(\begin{smallmatrix}\ell'\\k'\end{smallmatrix}\right)}\right) = \Phi_{\alpha\beta}\left(\begin{smallmatrix}\ell-\ell'\\kk'\end{smallmatrix}\right) \tag{3-3-2}$$

$$\Phi_{\alpha\beta\gamma}\left(\begin{smallmatrix}\ell\ell'\ell''\\kk'k''\end{smallmatrix}\right) = \left(\frac{\partial^3 \Phi}{\partial u_\alpha\left(\begin{smallmatrix}\ell\\k\end{smallmatrix}\right) \partial u_\beta\left(\begin{smallmatrix}\ell'\\k'\end{smallmatrix}\right) \partial u_\gamma\left(\begin{smallmatrix}\ell''\\k''\end{smallmatrix}\right)}\right) = \Phi_{\alpha\beta\gamma}\left(\begin{smallmatrix}\ell-\ell'\ \ell-\ell''\\kk'k''\end{smallmatrix}\right) .$$

The coefficients are written on the right-hand side in a notation which explicitly shows that the linear term is independent of ℓ, the quadratic term depends only on the relative coordinates $\ell - \ell'$ of the two particles, and so on.

Under the assumption that every particle is in its equilibrium position (which is distinct from the assumption that the configuration corresponds to vanishing stresses), the linear coefficients $\Phi_\alpha(k)$, are equal to zero. The potential energy of the system is then, to second-order, $\Phi = \frac{1}{2} \sum_{\substack{\alpha\beta \\ \ell\ell' \\ kk'}} \Phi_{\alpha\beta}\left(\begin{smallmatrix} \ell-\ell' \\ kk' \end{smallmatrix}\right) u_\alpha\left(\begin{smallmatrix} \ell \\ k \end{smallmatrix}\right) u_\beta\left(\begin{smallmatrix} \ell' \\ k' \end{smallmatrix}\right)$. The kinetic energy is $T = \sum_{\alpha k} \sum_{\ell} \frac{1}{2} m_k \left[\dot{u}_\alpha\left(\begin{smallmatrix} \ell \\ k \end{smallmatrix}\right)\right]^2$ where the dot indicates a time derivative. The Lagrangian for the system is

$$\mathcal{L} = T - V = \frac{1}{2} \sum_{\alpha k \ell} m_k \left[\dot{u}_\alpha\left(\begin{smallmatrix} \ell \\ k \end{smallmatrix}\right)\right]^2 - \frac{1}{2} \sum_{\substack{\alpha\beta \\ \ell\ell' \\ kk'}} \Phi_{\alpha\beta}\left(\begin{smallmatrix} \ell-\ell' \\ kk' \end{smallmatrix}\right) u_\alpha\left(\begin{smallmatrix} \ell \\ k \end{smallmatrix}\right) u_\beta\left(\begin{smallmatrix} \ell' \\ k' \end{smallmatrix}\right)$$

and Lagrange's equations of motion are

$$\frac{d}{dt}\left(\frac{\partial \mathcal{L}}{\partial \dot{u}_\alpha\left(\begin{smallmatrix} \ell \\ k \end{smallmatrix}\right)}\right) - \frac{\partial \mathcal{L}}{\partial u_\alpha\left(\begin{smallmatrix} \ell \\ k \end{smallmatrix}\right)} = 0 \qquad \alpha = 1, 2, 3$$

which for the crystal are

$$m_k \ddot{u}_\alpha\left(\begin{smallmatrix} \ell \\ k \end{smallmatrix}\right) + \sum_{\substack{\beta \ell' \\ k'}} \Phi_{\alpha\beta}\left(\begin{smallmatrix} \ell-\ell' \\ kk' \end{smallmatrix}\right) u_\beta\left(\begin{smallmatrix} \ell' \\ k' \end{smallmatrix}\right) = 0 \qquad \begin{matrix} \ell = 1, 2, 3, \ldots \\ \alpha = 1, 2, 3 \\ k = 0, n-1 \end{matrix} \quad . \tag{3-3-3}$$

Assume a plane wave solution to be a Bloch function of the form

$$u_\alpha\left(\begin{smallmatrix} \ell \\ k \end{smallmatrix}\right) = \frac{1}{\sqrt{m_k}} W_\alpha\left(k \,|\, \begin{smallmatrix} \gamma \\ j \end{smallmatrix}\right) e^{2\pi i \underline{\gamma} \cdot \underline{x}\left(\begin{smallmatrix} \ell \\ k \end{smallmatrix}\right) - i\omega t} \tag{3-3-4}$$

where $\underline{\gamma}$ is an arbitrary wave number vector and $j = 0, \ldots, 3n-1$ indexes the $3n$ solutions for a given $\underline{\gamma}$. For this assumed solution the equations of motion become

$$-\omega^2 W_\alpha(k) = -\sum_{l'k'\beta} \Phi_{\alpha\beta}\binom{l-l'}{kk'} \frac{1}{\sqrt{m_k m_{k'}}} e^{-2\pi i \underline{\chi}\cdot\underline{x}\binom{l-l'}{kk'}} W_\beta(k') \tag{3-3-5}$$

$$= \sum_{k'\beta} W_\beta(k') \frac{e^{-2\pi i \underline{\chi}\cdot(\underline{x}(k)-\underline{x}(k'))}}{\sqrt{m_k m_{k'}}} \sum_{l'} \Phi_{\alpha\beta}\binom{l-l'}{kk'} e^{-2\pi i \underline{\chi}\cdot(\underline{x}(l)-\underline{x}(l'))}$$

which can be written in the form

$$\omega^2 W_\alpha(k) = \sum_{k'\beta} C_{\alpha\beta}\binom{\chi}{kk'} W_\beta(k') \qquad k = 0, m-1 \qquad \alpha = 1,2,3 \tag{3-3-6}$$

where

$$C_{\alpha\beta}\binom{\chi}{kk'} = \frac{e^{-2\pi i \underline{\chi}\cdot[\underline{x}(k)-\underline{x}(k')]}}{\sqrt{m_k m_{k'}}} \sum_{l'} \Phi_{\alpha\beta}\binom{-l'}{kk'} e^{2\pi i \underline{\chi}\cdot\underline{x}(l')} . \tag{3-3-7}$$

Note that the original infinite number of equations of motion (3-3-3) have been reduced to the 3n equations (3-3-6). This was possible because $\Phi_{\alpha\beta}\binom{l-l'}{kk'}$ does not depend on both l and l', but only on the relative index $l - l'$. Hence in equation (3-3-7) it has been assumed, without loss of generality, that $l = 0$.

Following Huang (1949), let

$$\Phi_{\alpha\beta}\binom{-l'}{kk'} = \Phi^N_{\alpha\beta}\binom{-l'}{kk'} + \Phi^C_{\alpha\beta}\binom{-l'}{kk'} . \tag{3-3-8}$$

The second term is due solely to the coulombic interactions while the first term includes the rest. This separation allows the $C_{\alpha\beta}\binom{\chi}{kk'}$ to be separated into its coulombic and non-coulombic parts:

$$C^C_{\alpha\beta}\binom{\chi}{kk'} = \frac{e^{-2\pi i \underline{\chi}\cdot\underline{x}(k)}}{\sqrt{m_k m_{k'}}} \sum_{l'} \Phi^C_{\alpha\beta}\binom{-l'}{kk'} e^{2\pi i \underline{\chi}\cdot\underline{x}\binom{(l')}{(k')}} . \tag{3-3-9}$$

The lattice vibration equation (3-3-6) becomes

$$\omega^2 W_\alpha\left(k \middle| \begin{smallmatrix} \ell \\ j \end{smallmatrix}\right) = \sum_{k'\beta} C^N_{\alpha\beta}\left(\begin{smallmatrix} \ell \\ k k' \end{smallmatrix}\right) W_\beta\left(k' \middle| \begin{smallmatrix} \ell \\ j \end{smallmatrix}\right) + \tag{3-3-10}$$

$$+ \frac{1}{\sqrt{m_k}} \sum_\beta \Phi^C_{\alpha\beta}\left(\begin{smallmatrix} 0 \\ k k \end{smallmatrix}\right) \frac{1}{\sqrt{m_k}} W_\beta\left(k \middle| \begin{smallmatrix} \ell \\ j \end{smallmatrix}\right) +$$

$$+ \frac{e^{-2\pi i \underset{\sim}{\chi} \cdot \underset{\sim}{x}(k)}}{\sqrt{m_k}} \sum_\beta \sum_{\ell' k'}{}' \Phi^C_{\alpha\beta}\left(\begin{smallmatrix} -\ell' \\ k k' \end{smallmatrix}\right) \frac{1}{\sqrt{m_{k'}}} W_\beta\left(k' \middle| \begin{smallmatrix} \ell \\ j \end{smallmatrix}\right) e^{2\pi i \underset{\sim}{\chi} \cdot \underset{\sim}{x}\left(\begin{smallmatrix} \ell' \\ k' \end{smallmatrix}\right)} .$$

Note that the terms giving the coulombic restoring force on a particle due to its own displacement have been written separately in the second term. The prime on the summation in the third term indicates that the $\ell = 0$, $k = k'$ term has been omitted. This third term gives the coulombic force on particle $\left(\begin{smallmatrix} 0 \\ k \end{smallmatrix}\right)$ due to the displacements $\underset{\sim}{u}\left(\begin{smallmatrix} \ell' \\ k' \end{smallmatrix}\right)$ of all the other ions.

Written explicitly, the coulombic contribution to Φ is

$$\Phi^C = \tfrac{1}{2} \sum_{\ell k} \sum_{\substack{\ell' k' \\ \neq \ell k}} \frac{e_k e_{k'}}{\left| \underset{\sim}{x}\left(\begin{smallmatrix} \ell \\ k \end{smallmatrix}\right) + \underset{\sim}{u}\left(\begin{smallmatrix} \ell \\ k \end{smallmatrix}\right) - \underset{\sim}{x}\left(\begin{smallmatrix} \ell' \\ k' \end{smallmatrix}\right) - \underset{\sim}{u}\left(\begin{smallmatrix} \ell' \\ k' \end{smallmatrix}\right) \right|} . \tag{3-3-11}$$

For the case $\ell \neq 0$, $k \neq k'$, direct differentiation gives

$$\Phi^C_{\alpha\beta}\left(\begin{smallmatrix} \ell \\ k k' \end{smallmatrix}\right) = - e_k e_{k'} \left\{ \frac{\partial^2}{\partial x_\alpha \partial x_\beta} \frac{1}{|\underset{\sim}{x}|} \right\}_{\underset{\sim}{x} = \underset{\sim}{x}\left(\begin{smallmatrix} \ell \\ k k' \end{smallmatrix}\right)} . \tag{3-3-12}$$

For the case $\ell = 0$, $k = k'$, the coulombic field change experienced by ion k due to its displacement $\underset{\sim}{u}\left(\begin{smallmatrix} 0 \\ k \end{smallmatrix}\right)$ can be expressed as the change in the

coulombic field at $\binom{0}{k}$ due to a displacement $-\mathcal{U}\binom{0}{k}$ of all the other ions in the lattice.

$$\Phi_{\alpha\beta}\binom{0}{kk'} = e_k \sum_{\ell k'}{}' e_{k'} \left\{ \frac{\partial^2}{\partial X_\alpha \partial X_\beta} \frac{1}{|\underset{\sim}{X}|} \right\}_{\underset{\sim}{X} = \underset{\sim}{X}\binom{\ell}{kk'}} \tag{3-3-13}$$

Substituting equations (3-3-12) and (3-3-13) into the lattice vibration equation (3-3-10) gives:

$$\omega^2\binom{\chi}{j} W_\alpha(k|\tfrac{\chi}{j}) = \sum_{k'\beta} C^N_{\alpha\beta}\binom{\chi}{kk'} W_\beta(k'|\tfrac{\chi}{j}) +$$

$$+ \frac{e_k}{\sqrt{m_k}} \sum_\beta W_\beta(k|\tfrac{\chi}{j}) \sum_{\ell' k'}{}' \frac{e'_{k'}}{\sqrt{m_{k'}}} \left\{ \frac{\partial^2}{\partial X_\alpha \partial X_\beta} \frac{1}{|\underset{\sim}{X}(\ell'_{k'}) - \underset{\sim}{X}|} \right\}_{\underset{\sim}{X} = \underset{\sim}{X}(k)} - \tag{3-3-14}$$

$$- \frac{e_k e^{-2\pi i \underset{\sim}{\chi}\cdot\underset{\sim}{X}(k)}}{\sqrt{m_k}} \sum_\beta \sum_{\ell' k'}{}' \frac{e_{k'}}{\sqrt{m_{k'}}} W_\beta(k'|\tfrac{\chi}{j}) e^{2\pi i \underset{\sim}{\chi}\cdot\underset{\sim}{X}(\ell'_{k'})} \left\{ \frac{\partial^2}{\partial X_\alpha \partial X_\beta} \frac{1}{|\underset{\sim}{X}(\ell'_{k'}) - \underset{\sim}{X}|} \right\}.$$

A straightforward application of the method of long waves is not possible at this point because certain terms in the wave-number expansion are divergent. The physical problem is that ionic crystals are in general piezoelectric; one must specify both the strain and the macroscopic electric field before one has completely specified the forces acting on the particles. Huang (1949) resolved this problem by recognizing the analogy between (3-3-14) and the electric field in a dipole lattice, and then using Ewald's theta-function transformation to separate the macroscopic electric field from the effective coulombic field.

Analogy Between Vibration Equation and the Electric Field in a Dipole Lattice

It is interesting at this point to note that the second two terms in equation (3-3-14) have the exact form of the electric field in a dipole lattice. The field at a point $\underset{\sim}{x}$ due to a dipole $\underset{\sim}{p}(\ell)$ at $x(\ell)$ is given by (far-field approximation)

$$\underset{\sim}{\mathcal{E}}(\underset{\sim}{x}) = \nabla V = \nabla \left[\underset{\sim}{p}(\ell) \cdot \nabla \left(\frac{1}{\underset{\sim}{x}(\ell) - \underset{\sim}{x}} \right) \right] \tag{3-3-15}$$

in component form

$$\mathcal{E}_\alpha(\underset{\sim}{x}) = \sum_\beta p_\beta(\ell) \frac{\partial^2}{\partial x_\alpha \partial x_\beta} \left\{ \frac{1}{\underset{\sim}{x}(\ell) - \underset{\sim}{x}} \right\}. \tag{3-3-16}$$

In a Bravais lattice of such dipoles

$$\underset{\sim}{p}(\ell) = \underset{\sim}{p} e^{2\pi i \underset{\sim}{\chi} \cdot \underset{\sim}{x}(\ell)} \tag{3-3-17}$$

the field at $\underset{\sim}{x}$ is given by

$$\mathcal{E}_\alpha(\underset{\sim}{x}) = \sum_\beta p_\beta \frac{\partial^2}{\partial x_\alpha \partial x_\beta} \sum_\ell \frac{e^{2\pi i \underset{\sim}{\chi} \cdot \underset{\sim}{x}(\ell)}}{|\underset{\sim}{x}(\ell) - \underset{\sim}{x}|}. \tag{3-3-18}$$

Returning to equation (3-3-14), we see that the last term is just the field at $\underset{\sim}{x}\binom{0}{k}$ created by the displacements

$$u_\beta\binom{\ell'}{k'} = \frac{1}{\sqrt{m_{k'}}} W_\beta(k' | \underset{j}{\chi}) e^{2\pi i \underset{\sim}{\chi} \cdot \underset{\sim}{x}\binom{\ell'}{k'}} \tag{3-3-19}$$

which is seen, by comparison with (3-3-18), to be equivalent to the field at $\underset{\sim}{x}(k)$ due to a lattice of dipoles

$$p_\beta\binom{\ell'}{k'} = \frac{e_{k'}}{\sqrt{m_{k'}}} W_\beta(k' | \underset{j}{\chi}) \tag{3-3-20}$$

when the dipole at $\underline{x}(k)$ is excluded. Ewald (1921) called this the "exciting field". The second term in equation (3-3-14) is the exciting field at $\binom{0}{k}$ due to displacements $\underline{u}\binom{0}{k'} = -\underline{u}\binom{0}{k}$, which is equivalent to the exciting field in a lattice of dipoles

$$p_\beta\binom{l'}{k'} = \frac{e_{k'}}{\sqrt{m_{k'}}} W_\beta\left(k' \middle| \begin{matrix} \neq \\ j \end{matrix}\right). \tag{3-3-21}$$

Hence, as pointed out by Huang (1949) and Born and Huang (1962), the key to the solution of the vibration equation (3-3-14) is the formulation of the exciting field in the dipole lattice.

Ewald's Theta-Function Transformation

The use of Ewald's theta-function transformation in equation (3-3-14) accomplishes two purposes. First, it allows a separation from the vibration equation of a term corresponding to the macroscopic electric field. Second, it allows the coulombic sums to be written in more quickly convergent form.

Using the integral representation of $1/|\underline{x}(l) - \underline{x}|$

$$\frac{1}{|\underline{x}(l)-\underline{x}|} = \frac{2}{\sqrt{\pi}} \int_0^\infty e^{-|\underline{x}(l)-\underline{x}|^2\rho^2}\, d\rho \tag{3-3-22}$$

in equation (3-3-18) we obtain

$$\varepsilon_\alpha(\underline{x}) = \sum_\beta p_\beta \frac{\partial^2}{\partial x_\alpha \partial x_\beta} \int_0^\infty \left\{ \frac{2}{\sqrt{\pi}} \sum_l e^{-|\underline{x}(l)-\underline{x}|^2\rho^2 + 2\pi i \underline{\nu}\cdot(\underline{x}(l)-\underline{x})} \right\} e^{-2\pi i \underline{\nu}\cdot\underline{x}}\, d\rho. \tag{3-3-23}$$

Since the expression in the curly brackets is a periodic function of x with the periodicity of the lattice, it may be represented by a Fourier series with components

$$g(h_1h_2h_3) = \frac{1}{V_a} \int_{\substack{\text{zero}\\ \text{cell}}} \sum_{\ell} \left\{ \frac{2}{\sqrt{\pi}} e^{-|\underline{x}(\ell)-\underline{x}|^2\rho^2 + 2\pi i\, \underline{y}\cdot(\underline{x}(\ell)-\underline{x})} \right\} \cdot \tag{3-3-24}$$

$$\cdot\, e^{2\pi i\, \underline{y}(h)\cdot\underline{x}}\, d\underline{x}.$$

Interchange summation and integration; let $\underline{x}' = \underline{x} - \underline{x}(\ell)$ be the integration variable for a given ℓ.

$$g(h_1h_2h_3) = \frac{1}{V_a} \sum_{\ell} \int_{\substack{-\ell\\ \text{cell}}} \left\{ \frac{2}{\sqrt{\pi}} e^{-|\underline{x}'|^2\rho^2 - 2\pi i(\underline{y}(h)+\underline{y})\cdot\underline{x}'} \right\} dx' \cdot \tag{3-3-25}$$

$$\cdot\, e^{-2\pi i\, \underline{y}(h)\cdot\underline{x}(\ell)}.$$

Since the sum is equivalent to an integration over all space and since $e^{-2\pi i \underline{y}(h)\cdot x(\ell)} = 1$ we have

$$g(h_1h_2h_3) = \frac{1}{V_a} \int_{\substack{\text{All}\\ \text{space}}} \left\{ \frac{2}{\sqrt{\pi}} e^{-|\underline{x}|^2\rho^2 - 2\pi i(\underline{y}(h)+\underline{y})\cdot\underline{x}} \right\} dx \tag{3-3-26}$$

$$= \frac{2\pi}{V_a} \frac{1}{\rho^3} e^{-\frac{\pi^2}{\rho^2}|\underline{y}(h)+\underline{y}|^2}.$$

The Fourier expansion of the curly bracket in (3-3-23) can thus be written explicitly as

$$\frac{2}{\sqrt{\pi}} \sum_{\ell} e^{-|\underline{x}(\ell)-\underline{x}|^2\rho^2 + 2\pi i\, \underline{y}\cdot(\underline{x}(\ell)-\underline{x})} = \sum_{h} g(h_1h_2h_3)\, e^{2\pi i\, \underline{y}(h)\cdot\underline{x}} = \tag{3-3-27}$$

$$= \frac{2\pi}{V_a} \sum_{h} \frac{1}{\rho^3} e^{-\frac{\pi^2}{\rho^2}|\underline{y}(h)+\underline{y}|^2 + 2\pi i\, \underline{y}(h)\cdot\underline{x}}.$$

This is known as the theta-function transformation. Since the left-hand side is rapidly convergent for large values of ρ while the right-hand

side is rapidly convergent for small ρ, by dividing the integral in (3-3-23) into two parts and using the appropriate side of (3-3-27) in each we get

$$\mathcal{E}_\alpha(x) = \sum_\beta \rho_\beta \frac{\partial^2}{\partial x_\alpha \partial x_\beta}\left\{ \frac{2}{\sqrt{\pi}} \sum_\ell \int_R^\infty e^{-|\underline{x}(\ell)-\underline{x}|^2\rho^2 + 2\pi i \underline{y}\cdot(\underline{x}(\ell)-\underline{x})} d\rho + \right. \tag{3-3-28}$$

$$\left. + \frac{2\pi}{V_a} \sum_h \int_0^R \frac{1}{\rho^3} e^{-\pi^2/\rho^2 |\underline{y}(h)+\underline{y}|^2 + 2\pi i (\underline{y}(h)+\underline{y})\cdot \underline{x}} d\rho \right\}.$$

To simplify notation let

$$G(x) = \frac{e^{-x}}{x} \quad , \qquad H(x) = \frac{2}{\sqrt{\pi}} \frac{1}{x} \int_x^\infty e^{-x^2} dx \, . \tag{3-3-29}$$

The second term may be integrated directly, and the h = 0 term written separately to give

$$\mathcal{E}_\alpha(x) = \sum_\beta \rho_\beta \frac{\partial^2}{\partial x_\alpha \partial x_\beta} \left\{ \frac{1}{\pi V_a |\underline{y}|^2} e^{-\pi^2 |\underline{y}|^2/R^2 + 2\pi i \underline{y}\cdot\underline{x}} + \right.$$

$$+ R \sum_\ell H(R|x(\ell)-x|) e^{2\pi i \underline{y}\cdot\underline{x}(\ell)} + \tag{3-3-30}$$

$$\left. + \frac{\pi}{V_a} \frac{1}{R^2} \sum_h{}' G(\pi^2 |\underline{y}(h)+\underline{y}|^2/R^2) e^{2\pi i (\underline{y}(h)+\underline{y})\cdot\underline{x}} \right\}.$$

Carrying out the differentiation gives:

$$\mathcal{E}_\alpha(\underline{x}) = \sum_\beta p_\beta \Big\{ -\frac{4\pi}{V_a}\frac{y_\alpha y_\beta}{|\underline{y}|^2} e^{-\pi^2|\underline{y}|^2/R^2 + 2\pi i \underline{y}\cdot\underline{x}} + \\ + R^3 \sum_\ell H_{\alpha\beta}(R|\underline{x}(\ell)-\underline{x}|)\, e^{2\pi i \underline{y}\cdot\underline{x}(\ell)} - \\ - \frac{4\pi^3}{R^2 V_a} \sum_h{}' (y_\alpha(h)+y_\alpha)(y_\beta(h)+y_\beta)\, G(\pi^2|\underline{y}(h)+\underline{y}|^2/R^2) \cdot \\ \cdot e^{2\pi i(\underline{y}(h)+\underline{y})\cdot\underline{x}} \Big\} \qquad (3\text{-}3\text{-}31)$$

where

$$H_{\alpha\beta}(\underline{x}) = \frac{\partial^2}{\partial x_\alpha \partial x_\beta} H(|\underline{x}|) \qquad (3\text{-}3\text{-}32)$$

The next step is the key to the treatment of ionic lattices -- the separation of the macroscopic electrostatic field. For the lattice of dipoles under consideration, the macroscopic polarization (dipole moment per unit volume) is (in the limit of small $\underline{y}$)

$$\underset{\sim}{P}(\underline{x}) = \frac{\underline{p}}{V_a} e^{2\pi i \underline{y}\cdot\underline{x}} \qquad (3\text{-}3\text{-}33)$$

The corresponding macroscopic electric field can be found using

$$\nabla\cdot(\underline{E}(\underline{x}) + 4\pi \underline{P}(x)) = 0$$

to be

$$\underline{E}(\underline{x}) = \underline{E}\, e^{2\pi i \underline{y}\cdot\underline{x}}$$

where (3-3-34)

$$E_\alpha = -\frac{4\pi}{V_a}\left(\frac{y_\alpha}{|\underline{y}|}\right)\left(\frac{\underline{y}\cdot\underline{p}}{|\underline{y}|}\right) e^{2\pi i \underline{y}\cdot\underline{x}}$$

(See Born and Huang (1962) p. 249.)

Note that part of the first term in equation (3-3-31) can be identified as the macroscopic field if the term is rewritten as follows

$$\sum_\beta p_\beta \left\{ -\frac{4\pi}{V_a} \frac{y_\alpha y_\beta}{|\underline{y}|^2} e^{-\frac{\pi^2|\underline{y}|^2}{R^2} + 2\pi i \underline{y}\cdot\underline{x}} \right\} = \tag{3-3-35}$$

$$-\frac{4\pi}{V_a}\frac{y_\alpha}{|\underline{y}|}\left(\frac{\underline{y}\cdot\underline{p}}{|\underline{y}|}\right) e^{2\pi i \underline{y}\cdot\underline{x}} + \frac{4\pi}{V_a}\sum_\beta \frac{y_\alpha y_\beta p_\beta}{|\underline{y}|^2}\left\{ 1 - e^{-\pi^2|\underline{y}|^2/R^2} \right\} e^{2\pi i \underline{y}\cdot\underline{x}} .$$

Thus the coulombic field in the dipole lattice can be written in a form which explicitly contains the macroscopic field

$$\mathcal{E}_\alpha(\underline{x}) = E_\alpha(\underline{x}) + \sum_\beta p_\beta \left\{ \frac{4\pi}{V_a}\frac{y_\alpha y_\beta}{|\underline{y}|^2}\left[1 - e^{-\pi^2|\underline{y}|^2/R^2} \right] e^{2\pi i \underline{y}\cdot\underline{x}} \right.$$

$$+ R^3 \sum_l H_{\alpha\beta}(R|\underline{x}(l) - \underline{x}|)\, e^{2\pi i \underline{y}\cdot\underline{x}(l)} - \tag{3-3-36}$$

$$\left. - \frac{4\pi^3}{R^2 V_a} \sum_h{}' (y_\alpha(h) + y_\alpha)(y_\beta(h) + y_\beta)\, G(\pi^2|\underline{y}(h) + \underline{y}|^2/R^2)\, e^{2\pi i (\underline{y}(h) + \underline{y})\cdot\underline{x}} \right\} .$$

Note that for small y, the leading term in (3-3-31) goes as $y_\alpha y_\beta / |\underline{y}|^2$ and has no unique limit. After the separation of the macroscopic field, this term becomes $(y_\alpha y_\beta / |\underline{y}|^2)(1 - e^{-\pi^2|\underline{y}|^2/R^2})$, the leading term of which goes as $y_\alpha y_\beta$ as $y \to 0$. In the case of a composite lattice

$$\underline{p}\left(\begin{matrix} l' \\ k' \end{matrix}\right) = \underline{p}(k')\, e^{2\pi i \underline{y}\cdot\underline{x}\left(\begin{matrix} l' \\ k' \end{matrix}\right)}$$

$$E_\alpha = \left[-\frac{4\pi}{V_a}\left(\frac{y_\alpha}{|\underline{y}|}\right)\left(\frac{\underline{y}}{|\underline{y}|}\cdot\sum_{k'} \underline{p}(k')\right)\right] e^{2\pi i \underline{y}\cdot\underline{x}} \tag{3-3-37}$$

and equation (3-3-36) becomes:

$$\mathcal{E}_\alpha(\underline{x}) = E_\alpha + \sum_{k'}\sum_{\beta} p_\beta(k')\left\{\frac{4\pi}{V_a}\frac{\gamma_\alpha\gamma_\beta}{|\underline{\gamma}|^2}\left[1-e^{-\pi^2|\underline{\gamma}|^2/R^2}\right]e^{2\pi i\underline{\gamma}\cdot\underline{x}} + \right.$$

$$+ R^3\sum_{\ell'} H_{\alpha\beta}\left(R\,|\underline{x}(^{\ell'}_{k'})-\underline{x}|\right)\, e^{2\pi i\underline{\gamma}\cdot\underline{x}(^{\ell'}_{k'})} - \qquad (3\text{-}3\text{-}38)$$

$$\left. - \frac{4\pi^3}{V_a}\frac{e^{2\pi i\underline{\gamma}\cdot\underline{x}}}{R^2}\sum_{h}{}'(\gamma_\alpha(h)+\gamma_\alpha)(\gamma_\beta(h)+\gamma_\beta)G(\pi^2|\underline{\gamma}(h)+\underline{\gamma}|^2/R^2)\cdot \right.$$

$$\left. \cdot\, e^{2\pi i\underline{\gamma}(h)\cdot(\underline{x}-\underline{x}(^{\ell'}_{k'}))}\right\}.$$

In order to solve the vibration equation (3-3-14), we must evaluate the exciting field at a lattice point: i.e., we must evaluate $\mathcal{E}_\alpha(\underline{x})$ at a lattice site with the dipole at that site removed. The field due to the dipole at (^0_k) is

$$\sum_\beta p_\beta(k)\, e^{2\pi i\underline{\gamma}\cdot\underline{x}(^0_k)}\ \frac{\partial^2}{\partial x_\alpha \partial x_\beta}\ \frac{1}{|\underline{x}(^0_k)-\underline{x}|}\,. \qquad (3\text{-}3\text{-}39)$$

Subtracting this from the $\ell' = 0$, $k = k'$ contribution to the second term of equation (3-3-38) (see also equation (3-3-30)) gives

$$\sum_\beta p_\beta(k)\, e^{2\pi i\underline{\gamma}\cdot\underline{x}(^0_k)}\ \frac{\partial^2}{\partial x_\alpha \partial x_\beta}\left\{RH\left(R|\underline{x}(^0_k)-\underline{x}|\right) - \frac{1}{|\underline{x}(^0_k)-\underline{x}|}\right\}. \qquad (3\text{-}3\text{-}40)$$

Using the integral representation (3-3-22) for $1/|\underline{x}(k) - \underline{x}|$, this may be written:

$$\sum_\beta p_\beta(k)\, e^{2\pi i\underline{\gamma}\cdot\underline{x}(^0_k)}\ \frac{\partial^2}{\partial x_\alpha \partial x_\beta}\left\{\frac{-1}{|\underline{x}(^0_k)-\underline{x}|}\,\frac{2}{\sqrt{\pi}}\int_0^{R|\underline{x}(^0_k)-\underline{x}|} e^{-x^2}\,dx\right\}. \qquad (3\text{-}3\text{-}41)$$

Defining

$$H^{\circ}(x) = \frac{-2}{x\sqrt{\pi}} \int_0^x e^{-x^2} dx \qquad (3\text{-}3\text{-}42)$$

the effect of subtracting the contribution of the dipole at $\binom{0}{k}$ is the replacement of $H_{\alpha\beta}(\underline{x})$ with $H^0_{\alpha\beta}(\underline{x})$ in the $\ell = 0$, $k = k'$ term of equation (3-3-38). Following Born and Huang (1962) we write this exciting field at $\binom{0}{k}$ in the form

$$\mathcal{E}'_{\alpha}(\underline{x}(k)) = E_{\alpha} e^{2\pi i \underline{\gamma} \cdot \underline{x}(k)} + e^{2\pi i \underline{\gamma} \cdot \underline{x}(k)} \sum_{k'\beta} Q_{\alpha\beta}\binom{\gamma}{kk'} \rho_{\beta}(k') \qquad (3\text{-}3\text{-}43)$$

where

$$Q_{\alpha\beta}\binom{\gamma}{kk'} = \frac{4\pi}{V_a} \frac{\gamma_\alpha \gamma_\beta}{|\gamma|^2} \left[1 - e^{-\pi^2 |\gamma|^2 / R^2}\right] +$$

$$+ R^3 \sum_{\ell'} H_{\alpha\beta}\left(R x\binom{\ell'}{kk'}\right) e^{2\pi i \underline{\gamma} \cdot \underline{x}\binom{\ell'}{k'k}} - \qquad (3\text{-}3\text{-}44)$$

$$- \frac{4\pi^3}{R^2 V_a} \sum_{h}{}' \left(\gamma_\alpha(h) + \gamma_\alpha\right)\left(\gamma_\beta(h) + \gamma_\beta\right) G\left(\pi^2 |\underline{\gamma}(h) + \underline{\gamma}|^2 / R^2\right) \cdot$$

$$\cdot e^{2\pi i \underline{\gamma}(h) \cdot (\underline{x}(k) - \underline{x}(k'))} .$$

In the second term $H^0_{\alpha\beta}$ has to be substituted for $H_{\alpha\beta}$ for the term $\ell = 0$, $k = k'$. Equations (3-3-43) and (3-3-44) are valid for all vaules of $\underline{\gamma}$; however, only for $\underline{\gamma}$ small does the E_α term have its macroscopic significance.

Hence, we now have the required expression for the "exciting field" in a dipole lattice which can be used to solve the vibrational

equation(3-3-14). Upon using equation (3-3-43) in equation (3-3-14) one gets

$$\omega^2\left(\frac{\chi}{j}\right) W_\alpha(k|\frac{\chi}{j}) = \sum_{k'\beta} C^N_{\alpha\beta}\left(\frac{\chi}{kk'}\right) W_\beta(k'|\frac{\chi}{j}) +$$

$$+ \sum_{k'\beta} \frac{e_k e_{k'}}{m_k} Q_{\alpha\beta}\left(\frac{0}{kk'}\right) W_\beta(k|\frac{\chi}{j}) - \frac{e_k}{\sqrt{m_k}} E_\alpha - \qquad (3\text{-}3\text{-}45)$$

$$- \sum_{k'\beta} \frac{e_k e_{k'}}{\sqrt{m_k m_{k'}}} Q_{\alpha\beta}\left(\frac{\chi}{kk'}\right) W_\beta(k'|\frac{\chi}{j})$$

where (3-3-46)

$$E_\alpha = -\frac{4\pi}{V_a}\left(\frac{\chi_\alpha}{|\chi|}\right) \sum_\beta \left(\frac{\chi_\beta}{|\chi|}\right) \sum_{k'} \frac{e_{k'}}{\sqrt{m_{k'}}} W_\beta(k'|\frac{\chi}{j}) .$$

If this equation is written in the form

$$\omega^2\left(\frac{\chi}{j}\right) W_\alpha(k|\frac{\chi}{j}) = \sum_{k'\beta} C_{\alpha\beta}\left(\frac{\chi}{kk'}\right) W_\beta(k'|\frac{\chi}{j}) \qquad (3\text{-}3\text{-}47)$$

we can identify

$$C_{\alpha\beta}\left(\frac{\chi}{kk'}\right) = C^N_{\alpha\beta}\left(\frac{\chi}{kk'}\right) + \frac{4\pi}{V_a}\left(\frac{\chi_\alpha \chi_\beta}{|\chi|^2}\right) \frac{e_k e_{k'}}{\sqrt{m_k m_{k'}}}$$

$$+ \delta_{kk'} \frac{e_k}{m_k} \sum_{k''} e_{k''} Q_{\alpha\beta}\left(\frac{0}{kk''}\right) - \frac{e_k e_{k'}}{\sqrt{m_k m_{k'}}} Q_{\alpha\beta}\left(\frac{\chi}{kk'}\right) \qquad (3\text{-}3\text{-}48)$$

In the method of long-waves $C_{\alpha\beta}\left(\frac{\chi}{kk'}\right)$ is expanded in powers of $\underline{\chi}$. However, because of the $(\chi_\alpha \chi_\beta / \underline{\chi}^2)$ in the second term, the zero-order term in the expansion cannot be assumed to be independent of $\underline{\chi}$. We therefore leave this term explicitly in the wave equation, redefining $\overline{C}_{\alpha\beta}\left(\frac{\chi}{kk'}\right)$ as:

$$\bar{C}_{\alpha\beta}\left(\begin{smallmatrix}\underline{y}\\ kk'\end{smallmatrix}\right) = C^{N}_{\alpha\beta}\left(\begin{smallmatrix}\underline{y}\\ kk'\end{smallmatrix}\right) + \delta_{kk'}\frac{e_k}{m_k}\sum_{k''} e_{k''} Q_{\alpha\beta}\left(\begin{smallmatrix}0\\ kk''\end{smallmatrix}\right) - \frac{e_k e_{k'}}{\sqrt{m_k m_{k'}}} Q_{\alpha\beta}\left(\begin{smallmatrix}\underline{y}\\ kk'\end{smallmatrix}\right) \qquad (3\text{-}3\text{-}49)$$

The vibration equation (3-3-45) becomes:

$$\omega^2\left(\begin{smallmatrix}\underline{y}\\ j\end{smallmatrix}\right) W_\alpha\left(k\,|\,\begin{smallmatrix}\underline{y}\\ j\end{smallmatrix}\right) = \sum_{k'\beta} \bar{C}_{\alpha\beta}\left(\begin{smallmatrix}\underline{y}\\ kk'\end{smallmatrix}\right) W_\beta\left(k'\,|\,\begin{smallmatrix}\underline{y}\\ j\end{smallmatrix}\right) - \frac{e_k}{\sqrt{m_k}} E_\alpha \qquad (3\text{-}3\text{-}50)$$

Long Wave Expansion

In equation (3-3-49), replace $\underline{y}$ with $\epsilon\underline{y}$ and expand with respect to ϵ to get

$$\bar{C}_{\alpha\beta}\left(\begin{smallmatrix}\underline{y}\\ kk'\end{smallmatrix}\right) = \bar{C}^{(0)}_{\alpha\beta}(kk') + i\epsilon\sum_{\gamma}\bar{C}^{(1)}_{\alpha\beta\gamma}(kk')\,y_\gamma + \frac{1}{2}\epsilon^2\sum_{\gamma\lambda}\bar{C}^{(2)}_{\alpha\beta\gamma\lambda}(kk')\cdot \qquad (3\text{-}3\text{-}51)$$
$$\cdot\, y_\gamma y_\lambda + \cdots$$

where the coefficients are given by

$$\bar{C}^{(1)}_{\alpha\beta\gamma}(kk') = \left(\frac{\partial\bar{C}_{\alpha\beta}}{\partial\epsilon y_\gamma}\right)_{\underline{y}=0}, \qquad \bar{C}^{(2)}_{\alpha\beta\gamma\lambda} = \left(\frac{\partial^2\bar{C}_{\alpha\beta}}{\partial\epsilon y_\gamma\,\partial\epsilon y_\lambda}\right)_{\underline{y}=0}.$$

Differentiation of (3-3-49) and (3-3-44) gives the expansion coefficients

$$\bar{C}^{(0)}_{\alpha\beta}(kk') = \frac{1}{\sqrt{m_k m_{k'}}}\sum_{l}\Phi^{N}_{\alpha\beta}\left(\begin{smallmatrix}l\\ kk'\end{smallmatrix}\right) + \delta_{kk'}\frac{e_k}{m_k}\Big\{R^3\sum_{l''k''} e_{k''} H_{\alpha\beta}\left(R\,X\left(\begin{smallmatrix}l''\\ k''k\end{smallmatrix}\right)\right) -$$
$$- \frac{4\pi^3}{R^2 V_a}\sum_{k''} e_{k''}\sum_{h}{}' y_\alpha(h) y_\beta(h)\, G(\pi^2|\underline{y}(h)|^2/R^2)\; e^{2\pi i\,\underline{y}(h)\cdot(\underline{x}(k)-\underline{x}(k''))} \qquad (3\text{-}3\text{-}52)$$
$$- \frac{e_k e_{k'}}{\sqrt{m_k m_{k'}}}\Big\{R^3\sum_{l} H_{\alpha\beta}\left(R\,X\left(\begin{smallmatrix}l\\ kk'\end{smallmatrix}\right)\right) - \frac{4\pi^3}{R^2 V_a}\sum_{h}{}' y_\alpha(h)\, y_\beta(h)\, G(\pi^2|\underline{y}(h)|^2/R^2)\cdot$$
$$\cdot\, e^{2\pi i\,\underline{y}(h)\cdot(\underline{x}(k)-\underline{x}(k'))}\Big\}$$

$$\bar{C}^{(1)}_{\alpha\beta\gamma}(kk') = \frac{-2\pi}{\sqrt{m_k m_{k'}}} \sum_{l} \Phi^{N}_{\alpha\beta}\left(\begin{smallmatrix} l \\ kk' \end{smallmatrix}\right) X_\gamma\left(\begin{smallmatrix} l \\ kk' \end{smallmatrix}\right) -$$

$$- \frac{2\pi e_k e_{k'} R^3}{\sqrt{m_k m_{k'}}} \sum_{l'} H_{\alpha\beta}\left(R\,\underline{x}\left(\begin{smallmatrix} l' \\ k'k \end{smallmatrix}\right)\right) X_\gamma\left(\begin{smallmatrix} l' \\ k'k \end{smallmatrix}\right) - \qquad (3\text{-}3\text{-}53)$$

$$- \frac{4\pi^3 i e_k e_{k'}}{R^2 V_a \sqrt{m_k m_{k'}}} \sum_{h}{}' \left\{ \left(y_\alpha(h)\delta_{\beta\gamma} + y_\beta(h)\delta_{\alpha\gamma}\right) G(\pi^2 |\underline{y}(h)|^2/R^2) + \right.$$

$$\left. + \frac{2\pi^2}{R^2} y_\alpha(h) y_\beta(h) y_\gamma(h)\, G'(\pi^2 |\underline{y}(h)|^2/R^2) \right\} \cdot$$

$$\cdot e^{2\pi i \underline{y}(h)\cdot[\underline{x}(k) - \underline{x}(k')]}$$

$$\bar{C}^{2}_{\alpha\beta\gamma\lambda}(kk') = \frac{-4\pi^2}{\sqrt{m_k m_{k'}}} \sum_{l} \Phi^{N}_{\alpha\beta}\left(\begin{smallmatrix} l \\ kk' \end{smallmatrix}\right) X_\gamma\left(\begin{smallmatrix} l \\ kk' \end{smallmatrix}\right) X_\lambda\left(\begin{smallmatrix} l \\ kk' \end{smallmatrix}\right) -$$

$$- \frac{4\pi^3 e_k e_{k'}}{R^2 V_a \sqrt{m_k m_{k'}}} (\delta_{\alpha\gamma}\delta_{\beta\lambda} + \delta_{\alpha\lambda}\delta_{\beta\gamma}) +$$

$$+ \frac{4\pi^2 R^3 e_k e_{k'}}{\sqrt{m_k m_{k'}}} \sum_{l'} H_{\alpha\beta}\left(R\,\underline{x}\left(\begin{smallmatrix} l' \\ k'k \end{smallmatrix}\right)\right) X_\gamma\left(\begin{smallmatrix} l' \\ k'k \end{smallmatrix}\right) X_\lambda\left(\begin{smallmatrix} l' \\ k'k \end{smallmatrix}\right) + \qquad (3\text{-}3\text{-}54)$$

$$+ \frac{4\pi^3 e_k e_{k'}}{R^2 V_a \sqrt{m_k m_{k'}}} \sum_{h}{}' \left\{ (\delta_{\alpha\gamma}\delta_{\beta\lambda} + \delta_{\alpha\lambda}\delta_{\beta\gamma}) G(\pi^2 |\underline{y}(h)|^2/R^2) + \right.$$

$$+ \frac{4\pi^4}{R^4} y_\alpha(h) y_\beta(h) y_\gamma(h) y_\lambda(h)\, G''(\pi^2 |\underline{y}(h)|^2/R^2) +$$

$$+ \frac{2\pi^2}{R^2} \left\{ y_\alpha(h) y_\beta(h)\delta_{\gamma\lambda} + y_\alpha(h) y_\gamma(h)\delta_{\beta\lambda} + y_\alpha(h) y_\lambda(h)\delta_{\beta\gamma} + \right.$$

$$\left. \left. + y_\beta(h) y_\gamma(h)\delta_{\alpha\lambda} + y_\beta(h) y_\lambda(h)\delta_{\alpha\gamma} \right\} G'(\pi^2 |\underline{y}(h)|^2/R^2) \right\} \cdot$$

$$\cdot e^{2\pi i \underline{y}(h)\cdot(\underline{x}(k) - \underline{x}(k'))} \cdot$$

Note that the second order coefficient $\overline{C}^{(2)}_{\alpha\beta\gamma\lambda}(kk')$ given by (3-3-54) does not agree with the corresponding equation (31.23) in Born and Huang (1962). The difference is that Born and Huang's coefficient contains an extra factor of the form $y_\gamma(h)\, y_\lambda(h)\, \delta_{\alpha\beta}$ in the G' term which should not be there.

The following properties of the expansion coefficients will be useful in solving the vibrational equations. They are proved in Born and Huang (1962) §26.

$$\overline{C}^{(0)}_{\alpha\beta}(kk') = \overline{C}^{(0)}_{\beta\alpha}(k'k) \tag{3-3-55}$$

$$\overline{C}^{(1)}_{\alpha\beta\gamma}(kk') = -\overline{C}^{(1)}_{\beta\alpha\gamma}(k'k) \tag{3-3-56}$$

$$\overline{C}^{(2)}_{\alpha\beta\gamma\lambda}(kk') = \overline{C}^{(2)}_{\alpha\beta\lambda\gamma}(kk') = \overline{C}^{(2)}_{\beta\alpha\gamma\lambda}(kk') \tag{3-3-57}$$

$$\sum_{k'} \sqrt{m_{k'}}\, \overline{C}^{(0)}_{\alpha\beta}(kk') = \sum_{k'} \sqrt{m_{k'}}\, \overline{C}^{(0)}_{\beta\alpha}(k'k) = 0 \tag{3-3-58}$$

$$\sum_{k'} \sqrt{m_{k'}}\, \overline{C}^{(1)}_{\alpha\beta\gamma}(kk') = \sum_{k'} \sqrt{m_{k'}}\, \overline{C}^{(1)}_{\alpha\gamma\beta}(kk') \tag{3-3-59}$$

$$\sum_{kk'} \sqrt{m_k m_{k'}}\, \overline{C}^{(1)}_{\alpha\beta\gamma}(kk') = 0 \tag{3-3-60}$$

To solve the vibrational equation (3-3-50), expand $\omega(\frac{\underline{y}}{j})$, $W_\alpha(k|\frac{\underline{y}}{j})$, and E_α in terms of $\epsilon\, \underline{y}$.

(3-3-61)

$$W_\alpha(k|\epsilon_j^\gamma) = W_\alpha^{(0)}(k|_j^\gamma) + i\epsilon W_\alpha^{(1)}(k|_j^\gamma) + \tfrac{1}{2}\epsilon^2 W_\alpha^{(2)}(k|_j^\gamma) + \ldots \qquad (3\text{-}3\text{-}62)$$

$$E_\alpha = E_\alpha^{(0)} + i\epsilon E_\alpha^{(1)} + \tfrac{1}{2}\epsilon^2 E_\alpha^{(2)} + \ldots \qquad (3\text{-}3\text{-}63)$$

Substituting these expansions into the vibration equation (3-3-50) and collecting terms of equal order in ϵ gives the following perturbation equations

$$\sum_{k'\beta} \bar{C}_{\alpha\beta}^{(0)}(kk')\, W_\beta^{(0)}(k'|_j^\gamma) = \frac{e_k}{\sqrt{m_k}} E_\alpha^{(0)} \qquad (3\text{-}3\text{-}64)$$

$$\sum_{k'\beta} \bar{C}_{\alpha\beta}^{(0)}(kk')\, W_\beta^{(1)}(k'|_j^\gamma) = -\sum_{k'\beta\gamma} \bar{C}_{\alpha\beta\gamma}^{(1)}(kk')\, y_\gamma\, W_\beta^{(0)}(k'|_j^\gamma) + \frac{e_k}{\sqrt{m_k}} E_\alpha^{(1)} \qquad (3\text{-}3\text{-}65)$$

$$\sum_{k'\beta} \bar{C}_{\alpha\beta}^{(0)}(kk')\, W_\beta^{(2)}(k'|_j^\gamma) = -\sum_{k'\beta\gamma\lambda} \bar{C}_{\alpha\beta\gamma\lambda}^{(2)}(kk')\, y_\gamma y_\lambda\, W_\beta^{(0)}(k'|_j^\gamma) + \qquad (3\text{-}3\text{-}66)$$

$$+ 2\sum_{k'\beta\gamma} \bar{C}_{\alpha\beta\gamma}^{(1)}(kk')\, y_\gamma\, W_\beta^{(1)}(k'|_j^\gamma) + \frac{e_k}{\sqrt{m_k}} E_\alpha^{(2)} + 2\left[\omega^{(1)}(_j^\gamma)\right]^2 W_\alpha^{(0)}(k|_j^\gamma) .$$

The Zero-Order Equation

The zero-order equation (3-3-64) has non-trivial solutions of the form $W_\beta^{(0)}(k'|_j^\gamma) = \sqrt{m_{k'}}\, \mathcal{U}_\beta(j)$ where $\underline{\mathcal{U}}(j)$ is an arbitrary vector in space. That this is indeed a solution follows from equation (3-3-58) together with the observation that (because the unit cell is

electrically neutral)

$$E_\alpha^{(0)} = -\frac{4\pi}{V_\alpha}\left(\frac{V_\alpha}{|V|}\right)\left[\sum_\beta \left(\frac{V_\beta}{|V|}\right) U_\beta(j)\right] \sum_{k'} e_{k'} = 0 \quad . \tag{3-3-67}$$

The First-Order Equation

Substituting the zero-order solution into the first-order equation (3-3-65) gives

$$\sum_{k'\beta} \bar{C}^{(0)}_{\alpha\beta}(kk') W^{(1)}_\beta(k'|\tfrac{V}{j}) = -\sum_{k'\beta\gamma} \sqrt{m_{k'}}\, \bar{C}^{(1)}_{\alpha\beta\gamma}(kk') V_\gamma U_\beta(j) + \frac{e_k}{\sqrt{m_k}} E^{(1)}_\alpha \quad . \tag{3-3-68}$$

Even though $E^{(1)}_\alpha$ contains $W^{(1)}_\beta(k'|\frac{V}{j})$, it is considered independent. Hence, the left-hand side is considered the homogeneous part of the system of equations; the right-hand side is the inhomogeneous part.

According to the theory of linear equations if

$$\underset{\approx}{C}\,\underset{\sim}{W} = \underset{\sim}{D}$$

and $\underset{\sim}{W}'$ is a solution of the system of homogeneous equations $\underset{\approx}{C}\,\underset{\sim}{W}' = 0$, then the necessary and sufficient condition for the inhomogeneous equations to be solvable is that the inner product $(\underset{\sim}{W}', \underset{\sim}{D}) = 0$. In component form

$$\sum_{m=1}^{S} W'_m D_m = 0 \quad .$$

For equation (3-3-68) this solvability equation becomes (recognizing $\sqrt{m_k}\, U(j)$ as a solution of the homogeneous equations)

$$\sum_k \sqrt{m_k}\left[-\sum_{k'\beta\gamma}\sqrt{m_{k'}}\,\bar{C}^{(1)}_{\alpha\beta\gamma}(kk')\,y_\gamma u_\beta(j) + \frac{e_k}{\sqrt{m_k}}E^{(1)}_\alpha\right] = 0 =$$

$$= \sum_{\beta\gamma}\left\{\sum_{kk'}\sqrt{m_k m_{k'}}\,\bar{C}^{(1)}_{\alpha\beta\gamma}(kk')\right\} y_\gamma u_\beta(j) + E^{(1)}_\alpha \sum_k e_k = 0 \,. \qquad (3\text{-}3\text{-}69)$$

The first term is zero because of equation (3-3-60); the second term is zero because the unit cell is electrically neutral; hence the solvability equation is satisfied.

The first-order equation (3-3-69) may be given a physical interpretation if the displacement due to the zero-order wave

$$u^{(0)}_\alpha(\underline{x}) = \frac{1}{\sqrt{m_k}} W^{(0)}_\alpha(\underline{k}|\underline{\gamma}_j) e^{2\pi i \epsilon \underline{\gamma}\cdot\underline{x}} = u_\alpha(j) e^{2\pi i \epsilon \underline{\gamma}\cdot\underline{x}} \qquad (3\text{-}3\text{-}70)$$

is described as a homogeneous deformation in a region small compared to the wavelength of a long wave. This homogeneous deformation may be described as

$$x'_\alpha = x_\alpha + \sum_\beta u_{\alpha\beta} x_\beta \qquad \alpha, \beta = 1, 2, 3 \qquad (3\text{-}3\text{-}71)$$

where the deformation parameters are given by

$$u_{\alpha\beta} = \frac{\partial u_\alpha}{\partial x_\beta} = \frac{\partial}{\partial x_\beta}\left[u_\alpha(j) e^{2\pi i \epsilon \underline{\gamma}\cdot\underline{x}}\right] =$$

$$= 2\pi i \epsilon \gamma_\beta u_\alpha(j) e^{2\pi\epsilon \underline{\gamma}\cdot\underline{x}} \,. \qquad (3\text{-}3\text{-}72)$$

The exponential factor is considered a constant within the region under consideration. Using this result, rewrite the first-order equation (3-3-68) as follows:

$$\sum_{k'\beta} \bar{C}^{(0)}_{\alpha\beta}(kk')\, W^{(1)}_{\beta}(k'|\underset{j}{\chi}) = -\sum_{k'\beta\gamma} \sqrt{m_{k'}}\, \bar{C}^{(1)}_{\alpha\beta\gamma}(kk')\, u_{\beta\gamma}\left(\frac{i}{2\pi\epsilon}\right) e^{-2\pi i \epsilon \underset{\sim}{\chi}\cdot\underset{\sim}{x}} + \frac{e_k}{\sqrt{m_k}} E^{(1)}_{\alpha} . \tag{3-3-73}$$

let

$$u^{(1)}_{\beta}(k') = \frac{i\epsilon}{\sqrt{m_{k'}}} W^{(1)}_{\beta}(k'|\underset{j}{\chi})\, e^{2\pi i \epsilon \underset{\sim}{\chi}\cdot\underset{\sim}{x}} \tag{3-3-74}$$

then

$$\sum_{k'\beta} \bar{C}^{(0)}_{\alpha\beta}(kk')\frac{\sqrt{m_{k'}}}{i\epsilon}\, e^{-2\pi i \epsilon \underset{\sim}{\chi}\cdot\underset{\sim}{x}}\, u^{(1)}_{\beta}(k') = \sum_{k'\beta\gamma} \sqrt{m_{k'}}\, \bar{C}^{(1)}_{\alpha\beta\gamma}\, u_{\beta\gamma} \cdot \left(\frac{i}{2\pi\epsilon}\right) e^{-2\pi i \epsilon \underset{\sim}{\chi}\cdot\underset{\sim}{x}} + \frac{e_k}{\sqrt{m_k}} E^{(1)}_{\alpha} . \tag{3-3-75}$$

If we write

$$\bar{C}^{(0)}_{\alpha\beta} = \frac{1}{\sqrt{m_k m_{k'}}} \sum_{l} \bar{\bar{\Phi}}_{\alpha\beta}\binom{l}{kk'} \tag{3-3-76}$$

$$\bar{C}^{(1)}_{\alpha\beta} = -\frac{2\pi}{\sqrt{m_k m_{k'}}} \sum_{l} \bar{\bar{\Phi}}_{\alpha\beta}\binom{l}{kk'} \chi_{\gamma}\binom{l}{kk'}$$

equation (3-3-73) may be written

$$\sum_{k'\beta} \sum_{l} \bar{\bar{\Phi}}_{\alpha\beta}\binom{l}{kk'} u_{\beta}(k') = -\sum_{k'\beta\gamma} \sum_{l} \bar{\bar{\Phi}}_{\alpha\beta}\binom{l}{kk'} u_{\beta\gamma}\, \chi_{\gamma}\binom{l}{kk'} + i\epsilon\, e_k E^{(1)}_{\alpha}\, e^{2\pi i \epsilon \underset{\sim}{\chi}\cdot\underset{\sim}{x}} . \tag{3-3-77}$$

The first term on the right-hand side is the force on particle k due to the external strain caused by the zero-order wave. The term on the left-hand side is the counter-force due to the induced internal strain $u_{\beta}(k')$.

We thus see that equation (3-3-77) describes the balance of forces in a volume element in a state of homogeneous strain (both external and internal) and subject at the same time to an electric field. Equations (3-3-68) are 3n in number ($k = 0, 1, \ldots, n-1 : \alpha = 1, 2, 3$). However, if these equations are multiplied by $\sqrt{k}$ and summed over k, both sides are identically zero. Hence of the n equations for a given α, only n - 1 are independent. We can thus take the displacement of one of the base particles to be zero, and measure all other displacements relative to it. Taking $W_\alpha^{(1)}(0 \mid \frac{\gamma}{j}) = 0$, we thus reduce (3-3-68) to 3(n-1) equations in 3(n-1) unknowns.

The formal solution of (3-3-68) is found by operating with the inverse $\underset{\approx}{\Gamma}^{(3n-3)} = \left(\underset{\approx}{C}^{(0)}\right)^{-1}$ defined such that

$$\sum_{k'\beta} \Gamma_{\alpha\beta}^{(3n-3)}(kk')\, C_{\beta\gamma}^{(0)}(k'k'') = \delta_{kk''}\,\delta_{\alpha\gamma} . \qquad (3\text{-}3\text{-}78)$$

If we make $\underset{\approx}{\Gamma}$ a 3n x 3n matrix by bordering it with zeros $\left(\Gamma_{\alpha\beta}(kk') = 0 \text{ if } k = 0 \text{ or if } k' = 0\right)$ and operate on equation (3-3-68) we get:

$$W_\alpha^{(1)}(k \mid \frac{\gamma}{j}) = -\sum_{k'\mu} \Gamma_{\alpha\mu}(kk') \sum_{k''} \sum_{\beta\gamma} \sqrt{m_{k''}}\; \bar{C}_{\mu\beta\gamma}^{(1)}(k'k'')\, y_\gamma\, u_\beta(j) \qquad (3\text{-}3\text{-}79)$$

$$+ \sum_{k'\beta} \Gamma_{\alpha\beta}(kk') \frac{e_{k'}}{\sqrt{m_{k'}}} E_\beta^{(1)} .$$

The Second-Order Equation

Substitution of the zero- and first-order solutions into the second-order equation (3-3-66) gives:

$$\tfrac{1}{2}\sum_{k'\beta} C^{(0)}_{\alpha\beta}(kk')\,W^{(2)}_{\beta}(k'|\,{}^{\gamma}_{j}) = \left[\omega^{(1)}({}^{\gamma}_{j})\right]^2\sqrt{m_k}\;u_\alpha(j) -$$

$$-\tfrac{1}{2}\sum_{k'\beta\gamma\lambda}\sqrt{m_{k'}}\;\bar{C}^{(2)}_{\alpha\beta\gamma\lambda}(kk')\,y_\gamma y_\lambda\,u_\beta(j) - \qquad (3\text{-}3\text{-}80)$$

$$-\sum_{k'}\sum_{\mu\gamma}\bar{C}^{(1)}_{\alpha\mu\gamma}(kk')\,y_\gamma\sum_{k''\gamma}\Gamma_{\mu\nu}(k'k'')\sum_{k'''}\sum_{\beta\lambda}\bar{C}^{(1)}_{\gamma\beta\lambda}(k''k''')\sqrt{m_{k'''}}\;y_\lambda\,u_\beta(j) +$$

$$+\sum_{k'}\sum_{\mu\beta}\bar{C}^{(1)}_{\alpha\mu\gamma}(kk')\,y_\gamma\sum_{k''\beta}\Gamma_{\mu\beta}(k'k'')\,\frac{e_{k''}}{\sqrt{m_{k''}}}\,E^{(1)}_{\beta} \;+\; \frac{e_k}{\sqrt{m_k}}\,E^{(2)}_{\alpha}\,.$$

Recognizing that $\sqrt{m_k}\,u(j)$ is again a solution of the homogeneous equation, its inner product with the inhomogeneous part gives the following solubility condition.

$$\left(\frac{\sum_k m_k}{Va}\right)\left[\omega^{(1)}({}^{\gamma}_{j})\right]^2 u_\alpha(j) = 4\pi^2\sum_{\beta}\sum_{\gamma\lambda}\left\{[\alpha\beta,\gamma\lambda]+(\alpha\gamma,\beta\lambda)\right\}\cdot \qquad (3\text{-}3\text{-}81)$$

$$\cdot\, y_\gamma y_\lambda u_\beta(j) - 2\pi\sum_{\beta}\left\{\sum_{\gamma}[\beta,\alpha\gamma]\,y_\gamma\right\}E^{(1)}_{\beta}$$

where

$$[\alpha\beta,\gamma\lambda] = \frac{1}{8\pi^2 Va}\sum_{kk'}\sqrt{m_k m_{k'}}\;\bar{C}^{(2)}_{\alpha\beta\gamma\lambda}(kk') \qquad (3\text{-}3\text{-}82)$$

$$(\alpha\gamma,\beta\lambda) = \frac{-1}{4\pi^2 V_a} \sum_{kk'} \sum_{\mu\nu} \Gamma_{\mu\nu}(kk') \left(\sum_{k''} \bar{C}^{(1)}_{\mu\alpha\gamma}(kk'') \sqrt{m_{k''}} \right) \cdot \tag{3-3-83}$$

$$\cdot \left(\sum_{k'''} \bar{C}^{(1)}_{\nu\beta\lambda}(k'k''') \sqrt{m_{k'''}} \right)$$

$$[\beta,\alpha\gamma] = \frac{1}{2\pi V_a} \sum_{kk'\mu} \sqrt{m_k}\, \bar{C}^{(1)}_{\alpha\mu\gamma}(kk') \left(\sum_{k''} \Gamma_{\mu\beta}(k'k'') \frac{e_{k''}}{\sqrt{m_{k''}}} \right). \tag{3-3-84}$$

Symmetry Properties of the Round and Square Brackets

The square brackets are symmetric with respect to the interchange of indices within each pair

$$[\alpha\beta,\gamma\lambda] = [\beta\alpha,\gamma\lambda] = [\alpha\beta,\lambda\gamma] \tag{3-3-85}$$

as is easily seen from the symmetry of the $\bar{C}^{(2)}_{\alpha\beta\gamma\lambda}(kk')$ (3-3-57). The round brackets are symmetric with respect to both interchange within each pair and with respect to the interchange of the first and second pairs, as can be seen from equation (3-3-59).

$$(\alpha\beta,\gamma\lambda) = (\beta\alpha,\gamma\lambda) = (\alpha\beta,\lambda\gamma) = (\gamma\lambda,\alpha\beta) \tag{3-3-86}$$

Hence the round brackets have the full symmetry of the elastic constants while the square brackets do not.

Continuum Wave Equation for the Propagation of Small Amplitude Waves in a Prestressed, Piezoelectric Medium

We wish now to write the analogous equation to (3-1-20) for the case of a piezoelectric medium, such that the elastic constants (and peizoelectric constants) may be defined in terms of the brackets through a direct comparison with (3-3-81).

For a piezoelectric medium, one must use, in place of Hooke's Law, the constitutive stress-strain relation

$$S_{\alpha\gamma} = \sum_{\beta\lambda} \mathcal{S}_{\alpha\gamma\beta\lambda}\, u_{\beta\lambda} - \sum_{\beta} e_{\beta\alpha\gamma}\, E_{\beta} . \tag{3-3-87}$$

The equations of motion are

$$\rho \ddot{u}_{\alpha} = \sum_{\gamma} \frac{\partial S_{\alpha\gamma}}{\partial x_{\gamma}} = \sum_{\beta\gamma\lambda} \mathcal{S}_{\alpha\gamma\beta\lambda} \frac{\partial^2 u_{\beta}}{\partial x_{\gamma}\partial x_{\lambda}} - \sum_{\beta\gamma} e_{\beta\alpha\gamma} \frac{\partial E_{\beta}}{\partial x_{\gamma}} . \tag{3-3-88}$$

Assuming a plane elastic wave solution

$$u_{\alpha}(x,t) = \bar{u}_{\alpha}\, e^{2\pi i\, \gamma\cdot x - i\omega t} \tag{3-3-89}$$

and associated electric field

$$E_{\alpha} = \bar{E}_{\alpha}\, e^{2\pi i\, \gamma\cdot x - i\omega t} \tag{3-3-90}$$

the equation of motion (3-3-88) becomes

$$\rho\omega^2 \bar{u}_{\alpha} = 4\pi^2 \sum_{\beta} \left(\sum_{\gamma\lambda} \mathcal{S}_{\alpha\gamma\beta\lambda}\, \gamma_{\gamma}\gamma_{\lambda} \right) \bar{u}_{\beta} + 2\pi i \sum_{\beta} \left(\sum_{\gamma} e_{\beta\alpha\gamma}\gamma_{\gamma} \right) \bar{E}_{\beta} . \tag{3-3-91}$$

Comparison of this continuum wave equation (3-3-91) with the long-wave limit of the lattice vibration equation (3-3-81) allows the elastic and

piezoelectric constants to be expressed in terms of the interatomic potential.

$$\sum_{\gamma\lambda} \delta_{\alpha\gamma\beta\lambda}\, y_\gamma y_\lambda \equiv \sum_{\gamma\lambda} [\alpha\beta,\gamma\lambda]\, y_\gamma y_\lambda + \sum_{\gamma\lambda} (\alpha\gamma,\beta\lambda)\, y_\gamma y_\lambda \tag{3-3-92}$$

$$\sum_{\gamma} e_{\beta\alpha\gamma}\, y_\gamma \equiv \sum_{\gamma} [\beta,\alpha\gamma]\, y_\gamma \tag{3-3-93}$$

Since we will not be interested in the piezoelectric constants in the application to follow, they will not be discussed further.

For any value of χ (3-3-92) gives

$$\delta_{\alpha\gamma\beta\lambda} + \delta_{\alpha\lambda\beta\gamma} = 2[\alpha\beta,\gamma\lambda] + (\alpha\gamma,\beta\lambda) + (\alpha\lambda,\beta\gamma). \tag{3-3-94}$$

The problem here is that $[\alpha\beta,\gamma\lambda]$ is not symmetric with respect to interchange of the index pairs and thus does not have the full symmetry of the elastic constants. Following Born and Huang, § 27, we define new constants

$$d_{\alpha\gamma\beta\lambda} + d_{\alpha\lambda\beta\gamma} = 2[\alpha\beta,\gamma\lambda] \tag{3-3-95}$$

which satisfy the required symmetry relations

$$d_{\alpha\gamma\beta\lambda} = d_{\gamma\alpha\beta\lambda} \tag{3-3-96}$$

$$d_{\alpha\gamma\beta\lambda} = d_{\beta\lambda\alpha\gamma}. \tag{3-3-97}$$

It is easily verified that

$$d_{\alpha\gamma\beta\lambda} = [\alpha\beta,\gamma\lambda] + [\beta\gamma,\alpha\lambda] - [\beta\lambda\alpha\gamma] \tag{3-3-98}$$

satisfies both (3-3-95) and (3-3-96). However, (3-3-97) requires that $[\beta\gamma,\alpha\lambda] = [\alpha\lambda,\beta\gamma]$. Although this symmetry property of the square brackets cannot be directly demonstrated, it follows from the fact that (3-3-81) and (3-3-91) are physically equivalent. Born and Huang (1962) claim this is a consequence of the disappearance of the initial stress. However, this pair-wise symmetry is actually a condition for the existence of the strain-energy function and thus requires only that the initial stress be specified, not that it be specified to be equal to zero as implied by Born and Huang. Hence, for the case of a medium under hydrostatic prestress

$$\mathcal{S}_{\alpha\gamma\beta\lambda} = [\alpha\beta,\gamma\lambda] + [\beta\gamma,\alpha\lambda] - [\beta\lambda,\alpha\gamma] + (\alpha\gamma,\beta\lambda). \qquad (3\text{-}3\text{-}99)$$

Central Forces

By considering only central forces, the non-coulombic contributions to the elastic constants may be written directly in terms of radial derivatives of the non-coulombic potential. The total non-coulombic potential may be written

$$\Phi^N = \frac{1}{2} \sum_{lk} \sum_{l'k'} \Phi^N_{kk'} \left(\left| \underset{\sim}{\chi}\left(\begin{smallmatrix} l-l' \\ kk' \end{smallmatrix}\right) + \underset{\sim}{u}\left(\begin{smallmatrix} l \\ k \end{smallmatrix}\right) - \underset{\sim}{u}\left(\begin{smallmatrix} l' \\ k' \end{smallmatrix}\right) \right| \right) \qquad (3\text{-}3\text{-}100)$$

where $\Phi^N_{kk'}(r_{kk'})$ is the two-body short-range potential acting between particle type k and particle type k'. The coefficients in the displacement expansion (3-3-2) may be obtained by direct differentiation of (3-3-100) (see Born and Huang, § 29).

$$\Phi^N_\alpha(k) = \sum_{l'k'} P^{l}_{kk'}\, \chi_\alpha(\overset{l}{kk'})$$

$$\Phi^N_{\alpha\beta}(\overset{l}{kk'}) = -\delta_{\alpha\beta} P^{l}_{kk'} - Q^{l}_{kk'}\, \chi_\alpha(\overset{l}{kk'})\chi_\beta(\overset{l}{kk'}) \qquad k' \neq k \tag{3-3-101}$$

$$\Phi^N_{\alpha\beta}(\overset{\circ}{kk}) = \sum_{l'k'} \left\{ \delta_{\alpha\beta} P^{l}_{kk'} + Q^{l}_{kk'}\, \chi_\alpha(\overset{l}{kk'})\chi_\beta(\overset{l}{kk'}) \right\}$$

where

$$P^{l}_{kk'} = \left(\frac{1}{r}\frac{d\Phi^N_{kk'}}{dr}\right)_{r^{l}_{kk'}}$$

$$Q^{l}_{kk'} = \left[\frac{1}{r}\frac{d}{dr}\left(\frac{1}{r}\frac{d\Phi^N_{kk'}}{dr}\right)\right]_{r^{l}_{kk'}} \tag{3-3-102}$$

Using (3-3-101), the non-coulombic contribution to the coefficients of the wave-number expansion (3-3-51) may be written

$$C^{(0)}_{\alpha\beta}(kk') = \frac{1}{(m_k m_{k'})^{1/2}}\left\{ -\delta_{\alpha\beta}\sum_l P^{l}_{kk'} - \sum_l Q^{l}_{kk'}\, \chi_\alpha(\overset{l}{kk'})\chi_\beta(\overset{l}{kk'}) \right\} \qquad k \neq k'$$

$$C^{(0)}_{\alpha\beta}(kk) = \frac{1}{m_k}\left\{ \delta_{\alpha\beta}\sum_{k'\neq k}\sum_l P^{l}_{kk'} + \sum_{k'\neq k}\sum_l Q^{l}_{kk'}\, \chi_\alpha(\overset{l}{kk'})\chi_\beta(\overset{l}{kk'}) \right\} \tag{3-3-103}$$

$$C^{(1)}_{\alpha\beta\gamma}(kk') = \frac{2\pi}{(m_k m_{k'})^{1/2}}\left\{ \delta_{\alpha\beta}\sum_l P^{l}_{kk'}\chi_\gamma(\overset{l}{kk'}) + \sum_l Q^{l}_{kk'}\, \chi_\alpha(\overset{l}{kk'})\chi_\beta(\overset{l}{kk'})\chi_\gamma(\overset{l}{kk'}) \right\}$$

$$C^{(2)}_{\alpha\beta\gamma\lambda}(kk') = \frac{4\pi^2}{(m_k m_{k'})^{1/2}}\left\{ \delta_{\alpha\beta}\sum_l P^{l}_{kk'}\chi_\gamma(\overset{l}{kk'})\chi_\lambda(\overset{l}{kk'}) + \sum_l Q^{l}_{kk'}\, \chi_\alpha(\overset{l}{kk'})\chi_\beta(\overset{l}{kk'})\chi_\gamma(\overset{l}{kk'})\chi_\lambda(\overset{l}{kk'}) \right\}.$$

Using (3-3-103) in (3-3-82), the non-coulombic contribution to the square brackets may be written

$$[\alpha\beta,\gamma\lambda]^N = \frac{1}{2V_a}\sum_{kk'l}\left\{ \delta_{\alpha\beta} P^{l}_{kk'}\chi_\gamma(\overset{l}{kk'})\chi_\lambda(\overset{l}{kk'}) + \right. \tag{3-3-104}$$

$$\left. + Q^{l}_{kk'}\, \chi_\alpha(\overset{l}{kk'})\chi_\beta(\overset{l}{kk'})\chi_\gamma(\overset{l}{kk'})\chi_\lambda(\overset{l}{kk'}) \right\}.$$

In general, the round brackets defined by (3-3-83) cannot be separated into coulombic and non-coulombic parts because of the matrix inverse in the definition. Only for very special geometries can this term be simply expressed. For example, if every particle is a symmetry center, the round brackets are equal to zero. This is because $\underset{\approx}{C}^{(1)}$ is an odd function function of x_γ; for a centrosymmetric lattice the k'' and k''' sums in (3-3-83) are zero. The next simplest case is a cubic diagonal lattice; i.e., a cubic lattice in which the origin of each sublattice k lies on the cube diagonal. Inspection of (3-3-103) shows, in this case, the only non-zero $\underset{\approx}{C}^{(1)}(kk')$ are those with $\alpha \neq \beta \neq \gamma$. Hence in diagonal lattices, the internal deformations contribute only to C_{44}. Examples are the ZnS and CaF_2 structures. For all other geometries the full expression (3-3-83) must be evaluated for each elastic constant.

TABLE 3-1-1

Comparison of Stress-Strain Notations

This Work	Thurston (1964)	Wallace (1967)	Wallace (1965)	Thurston & Brugger (1964)	Thomsen (1970b)
a_i	a_i	$\bar{\bar{X}}_i$	a_i	a_i	a_i
t_{ij}	t_{ij}		t_{ij}	t_{ij}	
ρ_o	ρ_o	ρ_o	ρ_o	ρ_o	
$\bar{X}_i$	$\bar{X}_i$	$\bar{X}_i$	r_i	$\bar{X}_i$	$\bar{X}_i$
$\bar{T}_{ij}$	$\bar{T}_{ij}$	C_{ij}	T_{ij}		
$\bar{\rho}$	$\bar{\rho}$	ρ_1	ρ_1		
x_i	x_i	x_i	x_i	x_i	x_i
T_{ij}	T_{ij}	T_{ij}	τ_{ij}	τ_{ij}	T_{ij}
ρ	ρ	ρ	ρ	ρ	ρ_x
μ_i			μ_i		
η_{ij}	n_{ij}	$\bar{n}_{ij}$	s_{ij}	n_{ij}	n_{ij}
J_o	J		J_o	J	
U_i	μ_i	μ_i	U_i	μ_i	μ_i
S_{ij}	S_{ij}	n_{ij}	S_{ij}		
J		J	J_1		
ϵ_{ij}	ϵ_{ij}	ϵ_{ij}			
ω_{ij}	ω_{ij}	ω_{ij}			
f_{ij}		$\bar{\alpha}_{ij}$	q_{ij}		$(\underset{\sim}{1}+\underset{\sim}{e})_{ij}$
g_{ij}			b_{ij}		
u_{ij}					e_{ij}
c_{ijkl}	c_{ijkl}	$\bar{C}_{ijkl}$	c_{ijkl}	c_{ijkl}	
F_{ij}		α_{ij}			
G_{ij}					
U_{ij}		u_{ij}			μ_{ij}
C_{ijkl}	G_{ijkl}	C_{ijkl}	C_{ijkl}		
S_{ijkl}		S_{ijkl}			
A_{ijkl}	E_{ijkl}				
B_{ijkl}	S_{ijkl}	B_{ijkl}			C_{ijkl}
E_{ijkl}	B_{ijkl}	S_{ijkl}	E_{ijkl}		
β_{ijkl}	β_{ijkl}				

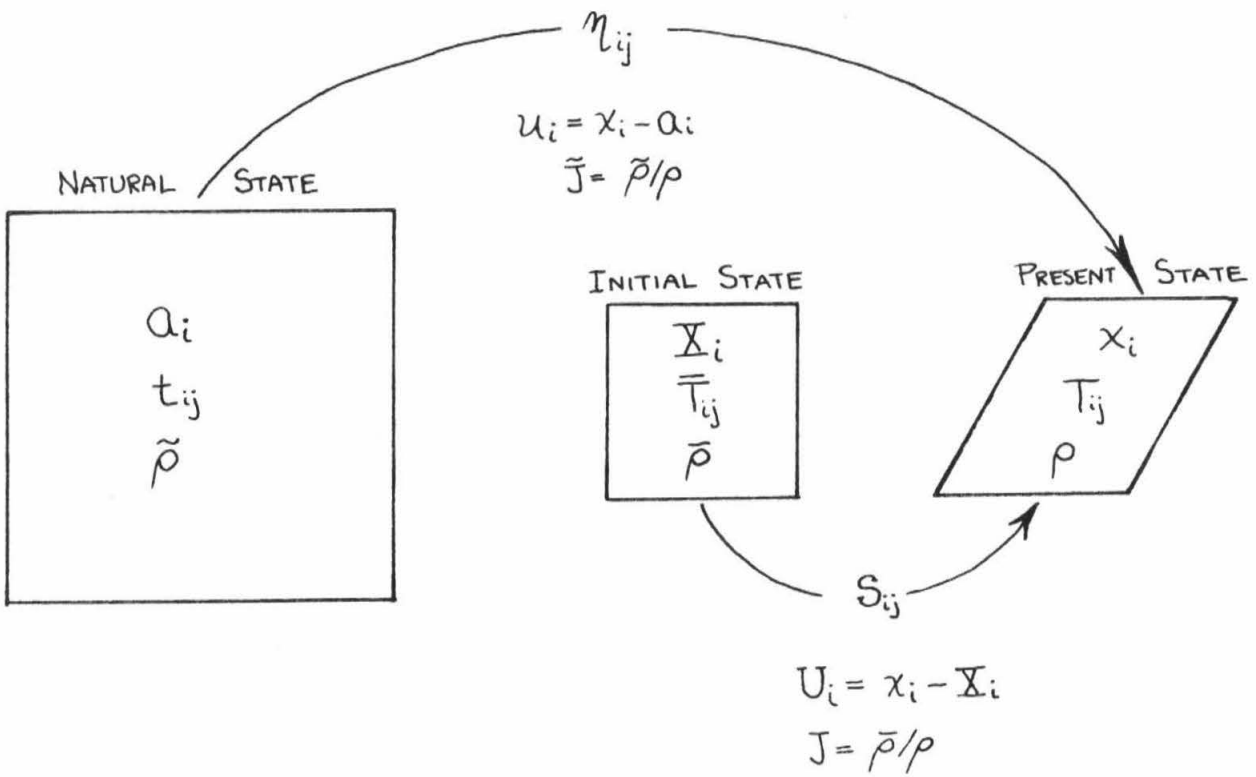

Figure 3-1-1. Stress-strain reference states.

IV. THE INTERATOMIC POTENTIAL

One of the basic assumptions of the Born model is that the cohesive energy of a static lattice can be represented as a sum of two-body interactions of the form

$$\Phi_{ij}(r_{ij}) = V_{ij}^{(e)}(r_{ij}) + V_{ij}^{(VDW)}(r_{ij}) + V_{ij}^{(r)}(r_{ij}) \qquad (4\text{-}0\text{-}1)$$

where

$V_{ij}^{(e)}(r_{ij})$ = electrostatic potential energy between the i^{th} and j^{th} ions $= q_i q_j / r_{ij} \qquad i \neq j$

q_i = change on i^{th} ion

r_{ij} = distance between i^{th} and j^{th} ions

$V_{ij}^{(VDW)}(r_{ij})$ = van der Waals or London interaction

$$= C_{ij}/r_{ij}^6 + f_{ij}/r_{ij}^8 + \ldots \qquad (4\text{-}0\text{-}2)$$

C_{ij} = van der Waals dipole-dipole constant

f_{ij} = van der Waals dipole-quadrupole constant

$V_{ij}^{(r)}$ = empirical repulsive potential opposing the interpenetration of the i^{th} and j^{th} ions. Its functional form is usually assumed to be either B/r_{ij}^n or $\lambda e^{-r_{ij}/\rho}$.

The potential energy of an i-type ion is then given by

$$\Phi_i = \sum_j \Phi_{ij}(r_{ij}) \qquad i \neq j \qquad (4\text{-}0\text{-}3)$$

It is convenient to make a distinction between the long-range electrostatic potential which must be summed over all ions in the

lattice and the van der Waals and repulsive terms which are short range; falling off as $1/r_{ij}^{n}$ or $e^{-r_{ij}/\rho}$ where n and the exponent are greater than 4. Hence it is usually adequate to sum only over nearest neighbors; i.e.

$$\Phi_i = \sum_{\text{all } j} V_{ij}^{(e)} + \sum_{\substack{j \text{ nearest} \\ \text{neighbors}}} \left(V_{ij}^{(VDW)} + V_{ij}^{(r)} \right) \qquad (4\text{-}0\text{-}4)$$

While the cohesive energy of an infinite crystal

$$\Phi = \tfrac{1}{2} \sum_i \Phi_i = \tfrac{1}{2} \sum_{ij} \Phi_{ij} \qquad (4\text{-}0\text{-}5)$$

is infinite, the energy density W is finite.

$$W = \tfrac{1}{2} N_A \sum_{\nu=1}^{S} \Phi_\nu \qquad \text{energy/mole} \qquad (4\text{-}0\text{-}6)$$

$\nu = 1, \ldots, S$ indexes the ions of one molecule

S = total number of ions in one molecule

N_A = Avogadro's number

The utility of the Born model in predicting elastic constants of geophysically interesting minerals at high pressures is ultimately determined by how accurately equations (4-0-1) - (4-0-6) represent the volume dependence of the energy density. The basic assumption that the complex bonding forces can be adequately represented by a sum of two-body central interactions having the simple functional forms given above can be tested either experimentally or by detailed quantum mechanical calculations. The experimental testing is one of the objectives of Chapter V where the Born model predictions are compared

with recent high-precision ultrasonic data for a number of structures pertinent to the lower mantle. The detailed quantum mechanical (q.m.) theory for alkalide-halides has been worked out principally by Landshoff (1936), Löwdin (1948), and Lundqvist (1955). Although such a quantum treatment is beyond the scope of this thesis, the results will be sketched in the next section, particularly as they relate to Born approximation.

4-1. Quantum Mechanical Calculations for Ionic Solids

The earliest q.m. calculation bearing on the problem of ionic crystals was the demonstration by Unsöld (1927), Brück (1928), and Pauling (1928) that the repulsion between closed ionic shells was of an exponential form, rather than the power law form derived by Born and Landé (1918a) from the Bohr electrostatic atom model which was popular at that time. Using this same approximation of closed electron shells, the sodium chloride lattice was originally treated by Landshoff (1936, 1937) and, in more detail, by Löwdin (1947, 1948). These early works by Löwdin, plus a later major paper (Löwdin, 1956), represent the most comprehensive quantum calculations of the cohesive and elastic properties of a solid yet attempted. Since Löwdin's calculations clearly show strengths and weaknesses of the Born formulation used in this thesis, his approach will now be outlined.

Löwdin considered a static system of ions for which the Hamiltonian operator is (using Löwdin's notation)

$$H_{op} = W + \sum_i H_i + \sum_{ik}{}' G_{ik}$$

where

$$W = \frac{e^2}{2} \sum_{gg'}{}' \frac{Z_g Z'_g}{r'_{gg}} = \text{ion-ion interaction}$$

$$H_i = \frac{1}{2m} \vec{p}_i^{\,2} - e^2 \sum_g \frac{Z_g}{r_i} = \text{kinematic energy of electrons + electron-ion interaction} \quad (4\text{-}1\text{-}1)$$

$$G_{ik} = \frac{e^2}{2r_{ik}} = \text{electron-electron interaction}$$

g, g' index the ion positions

i, k index the electron positions.

The ground state energy of the system is given by the lowest-eigenvalue $\mathcal{E}'$ of Schrödinger's equation

$$H_{op}\Phi = \mathcal{E}\Phi \quad (4\text{-}1\text{-}2)$$

where Φ is an antisymmetric wave function of the space and spin coordinates of the electrons.

The ground state energy is given by the lower bound of the integral equation

$$\mathcal{E} = \frac{\int \Phi^* H_{op} \Phi \, d\tau_1 d\tau_2 \cdots d\tau_N}{\int \Phi^* \Phi \, d\tau_1 d\tau_2 \cdots d\tau_N} . \quad (4\text{-}1\text{-}3)$$

Since the exact solution of Schrödinger's equation for a many-electron system is almost hopelessly complex, Löwdin made the following approximations

A. Instead of solving the exact Schrödinger equation, he used the one-electron approximation scheme also called the

Hartree-Fock self-consistent field method.

B. Instead of finding the one-electron wave functions by the self-consistent field method, Löwdin used the free-ion wave functions in the Hartree-Fock energy equation. He thus assumed that the solid was fully ionic, and neglected the mutual deformation of the ions. Hence there are no van der Waals or other multipole interactions in his formulation. As Slater (1967) points out: "The characteristic of this problem of interacting closed-shell atoms or ions is that a single determinantal wave function forms a satisfactory description, and configuration interaction is much less necessary than in such a problem as the H_2 molecule, involving covalent binding."

C. The overlap integrals are only worked out for nearest neighbors, and higher order terms in the overlap integrals have been neglected.

Löwdin computed the cohesive energy by subtracting the free-ion energy from the Hartree-Fock energy, writing his results in the form

$$E_{coh} = E_m + E_{corr} + E_{ex} + E_s$$

where

E_m = Madelung energy

E_{corr} = Coulomb correction due to overlap

E_{ex} = Exchange energy

E_s = Overlap energy between nearest neighbors

Without giving the detailed form of these terms, the important result as regards the Born approximation is that the first three terms and part of the fourth can be represented as a sum of two-body interaction. By expressing $E_{coh} = E_m + E_{rep}$, where $E_{rep} = E_{corr} + E_{ex} + E_s$, Löwdin found that computed values of E_{rep} as a function of R could be fit with an exponential function of the form $\lambda e^{-R/\rho}$. Thus the quantum results could be cast into a functional form equivalent to that assumed by Born and Mayer (1932). However, although the results look formally the same, there is one important difference. Part of E_s is given by three-body integrals and cannot be expressed as a sum of two-body interactions. One of Löwdin's more important results was the demonstration that these three-body interactions explain the deviation from Cauchy's relation ($C_{12} = C_{44}$) observed for alkali-halides in the NaCl structure. On this same point, La and Barsch (1968) extended Löwdin's approach to include the overlap of second neighbor anions. They were then able to explain the rather large deviations from Cauchy's relations observed in MgO.

By using a different expansion of the ion wave functions, Lundqvist (1955) showed that the main effect of the three-body interaction term is the introduction of an effective ionic charge, q* in the coulombic term, where $q^* \leq q$. In the Born approximation, this quantum result will be incorporated by introducing an ionicity factor, $0 < \phi \leq 1$, in the coulomb terms. In the treatment of MgO in Chapter V, it will be shown that by reducing ϕ from 1.0 to 0.7 much better agreement is obtained between the Born model calculations and the ultrasonic data.

The improvement of these quantum calculations represents the forefront of atomistic elasticity. However, even the qualitative insights provided by the crude approximations sketched above show that, with the exception of the effects of three-body interactions on the shear constants, the Born model can be expected to give a fairly good approximation to the volume dependence of the energy in ionic crystals. Quoting Slater (1967), "What Löwdin found, in fact, was a far-reaching resemblance between the quantum-mechanical calculation and the Born-Landé theory."

4-2. The Born Approximation

Having established that the empirical Born formulation given by equations (4-0-1) - (4-0-6) closely parallels the detailed quantum mechanical results, each of the terms in the Born potential will now be discussed.

The Electrostatic Potential

The electrostatic term in the energy density is usually written (Kittel, 1966)

$$W^{(e)} = \frac{N_A}{2} \sum_{ij}{}' \Phi_{ij}^{(e)} = \frac{N_A}{2} \sum_{ij}{}' \frac{q_i q_j}{r_{ij}} = \frac{N_A q_0^2}{R} \frac{1}{2} \sum_{ij} \frac{(\pm)}{p_{ij}} = \frac{N_A \alpha_M q_0^2}{R} \qquad (4\text{-}2\text{-}1)$$

where $r_{ij} = R p_{ij}$

R = reference dimension

p_{ij} = dimensionless scale factor

α_m = Madelung constant = $\frac{1}{2} \sum_{ij} \frac{(\pm)}{p_{ij}}$.

The factor 1/2 corrects for counting each interaction twice in the sum. The symbol (±) indicates that the sign of each term in the sum is dependent upon the sign of the charge on the i^{th} and j^{th} ions.

The Madelung constant is conditionally convergent and cannot be summed directly. There are two well-established methods of calculating α_m, the Evjen (1932) and the Ewald (1921) techniques. The Evjen technique involves grouping terms into electrically neutral cells, thus speeding the convergence. This technique is at its best for simple, highly symmetric structures. The Ewald method rewrites the sum given above as a sum over the direct lattice plus a sum over the reciprocal lattice, each of which converges faster than the original sum in direct space. This method is more generally applicable to complex lattices and is further described in Appendix 2.

In treating the electrostatic term for "essentially ionic" oxides and silicates, an empirical ionicity factor will be introduced

$$W^{(e)} = N_A \alpha_M \phi q^2 / R \qquad (4\text{-}2\text{-}2)$$

where $0 < \phi \leq 1$

in order to allow for an "effective ionicity" of less than 100%. The ionicity factor will be determined by requiring the best fit to the elastic constants and their pressure derivatives.

The concept of an effective ionic charge is not a new one. It was first introduced by Lyddane, Sachs, and Teller (1941). Szigeti (1949)

related the effective ionicity to the dielectric constants.

$$\epsilon = n^2 + \left(\frac{n^2+2}{3}\right)^2 \frac{\beta (ze)^2 N_A}{\pi \nu_t^2} \left(\frac{1}{m_1} + \frac{1}{m_2}\right) \qquad (4\text{-}2\text{-}3)$$

where ϵ = dielectric constant

n = index of refraction

ν_t = frequency of long wavelength transverse optical vibrations

z = valence

m_i = mass of ion

β = ionicity factor

Since all the variables except β are known for many crystals, Szigeti was able to calculate β. For materials to be investigated in this thesis he found:

Material	β
NaCl	0.74
MgO	0.88
TiO_2 (Rutile)	0.65 - 0.88

Although treated empirically by Szigeti and in this thesis, the coulomb correction is a result of the q.m. treatment of Lundqvist (1955) as shown in the previous section.

The van der Waals Potential

The van der Waals interaction can be understood semiclassically as the interaction of the instantaneous dipole moments (Kittel, 1966). One instantaneous dipole moment of magnitude p_i produces an electric

field $E = 2p_i/r^3$ which induces a dipole moment on a second ion given by

$$p_j = A_j E = 2A_j p_i / r_{ij}^3$$

A_j = electronic polarizability of ion j .

The potential energy of the dipole interaction is

$$V_{ij}^{(VDW.)} \approx -2p_i p_j / r_{ij}^3 = -\frac{4A_j p_i^2}{r_{ij}^6} \equiv \frac{C_{ij}}{r_{ij}^6} .$$

It should be pointed out that, unlike the interaction of two permanent dipoles which depends upon their relative orientation, the van der Waals interaction is a central interaction depending only on the separation r_{ij} between the two ions.

The van der Waals constant C_{ij} can be related to the principal absorption lines and polarizability of the ions

$$C_{ij} \simeq \frac{3}{2} A_i A_j \frac{E_i E_j}{E_i + E_j} \qquad (4\text{-}2\text{-}4)$$

where $E_i = h\nu_i$ = energies corresponding to main frequencies of the ions

A_i = ionic polarizability .

Although this seems very straightforward, the actual evaluation of the van der Waals constant in solids is subject to considerable uncertainties.

As Pitzer (1959) points out in his review article, London energies agree reasonably well for He and H_2, but for larger molecules serious disagreement, frequently by a factor of two, arises between theory and

experiment. Mayer (1933) found that the London calculations of the van der Waals coefficients were only half as large as those given by optical data for the alkali-halides. His experimental values for the dipole-dipole and dipole-quadrupole interactions for NaCl are given in Table 4-2-1. Mayer found that the dipole-quadrupole contribution to the cohesive energy, $\frac{C_2}{R^8}$ is between 10% and 20% of the dipole-dipole, $\frac{C}{R^6}$, contribution, while the quadrupole-quadrupole interaction, $\frac{C}{R^{10}}$, is negligible. More recently, Hajj (1966) has given the smaller values also given in Table 4-2-1.

Lennard-Jones and Dent (1927) observed that the O^{2-} ion is isoelectronic with the neon atom and used the coefficients found for the inert gas to describe the interaction of the O^{2-} ions in some rutile structures. The Lennard-Jones potential may be written in the form

$$\Phi_{ij}(\tilde{r}_{ij}) = 4\epsilon\left[\left(\frac{\sigma}{\tilde{r}_{ij}}\right)^{12} - \left(\frac{\sigma}{\tilde{r}_{ij}}\right)^{6}\right] = \tag{4-2-5}$$

$$= \frac{4\epsilon\sigma^{12}}{\tilde{r}_{ij}^{12}} - \frac{4\epsilon\sigma^{6}}{\tilde{r}_{ij}^{6}} = \frac{D}{\tilde{r}_{ij}^{12}} - \frac{C}{\tilde{r}_{ij}^{6}} .$$

Identifying $C_{BB} = 4\epsilon\sigma^6$, these values are given in Table 4-2-1 for Ne and Ar. The values of ϵ and σ are found from the measured bulk modulus and density of the inert gas crystals (Kittel, 1966) and are given in Table 4-2-1. Note that the C_{BB} is close to Mayer's value. Margenau (1939) computes the van der Waals constants for Ar and Ne to be

$$\Phi^{VDW} = -\frac{C_1}{R^6} - \frac{C_2}{R^8} - \frac{C_3}{R^{10}}$$

where for Ne: $C_1 = 4.67 \times 10^{-60}$, $C_2 = 6.9 \times 10^{-76}$, $C_3 = 5.3 \times 10^{-92}$

for Ar: $C_1 = 55.4 \times 10^{-60}$, $C_2 = 120 \times 10^{-76}$, $C_3 = 136 \times 10^{-92}$.

Hence, the larger value of C_{BB} found in the Lennard-Jones treatment is probably an effective sum of the dipole-dipole and higher order multipole interactions. For argon

$$-\frac{C_{BB}}{R^6} \text{ (Meyer)} = -\frac{103 \times 10^{-60}}{(3.76)^6 \times 10^{-48}} = .036 \times 10^{-12}$$

$$-\frac{C_1}{R^6} - \frac{C_2}{R^8} - \frac{C_3}{R^{10}} \text{ (Margenau)} = -\frac{55.4 \times 10^{-60}}{(3.76)^6 \times 10^{-48}} - \frac{120 \times 10^{-76}}{(3.76)^8 (10^{-64})}$$

$$- \frac{136 \times 10^{-92}}{(3.76)^{10} (10^{-80})} = .0196 + .003 + .00024$$

$$= .023 \times 10^{-12}.$$

In the remainder of this thesis, I will use the inert crystal potentials to characterize the anion-anion second neighbor interactions, since these contain the repulsive term as well as the van der Waals dipole-dipole term. This will be called the "inert crystal assumption".

The effect of these uncertainties in the van der Waals coefficients on the elastic constants and their pressure derivatives will be investigated in Chapter V where the individual structures are treated in detail. As Tosi (1964) points out, this uncertainty is not very important in

calculations of the cohesive energy since the van der Waals energy is only a few per cent of the total. Furthermore, uncertainties in the van der Waals energy are largely compensated by the adjustable parameters in the repulsive term $V_{ij}^{(r)}$. Born and Huang (1962, p. 28) state this quantitatively. They show that any term of the form A/R^n added to the energy expression will only change the total cohesive energy by

$$\Delta W = \frac{\left[\left(\frac{R_o}{\rho} - n\right)^2 + n\right]}{(R_o/\rho)^2} \left(\frac{A}{R^n}\right) . \qquad (4\text{-}2\text{-}6)$$

For a typical $R_o/\rho = 10$ the multiplicative factor is 0.2 for n = 6 and 0.1 for n = 8. Even though they contribute very little to the cohesive energy, Tosi (1964) has shown that the inclusion of the van der Waals terms systematically improves the fit between experimental and calculated cohesive energies for the alkali-halides.

It will be shown in the section on elastic constants that these terms are quite important, particularly in certain cases like the shear constant C_{44} for the NaCl structure, where the electrostatic and nearest-neighbor repulsive contributions are very small.

The Empirical Repulsive Potential

The two-body repulsive potential has traditionally been given one of the following two functional forms.

$$V_{ij}^{(r)} = B/r_{ij}^n \qquad \text{(Born and Landé, 1918a)}$$
$$V_{ij}^{(r)} = \lambda e^{-r_{ij}/\rho} \qquad \text{(Born and Mayer, 1932)} \qquad (4\text{-}2\text{-}7)$$

Each has two empirical parameters which are evaluated from the experimental values of the first and second volume derivatives of the energy; namely the density and bulk modulus at p = 0. Equations (4-2-7) represent the most basic assumption of the Born theory.

As discussed in section 4-1, quantum calculations for closed shell systems verify the exponential form as do the experimental cohesive energies calculated by Tosi (1964) and the elastic constant calculations given in Chapter V of this work. However, since the experimental tests are at low pressures, and for geophysical applications we wish to compute the elastic constants to strains of $V/V_o \approx 4.0/5.5 = .73$ at the base of the mantle, we wish to know if the exponential form is a good representation of the quantum repulsive energy over this compression range. In one attempt to answer this question, Kalinin (1960) has investigated the interaction between the closed shell systems He-He, Li^+- Li^+, and Be^{++}- Be^{++} on the quantum mechanical level. By minimizing the energy with respect to the constant $1/\rho$ in the exponent for various fixed values of the separation R, he computed $1/\rho$ as a function of R. He found that $1/\rho$ varied by less than 1% to pressures of the order of 10^4 kilobar for all three systems and concluded that the exponential form was a good representation of the energy of repulsion between atoms and ions with filled shells over the entire pressure range of geophysical interest. Of course, these calculations are for a 1-s shell which one would expect to be less deformable than the outer shells of more complex ions. However, Löwdin has shown that for alkali halides, the repulsive energy is approximately

exponential for compressions of at least 0.64.

The Cohesive Energy and Evaluation of the Empirical Parameters

The various terms discussed above will now be used in equation (4-0-6) for the internal energy density.

$$W = \frac{1}{2} N_A \sum_{\nu=1}^{S} \Phi_\nu \qquad \text{energy/mole}$$

$$\Phi_\nu = \text{potential energy of a } \nu\text{-type ion} \qquad (4\text{-}2\text{-}8)$$

$$S = \text{number of ions per molecule}$$

For ν = a cation, Φ_ν has the following form:

$$\Phi_\nu = \sum_{\text{all } j} \frac{q_\nu q_j}{r_{\nu j}} + \sum_{\substack{k \text{ nearest} \\ \text{anions}}} \left\{ -\frac{C_{\nu k}}{r_{\nu k}^6} + \lambda_{\nu k} e^{-r_{\nu k}/\rho_\nu} \right\}. \qquad (4\text{-}2\text{-}9)$$

For ν = an anion, Φ_ν has the form

$$\Phi_\nu = \sum_{\text{all } j} \frac{q_\nu q_j}{r_{\nu j}} + \sum_{\substack{k \text{ nearest} \\ \text{cations}}} \left\{ -\frac{C_{\nu k}}{r_{\nu k}^6} + \lambda_{\nu k} e^{-r_{\nu k}/\rho_\nu} \right\} \qquad (4\text{-}2\text{-}10)$$

$$+ \sum_{\substack{\ell \text{ nearest} \\ \text{anions} \\ \text{(second-neighbors)}}} \left\{ -\frac{C_{\nu \ell}}{r_{\nu \ell}^6} + \frac{D_{\nu \ell}}{r_{\nu \ell}^{12}} \right\}.$$

Notice that anion-anion interactions have been included while cation-cation interactions have not. This is because for all materials considered in this thesis the anion is larger than the cation. Hence, the anion overlap is greater than that of the cations. The energy density can thus be written

$$W = -\frac{N_A \alpha_M \phi q^2}{R} + \sum_{\nu \text{ cations}} Z_\nu \left\{ -\frac{C_{AB}}{(\rho_{\nu k} R)^6} + \lambda_\nu e^{-\frac{\rho_{\nu k} R}{\rho_\nu}} \right\}$$

$$+ \sum_{\nu' \text{anions}} \tfrac{1}{2} \eta_{\nu'} \left\{ -\frac{C_{BB}}{(\rho_{\nu' k} R)^6} + \frac{D_{BB}}{(\rho_{\nu' k} R)^{12}} \right\}$$

where Z_ν = number of nearest neighbors of ν-type cation

$\eta_{\nu'}$ = number of second neighbors of ν'-type anion

C_{AB} = cation-anion van der Waals coefficient

C_{BB} = anion-anion van der Waals coefficient

D_{BB} = Lennard-Jones anion-anion repulsive term

R = reference dimension

$r_{\nu k} = R\rho_{\nu k}$.

The equilibrium condition is $(dU/dR)_{\tilde{R}} = 0$ and the zero pressure bulk modulus is given by

$$\tilde{K} = \tilde{V}\left(\frac{\partial^2 U}{\partial V^2}\right)_{\sim} = \tilde{V}\left(\frac{\partial^2 U}{\partial R^2}\right)_{\sim}\left(\frac{\partial R}{\partial V}\right)_{\sim}^2 \quad = \text{Bulk modulus of the static lattice}.$$

Expressing $\tilde{V} = \tilde{R}^3/C_1$ = volume/mole of the static lattice

$R = (C_1 V)^{1/3}$ = linear edge of cubic reference cell

where C_1 = moles/reference cell = η_1 / N_A

η_1 = molecules/reference cell .

A tilde over a quantity means it is evaluated for the static lattice. The derivatives are easily performed. These two pieces of data allow two of the cation-anion repulsive parameters (λ_ν, ρ_ν) to be determined. The algebra will not be worked out here, but will be carried through as each structure is treated in Chapter V.

It is important to point out that $\tilde{K}$ and $\tilde{R}$ must be the bulk modulus and reference dimension of the static lattice which are obtained by linear extrapolation from the high-temperature data as explained in the next section.

4-3. Obtaining the Bulk Modulus and Density Appropriate to the Static Lattice

The P, V, T equation of state of a solid under hydrostatic pressure is

$$P = -(\partial F / \partial V)_T .$$

The harmonic vibrational spectrum of a collection of N_A ions can be represented by $3N_A$ independent oscillators having frequencies ν_i . Following the methods of statistical mechanics, we consider a canonical ensemble of microstates of possible energies

$$W(V) + \tfrac{1}{2}\sum_i h\nu_i + \sum_i n_i h\nu_i \qquad n_i = \text{integer} \qquad (4\text{-}3\text{-}1)$$

Since the oscillators are independent, the partition function Z may be written as a product of single oscillator partition functions

$$Z_1 = e^{-\left(W(V)/kT + \frac{1}{2kT}\sum_i h\nu_i\right)} \; Z_1 Z_2 Z_3 \ldots Z_{3N_A} \qquad (4\text{-}3\text{-}2)$$

$$Z_i = \sum_{n_i=1}^{\infty} e^{-hn_i\nu_i/kT} = \left(1 - e^{-h\nu_i/kT}\right)^{-1} .$$

The Helmholtz free energy may be calculated from the partition function as

$$F(V,T) = -kT \ln Z$$

$$= W(V) + \sum_i \left[\tfrac{1}{2} h\nu_i + kT \ln\left(1 - e^{-h\nu_i/kT}\right)\right] \qquad (4\text{-}3\text{-}3)$$

$$= W(V) + F_{vib}(V,T) .$$

The equation of state is thus

$$P = -(\partial F/\partial V)_T = -\frac{\partial W(V)}{\partial V} - \frac{1}{V}\sum_i \left[\frac{1}{2} h\nu_i + \frac{h\nu_i}{e^{h\nu_i/kT} - 1}\right] \frac{\partial \ln \nu_i}{\partial \ln V} . \qquad (4\text{-}3\text{-}4)$$

If one now makes the Einstein approximation that all ν_i are the same, and the Grüneisen approximation that all $\gamma_i = -\frac{\partial \ln \nu_i}{\partial \ln V} = \gamma$ are the same, one gets the Grüneisen equation of state

$$P = -\left(\frac{\partial W}{\partial V}\right) + \frac{\gamma E_{vib}}{V} \qquad (4\text{-}3\text{-}5)$$

where

$$E_{vib} = F_{vib} + TS = F_{vib} - T\left(\frac{\partial F}{\partial T}\right)_V = \frac{1}{2}\sum_i h\nu_i + kT \sum_i \frac{(h\nu_i/kT)}{e^{h\nu_i/kT} - 1} .$$

One need not make the Einstein approximation to get the Mie-Grüneisen equation of state. Tosi (1964) shows that the Mie-Grüneisen equation follows from the less restrictive assumption that the vibrational energy of the solid, divided by its temperature, be a function only of the

ratio between the temperature and a purely volume-dependent characteristic temperature. Thus equation (4-3-5) is also true for a Debye solid as shown in Born and Huang (1962, § 4).

Consider now the problem of evaluating the empirical repulsive parameters for the static lattice. The simplest assumption is that F_{vib} in equation (4-3-3) does not depend on the volume. To this approximation:

$$P = -\frac{\partial W}{\partial V} \qquad \left(\frac{\partial W}{\partial V}\right)_{\substack{P=0 \\ T=300^\circ K}} = 0$$

$$K(P=0, T=300^\circ K) = \left[V\left(\frac{\partial^2 W}{\partial V^2}\right)\right]_{\substack{P=0 \\ T=300}} . \tag{4-3-6}$$

Tosi (1964) has shown that this approximation of neglecting the volume dependence of F_{vib} leads to larger discrepancies in the calculated cohesive energy than neglecting van der Waals terms. A more realistic approach is to work with the Mie-Grüneisen equation (4-3-5). At P = 0, $T = T_o$

$$\left(\frac{dW}{\partial V}\right)_{V_o} = \frac{\gamma E_{vib}(T_o)}{V_o}$$

$$K(0,T_o) = -V_o\left(\frac{\partial P}{\partial V}\right)_{T_o} = V_o\left(\frac{\partial^2 W}{\partial V^2}\right)_{V_o} - V_o \frac{\partial}{\partial V}\left(\frac{\gamma E_{vib}}{V}\right)_{T_o, V_o} . \tag{4-3-7}$$

These equations may be used directly as outlined in Tosi (1964). However, often the temperature dependence of the density and the bulk modulus is known for temperatures above the Debye temperature. In this case a linear extrapolation from the high-temperature regime to

$T = 0°K$ gives $\tilde{V}$ and $\tilde{K}$, the molar volume and bulk modulus of the static lattice, as will now be demonstrated.

Following Born and Huang (1962, § 4) expand $W(V)$ about equilibrium volume $\tilde{V}$ defined by $(dW/dV)_{\tilde{V}} = 0$.

$$W(V) = \tilde{W} + \frac{1}{2}\frac{\partial^2 W}{\partial V^2}\Big|_{\tilde{V}}(V-\tilde{V})^2 + \frac{1}{3!}\frac{\partial^3 W}{\partial V^3}\Big|_{\tilde{V}}(V-\tilde{V})^3 + \cdots$$

Retaining only linear terms

$$\left(\frac{\partial W}{\partial V}\right) = \frac{\partial^2 W}{\partial V^2}\Big|_{\tilde{V}}(V-\tilde{V}) + \cdots$$

$$\left(\frac{\partial^2 W}{\partial V^2}\right) = \frac{\partial^2 W}{\partial V^2}\Big|_{\tilde{V}} + \frac{\partial^3 W}{\partial V^3}\Big|_{\tilde{V}}(V-\tilde{V}) + \cdots \quad . \tag{4-3-8}$$

At $P = 0$,

$$\frac{\partial^2 W}{\partial V^2}\Big|_{\tilde{V}}(V-\tilde{V}) = \frac{\gamma E_{vib}(T)}{V}$$

$$V = \tilde{V} + \frac{\tilde{V}}{\tilde{K}}\frac{\gamma}{V}E_{vib}(T) \quad .$$

If it can now be shown that the second term on the right-hand side is a linear function of T at high temperature, then the high-temperature data may be linearly extrapolated to $T = 0$ to get the equilibrium volume of the static lattice $\tilde{V}$.

Consider first the vibrational energy

$$E_{vib} = \tfrac{1}{2}\sum_i h\nu_i + kT\sum_i \frac{h\nu_i/kT}{e^{h\nu_i/kT}-1} \quad .$$

Let $x_i = h\nu_i/kT$. In the high-temperature limit $x_i << 1$

$$\approx \frac{1}{2}\sum_i h\nu_i + kT\sum_i \frac{x_i}{1+x_i+\frac{1}{2}x_i^2+\ldots-1}$$

$$\approx \frac{1}{2}\sum_i h\nu_i + kT\sum_i \frac{1}{1+\frac{1}{2}x_i}$$

$$\approx \frac{1}{2}\sum_i h\nu_i + kT\sum_i \left(1-\frac{1}{2}x_i\right)$$

$$= \frac{1}{2}\sum_i h\nu_i + 3N\,kT - \frac{kT}{2}\sum_i x_i$$

$$= \frac{1}{2}\sum_i h\nu_i + 3N\,kT - \frac{1}{2}\sum_i h\nu_i$$

$$= 3NkT \quad .$$

Thus at high temperatures

$$V = \tilde{V} + \frac{\tilde{V}}{\tilde{K}}\left(\frac{\gamma}{V}\right) 3NkT \quad . \tag{4-3-9}$$

If (γ/V) is a constant, then V may be extrapolated from the high-temperature regime to get $\tilde{V}$ as illustrated in Figure 4-3-1.

Consider now the bulk modulus in the high-temperature regime

$$\frac{K_T}{V} = -\left(\frac{\partial P}{\partial V}\right)_T = \frac{\partial^2 W}{\partial V^2} - \left[\frac{\partial}{\partial V}\left(\frac{\gamma}{V} E_{vib}\right)\right] \quad .$$

If (γ/V) is a constant (see Swenson, 1968), $(d/dV)(\gamma/V) = 0$ and we have

$$\frac{K}{V} = \frac{\partial^2 W}{\partial V^2} - \left(\frac{\gamma}{V}\right)\frac{\partial E_{vib}}{\partial V} .$$

Using (4-3-8) gives

$$\frac{K}{V} = \left.\frac{\partial^2 W}{\partial V^2}\right|_{\tilde{V}} + \left.\frac{\partial^3 W}{\partial V^3}\right|_{\tilde{V}}(V-\tilde{V}) - \left(\frac{\gamma}{V}\right)\frac{\partial E_{vib}}{\partial V} .$$

Identifying the first term as $\tilde{K}/\tilde{V}$ and using (4-3-9) on the second term gives

$$\frac{K}{V} = \frac{\tilde{K}}{\tilde{V}} + \left.\frac{\partial^3 W}{\partial V^3}\right|_{\tilde{V}}\frac{\tilde{V}}{\tilde{K}}\left(\frac{\gamma}{V}\right)3NkT - \left(\frac{\gamma}{V}\right)\frac{\partial E_{vib}}{\partial V} .$$

Differentiating equation (4-3-5) for E_{vib} and using the definition $C_V = (dE_{vib}/dT)_V$ one gets

$$\frac{\partial E_{vib}}{\partial V} = \left(E_{vib} - C_v T\right)\left(\frac{\gamma}{V}\right) .$$

So

$$\frac{K}{V} = \frac{\tilde{K}}{\tilde{V}} + \left[\left.\frac{\partial^3 W}{\partial V^3}\right|_{\tilde{V}}\frac{\tilde{V}}{\tilde{K}}\left(\frac{\gamma}{V}\right)3Nk - \left(\frac{\gamma}{V}\right)^2\left(3Nk - C_v\right)\right] T .$$

Under the assumption that (γ/V) is constant, K/V has the form

$$\frac{K}{V} = \frac{\tilde{K}}{\tilde{V}} + (\text{constant})\,T .$$

Thus a plot of K/V vs. T at $P = 0$ has an intercept of $\tilde{K}/\tilde{V}$ when extrapolated from the high-temperature regime.

All these arguments are hinged on the assumption that (γ/V) is a constant. Swenson (1968) gives arguments as to why this should be true, and Bassett et al. (1968) give data which show that in the relation

$\gamma/\gamma_o = (V/V_o)^a$, $a \approx 1$ for a wide range of solids.

Tosi (1964) reviews the various methods which have been used to handle the vibrational energy and thus arrive at empirical repulsive parameters appropriate to the static lattice. He finds that the difference between repulsive parameters found by equations (4-3-6) and those found for the static lattice after correcting for the vibrational contributions differ by up to 25%. Further he finds that the agreement between theoretical and experimental cohesive energies for the alkali halides are systematically improved upon making the thermodynamic corrections and that the magnitude of this improvement is larger than those caused by including van der Waals forces or second neighbors.

Table 4-2-1

Multipole Coefficients

The cation-anion interaction is $\phi_{AB}^{VDW} = -\frac{C_{AB}}{r_{AB}^6} - \frac{C_{AB}^+}{r_{AB}^8}$

The anion-anion interaction is $\phi_{BB}^{VDW} = -\frac{C_{BB}}{r_{BB}^6} + \frac{D_{BB}}{r_{BB}^{12}}$

NaCl	C_{AB} (10^{-60} ergs cm^6)	C_{BB} (10^{-60} ergs cm^6)	D_{BB} (10^{-106} ergs cm^{12})
Mayer (1933)	11.2	116	-
Hajj (1966)	11.7	64.5	-
Inert Crystal (Argon)		103	1594
MgO			
Huggins & Sakamoto (1957)	7.8	-	
Inert Crystal (Neon)	-	8.46	35.8

Table 4-2-1 (Continued)

Inert Crystal Parameters in the Lennard Jones

Potential $\phi_{BB} = 4\varepsilon \left[\left(\frac{\sigma}{r_{AB}} \right)^{12} - \left(\frac{\sigma}{r_{AB}} \right)^{6} \right]$

from Kittel (1966)

	σ (Å)	ε (10^{-16} ergs)	$(r_{AB})_o$ (Å)	$C_{BB} = 4\varepsilon\sigma^6$ (10^{-60} erg cm^6)	$D_{BB} = 4\varepsilon\sigma^{12}$ (10^{-106} ergs cm^{12})
Argon	3.40	167	3.76	103	1594
Neon	2.74	50	3.13	8.46	35.8

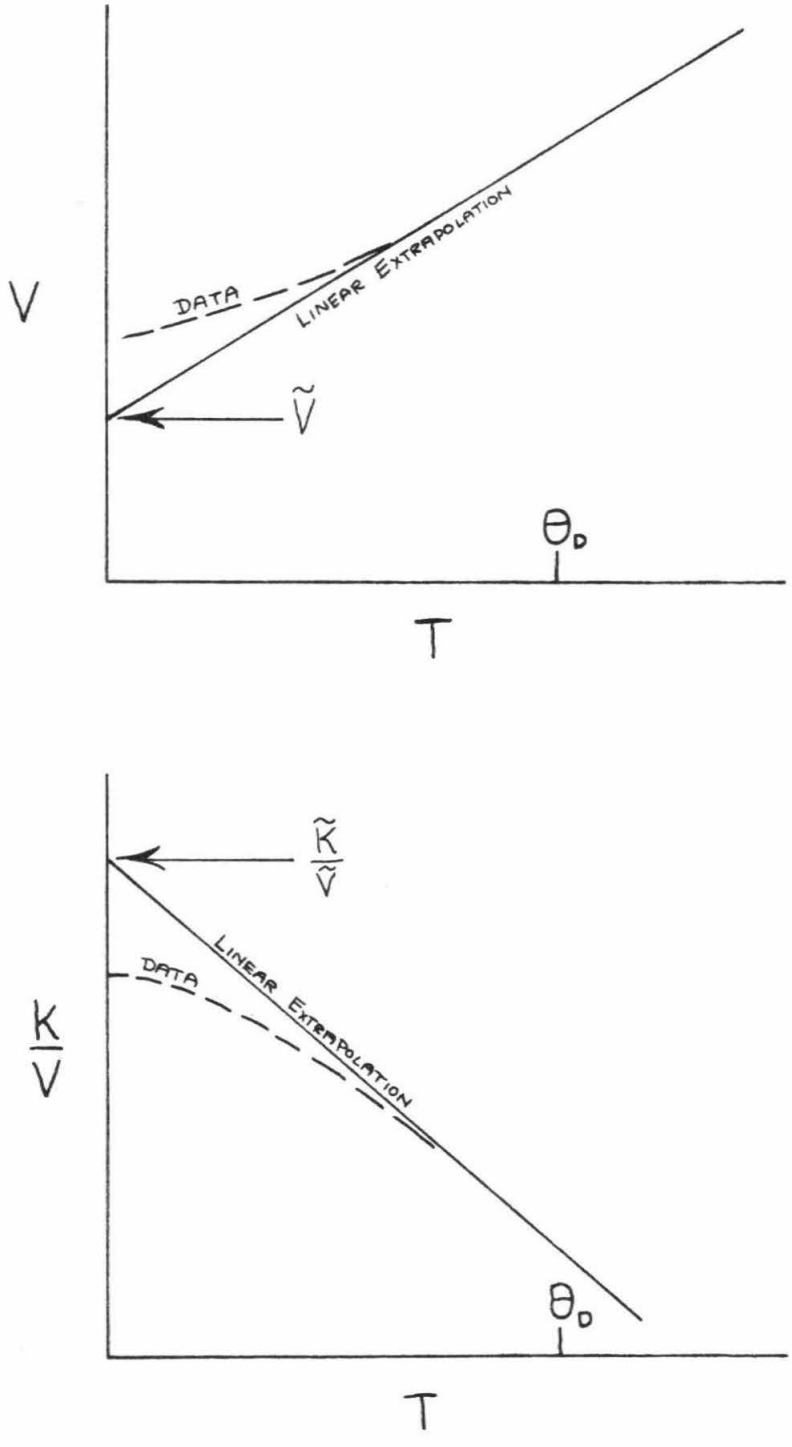

Figure 4-3-1. Linear extrapolation to obtain static lattice parameters.

V. SPECIALIZATION OF THE INTERATOMIC POTENTIAL MODEL TO SPECIFIC STRUCTURES OF GEOPHYSICAL INTEREST

5-1. The Sodium Chloride Structure

In this section equations (3-3-99) for the elastic constants will be specialized to the case of the cubic sodium chloride (rock salt) structure. Equations are given for the volume dependence of the elastic constants, as well as closed form expressions for their first and second pressure derivatives at P = 0. These expressions contain the electrostatic interactions, the empirical cation-anion repulsion, the cation-anion van der Waals interaction, and the anion-anion interaction as discussed in Chapter IV.

This section has two objectives. The first is to show how the general equations given in Chapter III, §3 are evaluated for an extremely simple, diatomic, cubic solid before investigating the more complicated, polyatomic, low-symmetry structures. The second objective is to explore the effects of the various terms in the potential on the elastic constants and their pressure derivatives.

The elastic constants and their pressure derivatives are evaluated for NaCl and MgO for direct comparison with the ultrasonic measurements of Spetzler, Sammis, and O'Connell (1970) and Spetzler (1970). MgO is of direct interest as a candidate material for the lower mantle below the 600 km discontinuity (Ringwood, 1970). NaCl is of interest because of its low bulk modulus relative to MgO (238 kbar vs. 1680 kbar). Since it undergoes a larger compression in the 10 kbar range presently accessible to ultrasonics than does MgO, it has been possible to

measure second pressure derivatives as well as the simultaneous temperature data necessary to make a first-order extrapolation to T = 0 for comparison with the static lattice results.

Specialization to the NaCl Structure

Because the elastic constants are symmetric with respect to the interchange of indices within each pair, each pair may be represented by one index as follows $\mathcal{S}_{\alpha\beta\gamma\lambda}$ $(\alpha,\beta,\gamma,\lambda = 1, 3) \rightarrow C_{ij}$ $(i, j = 1, 6)$.

Tensor Notation	Voigt Notation
11	1
22	2
33	3
23	4
31	5
12	6

(5-1-1)

For the special case of cubic symmetry, we have (see, for example, Nye, 1964, p. 140) three independent constants

$$C_{11} = C_{22} = C_{33} \qquad C_{12} = C_{21} = C_{23} = C_{32} = C_{13} = C_{31}$$

$$C_{44} = C_{55} = C_{66} .$$

All of the rest of the 6 x 6 = 36 possible C_{ij} are zero. From equation (3-3-99) we get

$$\begin{aligned} C_{11} &= \mathcal{S}_{1111} = [11, 11] + (11, 11) \\ C_{12} &= \mathcal{S}_{1122} = 2[12, 12] - [22, 11] + (11, 22) \\ C_{44} &= \mathcal{S}_{2323} = [22, 33] + (23, 23) . \end{aligned} \qquad (5\text{-}1\text{-}2)$$

Since the NaCl structure is centrosymmetric, the $\overline{C}^{(1)}_{\alpha\beta\gamma}(kk')$ vanish identically and thus so do the round brackets. The square brackets are written in terms of coulombic and non-coulombic parts

$$[\alpha\gamma,\beta\lambda] = [\alpha\gamma,\beta\lambda]^C + [\alpha\gamma,\beta\lambda]^N \qquad (5\text{-}1\text{-}3)$$

where the coulombic part is given by (3-3-54) (the details of the coulombic sums are given in Appendix 2) and the non-coulombic part by (3-3-103).

$$C_{11} = C^C_{11} + C^N_{11} = \frac{\alpha_{11} q^2}{2R^4} + \frac{1}{2V_a}\sum_{kk'\ell}\left\{P^{\ell}_{kk'}\chi_1(\overset{\ell}{kk'})^2 + Q^{\ell}_{kk'}\chi_1(\overset{\ell}{kk'})^4\right\}$$

$$C_{12} = C^C_{12} + C^N_{12} = \frac{\alpha_{12} q^2}{2R^4} + \frac{1}{2V_a}\sum_{kk'\ell}\left\{-P^{\ell}_{kk'}\chi_1(\overset{\ell}{kk'})^2 + Q^{\ell}_{kk'}\chi_1(\overset{\ell}{kk'})^2\chi_2(\overset{\ell}{kk'})^2\right\} \qquad (5\text{-}1\text{-}4)$$

$$C_{44} = C^C_{44} + C^N_{44} = \frac{\alpha_{44} q^2}{2R^4} + \frac{1}{2V_a}\sum_{kk'\ell}\left\{P^{\ell}_{kk'}\chi_1(\overset{\ell}{kk'})^2 + Q^{\ell}_{kk'}\chi_1(\overset{\ell}{kk'})^2\chi_2(\overset{\ell}{kk'})^2\right\}.$$

In these expressions

R = Nearest Neighbor Distance

$$P^{\ell}_{kk'} = \left[\frac{1}{r}\frac{\partial\Phi^N_{kk'}(r)}{\partial r}\right]_{r^{\ell}_{kk'}} \qquad (5\text{-}1\text{-}5)$$

$$Q^{\ell}_{kk'} = \left[\frac{1}{r}\frac{\partial}{\partial r}\left(\frac{1}{r}\frac{\partial\Phi^N_{kk'}(r)}{\partial r}\right)\right]_{r^{\ell}_{kk'}}$$

$\Phi^N_{kk'}(r)$ = Non-coulombic two-body potential between k and k' type ions

$$r^{\ell}_{kk'} = \left|\underset{\sim}{\chi}(\overset{\ell}{kk'})\right|$$

$$\underset{\sim}{\chi}(\overset{\ell}{kk'}) = \underset{\sim}{\chi}(\overset{o}{k}) - \underset{\sim}{\chi}(\overset{o}{k'}) + \ell_1\underset{\sim}{a}_1 + \ell_2\underset{\sim}{a}_2 + \ell_3\underset{\sim}{a}_3$$

$$\underset{\sim}{a}_1 = R(0, 1, 1)$$

$$\underset{\sim}{a}_2 = R(1, 0, 1)$$

$$\underset{\sim}{a}_3 = R(1, 1, 0)$$

$$V_a = \text{Volume of unit cell} = \underset{\sim}{a}_1 \cdot (\underset{\sim}{a}_2 \times \underset{\sim}{a}_3) = 2R^3 .$$

The α_{ij} in the coulombic parts of equations are dimensionless Madelung-like constants. The details of their calculation from equation (3-3-54) is given in Appendix 2 . Cowley (1962) gives for the NaCl structure

$$\alpha_{11} = -2.55604$$

$$\alpha_{12} = 0.11298$$

$$\alpha_{44} = 1.27802 .$$

These constants have certain internal cross-checks, $\alpha_{11} = -2\alpha_{44}$ and $(\alpha_{11}+2\alpha_{12})\frac{V_a}{2R^3} = -\frac{4}{3}\alpha_M$ which will be useful in checking these constants for more complex structures.

Indices $k = 0, n-1$ index the n primitive sublattices. For any compound AB in the rock salt structure, $n = 2$ and therefore three distinct two-body potentials $\Phi_{kk'}(r)$ must be specified. For the most general case considered in this section, we have for the non-coulombic $\Phi^N_{kk'}(r)$

$$\text{cation-cation} \quad \Phi^N_{AA}(r) = 0$$

$$\text{cation-anion} \quad \Phi^N_{AB}(r) = V_{AB}(r) - \frac{C_{AB}}{\left(r^{\ell}_{AB}\right)^6} \qquad (5\text{-}1\text{-}6)$$

$$\text{anion-anion} \quad \Phi^N_{BB}(r) = -\frac{C_{BB}}{\left(r^{\ell}_{BB}\right)^6} + \frac{D_{BB}}{\left(r^{\ell}_{BB}\right)^{12}} .$$

The terms on the r.h.s. of these equations are discussed in section 4-2 on the potential. In this section we will make calculations for both the Born-Landé (1918a) and the Born-Mayer (1932) forms of the empirical, two-body, repulsive potential. Respectively, these are

$$V_{AB}(r) = \frac{B}{(r_{AB}^{\ell})^n}$$
$$V_{AB}(r) = \lambda e^{-r_{AB}^{\ell}/\rho} . \qquad (5-1-7)$$

The cation-anion interaction is over nearest neighbors, while the anion-anion interaction is over what are usually termed second neighbors. These sums are worked out in Table 5-1-1. For the cation-anion interaction

$$P_{AB} = \left[\frac{1}{r}\frac{d\Phi_{AB}^{N}}{dr}\right]_R = \frac{1}{R}\left(V_{AB}'\right)_R + \frac{6C_{AB}}{R^8}$$
$$Q_{AB} = \left[\frac{1}{r}\frac{d}{dr}\left(\frac{1}{r}\frac{d\Phi_{AB}^{N}}{dr}\right)\right]_R = -\frac{1}{R^3}\left(V_{AB}'\right)_R + \frac{1}{R^2}\left(V_{AB}''\right)_R - \frac{48C_{AB}}{R^{10}} . \qquad (5-1-8)$$

For the anion-anion interaction

$$P_{BB} = \left[\frac{1}{r}\frac{d\Phi_{BB}^{N}}{dr}\right]_{r_{BB}} = \frac{6C_{BB}}{r_{BB}^8} - \frac{12D_{BB}}{r_{BB}^{14}} = \frac{3}{8}\frac{C_{BB}}{R^8} - \frac{3}{32}\frac{D_{BB}}{R^{14}}$$
$$Q_{BB} = \left[\frac{1}{r}\frac{d}{dr}\left(\frac{1}{r}\frac{d\Phi_{BB}^{N}}{dr}\right)\right]_{r_{BB}} = -\frac{48C_{BB}}{r_{BB}^{10}} + \frac{168D_{BB}}{r_{BB}^{16}} \qquad (5-1-9)$$
$$= -\frac{3}{2}\frac{C_{BB}}{R^{10}} + \frac{21}{32}\frac{D_{BB}}{R^{16}} .$$

The prime denotes differentiation w.r.t. r.

After doing the short-range sums, the expressions for the elastic constants become

$$C_{11} = \frac{\alpha_{11} \vartheta q^2}{2R^4 v_0} + \frac{1}{V_a}\left\{\left(2P_{AB} + 4P_{BB}\right)R^2 + \left(2Q_{AB} + 4Q_{BB}\right)R^4\right\}$$

$$C_{12} = \frac{\alpha_{12} \vartheta q^2}{2R^4 v_0} + \frac{1}{V_a}\left\{\left(-2P_{AB} - 4P_{BB}\right)R^2 + 2Q_{BB}R^4\right\} \qquad (5\text{-}1\text{-}10)$$

$$C_{44} = \frac{\alpha_{44} \vartheta q^2}{2R^4 v_0} + \frac{1}{V_a}\left\{\left(2P_{AB} + 4P_{BB}\right)R^2 + 2Q_{BB}R^4\right\}.$$

Note that the identical terms $P_{AB} = P_{BA}$ and $Q_{AB} = Q_{BA}$ have already been combined, thus eliminating one factor of one-half. However, the P_{BB} and Q_{BB} terms must still be divided by two to avoid counting the B–B interaction twice. Substituting equations (5-1-8) and (5-1-9) for $P_{kk'}$ and $Q_{kk'}$ gives

$$C_{11} = \frac{\alpha_{11} \vartheta q^2}{2R^4 v_0} + \frac{V''_{AB}}{R} - \frac{42C_{AB}}{R^9} - \frac{9}{4}\frac{C_{BB}}{R^9} + \frac{9}{8}\frac{D_{BB}}{R^{15}}$$

$$C_{12} = \frac{\alpha_{12} \vartheta q^2}{2R^4 v_0} - \frac{V'_{AB}}{R^2} - \frac{6C_{AB}}{R^9} - \frac{9}{4}\frac{C_{BB}}{R^9} + \frac{27}{32}\frac{D_{BB}}{R^{15}} \qquad (5\text{-}1\text{-}11)$$

$$C_{44} = \frac{\alpha_{44} \vartheta q^2}{2R^4 v_0} + \frac{V'_{AB}}{R^2} + \frac{6C_{AB}}{R^9} - \frac{3}{4}\frac{C_{BB}}{R^9} + \frac{15}{32}\frac{D_{BB}}{R^{15}}.$$

Evaluation of the Empirical Parameters in V_{AB} and Expressions for the Bulk Modulus

Before the elastic constants may be calculated, we need to evaluate the two empirical constants in the cation-anion repulsive potential. These are obtained from the zero-pressure density and bulk modulus as follows.

The energy density of the static lattice is given by

$$W = \tfrac{1}{2}N_A(U_A + U_B) \text{ energy/mole} \qquad (5\text{-}1\text{-}12)$$

where U_A = energy per cation and U_B = energy per anion. The factor of one-half corrects for having counted each interaction twice.

$$U_A = -\frac{\alpha_M q^2}{R} + Z_{AB}\left[V_{AB}(R) - \frac{C_{AB}}{R^6}\right]$$

$$U_B = -\frac{\alpha_M q^2}{R} + Z_{AB}\left[V_{AB}(R) - \frac{C_{AB}}{R^6}\right] + \tag{5-1-13}$$

$$+ Z_{BB}\left[-\frac{C_{BB}}{8R^6} + \frac{D_{BB}}{64R^{12}}\right]$$

Where α_M = Madelung constant = 1.747558

Z_{AB} = # of nearest neighbors = 6

Z_{BB} = # of second neighbors = 12 .

Equation (5-1-13) becomes

$$W = \tfrac{1}{2}N_A\{U_A + U_B\} = N_A\left\{-\frac{\alpha_M q^2}{R} + Z_{AB}\left[V_{AB}(R) - \frac{C_{AB}}{R^6}\right] + \right. \tag{5-1-14}$$

$$\left. + \frac{Z_{BB}}{2}\left[-\frac{C_{BB}}{8R^6} + \frac{D_{BB}}{64R^{12}}\right]\right\} .$$

The equilibrium equation may be written as

$$(dW/dR)\Big|_{\tilde{R}} = 0$$

where the $\sim$ denotes the equilibrium state for the static lattice.

$$\left.\frac{dW}{dR}\right|_{\tilde{R}} = N_A\left\{\frac{\alpha_M q^2}{\tilde{R}^2} + Z_{AB}\left[V'_{AB}(\tilde{R}) + \frac{6C_{AB}}{\tilde{R}^7}\right] + \right. \tag{5-1-15}$$

$$\left. + \frac{Z_{BB}}{2}\left[\frac{3C_{BB}}{4R^7} - \frac{3D_{BB}}{16\tilde{R}^{13}}\right]\right\} = 0$$

The bulk modulus is computed according to the relation

$$K = V \frac{d^2 W}{dV^2}$$

where V = volume/mole = $2N_A R^3$. Since the energy is expressed as a function of the nearest neighbor distance R, the volume derivative may be more easily evaluated if it is transformed to a derivative with respect to R using the chain rule.

$$\frac{\partial^2 W}{\partial V^2} = \frac{\partial^2 W}{\partial R^2}\left(\frac{\partial R}{\partial V}\right)^2 + \frac{\partial W}{\partial R}\frac{\partial^2 R}{\partial V^2} \tag{5-1-16}$$

Since

$$R = \left(\frac{V}{2N_A}\right)^{1/3} \quad ; \quad \frac{\partial R}{\partial V} = \frac{1}{6N_A}\left(\frac{1}{R}\right)^2 \tag{5-1-17}$$

$$\frac{\partial^2 R}{\partial V^2} = \frac{-1}{18 N_A^2}\left(\frac{1}{R}\right)^5 .$$

At equilibrium

$$\left.\frac{\partial^2 W}{\partial V^2}\right|_{\tilde{V}} = \left.\frac{\partial^2 W}{\partial R^2}\right|_{\tilde{R}} \left[\frac{1}{36 N_A^2 \tilde{R}^4}\right] . \tag{5-1-18}$$

Differentiating equation (5-1-15) one more time gives

$$\frac{\partial^2 W}{\partial R^2} = N_A \left\{ -\frac{2\alpha m q^2}{R^3} + Z_{AB}\left[V''_{AB}(R) - \frac{42\, C_{AB}}{R^8}\right] \right. \tag{5-1-19}$$

$$\left. + \frac{Z_{BB}}{2}\left[-\frac{21}{4}\frac{C_{BB}}{R^8} + \frac{39}{16}\frac{D_{BB}}{R^{14}}\right]\right\} .$$

At equilibrium

$$\tilde{K} = \tilde{V}\left.\frac{\partial^2 W}{\partial V^2}\right|_{\tilde{V}} = 2N_A\tilde{R}^3\left[\frac{1}{36N_A^2\tilde{R}^4}\right]N_A\left\{-\frac{2\alpha_m d q^2}{\tilde{R}^3} + \right. \tag{5-1-20}$$

$$\left. + Z_{AB}\left[V''_{AB}(\tilde{R}) - \frac{42C_{AB}}{\tilde{R}^8}\right] + \frac{Z_{BB}}{2}\left[-\frac{42C_{BB}}{8\tilde{R}^8} + \frac{156D_{BB}}{64\tilde{R}^{14}}\right]\right\}$$

which simplifies to

$$\tilde{K} = \frac{1}{18}\left\{-\frac{2\alpha_m d q^2}{\tilde{R}^4} + Z_{AB}\left[\frac{V''_{AB}(\tilde{R})}{\tilde{R}} - \frac{42C_{AB}}{\tilde{R}^9}\right]\right. \tag{5-1-21}$$

$$\left. + \frac{Z_{BB}}{2}\left[-\frac{21}{4}\frac{C_{BB}}{\tilde{R}^9} + \frac{39}{16}\frac{D_{BB}}{\tilde{R}^{15}}\right]\right\}.$$

We now wish to use equations (5-1-15) and (5-1-21) to evaluate the two empirical parameters in $V_{AB}(R)$ in terms of the experimental values of $\tilde{K}$ and $\tilde{R} = (M/2N_A\tilde{\rho})^{1/3}$ where M is the atomic weight and $\tilde{\rho}$ is the density.

This may be done rather easily for both the power-law and the exponential forms of the potential because of the following properties of these functions.

Power Law	Exponential
$V_{AB} = B/R^n$	$V_{AB} = \lambda e^{-R/\rho}$
$V'_{AB} = \frac{-n}{R}V_{AB}$	$V'_{AB} = -\frac{V_{AB}}{\rho}$
$V''_{AB} = \frac{n(n+1)}{R^2}V_{AB}$	$V''_{AB} = \frac{V_{AB}}{\rho^2}$
$V'''_{AB} = \frac{-n(n+1)(n+2)}{R^3}V_{AB}$	$V'''_{AB} = -\frac{V_{AB}}{\rho^3}$
$V^{IV}_{AB} = \frac{n(n+1)(n+2)(n+3)}{R^4}V_{AB}$	$V^{IV}_{AB} = \frac{V_{AB}}{\rho^4}$

(5-1-22)

Note that for both functional forms of the potential

$$V''_{AB} = -\frac{\delta}{R} V'_{AB}$$

$$\delta = n + 1 \text{ for the power-law potential} \qquad (5\text{-}1\text{-}23)$$

$$\delta = \tilde{R}/\rho \text{ for the exponential potential} .$$

This has been pointed out by Anderson (1970), although it is not characteristic of a general potential as he suggests. Solving equation (5-1-15) for $(V'_{AB})|_{\tilde{R}}$

$$V'_{AB}\Big|_{\tilde{R}} = \frac{1}{Z_{AB}}\left\{-\frac{\alpha_m \tilde{q}^2}{\tilde{R}^2 \tilde{v}} - \frac{Z_{BB}}{2}\left[\frac{3}{4}\frac{C_{BB}}{\tilde{R}^7} - \frac{3}{16}\frac{D_{BB}}{\tilde{R}^{13}}\right]\right\} - \frac{6C_{AB}}{\tilde{R}^7} . \qquad (5\text{-}1\text{-}24)$$

So, according to equation (5-1-23)

$$V''_{AB} = -\frac{\delta}{R}\left\langle \frac{1}{Z_{AB}}\left\{\frac{-\alpha \tilde{q}^2}{R^2}\right\} - \frac{Z_{BB}}{2}\left[\frac{3}{4}\frac{C_{BB}}{R^7} - \frac{3}{16}\frac{D_{BB}}{R^{13}}\right]\right\} - \frac{6C_{AB}}{R^7}\Big\rangle . \qquad (5\text{-}1\text{-}25)$$

Substituting this expression into equation (5-1-21) gives

$$18\tilde{K} = -\frac{2\alpha \tilde{q}^2}{\tilde{R}^4 \tilde{v}} + \frac{Z_{AB}\delta}{\tilde{R}^2}\left\langle \frac{1}{Z_{AB}}\left[\frac{\alpha \tilde{q}^2}{\tilde{R}^2 \tilde{v}} + \frac{Z_{BB}}{2}\left(\frac{3}{4}\frac{C_{BB}}{\tilde{R}^7} - \frac{3}{16}\frac{D_{BB}}{\tilde{R}^{13}}\right)\right] + \right.$$

$$\left. + \frac{6C_{AB}}{\tilde{R}^7}\right\rangle - 42 Z_{AB}\frac{C_{AB}}{\tilde{R}^9} + \frac{Z_{BB}}{2}\left[-\frac{21}{4}\frac{C_{BB}}{\tilde{R}^9} + \frac{39}{16}\frac{D_{BB}}{\tilde{R}^{14}}\right] . \qquad (5\text{-}1\text{-}26)$$

Solving this equation for δ gives

$$\delta = \frac{18\tilde{K} + \frac{2\alpha \tilde{q}^2}{\tilde{R}^4 \tilde{v}} + \frac{42 Z_{AB} C_{AB}}{\tilde{R}^9} - \frac{Z_{BB}}{2}\left[-\frac{21}{4}\frac{C_{BB}}{\tilde{R}^9} + \frac{39}{16}\frac{D_{BB}}{\tilde{R}^{14}}\right]}{\frac{\alpha_m \tilde{q}^2}{\tilde{R}^4 \tilde{v}} + 6 Z_{AB}\frac{C_{AB}}{\tilde{R}^9} + \frac{Z_{BB}}{2}\left(\frac{3}{4}\frac{C_{BB}}{\tilde{R}^9} - \frac{3}{16}\frac{D_{BB}}{\tilde{R}^{15}}\right)} . \qquad (5\text{-}1\text{-}27)$$

Note that for the simpler case of nearest neighbor interactions only and no van der Waals terms, equation (5-1-27) above simplifies to

$$\delta = \frac{18\tilde{K}\tilde{R}^4}{\alpha_m \not{d} q^2} + 2$$

as given by Kittel (1966). It is interesting to note that the relation $\tilde{R}/\rho = n + 1$ follows from the relations (5-1-23) and (5-1-24) and is independent of the number of interactions added onto the potential. Once δ has been determined, the other constants in $V_{AB}(R)$ may be determined from equation (5-1-24).

$$B = \frac{\tilde{R}^{n+1}}{n Z_{AB}} \left\{ \frac{\alpha_m \not{d} q^2}{\tilde{R}^2} + 6 Z_{AB} \frac{C_{AB}}{\tilde{R}^7} + \frac{Z_{BB}}{2} \left[\frac{3}{4} \frac{C_{BB}}{\tilde{R}^7} - \frac{3}{16} \frac{D_{BB}}{\tilde{R}^{13}} \right] \right\} \tag{5-1-28}$$

$$\lambda = \frac{\tilde{R} e^{\tilde{R}/\rho}}{(R/\rho) Z_{AB}} \left\{ \frac{\alpha_m \not{d} q^2}{\tilde{R}^2} + 6 Z_{AB} \frac{C_{AB}}{\tilde{R}^7} + \frac{Z_{BB}}{2} \left[\frac{3}{4} \frac{C_{BB}}{\tilde{R}^7} - \frac{3}{16} \frac{D_{BB}}{\tilde{R}^{13}} \right] \right\}$$

The volume dependence of the bulk modulus is given by

$$K(R) = V \frac{\partial^2 W}{\partial V^2} = V \left[\frac{\partial^2 W}{\partial R^2} \left(\frac{\partial R}{\partial V} \right)^2 + \frac{\partial W}{\partial R} \frac{\partial^2 R}{\partial V^2} \right]$$

$$= \frac{1}{18} \left\{ -\frac{4 \alpha_m \not{d} q^2}{R^4} + Z_{AB} \left[\frac{V''_{AB}}{R} - \frac{2 V'_{AB}}{R^2} - \frac{54 C_{AB}}{R^9} \right] + \right. \tag{5-1-29}$$

$$\left. + \frac{Z_{BB}}{2} \left[-\frac{27}{4} \frac{C_{BB}}{R^9} + \frac{45}{16} \frac{D_{BB}}{R^{15}} \right] \right.$$

As a direct check on the algebra, this equation is identical term for term with $1/3\ (C_{11} + 2C_{12})$ calculated from equations (5-1-11).

At equilibrium (P = 0)

$$\frac{V''_{AB}}{\tilde{R}} - \frac{2V'_{AB}}{\tilde{R}^2} = -\frac{V'_{AB}|_{\tilde{R}}}{\tilde{R}^2}(\delta+2)$$

is the same for both functional forms of V_{AB}. This must be true since $K(\tilde{R})$ is one of the two input parameters. However, at $R \neq \tilde{R}$, the two potentials give a different predicted value of K(R) since in general the power-law expression

$$\frac{V''_{AB}(R)}{R} - \frac{2V'_{AB}(R)}{R^2} = n(n+3)\frac{V_{AB}(R)}{R^3}$$

does not equal the exponential expression

$$\frac{V''_{AB}(R)}{R} - \frac{2V'_{AB}(R)}{R^2} = \frac{R}{\rho}\left(\frac{R}{\rho}+2\right)\frac{V_{AB}(R)}{R^3}.$$

For the power-law potential

$$K(R) = \frac{1}{18}\left\{-\frac{4\alpha_M q^2}{R^4} + Z_{AB}\left[n(n+3)\frac{V_{AB}(R)}{R^3} - 54\frac{C_{AB}}{R^9}\right] + \right.$$
$$\left. + \frac{Z_{BB}}{2}\left[-\frac{27}{4}\frac{C_{BB}}{R^9} + \frac{45}{16}\frac{D_{BB}}{R^{15}}\right]\right\}. \qquad (5\text{-}1\text{-}30)$$

For the exponential potential

$$K(R) = \frac{1}{18}\left\{-\frac{4\alpha_M q^2}{R^4} + Z_{AB}\left[\frac{R}{\rho}\left(\frac{R}{\rho}+2\right)\frac{V_{AB}(R)}{R^3} - \frac{54C_{AB}}{R^9}\right] + \right.$$
$$\left. + \frac{Z_{BB}}{2}\left[-\frac{27}{4}\frac{C_{BB}}{R^9} + \frac{45}{16}\frac{D_{BB}}{R^{15}}\right]\right\}. \qquad (5\text{-}1\text{-}31)$$

The pressure volume relation is given by

$$P = -\frac{\partial W}{\partial V} = -\frac{\partial W}{\partial R}\frac{\partial R}{\partial V} = \tag{5-1-32}$$

$$= -\frac{1}{6}\left\{\frac{\alpha_M \not{d} q^2}{R^4} + Z_{AB}\left[\frac{V'_{AB}(R)}{R^2} + \frac{6C_{AB}}{R^9}\right] + \frac{Z_{BB}}{2}\left[\frac{3}{4}\frac{C_{BB}}{R^9} - \frac{3}{16}\frac{D_{BB}}{R^{15}}\right]\right\}.$$

Equations (5-1-11) for the volume dependence of the elastic constants may be written (using equations (5-1-22))

(a) Power-law Potential

$$C_{11} = \frac{\alpha_{11} \not{d} q^2}{2R^4} + \frac{n(n+1)V_{AB}}{R^3} - \frac{42C_{AB}}{R^9} - \frac{9}{4}\frac{C_{BB}}{R^9} + \frac{9}{8}\frac{D_{BB}}{R^{15}}$$

$$C_{12} = \frac{\alpha_{12} \not{d} q^2}{2R^4} + n\frac{V_{AB}}{R^3} - \frac{6C_{AB}}{R^9} - \frac{9}{4}\frac{C_{BB}}{R^9} + \frac{27}{32}\frac{D_{BB}}{R^{15}}$$

$$C_{44} = \frac{\alpha_{44} \not{d} q^2}{2R^4} - n\frac{V_{AB}}{R^3} + 6\frac{C_{AB}}{R^9} - \frac{3}{4}\frac{C_{BB}}{R^9} + \frac{15}{32}\frac{D_{BB}}{R^{15}} \tag{5-1-33}$$

(b) Exponential Potential

$$C_{11} = \frac{\alpha_{11} \not{d} q^2}{2R^4} + \left(\frac{R}{\rho}\right)^2\frac{V_{AB}}{R^3} - \frac{42C_{AB}}{R^9} - \frac{9}{4}\frac{C_{BB}}{R^9} + \frac{9}{8}\frac{D_{BB}}{R^{15}}$$

$$C_{12} = \frac{\alpha_{12} \not{d} q^2}{2R^4} + \frac{R}{\rho}\frac{V_{AB}}{R^3} - \frac{6C_{AB}}{R^9} - \frac{9}{4}\frac{C_{BB}}{R^9} + \frac{27}{32}\frac{D_{BB}}{R^{15}}$$

$$C_{44} = \frac{\alpha_{44} \not{d} q^2}{2R^4} - \frac{R}{\rho}\frac{V_{AB}}{R^3} + \frac{6C_{AB}}{R^9} - \frac{3}{4}\frac{C_{BB}}{R^9} + \frac{15}{32}\frac{D_{BB}}{R^{15}}.$$

Expressions for the First and Second Pressure Derivatives of the Elastic Constants at P = 0

Expressions will now be derived for the first and second pressure derivatives of the elastic constants at P = 0. These expressions are useful in making a direct comparison with the ultrasonic data.

The pressure derivatives are computed according to the relation

$$\frac{\partial C_{ij}}{\partial P} = \frac{\partial C_{ij}/\partial R}{\partial P/\partial R} \tag{5-1-34}$$

$$\frac{\partial^2 C_{ij}}{\partial P^2} = \frac{\partial}{\partial R}\left(\frac{\partial C_{ij}}{\partial P}\right)\frac{\partial R}{\partial P} .$$

The relation dR/dP = -R/3K allows these equations to be written (at P = 0)

$$\left.\frac{\partial C_{ij}}{\partial P}\right|_{\tilde{R}} = -\frac{\tilde{R}}{3\tilde{K}}\left.\left(\frac{\partial C_{ij}}{\partial R}\right)\right|_{\tilde{R}} \tag{5-1-35}$$

$$\frac{\partial^2 C_{ij}}{\partial P^2} = \frac{\tilde{R}}{3\tilde{K}}\left\{\frac{\tilde{R}}{3\tilde{K}}\left.\frac{\partial^2 C_{ij}}{\partial R^2}\right|_{\tilde{R}} + \frac{1}{\tilde{K}}\left[\left.\frac{\partial K}{\partial P}\right|_{\tilde{R}} + \frac{1}{3}\right]\left.\frac{\partial C_{ij}}{\partial R}\right|_{\tilde{R}}\right\}$$

$$\left.\frac{\partial^2 C_{ij}}{\partial P^2}\right|_{\tilde{R}} = \left(\frac{\tilde{R}}{3\tilde{K}}\right)^2 \left.\frac{\partial^2 C_{ij}}{\partial R^2}\right|_{\tilde{R}} - \frac{1}{\tilde{K}}\left[\left.\frac{\partial K}{\partial P}\right|_{\tilde{R}} + \frac{1}{3}\right]\left.\frac{\partial C_{ij}}{\partial P}\right|_{\tilde{R}} \tag{5-1-36}$$

where C_{ij} represents any one of the three independent elastic constants or the bulk modulus.

Consider first the bulk modulus

$$\left.\frac{\partial K}{\partial P}\right|_{\sim} = -\frac{\tilde{R}}{3\tilde{R}}\left.\frac{\partial K}{\partial R}\right|_{\sim} .$$

Differentiation of equation (5-1-30) for the power-law potential

$$\left.\frac{dK}{dP}\right|_{\sim} = \frac{-1}{54\tilde{K}}\left\{\frac{16\alpha_M \Phi q^2}{\tilde{R}^4} + Z_{AB}\left[-n(n+3)^2\frac{V_{AB}}{\tilde{R}^3} + 486\frac{C_{AB}}{\tilde{R}^9}\right] + \right.$$

$$\left. + \frac{Z_{BB}}{2}\left[\frac{243}{4}\frac{C_{BB}}{\tilde{R}^9} - \frac{675}{16}\frac{D_{BB}}{\tilde{R}^{15}}\right]\right\}. \qquad (5\text{-}1\text{-}37)$$

The equilibrium equation (5-1-15) may be used to further simplify the expression to

$$\left.\frac{dK}{dP}\right|_{\sim} = \frac{-1}{54\tilde{K}}\left\{Z_{AB}\left[-n(n+7)(n-1)\frac{V_{AB}}{\tilde{R}^3} + 390\frac{C_{AB}}{\tilde{R}^9}\right] + \right.$$

$$\left. + \frac{Z_{BB}}{2}\left[\frac{195}{4}\frac{C_{BB}}{\tilde{R}^9} - \frac{627}{16}\frac{D_{BB}}{\tilde{R}^{15}}\right]\right\}. \qquad (5\text{-}1\text{-}38)$$

For the case of nearest neighbor interaction only and no van der Waals terms $(dK/dP)|_{\sim}$ can be shown to have a simple form

$$\left.\frac{dK}{dP}\right|_{\sim} = \frac{n+7}{3} \quad .$$

Differentiation of equation (5-1-30) for the exponential potential gives

$$\left.\frac{dK}{dP}\right|_{\sim} = \frac{-1}{54\tilde{K}}\left\{\frac{16\alpha_M \Phi q^2}{\tilde{R}^4} + Z_{AB}\left[-\left\langle\left(\frac{\tilde{R}}{\rho}\right)^3 + 3\left(\frac{\tilde{R}}{\rho}\right)^2 + 4\frac{\tilde{R}}{\rho}\right\rangle\frac{V_{AB}}{\tilde{R}^3} + 486\frac{C_{AB}}{\tilde{R}^9}\right] + \right.$$

$$\left. + \frac{Z_{BB}}{2}\left[\frac{243}{4}\frac{C_{BB}}{\tilde{R}^9} - \frac{675}{16}\frac{D_{BB}}{\tilde{R}^{15}}\right]\right\}.$$

Again using the equilibrium equation to rewrite the first term gives

$$\left.\frac{dK}{dP}\right|_{\sim} = \frac{-1}{54\tilde{K}}\left\{Z_{AB}\left[\left\langle-\left(\frac{\tilde{R}}{\rho}\right)^3 - 3\left(\frac{\tilde{R}}{\rho}\right)^2 + 12\frac{\tilde{R}}{\rho}\right\rangle\frac{V_{AB}}{\tilde{R}^3} + 390\frac{C_{AB}}{\tilde{R}^9}\right] + \right.$$

$$\left. + \frac{Z_{BB}}{2}\left[\frac{195}{4}\frac{C_{BB}}{\tilde{R}^9} - \frac{627}{16}\frac{D_{BB}}{\tilde{R}^{15}}\right]\right\}. \qquad (5\text{-}1\text{-}39)$$

In the case of nearest neighbor interactions only and no van der Waals terms $(dK/dP)|_{\tilde{R}}$ again has a simple form

$$\left.\frac{dK}{dP}\right|_{\sim} = \frac{1}{3\left(\frac{\tilde{R}}{\rho}-2\right)}\left[\left(\tilde{R}/\rho+1\right)\left(\tilde{R}/\rho+2\right)-14\right].$$

The second pressure derivative of the bulk modulus is now computed according to equation (5-1-36). In this case equation (5-1-35) may be used to simplify equation (5-1-36) to the form

$$\left.\frac{d^2K}{dP^2}\right|_{\sim} = \left(\frac{\tilde{R}}{3\tilde{K}}\right)^2 \left.\frac{d^2K}{dR^2}\right|_{\sim} - \frac{1}{\tilde{K}}\left[\left.\frac{dK}{dP}\right|_{\sim} + \frac{1}{3}\right]\left.\frac{dK}{dP}\right|_{\sim}. \qquad (5\text{-}1\text{-}40)$$

Equation (5-1-38) or (5-1-39) is used for (dK/dP) depending on the assumed form of V_{AB}. Consider first the power-law potential. Differentiating equation (5-1-37) with respect to R and using the equilibrium condition gives

$$\left.\frac{d^2K}{dP^2}\right|_{\sim} = \frac{1}{162\tilde{K}^2}\left\{Z_{AB}\left[\left(n(n+4)(n+3)^2-80n\right)\frac{\tilde{V}_{AB}}{\tilde{R}^3} - 4380\frac{C_{AB}}{\tilde{R}^9}\right] + \right. \qquad (5\text{-}1\text{-}41)$$

$$\left. + \frac{Z_{BB}}{2}\left[-\frac{1095}{2}\frac{C_{BB}}{\tilde{R}^9} + 660\frac{D_{BB}}{\tilde{R}^{15}}\right]\right\} - \left[\left.\frac{dK}{dP}\right|_{\sim} + \frac{1}{3}\right]\frac{1}{\tilde{K}}\left.\frac{dK}{dP}\right|_{\sim}.$$

For the case of nearest neighbors only and no van der Waals terms, $(d^2K/dP^2)|_{\sim}$ has the simple form

$$\left.\frac{d^2K}{dP^2}\right|_{\sim} = -\frac{4}{9\tilde{K}}(n+3).$$

Next consider the exponential potential. Differentiating equation (5-1-30) twice with respect to R and using the equilibrium condition gives

$$\left.\frac{d^2K}{dP^2}\right|_{\sim} = \frac{1}{162\tilde{K}^2}\left\{Z_{AB}\left[\left\langle\frac{\tilde{R}}{\rho}\left(\frac{\tilde{R}}{\rho}+2\right)\left(\left(\frac{\tilde{R}}{\rho}\right)^2+2\frac{\tilde{R}}{\rho}+6\right)-80\frac{\tilde{R}}{\rho}\right\rangle\frac{V_{AB}}{R^3}-4380\frac{C_{AB}}{R^9}\right]+\right.$$

$$\left.+\frac{Z_{BB}}{2}\left[\frac{1095}{2}\frac{C_{BB}}{R^9}+660\frac{D_{BB}}{R^{15}}\right]\right\}- \qquad (5\text{-}1\text{-}42)$$

$$-\left[\left.\frac{dK}{dP}\right|_{\sim}+\frac{1}{3}\right]\frac{1}{\tilde{K}}\left.\frac{dK}{dP}\right|_{\sim}.$$

For the case of nearest neighbors only and no van der Waals interactions:

$$\left.\frac{d^2K}{dP^2}\right|_{\sim} = \frac{1}{9\tilde{K}(\tilde{R}/\rho-2)}\left\{\left(\frac{\tilde{R}}{\rho}+2\right)\left[\left(\frac{\tilde{R}}{\rho}\right)^2+2\frac{\tilde{R}}{\rho}+6\right)-80-\right.$$

$$\left.-\left[\frac{(\tilde{R}/\rho+2)^2-18}{(\tilde{R}/\rho-2)}\right]\left[\left(\frac{\tilde{R}}{\rho}+1\right)\left(\frac{\tilde{R}}{\rho}+2\right)-14\right]\right\}.$$

Equations (5-1-35) and (5-1-36) for the pressure derivatives of the elastic constants will now be evaluated. Differentiating equations (5-1-11) with respect to R gives, for the power-law potential

$$\frac{dC_{11}}{dR} = \frac{-2\alpha_{11}\mathcal{J}q^2}{R^5}-n(n+1)(n+3)\frac{V_{AB}}{R^4}+378\frac{C_{AB}}{R^{10}}+\frac{81}{4}\frac{C_{BB}}{R^{10}}-\frac{135}{8}\frac{D_{BB}}{R^{16}}$$

$$\frac{d^2C_{11}}{dR^2} = \frac{10\alpha_{11}\mathcal{J}q^2}{R^6}+n(n+1)(n+3)(n+4)\frac{V_{AB}}{R^5}-3780\frac{C_{AB}}{R^{11}}-\frac{405}{2}\frac{C_{BB}}{R^{11}}+270\frac{D_{BB}}{R^{17}} \qquad (5\text{-}1\text{-}43)$$

$$\frac{dC_{12}}{dR} = \frac{-2\alpha_{12}\mathcal{J}q^2}{R^5}-n(n+3)\frac{V_{AB}}{R^4}+54\frac{C_{AB}}{R^{10}}+\frac{81}{4}\frac{C_{BB}}{R^{10}}-\frac{405}{32}\frac{D_{BB}}{R^{16}}$$

$$\frac{d^2C_{12}}{dR^2} = \frac{10\alpha_{12}\mathcal{J}q^2}{R^6}+n(n+3)(n+4)\frac{V_{AB}}{R^5}-540\frac{C_{AB}}{R^{11}}-\frac{405}{2}\frac{C_{BB}}{R^{11}}+\frac{405}{2}\frac{D_{BB}}{R^{17}}$$

$$\frac{dC_{44}}{dR} = -\frac{2\alpha_{44}\Delta q^2}{R^5} + n(n+3)\frac{V_{AB}}{R^4} - 54\frac{C_{AB}}{R^{10}} + \frac{27}{4}\frac{C_{BB}}{R^{10}} - \frac{225}{32}\frac{D_{BB}}{R^{16}}$$

$$\frac{d^2C_{44}}{dR^2} = \frac{10\alpha_{44}\Delta q^2}{R^6} - n(n+3)\frac{V_{AB}}{R^5} + 540\frac{C_{AB}}{R^{11}} - \frac{135}{2}\frac{C_{BB}}{R^{11}} + \frac{225}{2}\frac{D_{BB}}{R^{17}}, \qquad (5\text{-}1\text{-}43)$$

For the case of the exponential potential

$$\frac{dC_{11}}{dR} = -\frac{2\alpha_{11}\Delta q^2}{R^5} - \left(\frac{R}{\rho}\right)^2\left(\frac{R}{\rho}+1\right)\frac{V_{AB}}{R^4} + 378\frac{C_{AB}}{R^{10}} + \frac{81}{4}\frac{C_{BB}}{R^{10}} - \frac{135}{8}\frac{D_{BB}}{R^{16}}$$

$$\frac{d^2C_{11}}{dR^2} = \frac{10\alpha_{11}\Delta q^2}{R^6} + \left(\frac{R}{\rho}\right)^2\left[\left(\frac{R}{\rho}\right)^2 + 2\frac{R}{\rho} + 2\right]\frac{V_{AB}}{R^5} - 3780\frac{C_{AB}}{R^{11}} - \frac{405}{2}\frac{C_{BB}}{R^{11}} + 270\frac{D_{BB}}{R^{17}}$$

$$\frac{dC_{12}}{dR} = -\frac{2\alpha_{12}\Delta q^2}{R^5} - \frac{R}{\rho}\left(\frac{R}{\rho}+2\right)\frac{V_{AB}}{R^4} + 54\frac{C_{AB}}{R^{10}} + \frac{81}{4}\frac{C_{BB}}{R^{10}} - \frac{405}{32}\frac{D_{BB}}{R^{16}} \qquad (5\text{-}1\text{-}44)$$

$$\frac{d^2C_{12}}{dR^2} = \frac{10\alpha_{12}\Delta q^2}{R^6} + \frac{R}{\rho}\left[\left(\frac{R}{\rho}\right)^2 + 4\frac{R}{\rho} + 6\right]\frac{V_{AB}}{R^5} - 540\frac{C_{AB}}{R^{11}} - \frac{405}{2}\frac{C_{BB}}{R^{11}} + \frac{405}{2}\frac{D_{BB}}{R^{17}}$$

$$\frac{dC_{44}}{dR} = -\frac{2\alpha_{44}\Delta q^2}{R^5} + \frac{R}{\rho}\left(\frac{R}{\rho}+2\right)\frac{V_{AB}}{R^4} - 54\frac{C_{AB}}{R^{10}} + \frac{27}{4}\frac{C_{BB}}{R^{10}} - \frac{225}{32}\frac{D_{BB}}{R^{16}}$$

$$\frac{d^2C_{44}}{dR^2} = \frac{10\alpha_{44}\Delta q^2}{R^6} - \frac{R}{\rho}\left[\left(\frac{R}{\rho}\right)^2 + 4\frac{R}{\rho} + 6\right]\frac{V_{AB}}{R^5} + 540\frac{C_{AB}}{R^{11}} - \frac{135}{2}\frac{C_{BB}}{R^{11}} + \frac{225}{2}\frac{D_{BB}}{R^{17}}.$$

Substitution of equations (5-1-43) into equations (5-1-35) and (5-1-36) gives the pressure derivatives for the power-law potential, while substitution of equations (5-1-44) into equations (5-1-35) and (5-1-36) gives these derivatives for the exponential potential. The expressions for these derivatives are the same except for the V_{AB} term. It was shown that at equilibrium

$$n(n+3)\left(\frac{V_{AB}}{\tilde{R}^3}\right) = \frac{\tilde{R}}{\rho}\left(\frac{\tilde{R}}{\rho}+2\right)\left(\frac{V_{AB}}{\tilde{R}^3}\right),$$

therefore $(dC_{12}/dP)|_{\sim}$ and $(dC_{44}/dP)|_{\sim}$ are the same for both forms of V_{AB}, while $(dC_{11}/dP)|_{\sim}$ is different. Each of the three second derivatives $(d^2C_{11}/dP^2)|_{\sim}$ is different for each functional form of the cation-anion repulsion.

For the case of nearest neighbor cation-anion interactions only, the pressure derivatives reduce to the simple expressions given below:

Power-Law Potential

$$\left.\frac{dC_{11}}{dP}\right|_{P=0} = \frac{6}{(n-1)}\left[\frac{(n+1)(n+3)}{Z_{AB}} + \frac{2\alpha_{11}}{\alpha_M}\right] = \frac{(n+1)(n+3) - 17.5516}{(n-1)}$$

$$\left.\frac{dC_{12}}{dP}\right|_{P=0} = \frac{6}{(n-1)}\left[\frac{n+3}{Z_{AB}} + \frac{2\alpha_{12}}{\alpha_M}\right] = \frac{(n+3) + 0.775803}{(n-1)} \qquad (5\text{-}1\text{-}45)$$

$$\left.\frac{dC_{44}}{dP}\right|_{P=0} = \frac{-6}{(n-1)}\left[\frac{n+3}{Z_{AB}} - \frac{2\alpha_{44}}{\alpha_M}\right] = \frac{-(n+3) + 8.77581}{(n-1)}$$

Exponential Potential

$$\left.\frac{dC_{11}}{dP}\right|_{P=0} = \frac{6}{(\tilde{R}/\rho-2)}\left[\frac{1}{Z_{AB}}\frac{\tilde{R}}{\rho}\left(\frac{\tilde{R}}{\rho}+1\right)+\frac{2\alpha_{11}}{\alpha_M}\right] = \frac{\frac{\tilde{R}}{\rho}\left(\frac{\tilde{R}}{\rho}+1\right)-17.5516}{\frac{\tilde{R}}{\rho}-2}$$

$$\left.\frac{dC_{12}}{dP}\right|_{P=0} = \frac{6}{(\tilde{R}/\rho-2)}\left[\frac{1}{Z_{AB}}\left(\frac{\tilde{R}}{\rho}+2\right)+\frac{2\alpha_{12}}{\alpha_M}\right] = \frac{\left(\frac{\tilde{R}}{\rho}+2\right)+0.775803}{\frac{\tilde{R}}{\rho}-2} \qquad (5\text{-}1\text{-}46)$$

$$\left.\frac{dC_{44}}{dP}\right|_{P=0} = \frac{-6}{(\tilde{R}/\rho-2)}\left[\frac{1}{Z_{AB}}\left(\tilde{R}/\rho+2\right)-\frac{2\alpha_{44}}{\alpha_M}\right] = -\frac{\left(\frac{\tilde{R}}{\rho}+2\right)+8.77581}{\frac{\tilde{R}}{\rho}-2}$$

As a check on the algebra, it can be readily shown that $1/3\left[\left(dC_{11}/dP\right)\big|_{\sim} + 2\left(dC_{12}/dP\right)\big|_{\sim}\right]$ calculated from equations (5-1-45) and (5-1-46) are equal to $(dK/dP)\big|_{\sim}$ as given by equations (5-1-38) and (5-1-39).

Numerical Predictions for NaCl and MgO

The two input parameters, $\tilde{K}$ and $\tilde{R}$, are obtained by the linear extrapolation of V(T) and (K/V)(T) from the high-temperature regime ($T \gtrsim \Theta_D$) to absolute zero, as discussed in section 4-3. The experimental data and extrapolation are shown in Figure 5-1-1 for NaCl and in Figure 5-1-2 for MgO. Note that for NaCl the thermal expanison coefficient rises very rapidly above the Debye temperature, and one might be tempted to make the dashed extrapolation of V shown in 5-1-1b. However, since this rapid rise in α may be due to the formation of vacancies (Enck and Dommel, 1965), it should be disregarded and the solid extrapolation used. This solid line extrapolation gives the same

$\tilde{V}$ and $\tilde{K}$ found by Thomsen (1970b) from the more rigorous solution of the fourth-order anharmonic equations. The extrapolated $\tilde{V}$ and $\tilde{K}$ values are given in Tables 5-1-1 and 5-1-2. The other input parameters are the multipole coefficients C_{AB}, C_{BB}, and D_{BB} which are discussed in Chapter IV and are summarized in Table 4-2-1.

Tables 5-1-4 through 5-1-10 give the theoretical predictions of the elastic constants and their first and second pressure derivatives at zero pressure. These calculations are made for a range of ionicity factors, δ, between 0.6 and 1.0. The effect of the multipole terms is investigated by repeating the calculations with and without these terms. The results of the calculations are compared with experiment in Figures (5-1-3) through (5-1-9). Finally, using the ionicity factor, δ, which gives the best agreement between experiment and theory at P = 0, the volume and the elastic constants are calculated as a function of pressure. These results are given in Tables 5-1-11 through 5-1-14; and in Figures 5-1-8 and 5-1-9.

Discussion and Conclusions

As stated earlier, the primary objective of this chapter is to understand the effects of the functional form of the potential and its various terms on the elastic constants and their pressure derivatives. The geophysical question is: Given the compressional properties, $\tilde{\rho}$ and $\tilde{K}$, of a material, how accurately can its shear properties be predicted. In order for the theory to be geophysically useful, the shear properties must be relatively insensitive to the potential, but strongly

dependent on the crystal structure. For both NaCl and MgO the precise ultrasonic data exist to make this test. Discrepancies between theoretical predictions and experimental values will be discussed in terms of uncertainties in the velocity at compressions corresponding to 600 km depth in the earth and 2892 km at the base of the mantle. At 600 km, $P \approx 215$ kbar and $\tilde{K} \approx 2000$ kbar so $P/\tilde{K} \approx 0.11$. At the base of the mantle $P \approx 1338$ kbar and $\tilde{K} \approx 2000$ kbar so $P/\tilde{K} \approx 0.67$.

We will first consider NaCl. Since NaCl is a better approximation to the Born ionic model than any other solid investigated in this thesis, one would hope for good agreement between theory and experiment. Table 5-1-2 shows that this is indeed the case. The largest discrepancy between theoretical and experimental elastic constants is 9.4% for C_{12}. This is a consequence of the central force model; Löwdin (1948) has shown that three-body interactions explain this deviation from Cauchy's relation. The discrepancies in the prediction of the other elastic constants are all less than 4%. The prediction of $dK/dP\big|_{\sim}$ is within 2% of experiment, while $dC_{11}/dP\big|_{\sim}$ and $dC_{12}/dP\big|_{\sim}$ are both within 5%. Although $dC_{44}/dP\big|_{\sim}$ is 200% low, this has very little effect on the high-pressure predictions since dC_{44}/dP is so small. At $(P/K_o) \approx 0.1$ (~600 km in the mantle), the error in C_{44} caused by this error in the predicted pressure derivative is only 8.6 kbar or 6%. The importance of taking data as a simultaneous function of temperature and pressure is clearly shown by Figure 5-1-5 for (dK/dP)(T). Note that $(dK/dP)\big|_{\sim}$ is 4.88, while $(dK/dP)_{298}$ is 5.35. It is essential that the pressure derivatives be extrapolated to T = 0 before a comparison is made with the static lattice

model prediction.

Even the second pressure derivatives have the correct sign and relative magnitudes, although they are all smaller than the experimental values by factors of 3 to 8. The second derivatives have virtually no effect on the predictions at P/K values comparable to those in the mantle. Since the second pressure derivatives of the elastic constants involve the fourth derivative of the interatomic potential with respect to the ion separation, it is quite remarkable that the predictions have the correct sign and order of magnitude.

Figures 5-1-8 and 5-1-9 summarize Tables 5-1-4 through 5-1-7 in which the effects of the functional form of the potential, the various multipole terms, and the ionicity are investigated. Note that the ionicity factor, λ , has the largest effect on the predictions with a value between 0.9 and 1.0 best satisfying the elastic data. This is fortunate since any significant lowering of the ionicity would cause an unacceptable discrepancy between the theoretical and experimental values for the cohesive energy. The functional form of the potential only effects $(dC_{11}/dP)\underset{\sim}{|}$ and hence also $(dK/dP)\underset{\sim}{|}$. It can be seen that the exponential form of the anion-anion repulsive energy gives the best fit to experiment. This is in accord with the conclusion reached by Löwdin (1948) from the q.m. calculation and by Tosi (1964) from the cohesive energy. The inclusion of van der Waals and anion-anion terms does not significantly improve the general agreement between theory and experiment; the effect is to slightly lower the ionicity at which the best total fit is achieved. The most striking effect of these terms is on the

pressure derivative of C_{44}. Note that in Figure 5-1-12, C_{44} goes to zero. This is a sufficient condition for a phase transformation (in this case to the CsCl structure) and has been discussed in some detail by Anderson and Liebermann (1970). However, the pressure at which the structure becomes unstable if the second neighbors are included is twice as large as that predicted by a nearest neighbor model. The conclusion to be drawn here is that while the occurrence of a shear instability is predicted, the exact transition pressure is very sensitive to the details of the potential and can therefore not be reliably predicted using Born lattice models. Returning to Figures 5-1-8 and 5-1-9, the shaded regions bound the predictions using the various multipole terms as summarized in Table 4-1-1 and should be thought of as a measure of the uncertainty in the theoretical predictions introduced by our incomplete understanding of van der Waals and anion-anion interactions.

One final note on NaCl; the compression curve given in Table 5-1-12 and Figure 5-1-12 is insensitive to second neighbor or anion-anion interactions and agrees within 3% of P with that given by Weaver, et al. (1968) and Thomsen (1970a). The Birch-Murnaghan curve gives 14% lower pressures at 200 kb.

We will now consider MgO. Figures 5-1-10 and 5-1-11 summarize the calculations given in Tables 5-1-8 through 5-1-10. As with NaCl, the ionicity factor, ϕ, has the largest effect on the prediction; but unlike NaCl, the MgO data are not best fit with $\phi \approx 1$. By looking only at dK/dP for $\phi = 1$, Anderson and Anderson (1970) concluded that the power law gives a better fit than the exponential, as is evident from

Figure 5-1-10. However at $\phi = 1$, note that the predicted value of $\tilde{C}_{11}$ is 50% too low. Note further that for $\phi \approx 0.7$, the predicted $\tilde{C}_{11}$ is only 10% too low, while the exponential potential gives an excellent fit to $dK/dP|_{\sim}$. Also, the fit for $(dC_{12}/dP)|_{\sim}$ gets progressively better as the ionicity is lowered. As for NaCl, the predicted (dC_{44}/dP) for MgO is too small, but because of the small size of this derivative, the uncertainty introduced in C_{44} at $P/K = 0.1$ (600 km in the mantle) is only 168 kbar or 10%. When translated into a velocity this gives an uncertainty of $\sim 5\%$. The large deviation from Cauchy's relation $(C_{12} = C_{44})_o$ observed in MgO is due to the large size of O^{2-} relative to Mg^{2+}. La and Barsch (1968) discuss this discrepancy using Löwdin's (1948) q.m. formulation. For the central force model discussed here, a 20% error in one or both of these elastic constants is inescapable. In spite of the problem of the deviation from Cauchy's relation, it appears that an exponential potential with $\phi = 0.7$ gives the best fit to the data.

Note that the van der Waals and anion-anion interactions have much less relative effect in MgO than in NaCl. There are two reasons for this. First, from Table 4-1-1 it can be seen that the coefficients are smaller for MgO than for NaCl. Second, because MgO is divalent, the electrostatic and repulsive terms make a larger relative contribution to the elastic constants. Since this is the case for all mantle candidate minerals, the calculations can be greatly simplified.

In Figure 5-1-13 the elastic constants and the volume have been plotted for $\phi = 0.7$ and $\phi = 0.6$. The compression curve is not sensitive to this small change in ionicity and is in good agreement with

the Birch-Murnaghan curve (Chapter 2 , eqn.2-1-19). As for NaCl, the transition pressure of MgO is very sensitive to the details of the potential, in this case ϕ , while the predicted values of C_{11} and C_{12} are relatively insensitive.

It should be noted that lowering the ionicity factor to 0.7 has important consequences in the calculation of the cohesive energy. The experimental value of the cohesive energy is not known since one step in the Born-Haber cycle, the heat of formation of O^{2-}, is not known. The usual procedure is to use a Born lattice model with $\phi = 1.0$ to calculate the cohesive energy and thus solve for the unknown $\Delta H_f^o(O^{2-})$. Gaffney and Ahrens (1969) found $\Delta H_f^o(O^{2-}) = 202.3$ kcal/mole by this method. However, upon redoing their calculation for $\phi = 0.7$, one gets the unacceptable result $\Delta H_f^o(O^{2-}) = -35.2$ kcal/mole. The conclusion is that while lowering the ionicity improves the shape of the cohesive energy curve, it introduces an error in the total depth of 10-20%. This energy calculation is given in Appendix 3 .

In summary, NaCl elastic data are best fit by an exponential potential with $0.9 < \phi < 1.0$. The MgO data are best fit by an exponential potential with $0.6 < \phi < 0.7$. Based on this simple structure for which good ultrasonic data exist as a simultaneous function of temperature and pressure, it appears that the Born model is capable of predicting elastic wave velocities of oxides in the lower mantle to an accuracy of 5%.

TABLE 5-1-1

Short-Range Sums for the Rock salt Structure

Cation-Anion

Neighbor Number	$x_{kk'}$	$y_{kk'}$	$z_{kk'}$	$(x_{kk'})^2$	$(y_{kk'})^2$	$(x_{kk'})^2 (y_{kk'})^2$	$x_{kk'}^4$
1	0	0	R	0	0	0	0
2	0	0	-R	0	0	0	0
3	0	R	0	0	R^2	0	0
4	0	-R	0	0	R^2	0	0
5	R	0	0	R^2	0	0	R^4
6	-R	0	0	R^2	0	0	R^4
			$\sum_{k'} \rightarrow$	$2R^2$	$2R^2$	0	$2R^4$

Anion-Anion

1	R	R	0	R^2	R^2	R^2	R^4
2	-R	-R	0	R^2	R^2	R^2	R^4
3	-R	R	0	R^2	R^2	R^2	R^4
4	R	-R	0	R^2	R^2	R^2	R^4
5	R	0	R	R^2	0	0	R^4
6	-R	0	-R	R^2	0	0	R^4
7	-R	0	R	R^2	0	0	R^4
8	R	0	-R	R^2	0	0	R^4
9	0	R	R	0	R^2	0	0
10	0	-R	-R	0	R^2	0	0
11	0	-R	R	0	R^2	0	0
12	0	R	-R	0	R^2	0	0
			$\sum_{k'} \rightarrow$	$8R^2$	$8R^2$	$4R^2$	$8R^4$

TABLE 5-1-2

Static Lattice Parameters for NaCl

Parameter	Units	Experimental Source	Experimental Value	Lattice Model Prediction Value	Lattice Model Prediction Model
$\tilde{V}$	cm /mole	Fig. 5-1-1	26.0		
$\tilde{R}$	Å	Fig. 5-1-1 Ref. (1)	2.784 2.785	Input	
$\tilde{K}$	kbar	Fig. 5-1-1 Ref. (1)	284.7 285.5	Input	
$\tilde{C}_{11}$	kbar	Fig. 5-1-3 Ref. (2)	600 614	577	D1E
$\tilde{C}_{12}$	kbar	Fig. 5-1-3 Ref. (2)	127 121	139	D1E
$\tilde{C}_{44}$	kbar	Fig. 5-1-3 Ref. (2)	140 139	139	D1E
$\tilde{K}'$		Fig. 5-1-5	4.88	4.78	D1E
$\tilde{C}_{11}'$		Fig. 5-1-4	11.3	10.7	D1E
$\tilde{C}_{12}'$		Fig. 5-1-4	1.7	1.8	D1E
$\tilde{C}_{44}'$		Fig. 5-1-4	0.15	-0.16	D1E
$\tilde{K}''$	per kbar	Fig. 5-1-5	-0.084	-0.02	D1E
$\tilde{C}_{11}''$	per kbar	Fig. 5-1-4	-0.13	-0.05	D1E
$\tilde{C}_{12}''$	per kbar	Fig. 5-1-4	-0.05	-0.006	D1E
$\tilde{C}_{44}''$	per kbar	Fig. 5-1-4	-0.01	-0.006	D1E

Model D1E has an ionicity factor $\downarrow = 1.0$, an exponential repulsive potential, and van der Waal constants from Mayer (1933) (see Table 5-1-7).

Ref. (1) - Thomsen (1970a)

Ref. (2) - Thomsen (1970b)

TABLE 5-1-3

Static Lattice Parameters for MgO

Parameter	Units	Experimental Source	Experimental Value	Lattice Model Prediction Value	Lattice Model Prediction Model
$\tilde{R}$	Å		2.093	Input	
		Ref. (1)	2.089		
$\tilde{K}$	kbar	Fig. 5-1-6	1687.7	Input	
		Ref. (1)	1733.8		
$\tilde{C}_{11}$	kbar	Fig. 5-1-6	3100	2680	G.7E
		Ref. (2)	3351		
$\tilde{C}_{12}$	kbar	Fig. 5-1-6	960	1190	G.7E
		Ref. (2)	924		
$\tilde{C}_{44}$	kbar	Fig. 5-1-6	1600	1190	G.7E
		Ref. (2)	1634		
$\tilde{K}'$		Fig. 5-1-7	3.8	3.9	G.7E
$\tilde{C}_{11}'$		Fig. 5-1-7	8.7	7.8	G.7E
$\tilde{C}_{12}'$		Fig. 5-1-7	1.5	2.0	G.7E
$\tilde{C}_{44}'$		Fig. 5-1-7	1.0	0.003	G.7E
$\tilde{K}''$	per kbar			-0.003	G.7E
$\tilde{C}_{11}''$	per kbar			-0.005	G.7E
$\tilde{C}_{12}''$	per kbar			-0.001	G.7E
$\tilde{C}_{44}''$	per kbar			-0.001	G.7E

Model G.7E has an ionicity factor $\downarrow = 0.7$, an exponential potential, and both van der Waals and anion-anion interaction.

Ref. (1) - Thomsen (1970a)

Ref. (2) - Thomsen (1970b)

TABLE 5-1-4

NaCl - Model A - No vdW or anion-anion interactions.

IONICITY FACTOR=1.00 CAB/R**9= 0.0 CBB/R**9= 0.0 CBB/R**15= 0.0

K	R	B/RO**N	N	LAMDA	RO/RHO
0.284700E 12	0.278400E-07	0.279454E-12	0.863626E 01	0.383442E-08	0.963626E 01

	ELECTR.	PWR.LAW	EXPON.	CAB	CBB	DBB	P.LAW TOT.	EXP. TOT.
C_{11}	-0.491E 12	0.108E 13	0.108E 13	0.0	0.0	0.0	0.587E 12	0.587E 12
C_{12}	0.217E 11	0.112E 12	0.112E 12	0.0	0.0	0.0	0.134E 12	0.134E 12
C_{44}	0.245E 12	-0.112E 12	-0.112E 12	0.0	0.0	0.0	0.134E 12	0.134E 12
C'_{11}	-0.230E 01	0.147E 02	0.134E 02	0.0	0.0	0.0	0.124E 02	0.111E 02
C'_{12}	0.102E 00	0.152E 01	0.152E 01	0.0	0.0	0.0	0.163E 01	0.163E 01
C'_{44}	0.115E 01	-0.152E 01	-0.152E 01	0.0	0.0	0.0	-0.375E 00	-0.375E 00

SECOND DERIVATIVES FOR POWER-LAW POTENTIAL

	ELECTR.	REPULSIVE	CAB	CBB	DBB	TOTAL
C''_{11}	0.313E-10	-0.688E-10	0.0	0.0	0.0	-0.375E-10
C''_{12}	-0.138E-11	-0.714E-11	0.0	0.0	0.0	-0.852E-11
C''_{44}	-0.157E-10	0.714E-11	0.0	0.0	0.0	-0.852E-11

SECOND DERIVATIVES FOR EXPONENTIAL POTENTIAL

	ELECTR.	REPULSIVE	CAB	CBB	DBB	TOTAL
C''_{11}	0.279E-10	-0.730E-10	0.0	0.0	0.0	-0.451E-10
C''_{12}	-0.123E-11	-0.636E-11	0.0	0.0	0.0	-0.760E-11
C''_{44}	-0.140E-10	0.636E-11	0.0	0.0	0.0	-0.760E-11

POWER LAW		EXPONENTIAL	
DK/DP	D2K/DP2	DK/DP	D2K/DP2
0.521E 01	-0.182E-10	0.479E 01	-0.201E-10

TABLE 5-1-5

NaCl - Model B - Including vdW from Mayer (1933), but no anion-anion interactions.

IONICITY FACTOR=1.00 CAB/R**9= 0.123E 10 CBB/R**9= 0.0 DBB/R**15= 0.0

K	R	B/RO**N	N	LAMDA	RC/RHO
0.284700E 12	0.278400E-07	0.303590E-12	0.847333E 01	0.353226E-08	0.947333E 01

	ELECTR.	PWR.LAW	EXPON.	CAB	CBB	DBB	P.LAW TOT.	EXP. TOT.
C_{11}	-0.491E 12	0.113E 13	0.113E 13	-0.516E 11	0.0	0.0	0.587E 12	0.587E 12
C_{12}	0.217E 11	0.119E 12	0.119E 12	-0.737E 10	0.0	0.0	0.134E 12	0.134E 12
C_{44}	0.245E 12	-0.119E 12	-0.119E 12	0.737E 10	0.0	0.0	0.134E 12	0.134E 12
C'_{11}	-0.230E 01	0.152E 02	0.138E 02	-0.543E 00	0.0	0.0	0.123E 02	0.116E 02
C'_{12}	0.102E 00	0.160E 01	0.160E 01	-0.776E-01	0.0	0.0	0.163E 01	0.163E 01
C'_{44}	0.115E 01	-0.160E 01	-0.160E 01	0.776E-01	0.0	0.0	-0.375E 00	-0.375E 00

SECOND DERIVATIVES FOR POWER-LAW POTENTIAL

	ELECTR.	REPULSIVE	CAB	CBB	DBB	TOTAL
C''_{11}	0.312E-10	-0.729E-10	0.419E-11	0.0	0.0	-0.376E-10
C''_{12}	-0.138E-11	-0.770E-11	0.598E-12	0.0	0.0	-0.848E-11
C''_{44}	-0.156E-10	0.770E-11	-0.598E-12	0.0	0.0	-0.848E-11

SECOND DERIVATIVES FOR EXPONENTIAL POTENTIAL

	ELECTR.	REPULSIVE	CAB	CBB	DBB	TOTAL
C''_{11}	0.270E-10	-0.760E-10	0.335E-11	0.0	0.0	-0.451E-10
C''_{12}	-0.122E-11	-0.677E-11	0.478E-12	0.0	0.0	-0.751E-11
C''_{44}	-0.138E-10	0.677E-11	-0.478E-12	0.0	0.0	-0.751E-11

POWER LAW		EXPONENTIAL	
DK/DP	D2K/DP2	DK/DP	D2K/DP2
0.519E 01	-0.182E-10	0.475E 01	-0.200E-10

TABLE 5-1-6

NaCl - Model C - vdW terms from Hajj (1966), including anion-anion terms.

IONICITY FACTOR=1.00 CAB/R**9= 0.118E 10 CBB/R**9= 0.810E 09 CBB/R**15= 0.541E 09

K	R	B/RO**N	N	LAMDA	RC/RHO
0.284700E 12	0.278400E-07	0.309269E-12	0.818216E 01	0.267930E-08	0.918216E 01

	ELECTR.	PWR.LAW	EXPON.	CAB	CBB	DBB	P.LAW TOT.	EXP. TOT.
C_{11}	-0.491E 12	0.108E 13	0.108E 13	-0.494E 11	-0.146E 11	0.390E 11	0.561E 12	0.561E 12
C_{12}	0.217E 11	0.117E 12	0.117E 12	-0.706E 10	-0.146E 11	0.292E 11	0.147E 12	0.147E 12
C_{44}	0.245E 12	-0.117E 12	-0.117E 12	0.706E 10	-0.486E 10	0.162E 11	0.147E 12	0.147E 12
C'_{11}	-0.230E 01	0.141E 02	0.128E 02	-0.520E 00	-0.154E 00	0.684E 00	0.118E 02	0.105E 02
C'_{12}	0.102E 00	0.154E 01	0.154E 01	-0.744E-01	-0.154E 00	0.513E 00	0.192E 01	0.192E 01
C'_{44}	0.115E 01	-0.154E 01	-0.154E 01	0.744E-01	-0.512E-01	0.285E 00	-0.780E-01	-0.780E-01

SECOND DERIVATIVES FOR POWER-LAW POTENTIAL

	ELECTR.	REPULSIVE	CAB	CBB	DBB	TOTAL
C''_{11}	0.314E-10	-0.738E-10	0.405E-11	0.120E-11	-0.523E-12	-0.377E-10
C''_{12}	-0.139E-11	-0.804E-11	0.579E-12	0.120E-11	-0.393E-12	-0.804E-11
C''_{44}	-0.157E-10	0.804E-11	-0.579E-12	0.399E-12	-0.218E-12	-0.804E-11

SECOND DERIVATIVES FOR EXPONENTIAL POTENTIAL

	ELECTR.	REPULSIVE	CAB	CBB	DBB	TOTAL
C''_{11}	0.280E-10	-0.708E-10	0.329E-11	0.970E-12	0.486E-12	-0.441E-10
C''_{12}	-0.124E-11	-0.725E-11	0.469E-12	0.970E-12	0.365E-12	-0.668E-11
C''_{44}	-0.140E-10	0.725E-11	-0.469E-12	0.323E-12	0.203E-12	-0.668E-11

POWER LAW		EXPONENTIAL	
DK/DP	D2K/DP2	DK/DP	D2K/DP2
0.522E 01	-0.179E-10	0.480E 01	-0.192E-10

TABLE 5-1-7

NaCl - Model D - vdW terms from Mayer (1933), including anion-anion interactions.

IONICITY FACTOR=1.00 CAB/R**9= 0.123E 10 CBB/R**9= 0.146E 10 CBB/R**15= 0.541E 09

K	R	B/RO**N	N	LAMDA	RC/RHO
0.284700E 12	0.278400E-07	0.323304E-12	0.810683E 01	0.259502E-08	0.910683E 01

	ELECTR.	PWR.LAW	EXPON.	CAB	CBB	DBB	P.LAW TOT.	EXP. TOT.
C_{11}	-0.491E 12	0.111E 13	0.111E 13	-0.516E 11	-0.262E 11	0.390E 11	0.577E 12	0.577E 12
C_{12}	0.217E 11	0.121E 12	0.121E 12	-0.737E 10	-0.262E 11	0.292E 11	0.139E 12	0.139E 12
C_{44}	0.245E 12	-0.121E 12	-0.121E 12	0.737E 10	-0.874E 10	0.162E 11	0.139E 12	0.139E 12
C'_{11}	-0.230E 01	0.144E 02	0.131E 02	-0.543E 00	-0.276E 00	0.684E 00	0.120E 02	0.107E 02
C'_{12}	0.102E 00	0.158E 01	0.158E 01	-0.776E-01	-0.276E 00	0.513E 00	0.184E 01	0.184E 01
C'_{44}	0.115E 01	-0.158E 01	-0.158E 01	0.776E-01	-0.921E-01	0.285E 00	-0.160E 00	-0.160E 00

SECOND DERIVATIVES FOR POWER-LAW POTENTIAL

	ELECTR.	REPULSIVE	CAB	CBB	DBB	TOTAL
C''_{11}	0.313E-10	-0.762E-10	0.422E-11	0.215E-11	-0.505E-12	-0.390E-10
C''_{12}	-0.138E-11	-0.837E-11	0.603E-12	0.215E-11	-0.379E-12	-0.738E-11
C''_{44}	-0.157E-10	0.837E-11	-0.603E-12	0.715E-12	-0.211E-12	-0.738E-11

SECOND DERIVATIVES FOR EXPONENTIAL POTENTIAL

	ELECTR.	REPULSIVE	CAB	CBB	DBB	TOTAL
C''_{11}	0.278E-10	-0.786E-10	0.340E-11	0.173E-11	0.532E-12	-0.452E-10
C''_{12}	-0.123E-11	-0.749E-11	0.485E-12	0.173E-11	0.399E-12	-0.611E-11
C''_{44}	-0.139E-10	0.749E-11	-0.485E-12	0.575E-12	0.222E-12	-0.611E-11

POWER LAW		EXPONENTIAL	
DK/DP	D2K/DP2	DK/DP	D2K/DP2
0.521E 01	-0.179E-10	0.478E 01	-0.191E-10

TABLE 5-1-8

MgO - Model E, ϕ = 1.0, No vdW or anion-anion interactions.

IONICITY FACTOR=1.00 CAB/R**9= 0.0 CBB/R**9= 0.0 CBB/R**15= 0.0

K	R	B/RO**N	N	LAMDA	RC/RHO
0.108770E 13	0.209300E-07	0.278233E-11	0.461516E 01	0.627667E-09	0.561516E 01

	ELECTR.	PWR.LAW	EXPON.	CAB	CBB	DBB	P.LAW TOT.	EXP. TOT.
C_{11}	-0.015E 13	0.786E 13	0.786E 13	0.0	0.0	0.0	0.172E 13	0.172E 13
C_{12}	0.272E 12	0.140E 13	0.140E 13	0.0	0.0	0.0	0.167E 13	0.167E 13
C_{44}	0.307E 13	-0.14CE 13	-0.140E 13	0.0	0.0	0.0	0.167E 13	0.167E 13
C'_{11}	-0.485E 01	0.118E 02	0.103E 02	0.0	0.0	0.0	0.697E 01	0.542E 01
C'_{12}	0.215E 00	0.211E 01	0.211E 01	0.0	0.0	0.0	0.232E 01	0.232E 01
C'_{44}	0.243E 01	-0.211E 01	-0.211E 01	0.0	0.0	0.0	0.321E 00	0.321E 00

SECOND DERIVATIVES FOR POWER-LAW POTENTIAL

	ELECTR.	REPULSIVE	CAB	CBB	DBB	TOTAL
C''_{11}	0.730E-11	-0.934E-11	0.0	0.0	0.0	-0.204E-11
C''_{12}	-0.323E-12	-0.166E-11	0.0	0.0	0.0	-0.199E-11
C''_{44}	-0.365E-11	0.166E-11	0.0	0.0	0.0	-0.199E-11

SECOND DERIVATIVES FOR EXPONENTIAL POTENTIAL

	ELECTR.	REPULSIVE	CAB	CBB	DBB	TOTAL
C''_{11}	0.581E-11	-0.872E-11	0.0	0.0	0.0	-0.290E-11
C''_{12}	-0.257E-12	-0.132E-11	0.0	0.0	0.0	-0.158E-11
C''_{44}	-0.291E-11	0.132E-11	0.0	0.0	0.0	-0.158E-11

POWER LAW		EXPONENTIAL	
DK/DP	D2K/DP2	DK/DP	D2K/DP2
0.387E 01	-0.201E-11	0.335E 01	-0.202E-11

TABLE 5-1-9

MgO - Model F, $\Phi = 0.7$, No vdW or anion-anion interactions.

IONICITY FACTOR=0.70 CAB/R**9= 0.0 CBB/R**9= 0.0 CBB/R**15= 0.0

K	R	B/RO**N	N	LAMDA	RC/RHO
0.166770E 13	0.209300E-07	0.145813E-11	0.616451E 01	0.162187E-08	0.716451E 01

	ELECTR.	PWR.LAW	EXPON.	CAB	CBB	DBB	P.LAW TOT.	EXP. TOT.
C_{11}	-0.430E 13	0.702E 13	0.702E 13	0.0	0.0	0.0	0.272E 13	0.272E 13
C_{12}	0.190E 12	0.980E 12	0.980E 12	0.0	0.0	0.0	0.117E 13	0.117E 13
C_{44}	0.215E 13	-0.980E 12	-0.980E 12	0.0	0.0	0.0	0.117E 13	0.117E 13
C'_{11}	-0.340E 01	0.127E 02	0.113E 02	0.0	0.0	0.0	0.932E 01	0.793E 01
C'_{12}	0.150E 00	0.177E 01	0.177E 01	0.0	0.0	0.0	0.192E 01	0.192E 01
C'_{44}	0.170E 01	-0.177E 01	-0.177E 01	0.0	0.0	0.0	-0.753E-01	-0.753E-01

SECOND DERIVATIVES FOR POWER-LAW POTENTIAL

	ELECTR.	REPULSIVE	CAB	CBB	CBB	TOTAL
C''_{11}	0.615E-11	-0.100E-10	0.0	0.0	0.0	-0.389E-11
C''_{12}	-0.272E-12	-0.140E-11	0.0	0.0	0.0	-0.167E-11
C''_{44}	-0.308E-11	0.140E-11	0.0	0.0	0.0	-0.167E-11

SECOND DERIVATIVES FOR EXPONENTIAL POTENTIAL

	ELECTR.	REPULSIVE	CAB	CBB	DBB	TOTAL
C''_{11}	0.522E-11	-0.100E-10	0.0	0.0	0.0	-0.482E-11
C''_{12}	-0.231E-12	-0.119E-11	0.0	0.0	0.0	-0.142E-11
C''_{44}	-0.261E-11	0.119E-11	0.0	0.0	0.0	-0.142E-11

POWER LAW		EXPONENTIAL	
DK/DP	D2K/DPZ	DK/DP	D2K/DPZ
0.439E 01	-0.241E-11	0.393E 01	-0.256E-11

TABLE 5-1-10

MgO - Model G - Including vdW and anion-anion interactions.

IONICITY FACTOR=0.70 CAB/R**9= 0.101E 11 CBB/R**9= 0.137E 10 DBB/R**15= 0.863E 09

K	R	B/RO**N	N	LAMDA	RC/RHO
0.168770E 13	0.209300E-07	0.156280E-11	0.609541E 01	0.161967E-08	0.709541E 01

	ELECTR.	PWR.LAW	EXPON.	CAB	CBB	DBB	P.LAW TOT.	EXP. TOT.
C_{11}	-0.430E 13	0.737E 13	0.737E 13	-0.425E 12	-0.247E 11	0.622E 11	0.268E 13	0.268E 13
C_{12}	0.190E 12	0.104E 13	0.104E 13	-0.607E 11	-0.247E 11	0.466E 11	0.119E 13	0.119E 13
C_{44}	0.215E 13	-0.104E 13	-0.104E 13	0.607E 11	-0.823E 10	0.259E 11	0.119E 13	0.119E 13
C'_{11}	-0.340E 01	0.132E 02	0.118E 02	-0.756E 00	-0.439E-01	0.184E 00	0.923E 01	0.777E 01
C'_{12}	0.150E 00	0.187E 01	0.187E 01	-0.108E 00	-0.439E-01	0.138E 00	0.200E 01	0.200E 01
C'_{44}	0.170E 01	-0.167E 01	-0.187E 01	0.108E 00	-0.140E-01	0.767E-01	0.288E-02	0.288E-02

SECOND DERIVATIVES FOR POWER-LAW POTENTIAL

	ELECTR.	REPULSIVE	CAB	CBB	DBB	TOTAL
C''_{11}	0.620E-11	-0.108E-10	0.632E-12	0.367E-13	0.642E-13	-0.390E-11
C''_{12}	-0.274E-12	-0.153E-11	0.903E-13	0.367E-13	0.482E-13	-0.162E-11
C''_{44}	-0.310E-11	0.153E-11	-0.903E-13	0.122E-13	0.268E-13	-0.162E-11

SECOND DERIVATIVES FOR EXPONENTIAL POTENTIAL

	ELECTR.	REPULSIVE	CAB	CBB	DBB	TOTAL
C''_{11}	0.522E-11	-0.106E-10	0.415E-12	0.241E-13	0.117E-12	-0.484E-11
C''_{12}	-0.231E-12	-0.128E-11	0.592E-13	0.241E-13	0.879E-13	-0.134E-11
C''_{44}	-0.261E-11	0.128E-11	-0.592E-13	0.803E-14	0.488E-13	-0.134E-11

POWER LAW		EXPONENTIAL	
DK/DP	D2K/DP2	DK/DP	D2K/DP2
0.441E 01	-0.238E-11	0.393E 01	-0.250E-11

TABLE 5-1-11

Predicted Volume Dependence of the Pressure and Elastic Constants for NaCl

Inputs: $\tilde{R}$ = 2.784 Å, $\tilde{K}$ = 284.7 kbar, ϕ = 1.0

Case 1: $C_{AB} = C_{BB} = D_{BB} = 0$

R (Å)	$V/\tilde{V}$	P (kb)	C_{44} (kb)	C_{12} (kb)	C_{11} (kb)	$C_{11} - C_{12}$ (kb)	K (kb)
2.784	1.000	0	133.5	133.5	587.0	453.5	284.7
2.700	.912	32.61	118.3	183.6	931.6	748.0	432.9
2.650	.862	60.05	102.6	222.7	1203	979.9	549.4
2.600	.815	95.41	80.1	271.0	1537	1266	692.9
2.550	.768	140.8	49.0	330.5	1948	1617	869.6
2.500	.724	198.7	6.7	404.0	2453	2049	1087
2.495	.720	205.3	1.7	412.3	2509	2097	1111

Case 2: $C_{AB} = 11.2 \times 10^{-60}$ erg cm^6, $C_{BB} = 116 \times 10^{-60}$ erg cm^6, $D_{BB} = 1594 \times 10^{-106}$ erg cm^{12} (Mayer, 1933)

R (Å)	$V/\tilde{V}$	P (kb)	C_{44} (kb)	C_{12} (kb)	C_{11} (kb)	$C_{11} - C_{22}$ (kb)	K (kb)
2.784	1.000	0	138.8	138.8	576.5	437.8	284.7
2.700	.912	32.60	131.3	196.5	905.7	709.2	432.9
2.600	.815	95.50	111.1	302.1	1482	1180	695.3
2.500	.724	199.6	73.9	473.0	2355	1882	1100
2.400	.641	370.3	15.5	756.2	3683	2926	1732
2.380	.625	415.9	1.2	832.9	4022	3190	1896

TABLE 5-1-12

Predicted 298°K Compression Curve for NaCl

$$P(V, T) = P_o(V) + P^*(V, T)$$

$$P_o(V) = \frac{-\partial W(V)}{\partial V} \qquad P^*(V, T) = \frac{\gamma}{V} W_{vib}$$

$$W_{vib} = \frac{9}{4} N_A k_B \Theta_D + 3 N_A k_B T D(\Theta_D/T), \qquad D(x) = \frac{3}{x^3}\int_0^x \frac{z^3}{e^z - 1}\, dz$$

Assume $P^*(V, 298)$ = constant

$\tilde{V}$ = 26.0 cm^3/mole $\quad \tilde{R}$ = 2.784 Å $\quad \Theta_D$ = 327 °K

V_{298} = 26.99 cm^3/mole $\quad R_{298}$ = 2.819 Å $\quad \tilde{K}$ = 284.7 kbar

γ = 1.0

Case 1, $C_{AB} = C_{BB} = D_{BB} = 0$

R (Å)	$V/\tilde{V}$	V/V_{298}	$P_o(V)$ (kb)	$P^*(V, T)$ (kb)	P (kb)	Birch-Murnaghan	% Diff.
2.819	1.038	1.000	-9.8	9.8	0	0	0
2.784	1.000	.963	0.0		9.8	9.7	1
2.700	.912	.879	32.61		42.4	39.9	6
2.650	.862	.830	60.05		69.9	65.0	8
2.600	.815	.785	95.41		105.2	95.1	11
2.550	.768	.740	140.8		150.6	134.2	12
2.500	.724	.697	198.7		208.5	183.2	14
2.495	.720	.694	205.3		215.1	187.2	15

Birch-Murnaghan Parameters:

K^T_{298} = 238.4, $\quad K'_{298}$ = 5.35 (Spetzler et. al., 1971)

continued...

TABLE 5-1-12 (continued)

Case 2, $C_{AB} = 11.2 \times 10^{-60}$ erg cm^6, $C_{BB} = 116 \times 10^{-60}$ erg cm^6
$D_{BB} = 1594 \times 10^{-106}$ erg cm^{12}

R (Å)	$V/\tilde{V}$	V/V_{CTB}	$P_o(V)$ (kb)	$P^*(V,T)$ (kb)	P (kb)	Birch-Murnaghan	% Diff.
2.819	1.038	1.000	-9.8	9.8	0	0	0
2.784	1.000	.963	0.0	↓	9.8	9.7	1
2.700	.912	.879	32.6	↓	42.4	39.9	6
2.600	.815	.785	95.5	↓	105.3	95.1	8
2.500	.724	.697	199.6	↓	209.4	183.2	14
2.400	.641	.617	370.3	↓	380.1	321.5	18
2.380	.625	.602	415.9	↓	425.7	357.3	19

TABLE 5-1-13

Predicted Volume Dependence of the Pressure and Elastic Constants for MgO

Inputs: $\tilde{R}$ = 2.093 Å C_{AB} = 7.8×10^{-60} ergs cm^6
$\tilde{K}$ = 1687.7 kbar C_{BB} = 8.46×10^{-60} ergs cm^6
D_{BB} = 35.8×10^{-106} ergs cm^{12}

Case 1, $\lambda = 0.7$

R (Å)	$V/\tilde{V}$	P (kb)	C_{44} (kb)	C_{12} (kb)	C_{11} (kb)	$C_{11} - C_{12}$ (kb)	K (kb)
2.093	1.000	0	1190	1190	2683	1492	1688
2.050	.940	118.7	1183	1420	3576	2156	2139
2.000	.873	300.4	1150	1751	4860	3109	2788
1.950	.809	542.0	1085	2169	6468	4299	3602
1.900	.748	861.3	977.7	2700	8479	5779	4627
1.850	.691	1281	817.2	3380	10991	7611	5918
1.800	.636	1832	591.6	4256	14130	9874	7548
1.750	.584	2555	289.3	5398	18061	12662	9619
1.712	.547	3251	2.3	6504	21706	15202	11571

Case 2, $\lambda = 0.6$

R (Å)	$V/\tilde{V}$	P (kb)	C_{44} (kb)	C_{12} (kb)	C_{11} (kb)	$C_{11} - C_{12}$ (kb)	K (kb)
2.093	1.000	0	1023	1023	3017	1994	1688
2.050	.940	119.8	1000	1240	4051	2811	2177
2.000	.873	306.6	943.6	1557	5561	4005	2892
1.950	.809	559.6	845.6	1965	7485	5520	3805
1.900	.748	900.0	692.8	2493	9932	7439	4972
1.850	.691	1355	469.2	3180	13040	9861	6467
1.800	.636	1963	155.5	4081	16991	12910	8385
1.780	.615	2259	-0.02	4518	18857	14339	9298

TABLE 5-1-14

Predicted 298 °K Compression Curve for MgO

$$P(V, T) = P_o(V) + P^*(V, T)$$

$$P_o(V) = \frac{-\partial W(V)}{\partial V} \qquad P^*(V, T) = \frac{\gamma}{V} W_{vib.}$$

$$W_{vib} = \frac{9}{4} N_A k_B \theta_D + 3 N_A k_B T D(\theta_D/T), \qquad D(x) = \frac{3}{x^3} \int_0^x \frac{z^3}{e^z - 1} dz$$

Assume $P^*(V, 298)$ = constant

$\tilde{V}$ = 11.045 cm^3/mole $\quad \tilde{R}$ = 2.093 Å $\quad \theta_D$ = 966 °K

V_{298} = 11.24 cm^3/mole $\quad R_{298}$ = 2.106 Å $\quad \tilde{K}$ = 1687.7 kbar

Case 1, δ = 0.7

R (Å)	$V/\tilde{V}$	V/V_{298}	$P_o(V)$ (kb)	$P^*(V,T)$ (kb)	P (kb)	Birch-Murnaghan	% Diff.
2.106	1.019	1.000	-30.2	30.2	0	0	0
2.093	1.000	.982	0.0		30.2	30.2	0
2.050	.940	.923	118.7		148.9	146.0	2
2.000	.873	.857	300.4		330.6	337.2	2
1.950	.809	.794	542.0		572.2	587.2	3
1.900	.748	.734	861.3		891.5	921.2	3
1.850	.691	.678	1281		1311	1357	4
1.800	.636	.624	1832		1862	1943	4
1.750	.584	.573	2555		2585	2720	5
1.712	.547	.537	3251		3281	3457	5

Birch-Murnaghan Parameters:

K'_{298} = 1605, $\quad K'_{298}$ = 3.89 (Spetzler, 1970)

continued...

TABLE 5-1-14 (continued)

Case 2, $\Delta = 0.6$

R (Å)	$V/\tilde{V}$	V/V_{298}	$P_o(V)$ (kb)	$P^*(V,T)$ (kb)	P (kb)	Birch-Murnaghan	% Diff.
2.106	1.019	1.0	-30.2	30.2	0	0	0
2.093	1.000	.982	0.0		30.2	30.2	0
2.050	.940	.923	119.8		150.0	146.0	3
2.000	.873	.857	306.6		336.8	337.0	.1
1.950	.809	.794	559.6		589.8	587.2	.4
1.900	.748	.734	900.0		930.2	921.2	1
1.850	.691	.678	1355		1385	1357	2
1.800	.636	.624	1963		1993	1943	3
1.780	.615	.064	2259		2289	2217	3

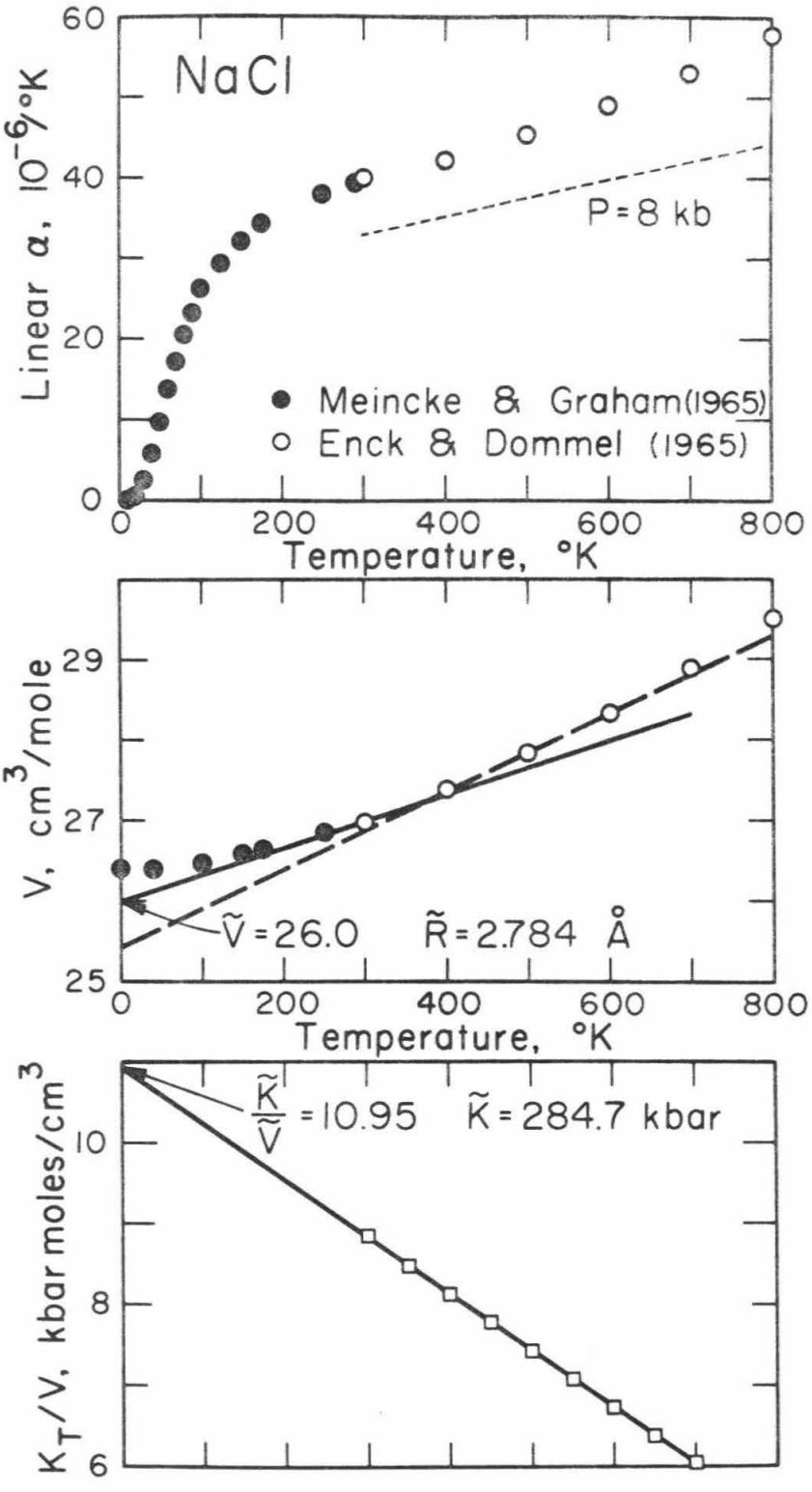

Figure 5-1-1. Static lattice parameters for NaCl.

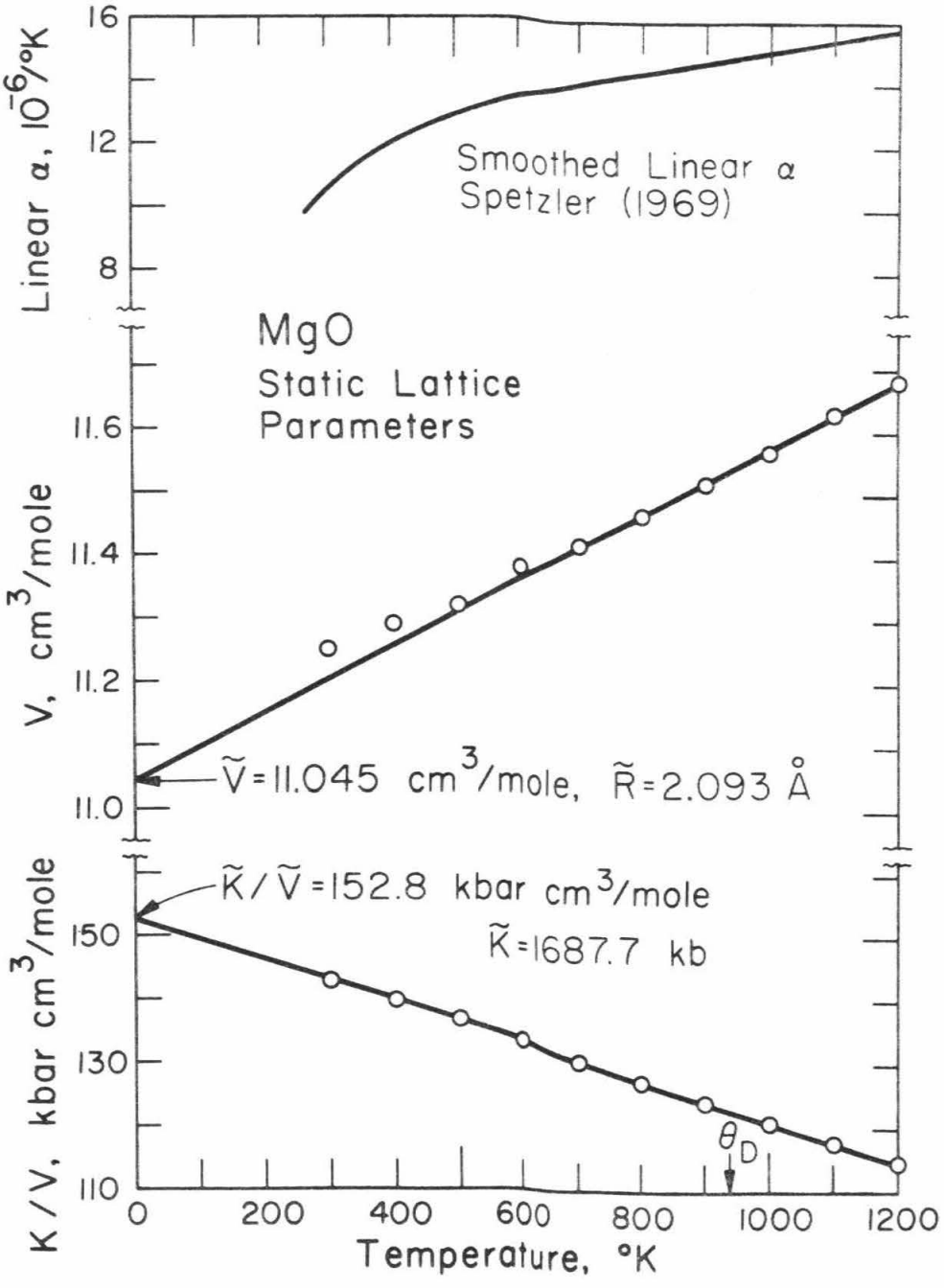

Figure 5-1-2. Static lattice parameters for MgO.

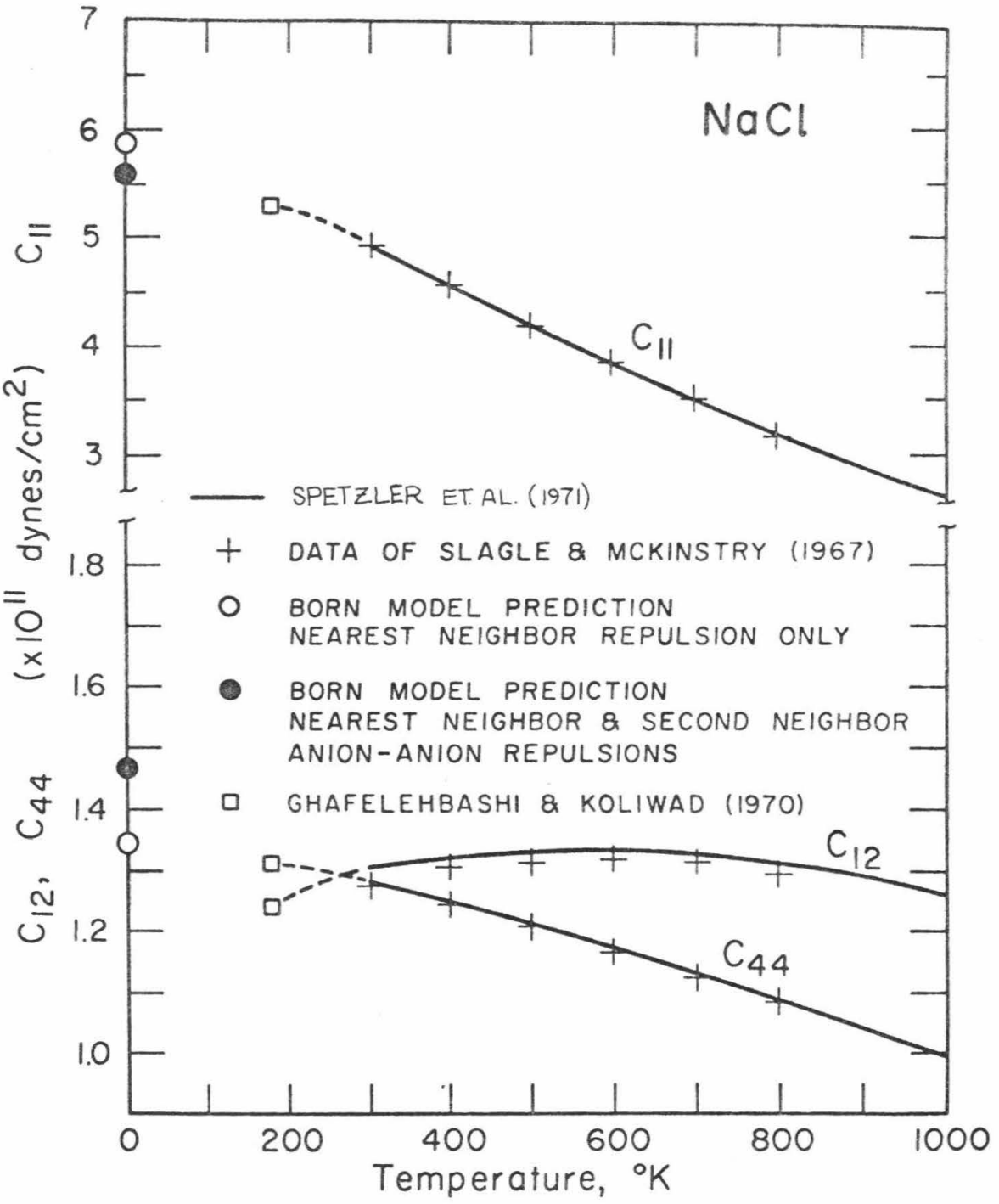

Figure 5-1-3. Temperature dependence of the elastic constants for NaCl.

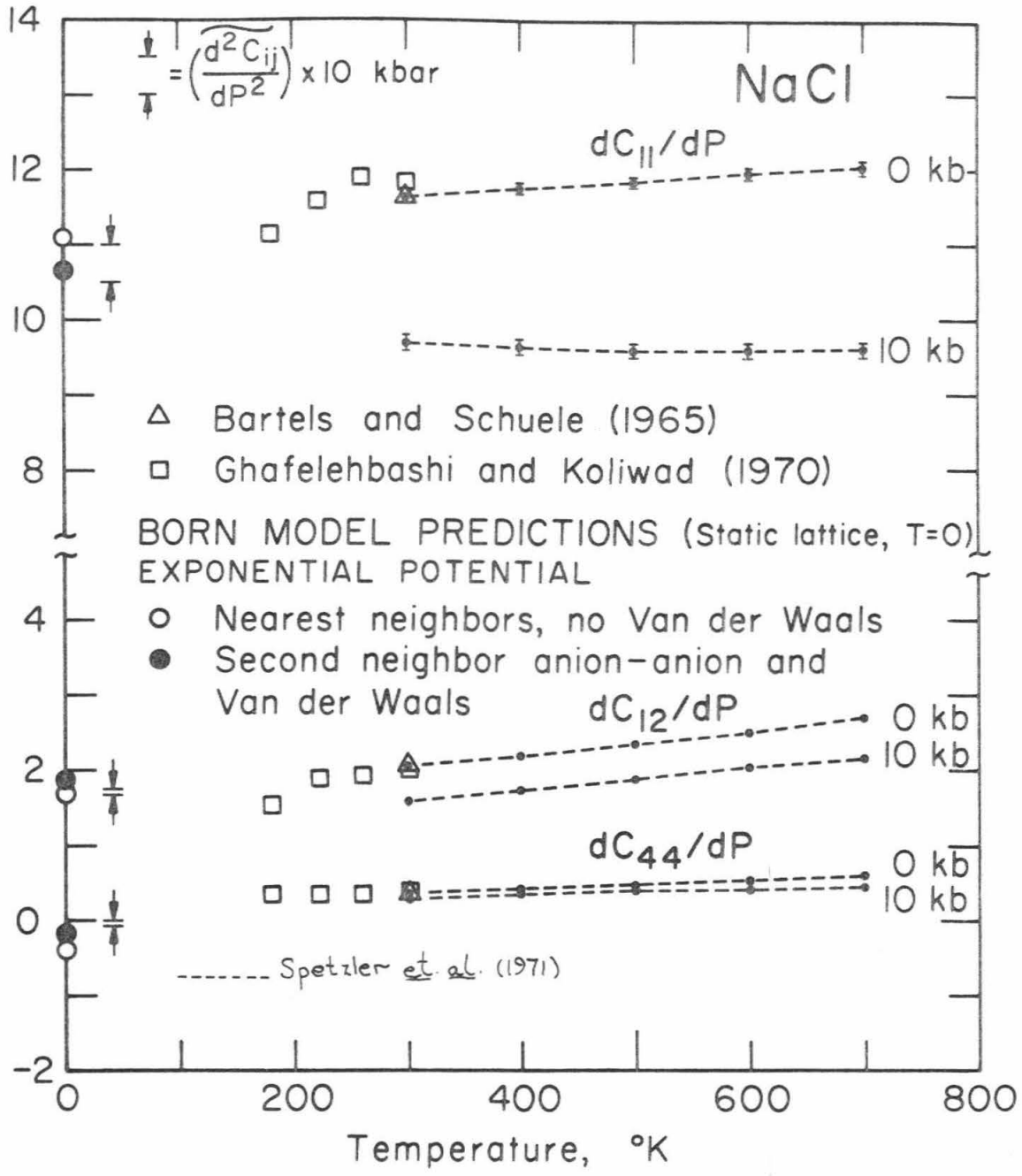

Figure 5-1-4. Temperature dependence of dC_{ij}/dP for NaCl.

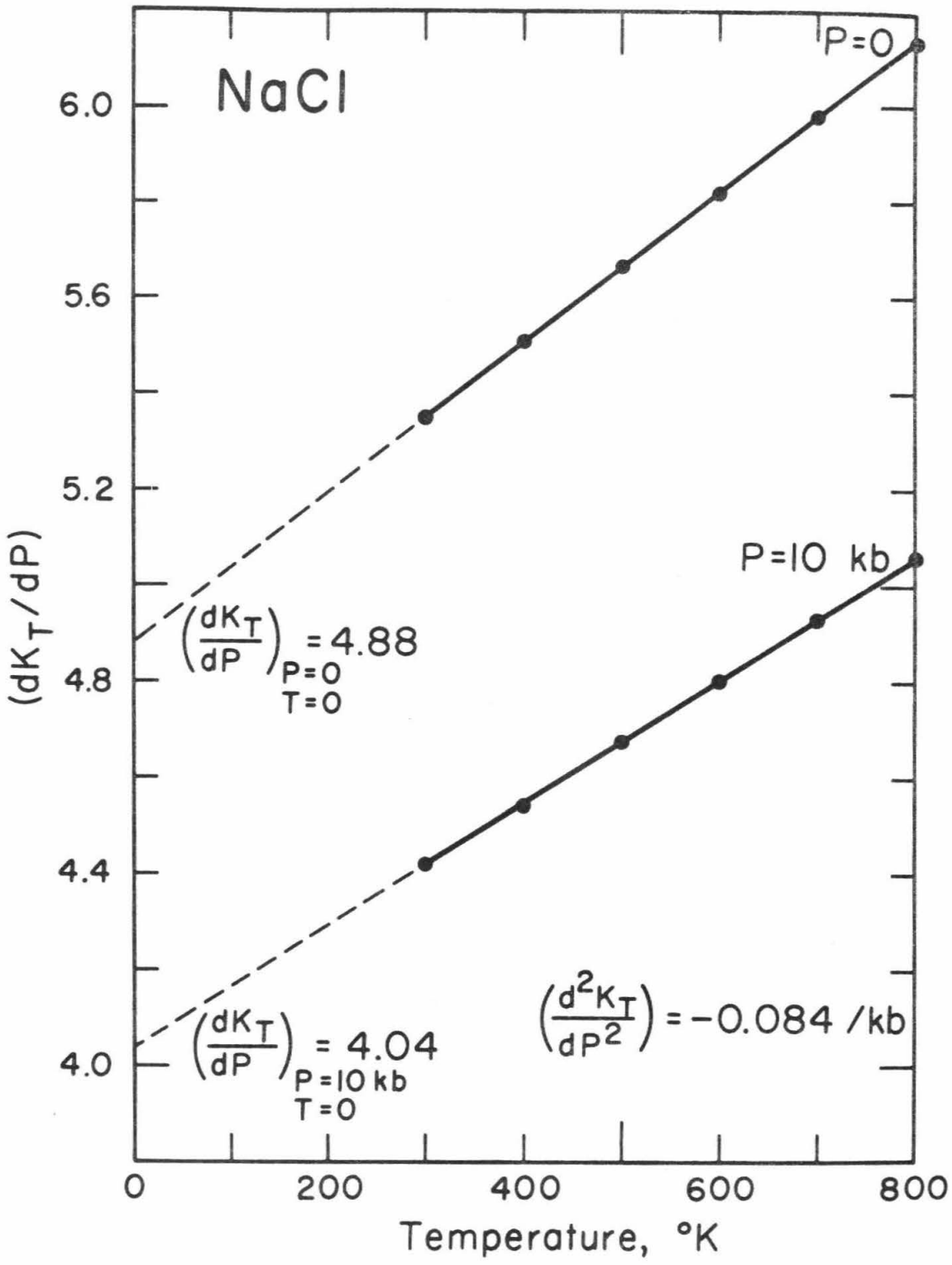

Figure 5-1-5. Temperature dependence of dK/dP for NaCl.

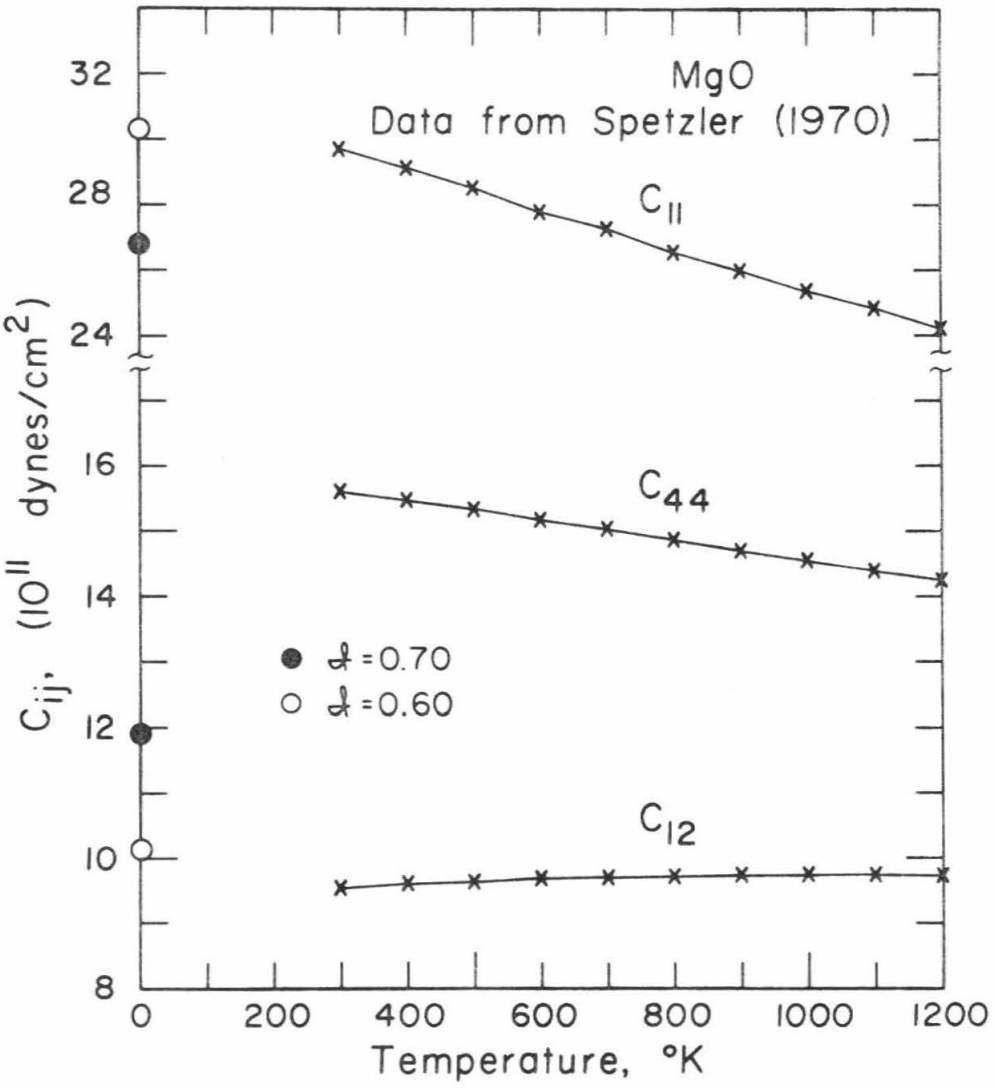

Figure 5-1-6. Temperature dependence of the elastic constants of MgO.

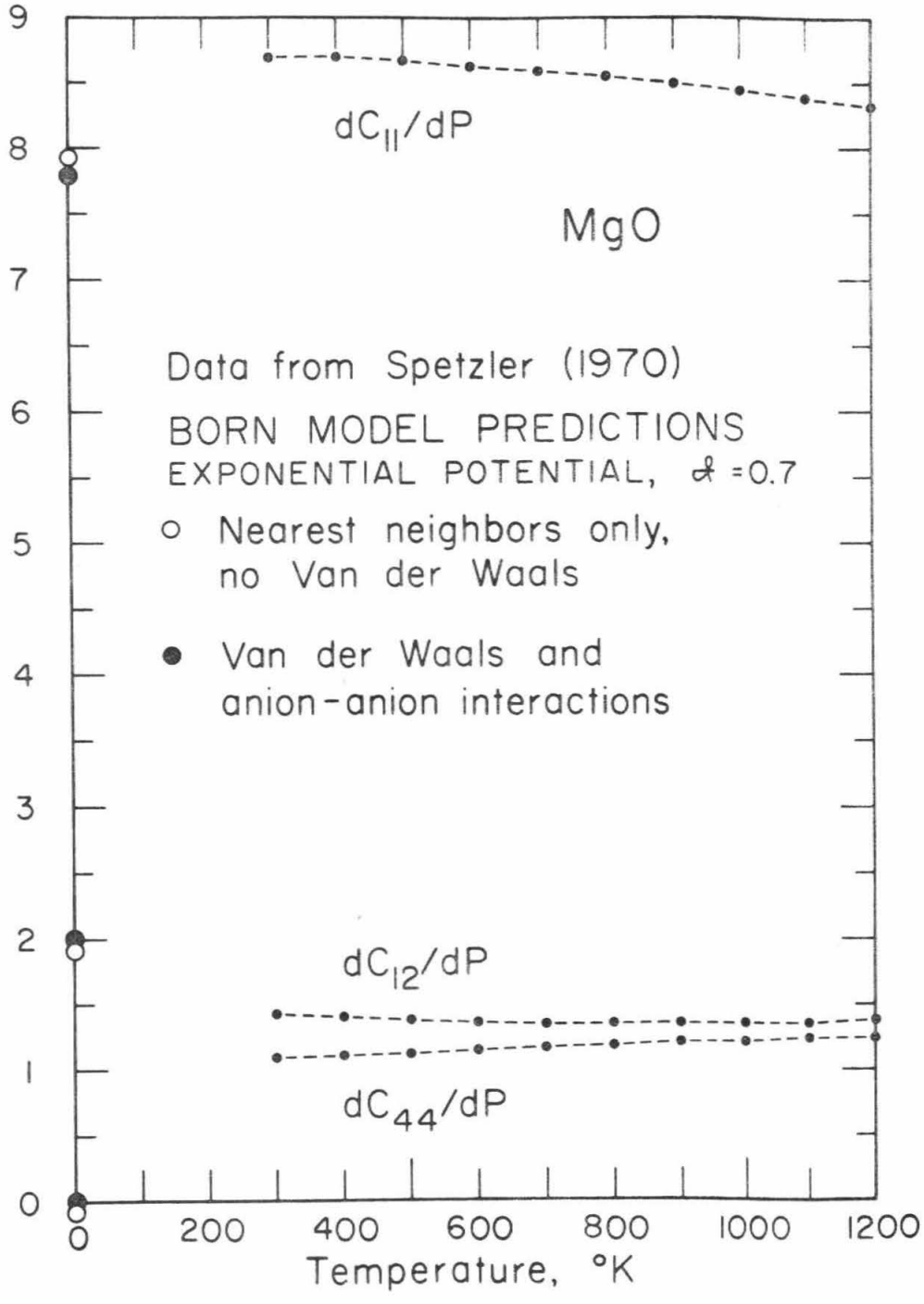

Figure 5-1-7. Temperature dependence of dC_{ij}/dP for MgO.

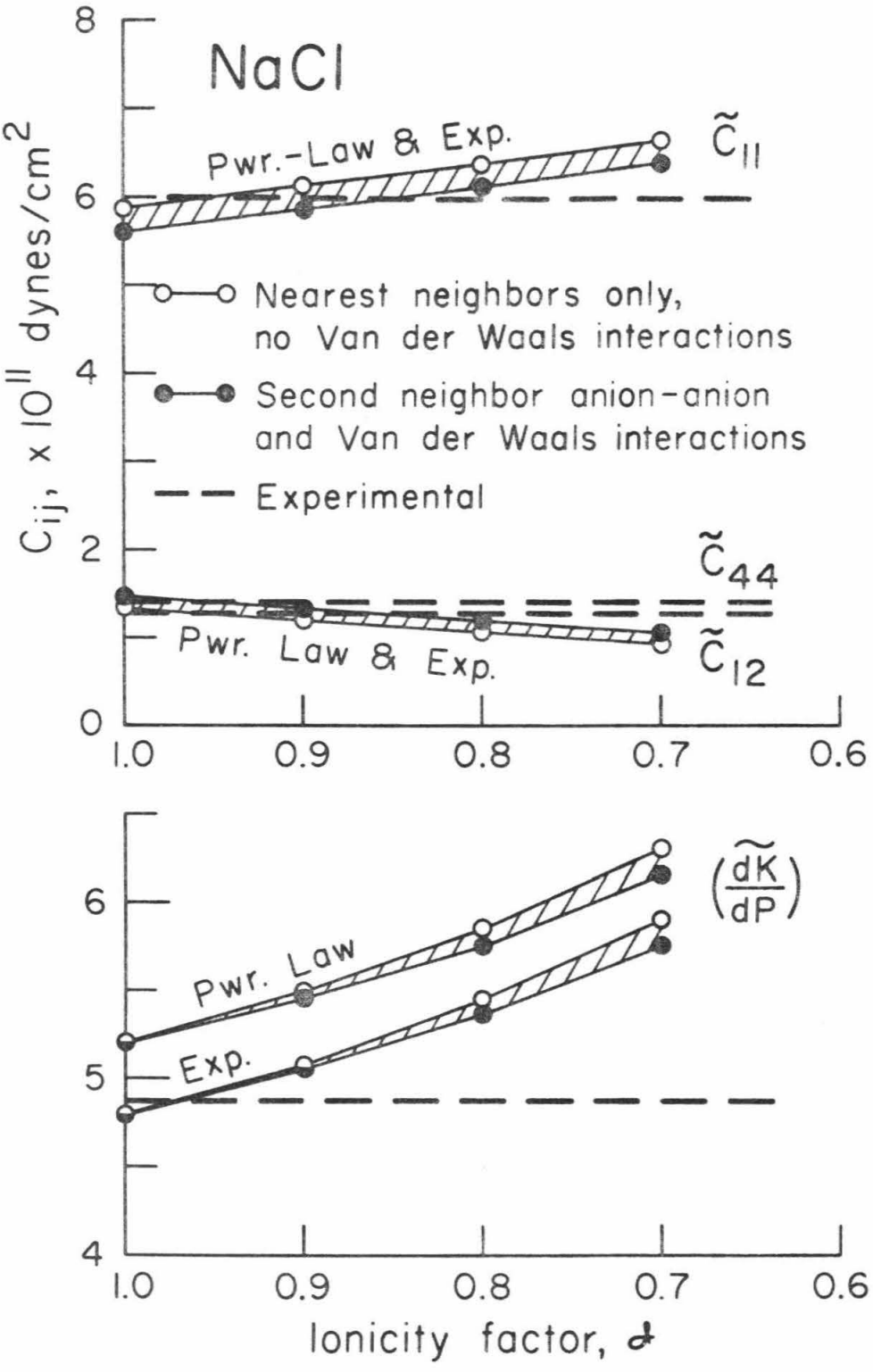

Figure 5-1-8. Comparison of theoretical and experimental elastic constants for NaCl.

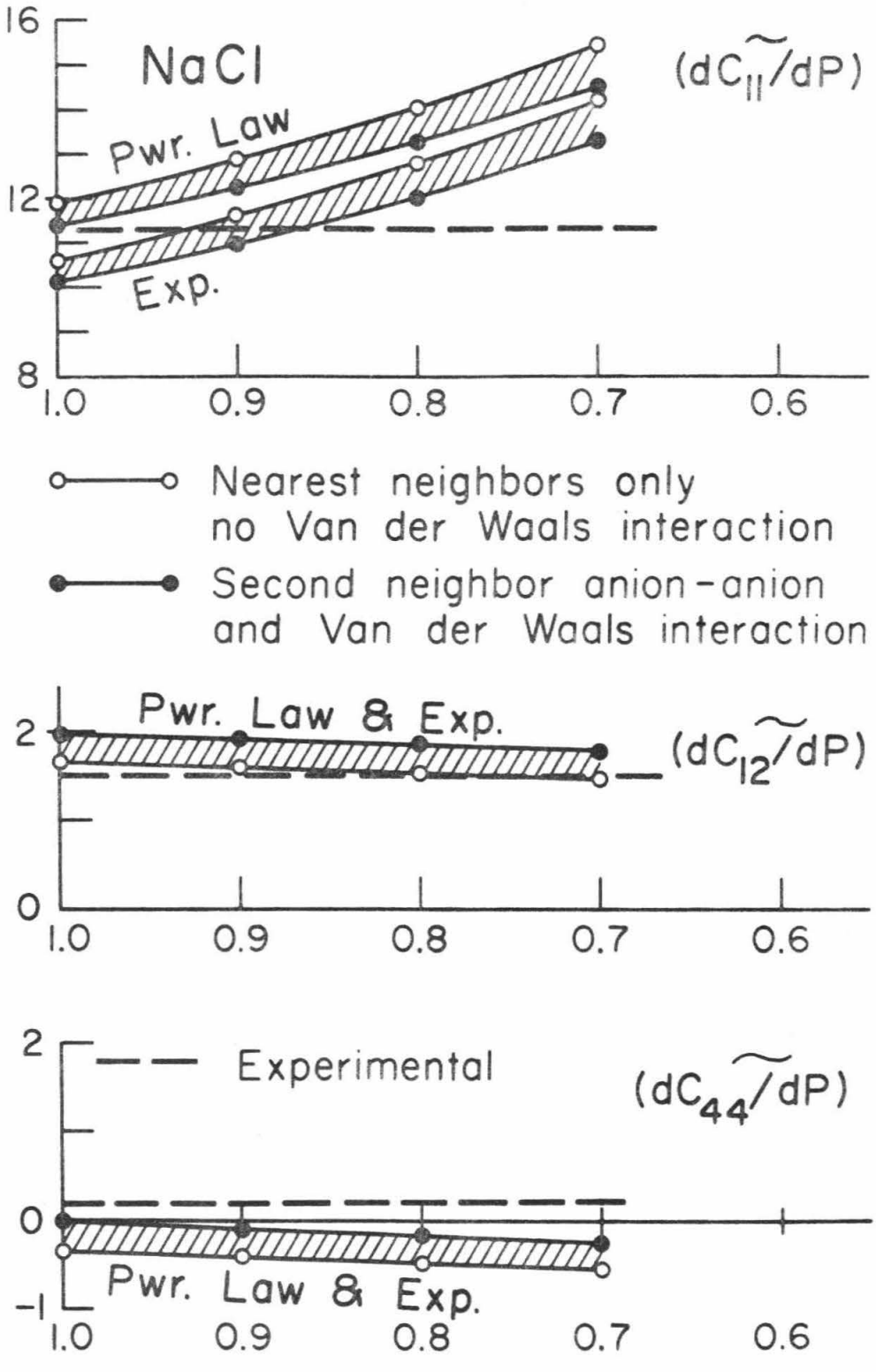

Figure 5-1-9. Comparison of theoretical and experimental elastic constants for NaCl.

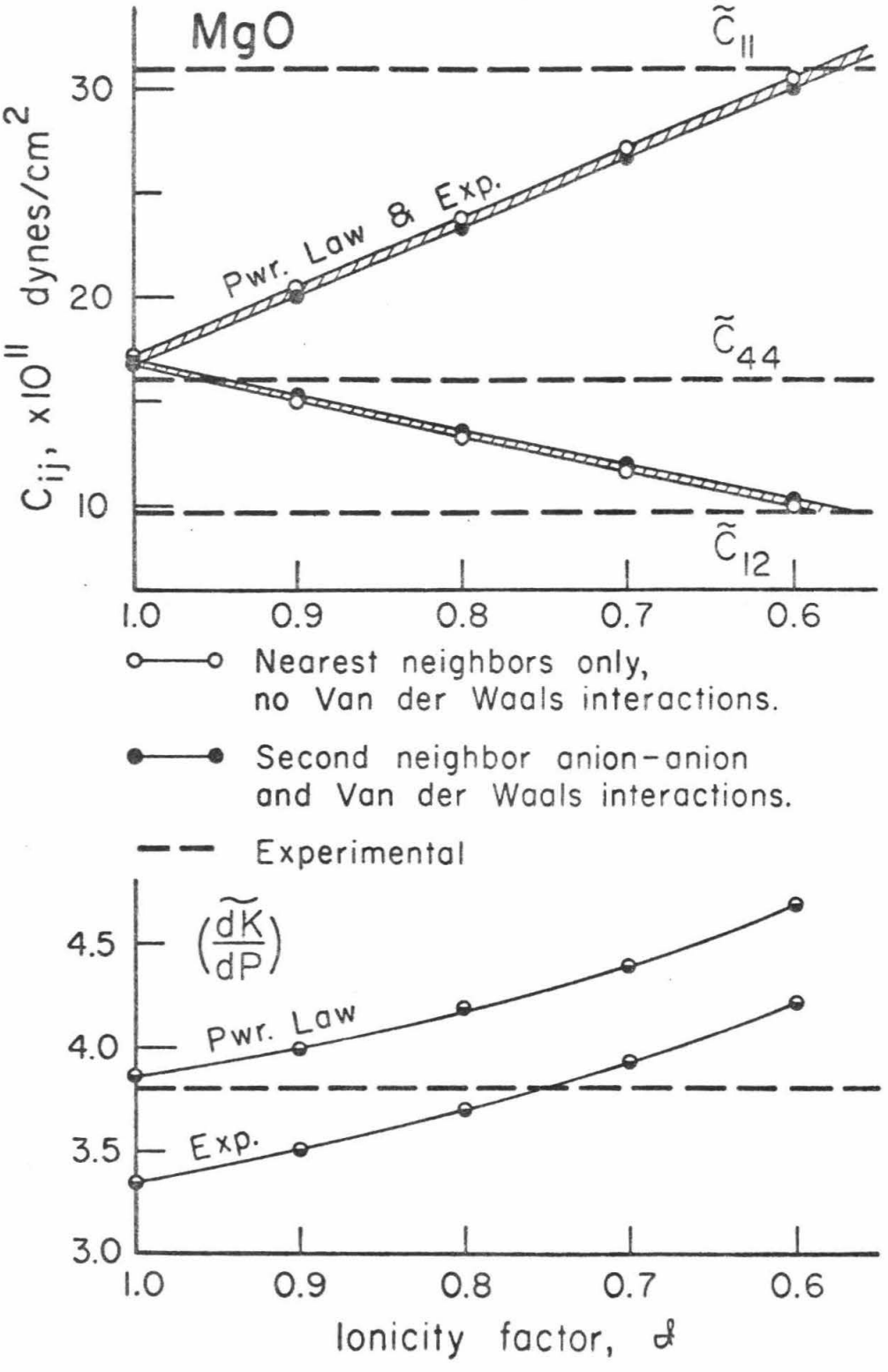

Figure 5-1-10. Comparison of theoretical and experimental elastic constants for MgO.

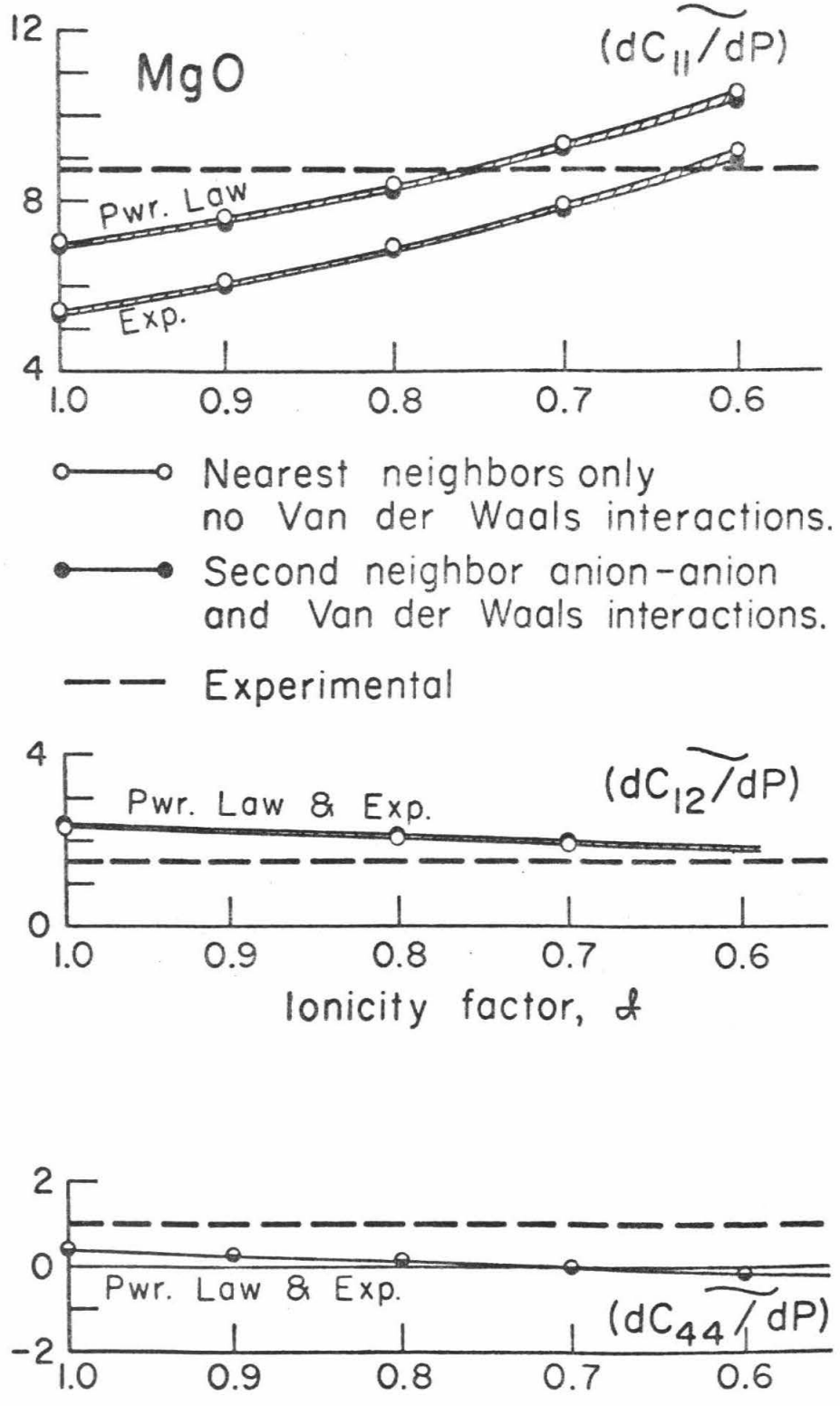

Figure 5-1-11. Comparison of theoretical and experimental elastic constants for MgO.

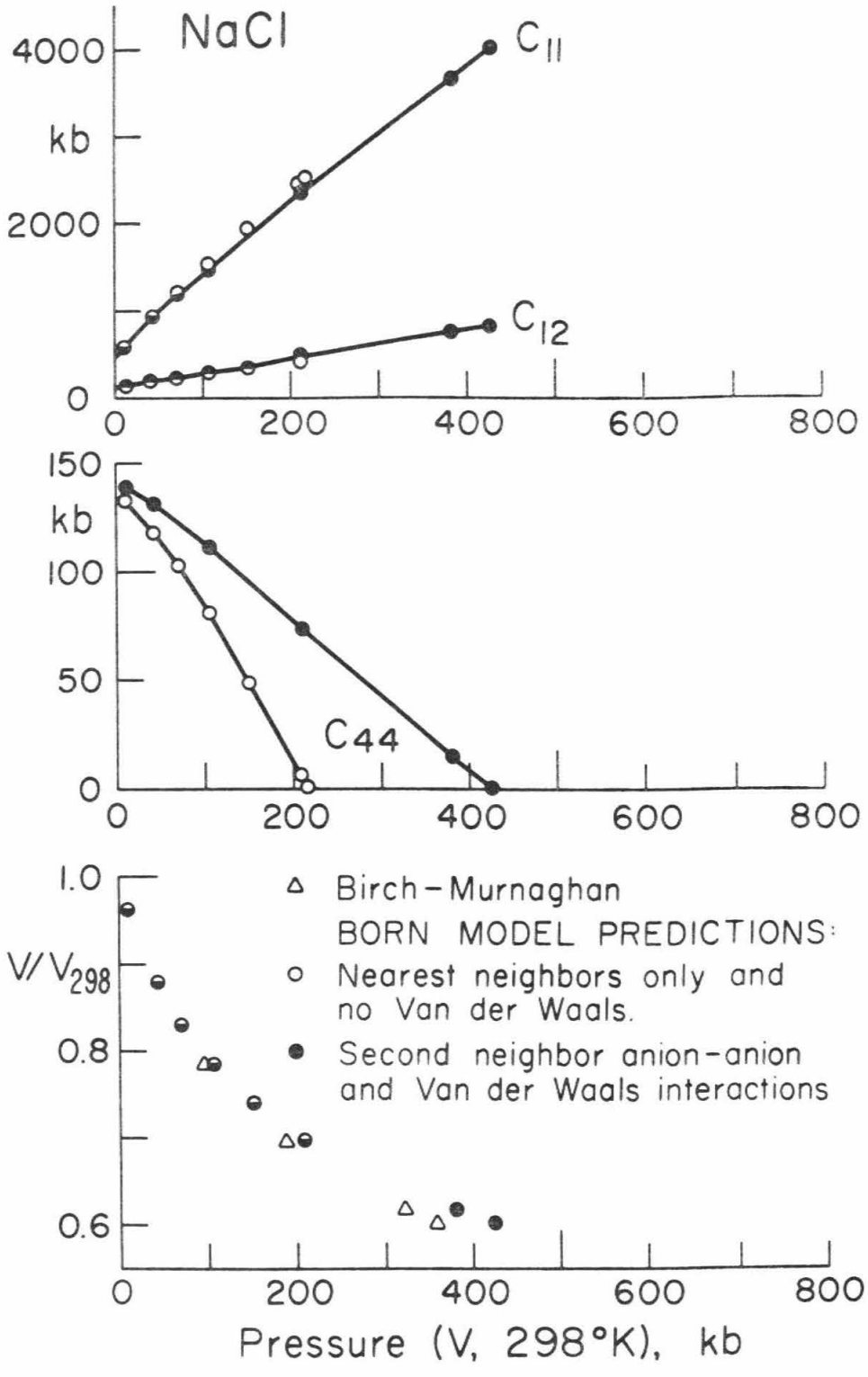

Figure 5-1-12. Theoretical pressure dependence of the elastic constants of NaCl.

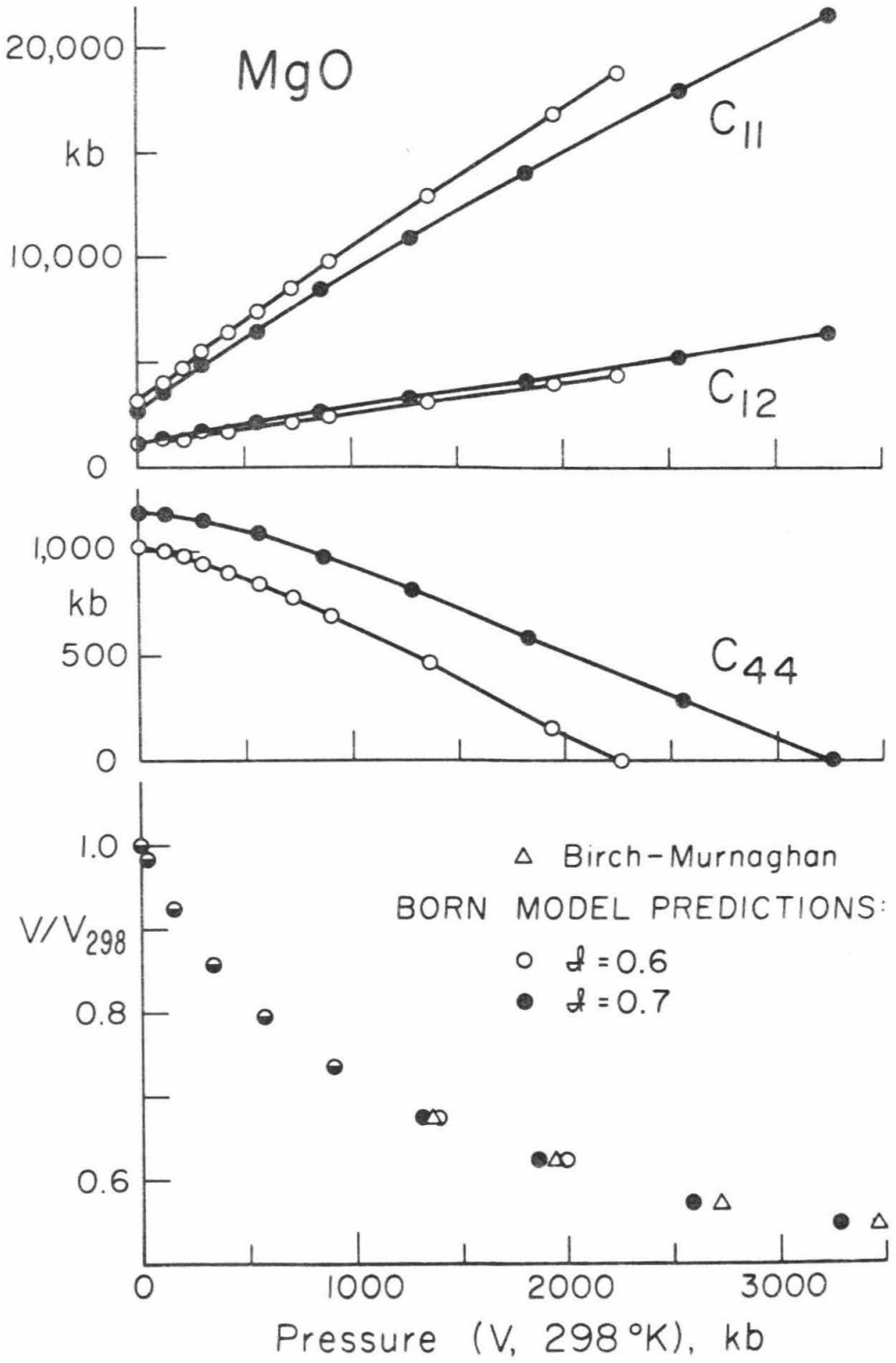

Figure 5-1-13. Theoretical pressure dependence of the elastic constants of MgO.

5-2. The Spinel Structure

In the last section, equations (3-3-99) for the elastic constants were specialized for the cubic, diatomic, sodium chloride structure. In this section, these equations are worked out for the more complex, triatomic, spinel lattice.

The Consistent Pair-Potential Assumption

When treating polyatomic solids in the Born approximation, it is important to differentiate between the various types of bonds rather than lump all cation-anion repulsive interactions into one term of the form B/R^n or $\lambda e^{-R/\rho}$, as is usually done in the literature. For example, in the case of A_2BO_4 spinel, there are six distinct two-body interactions, given below.

Cation-Cation Interactions:

$$\Phi_{AA}(r) = \frac{\mathcal{A} q_A^2}{r_{AA}^{\ell}} \quad , \quad \Phi_{BB}(r) = \frac{\mathcal{A} q_B^2}{r_{BB}^{\ell}} \tag{5-2-1}$$

$$\Phi_{AB}(r) = \frac{\mathcal{A} q_A q_B}{r_{AB}^{\ell}}$$

Cation-Anion Interactions:

$$\Phi_{AO}(r) = -\frac{\mathcal{A}|q_A q_O|}{r_{AO}^{\ell}} + V_{AO}(r) - \frac{C_{AO}}{(r_{AO}^{-1})^6} \tag{5-2-2}$$

$$\Phi_{BO}(r) = \frac{\mathcal{A} q_B q_O|}{r_{BO}^{\ell}} + V_{BO}(r) - \frac{C_{BO}}{(r_{BO}^{-1})^6}$$

Anion-Anion Interactions:

$$\Phi_{OO}(r) = \frac{\mathcal{A} q_O^2}{r_{OO}^{\ell}} - \frac{C_{OO}}{(r_{OO}^{-1})^6} + \frac{D_{OO}}{(r_{OO}^{-1})^{12}} \tag{5-2-3}$$

Note that there are now two empirical cation-anion repulsive functions ($V_{AO}(r)$, $V_{BO}(r)$), and hence four empirical parameters λ_{AO}, ρ_{AO}, λ_{BO}, ρ_{BO}. If only the bulk modulus and density of the spinel are known, only two of these parameters may be evaluated. However, this problem may be circumvented if one makes what I shall call the "consistent pair-potential assumption". This is the assumption that the two empirical parameters of the cation-anion repulsive interaction $V_{kk'}(r)$ depend only on the type of ions interacting. They are assumed to be independent of the specific solid in which this interaction takes place and of the coordination number of the cation in the solid. Thus, for the case of Al_2MgO_4, one can use the empirical λ_{MgO}, ρ_{MgO} in $V_{MgO}(r)$ that were determined from $\tilde{K}$ and $\tilde{R}$ of MgO in the last section. The measured values of $\tilde{K}$ and $\tilde{R}$ for Al_2MgO_4 can then be used to find the parameters λ_{AlO} and ρ_{AlO} in the aluminum oxygen repulsive potential $V_{AlO}(r)$. For the case of Mg_2SiO_4 spinel, which is of direct interest in the lower mantle, no ultrasonic or compression data exists. However, by using the consistent pair-potential assumption, $V_{SiO}(r)$ may be determined from the data on SiO_2 stishovite. In this way the elastic constants and their pressure dependence may be estimated.

The consistent pair-potential assumption can be tested using suites of solids containing the same cation-anion pairs for which good ultrasonic data exists. For example, $V_{MgO}(r)$ and $V_{AlO}(r)$ are shown to be self-consistent for the series MgO, Al_2O_3, and Al_2MgO_4 in Appendix 4. Further tests of this assumption should be one of the goals of future ultrasonics work in geophysics.

Tosi (1963) reached the conclusion that repulsive parameters cannot be transferred from structure to structure, since he could not accurately calculate the observed energy change associated with the transformation of NaCl from the rock salt to the CsCl structure using only one set of bond parameters. However, since the energy change is such a small part of the cohesive energy (typically 1%), and since volume dependence of the Gibbs free energy of the two structures are subparallel in G, V space, the requirement that the Born model describe such phase transitions is far more stringent than the requirement that it reflect the effect of structure on the elastic constants. When the elastic constants are measured through such a phase change, this test will be possible.

Specialization to the Spinel Structure

The spinel unit cell, with cube edge R, contains eight A_2BO_4 molecules and is diagrammed in Figure 5-2-1. It may be described in terms of fourteen interpenetrating F.C.C. Bravais lattices as (Wyckoff, Vol. 3, 1965)

$$
\begin{aligned}
&\text{Mg: } 000;\ \tfrac{1}{4}\tfrac{1}{4}\tfrac{1}{4} \\
&\text{Al: } \tfrac{5}{8}\tfrac{5}{8}\tfrac{5}{8};\ \tfrac{5}{8}\tfrac{7}{8}\tfrac{7}{8};\ \tfrac{7}{8}\tfrac{5}{8}\tfrac{7}{8};\ \tfrac{7}{8}\tfrac{7}{8}\tfrac{5}{8} \\
&\text{O: } uuu;\ u\bar{u}\bar{u};\ \tfrac{1}{4}-u, \tfrac{1}{4}-u, \tfrac{1}{4}-u;\ \tfrac{1}{4}-u, u+\tfrac{1}{4}, u+\tfrac{1}{4} \\
&\qquad \bar{u}\bar{u}u;\ \bar{u}u\bar{u};\ u+\tfrac{1}{4}, \tfrac{1}{4}-u, u+\tfrac{1}{4};\ u+\tfrac{1}{4}, u+\tfrac{1}{4}, \tfrac{1}{4}-u\ .
\end{aligned}
\qquad (5\text{-}2\text{-}4)
$$

Any lattice site may be reached from one of the above fourteen sublattice origins by a linear combination of the F.C.C. basis vectors:

$$\underset{\sim}{a}_1 = R(0,\tfrac{1}{2},\tfrac{1}{2}) \; ; \; \underset{\sim}{a}_2 = R(\tfrac{1}{2},0,\tfrac{1}{2}) \; ; \; \underset{\sim}{a}_3 = R(\tfrac{1}{2},\tfrac{1}{2},0) \; . \tag{5-2-5}$$

The u parameter is 0.375 for oxygen ions in perfect cubic close packing; for Al_2MgO_4, $u = 0.387$.

Since spinel has cubic symmetry, there are three independent elastic constants

$$\begin{aligned} C_{11} &= C_{22} = C_{33} = \mathcal{S}_{1111} = [1111] + (1111) \\ C_{12} &= C_{21} = C_{23} = C_{32} = C_{13} = C_{31} = \mathcal{S}_{1122} = 2[1212] - [2211] + (1122) \\ C_{44} &= C_{55} = C_{66} = \mathcal{S}_{2323} = [2233] + (2323) \; . \end{aligned} \tag{5-2-6}$$

For the spinel structure, internal deformations make a contribution to the elastic constants since the B-type site is not a symmetry center. The round brackets were computed according to their definition

$$(\alpha\beta\gamma\lambda) = \frac{-1}{4\pi^2 V_a} \sum_{kk'} \sum_{\mu\nu} \Gamma_{\mu\nu}(kk') \left(\sum_{k''} C^{(1)}_{\mu\alpha\gamma}(kk'') \sqrt{m_{k''}} \right) \cdot \left(\sum_{k'''} C^{(1)}_{\nu\beta\lambda}(k'k''') \sqrt{m_{k'''}} \right) \tag{5-2-7}$$

where

$$C^{(1)}_{\mu\alpha\gamma}(kk'') = \frac{-2\pi}{\sqrt{m_k m_{k''}}} \sum_{l} \Phi_{\alpha\beta}\begin{pmatrix} l \\ kk'' \end{pmatrix} \chi_\gamma \begin{pmatrix} l \\ kk'' \end{pmatrix} \tag{5-2-8}$$

as was derived in Chapter III.

It is not possible to compute the coulombic and non-coulombic contributions to the round brackets separately since the entire $\underset{\approx}{C}^{(0)}$ matrix must be inverted to yield $\underset{\approx}{\Gamma}$.

Writing the square brackets in terms of coulombic and non-coulombic parts

$$[\alpha\beta\gamma\lambda] = [\alpha\beta\gamma\lambda]^C + [\alpha\beta\gamma\lambda]^N .$$

The coulombic sums were computed directly according to equations (3-3-52) - (3-3-54). The sublattice indices k, k' ranged from 1 to 14 with x(k) given by (5-2-4). The sum over the direct lattice was taken over the vectors $x(\ell_{kk'}) = x(k') - x(k) + \ell_1 a_1 + \ell_2 a_2 + \ell_3 a_3$ where the basis vectors a_i are given by (5-2-5). The h sum was taken over the reciprocal lattice vectors

$$\underset{\sim}{b}(h) = h_1 b_1 + h_2 b_2 + h_3 b_3$$

where

$$b_1 = \frac{1}{R}(-1, 1, 1); \quad b_2 = \frac{1}{R}(1, -1, 1); \quad b_3 = \frac{1}{R}(1, 1, -1) .$$

The details of these lattice sums are given in Appendix 3. The results are

$u = 0.375$ (perfect cubic close packing of oxygens)

Madelung constant $\alpha_M = 128.6$ for R = 8.09 Å, q = 1e

Electrostatic Contributions to the Square Brackets	$[1111]^e$	= -1973.	$\mathcal{J}q^2/2R^4$ (5-2-9)
	$[1122]^e$	= 986.4	
	$[1212]^e$	= 300.8	

$u = 0.387$ (Al_2MgO_4)

Madelung constant $\alpha_M = 132.6$ for R = 8.09 Å, q = 1e

Electrostatic Contributions to the Square Brackets	$[1111]^e$	= -2069	$\mathcal{J}q^2/2R^4$ (5-2-10)
	$[1122]^e$	= 1034	
	$[1212]^e$	= 326.9	

The square brackets are plotted as a function of u in Figure 5-2-6. The Madelung constant for $u = .375$ is in agreement with that given by

Waddington (1959). Although the trend is the same for larger u, the values computed here using the Ewald method are $\sim 2\%$ smaller than those reported by Waddington (1959) based on an Evjen calculation. The electrostatic contribution to the elastic constants have not previously been computed for the spinel structure.

The expressions for the elastic constants are formally identical with equations (5-1-4) given in the previous section. For these equations

$$\alpha_{11} = [1111]^C \frac{2R^4}{\Delta q^2} = -1973. \ , \ (-2069.)$$

$$\alpha_{12} = \left\{ 2[1212]^C - [1122]^f \right\} \frac{2R^4}{\Delta q^2} = -384.8 \ , \ (-380.4) \qquad (5\text{-}2\text{-}11)$$

$$\alpha_{44} = [1122] \frac{2R^4}{\Delta q^2} = 986.4 \ , \ (1034)$$

where the numbers in parentheses are for $u = 0.387$. Note that these sums meet the required internal consistency checks

$$\alpha_{11} = -2\alpha_{44}$$

$$(\alpha_{11} + 2\alpha_{12}) \frac{V_a}{2R^3} = -\frac{4}{3} \frac{\alpha_M}{n_1}$$

where n_1 = number of molecules per reference cell of volume V_a.

The short-range sums in the C_{ij}^N part of equation (5-1-4) may be easily done by hand with the help of Table 5-2-1 which gives the nearest and relevant next-nearest neighbor positions of the cations and anions. With the help of this table, the elastic constants may be written as,

$$C_{11} = \frac{\alpha_{11}\hbar q^2}{2R^4} + \frac{1}{2Va}\left\{4\left[P_{BO}\frac{4}{3}\Gamma_{BO}^2 + Q_{BO}\frac{4}{9}\Gamma_{BO}^4\right] + \right.$$

$$+ 8\left[P_{AO}(2\beta^2+4\delta^2) + Q_{AO}(2\beta^4+4\delta^2)\right] + 8\left[P_{OO}(2\psi^2+2\xi^2+8\delta^2+R^2/4) + \right.$$

$$\left.\left. + Q_{OO}(2\psi^4+2\xi^4+32\delta^4+R^4/64)\right]\right\} + (1111)$$

$$C_{12} = \frac{\alpha_{12}\hbar q^2}{2R^4} + \frac{1}{2Va}\left\{4\left[-P_{BO}\frac{4}{3}\Gamma_{BO}^2 + Q_{BO}\frac{4}{9}\Gamma_{BO}^4\right] + \right.$$

$$\left. + 8\left[-P_{OO}(2\psi^4+2\xi^2+8\delta^2+R^2/4) + Q_{OO}(\psi^4+\xi^4+\delta^4+R^4/128)\right]\right\} + (1122) \qquad (5\text{-}2\text{-}12)$$

$$C_{44} = \frac{\alpha_{44}\hbar q^2}{2R^4} + \frac{1}{2Va}\left\{4\left[P_{BO}\frac{4}{3}\Gamma_{BO}^2 + Q_{BO}\frac{4}{9}\Gamma_{BO}^4\right] + \right.$$

$$+ 8\left[P_{AO}(2\beta^2+4\delta^2) + Q_{AO}(4\beta^2\delta^2+2\delta^4)\right] + 8\left[P_{OO}(2\psi^2+2\xi^2+8\delta^2+R^2/4) + \right.$$

$$\left.\left. + Q_{OO}(\psi^4+\xi^4+\delta^4+R^4/128)\right]\right\} + (1212)$$

The β, δ , and ξ parameters are defined in terms of the reference dimension R and u parameter according to (see Table 5-2-1)

$$r_{AO} = \sqrt{\beta^2+2\delta^2} \qquad \beta = (5/8-u)R$$

$$r_{BO} = \sqrt{3}\,(u-1/4)R \qquad \xi = (u-1/8)R \qquad (5\text{-}2\text{-}13)$$

$$r_{OO} \approx \sqrt{2}\,R/4 \qquad \delta = (u-3/8)R$$

Since the O—O interactions are relatively unimportant, we have taken all r_{OO} to be equal. The various $P_{kk'}$ and $Q_{kk'}$, k = A, B, O are given in terms of the two-body potentials by

$$
\begin{aligned}
P_{AO} &= \left[\frac{1}{r}\left(\frac{d\Phi_{AO}}{dr}\right)\right]_{r_{AO}} &&= \frac{V'_{AO}}{r_{AO}} + \frac{6C_{AO}}{r_{AO}^{8}} \\
Q_{AO} &= \left[\frac{1}{r}\frac{d}{dr}\left(\frac{1}{r}\frac{d\Phi_{AO}}{dr}\right)\right]_{r_{AO}} &&= -\frac{V'_{AO}}{r_{AO}^{3}} + \frac{V''_{AO}}{r_{AO}^{2}} - \frac{48C_{AO}}{r_{AO}^{10}} \\
P_{BO} &= \left[\frac{1}{r}\left(\frac{d\Phi_{BO}}{dr}\right)\right]_{r_{BO}} &&= \frac{V'_{BO}}{r_{BO}} + \frac{6C_{BO}}{r_{BO}^{8}} \\
Q_{BO} &= \left[\frac{1}{r}\frac{d}{dr}\left(\frac{1}{r}\frac{d\Phi_{BO}}{dr}\right)\right]_{r_{BO}} &&= -\frac{V'_{BO}}{r_{BO}^{3}} + \frac{V''_{BO}}{r_{BO}^{2}} - \frac{48C_{BO}}{r_{BO}^{10}} \\
P_{OO} &= \left[\frac{1}{r}\left(\frac{d\Phi_{OO}}{dr}\right)\right]_{r_{OO}} &&= \frac{6C_{OO}}{r_{OO}^{8}} - \frac{12D_{OO}}{r_{OO}^{14}} \\
Q_{OO} &= \left[\frac{1}{r}\frac{d}{dr}\left(\frac{1}{r}\frac{d\Phi_{OO}}{dr}\right)\right]_{r_{OO}} &&= -\frac{48C_{OO}}{r_{OO}^{10}} + \frac{168D_{OO}}{r_{OO}^{16}} .
\end{aligned}
\qquad (5\text{-}2\text{-}14)
$$

In equations (5-2-12) for the elastic constants, note that the identical terms $P_{BO} = P_{OB}$, $P_{AO} = P_{OA}$, $Q_{BO} = Q_{OB}$, $Q_{AO} = Q_{OA}$ have been combined.

Evaluation of the Empirical Parameters in V_{AO} and V_{BO}

Before the elastic constants can be calculated, we need to evaluate two of the empirical constants, λ_A and ρ_A or λ_B and ρ_B, depending upon whether the A–O or the B–O is known from data on the relevant diatomic solid. The energy density of the static lattice is given by

$$
\begin{aligned}
W &= \tfrac{1}{2}N_A\left(2U_A + U_B + 4U_O\right) \quad \text{ergs/mole} \\
&= N_A\left\{-\frac{\alpha m_d q^2}{R} + 2Z_{AO}\left[V_{AO}(r) - \frac{C_{AO}}{r_{AO}^{6}}\right] + \right. \\
&\qquad \left. + Z_{BO}\left[V_{BO}(r) - \frac{C_{BO}}{r_{BO}^{6}}\right] + 2Z_{OO}\left[-\frac{C_{OO}}{r_{OO}^{6}} + \frac{D_{OO}}{r_{OO}^{12}}\right]\right\}
\end{aligned}
\qquad (5\text{-}2\text{-}15)
$$

where

Z_{AO} = Coordination number of the A-type ion = 6

Z_{BO} = Coordination number of the B-type ion = 4

Z_{OO} = Number of oxygen second neighbors to a given oxygen = 12

Since we now wish to take derivatives with respect to the lattice constant R, it will be more convenient to rewrite equation (5-2-15) in terms of R using (5-2-13).

$$W = N_A \left\{ -\frac{\alpha_m \beta q^2}{R} + 2Z_{AO}\left[\mathcal{V}_{AO}(R) - \frac{\mathcal{C}_{AO}}{R^6} \right] + \right.$$
$$\left. + Z_{BO}\left[\mathcal{V}_{BO}(R) - \frac{\mathcal{C}_{BO}}{R^6} \right] + 2Z_{OO}\left[-\frac{\mathcal{C}_{OO}}{R^6} + \frac{\mathcal{D}_{OO}}{R^{12}} \right] \right. \tag{5-2-16}$$

where

$$\mathcal{V}_{AO}(R) = \lambda_{AO} e^{-\sqrt{43/64 - 11/4\,u + 3u^2}\, R/\rho_{AO}}$$
$$\mathcal{V}_{BO}(R) = \lambda_{BO} e^{-\sqrt{3}(u-1/4) R/\rho_{BO}}$$
$$\mathcal{C}_{AO} = C_{AO}/(43/64 - 11/4\,u + 3u^2)^3$$
$$\mathcal{C}_{BO} = C_{BO}/27(u-1/4)^6 \tag{5-2-17}$$
$$\mathcal{C}_{OO} \quad 512\, C_{OO}$$
$$\mathcal{D}_{OO} \approx 262144\, D_{OO}$$

To save needless algebra, the C_{OO} and D_{OO} parameters have been written as though the O^{2-} ions were in perfect close packing. This approximation was made in light of the result from the previous section that the O–O interactions have little effect on the bulk modulus. The equilibrium condition has the form

$$\left(\frac{\partial W}{\partial R}\right)_{\tilde{R}} = 0 = N_A \left\{ \frac{\alpha_m \beta q^2}{R^2} + 2Z_{AO}\left[\mathcal{V}'_{AO}(R) + \frac{6\mathcal{C}_{AO}}{R^7} \right] + \right.$$
$$\left. + Z_{BO}\left[\mathcal{V}'_{BO}(R) + \frac{6\mathcal{C}_{BO}}{R^7} \right] + 2Z_{OO}\left[\frac{6\mathcal{C}_{OO}}{R^7} - \frac{12\mathcal{D}_{OO}}{R^{13}} \right] \right\} \tag{5-2-18}$$

where the prime denotes differentiation w.r.t. R.

The bulk modulus is computed according to the relation

$$K = V \frac{\partial^2 W}{\partial V^2} .$$

An expression for the volume per mole V in terms of the reference dimension R may be written in a form applicable to any structure as

$$V = \frac{R^3}{C_1} \qquad R = (C_1 V)^{1/3} \tag{5-2-19}$$

where C_1 = moles/reference cell = η_1 / N_A

where η_1 = molecules/reference cell.

$$\frac{\partial R}{\partial V} = \frac{C_1}{3}(C_1 V)^{-2/3} = \frac{C_1}{3}\left(\frac{1}{R}\right)^2$$

$$\frac{\partial^2 R}{\partial V^2} = -\frac{2}{9} C_1^2 (C_1 V)^{-5/3} = -\frac{2C_1^2}{9}\left(\frac{1}{R}\right)^5$$

For the NaCl structure $\eta_1 = 1/2$, $C_1 = 1/2N_A$.

For the spinel structure $\eta_1 = 8$, $C_1 = 8/N_A$.

At equilibrium:

$$\left(\frac{\partial^2 W}{\partial V^2}\right)_{\tilde{V}} = \frac{\partial^2 W}{\partial R^2}\left[\frac{C_1^2}{9}\left(\frac{1}{R}\right)^4\right] . \tag{5-2-20}$$

Differentiating equation (5-2-18) with respect to R gives

$$\frac{\partial^2 W}{\partial R^2} = N_A \left\{ -\frac{2\alpha_m \phi q^2}{R^3} + 2Z_{AO}\left[V_{AO}''(R) - \frac{42 C_{AO}}{R^8}\right] + \right. \tag{5-2-21}$$

$$\left. + Z_{BO}\left[V_{BO}'' - \frac{42 C_{BO}}{R^8}\right] + 2Z_{OO}\left[-\frac{42 C_{OO}}{R^8} + \frac{156 D_{OO}}{R^{14}}\right]\right\} .$$

So the bulk modulus may be written

$$\tilde{K} = \frac{8}{9}\left\{ -\frac{2\alpha_m \phi q^2}{\tilde{R}^4} + 2Z_{AO}\left[\frac{V_{AO}''(\tilde{R})}{\tilde{R}} - \frac{42 C_{AO}}{\tilde{R}^9}\right] + \right.$$

$$\left. + Z_{BO}\left[\frac{V_{BO}''(\tilde{R})}{\tilde{R}} - \frac{42 C_{BO}}{\tilde{R}^9}\right] + 2Z_{OO}\left[-\frac{42 C_{OO}}{\tilde{R}^9} + \frac{156 D_{OO}}{\tilde{R}^{15}}\right]\right\} . \tag{5-2-22}$$

As for the case of NaCl, we can write

$$V''_{AO} = -\frac{\delta_{AO}}{R} V'_{AO}$$
$$V''_{BO} = -\frac{\delta_{BO}}{R} V'_{BO} \quad . \tag{5-2-23}$$

Using the equilibrium condition (equation 5-2-18)

$$V'_{AO} = \frac{-1}{2Z_{AO}}\left(\frac{\alpha_m \phi q^2}{\tilde{R}^2} + Z_{BO}\left[V'_{BO}(\tilde{R}) + \frac{6C_{BO}}{\tilde{R}^7}\right] + 2Z_{OO}\left[\frac{6C_{OO}}{\tilde{R}^7} - \frac{12D_{OO}}{\tilde{R}^{13}}\right]\right) - \frac{6C_{AO}}{\tilde{R}^7}$$
$$V'_{BO} = -\frac{1}{Z_{BO}}\left(\frac{\alpha_m \phi q^2}{\tilde{R}^2} + 2Z_{AO}\left[V'_{AO}(\tilde{R}) + \frac{6C_{AO}}{\tilde{R}^7}\right] + 2Z_{OO}\left[\frac{6C_{OO}}{\tilde{R}^7} - \frac{12D_{OO}}{\tilde{R}^{13}}\right]\right) - \frac{6C_{BO}}{\tilde{R}^7} \quad . \tag{5-2-24}$$

Equation (5-2-22) gives

$$\frac{V''_{AO}}{\tilde{R}} = \frac{1}{2Z_{AO}}\left\{\frac{9}{8}\tilde{K} + \frac{2\alpha_m \phi q^2}{\tilde{R}^4} - Z_{BO}\left[\frac{V''_{BO}}{\tilde{R}} - \frac{42C_{BO}}{\tilde{R}^9}\right] - 2Z_{OO}\left[\frac{-42C_{OO}}{\tilde{R}^9} + \frac{156D_{OO}}{\tilde{R}^{15}}\right]\right\} + \frac{42C_{AO}}{\tilde{R}^9} \quad . \tag{5-2-25}$$

Equation (5-2-23) may be written

$$\delta_{AO} = -\frac{\tilde{R}^2}{V'_{AO}}\left(\frac{V''_{AO}}{\tilde{R}}\right)$$

which, together with (5-2-24) and (5-2-25) gives

$$\delta_{AO} = \frac{\frac{1}{2Z_{AO}}\left\{\frac{9}{8}\tilde{K} + \frac{2\alpha_m \phi q^2}{\tilde{R}^4} - Z_{BO}\left[\frac{V''_{BO}}{\tilde{R}} - \frac{42C_{BO}}{\tilde{R}^9}\right] - 2Z_{OO}\left[\frac{-42C_{OO}}{\tilde{R}^9} + \frac{156D_{OO}}{\tilde{R}^{15}}\right]\right\} + \frac{42C_{AO}}{\tilde{R}^9}}{\frac{1}{2Z_{AO}}\left\{\frac{\alpha_m \phi q^2}{\tilde{R}^4} + Z_{BO}\left[\frac{V'_{BO}}{\tilde{R}^2} + \frac{6C_{BO}}{\tilde{R}^9}\right] + 2Z_{OO}\left[\frac{6C_{OO}}{\tilde{R}^9} - \frac{12D_{OO}}{\tilde{R}^{15}}\right]\right\} + \frac{6C_{AO}}{\tilde{R}^9}} \quad . \tag{5-2-26}$$

By identical algebra, one may also obtain

$$\delta_{BO} = \frac{\frac{1}{Z_{BO}}\left\{\frac{9}{8}\tilde{K} + \frac{2\alpha_m \phi q^2}{\tilde{R}^4} - 2Z_{AO}\left[\frac{V''_{AO}}{\tilde{R}} - \frac{42C_{AO}}{\tilde{R}^9}\right] - 2Z_{OO}\left[\frac{-42C_{OO}}{\tilde{R}^9} + \frac{156D_{OO}}{\tilde{R}^{15}}\right]\right\} + \frac{42C_{OO}}{\tilde{R}^9}}{\frac{1}{Z_{BO}}\left\{\frac{\alpha_m \phi q^2}{\tilde{R}^4} + 2Z_{AO}\left[\frac{V'_{AO}}{\tilde{R}^2} + \frac{6C_{AO}}{\tilde{R}^9}\right] + 2Z_{OO}\left[\frac{6C_{OO}}{\tilde{R}^9} - \frac{12D_{OO}}{\tilde{R}^{15}}\right]\right\} + \frac{6C_{BO}}{\tilde{R}^9}} \quad . \tag{5-2-27}$$

For the exponential form of the cation-anion potential, which is the only one we will investigate for the spinel structure, equations (5-2-17) give

$$\delta_{AO} = \sqrt{43/64 - 11/4\,u + 3u^2}\;\frac{\tilde{R}}{\rho_{AO}}$$

$$\delta_{BO} = \sqrt{3}\,(u - 1/4)\,\frac{\tilde{R}}{\rho_{BO}}\,. \qquad (5\text{-}2\text{-}28)$$

The second empirical parameters, λ_{AO} or λ_{BO}, may now be evaluated using equations (5-2-24) and (5-2-17).

$$(V'_{AO})_{\tilde{R}} = -\frac{\lambda_{AO}}{\tilde{R}}\sqrt{\frac{43}{64} - \frac{11}{4}u + 3u^2}\left(\frac{\tilde{R}}{\rho_{AO}}\right)e^{-\sqrt{\frac{43}{64} - \frac{11}{4}u + 3u^2}\;\tilde{R}/\rho_{AO}}$$

$$= \frac{-1}{2Z_{AO}}\left(\frac{\alpha_m \delta q^2}{\tilde{R}^2} + Z_{BO}\left[V'_{BO}(\tilde{R}) + \frac{6C_{BO}}{\tilde{R}^7}\right] + 2Z_{OO}\left[\frac{6C_{OO}}{\tilde{R}^7} - \frac{12D_{OO}}{\tilde{R}^{13}}\right]\right) - \frac{6C_{AO}}{\tilde{R}^7} \qquad (5\text{-}2\text{-}29)$$

so

$$\lambda_{AO} = \frac{\rho_{AO}\, e^{\sqrt{43/64 - 11/4\,u + 3u^2}\,\tilde{R}/\rho}}{\sqrt{\frac{43}{64} - \frac{11}{4}u + 3u^2}}\left\{\frac{1}{2Z_{AO}}\left(\frac{\alpha_m \delta q^2}{\tilde{R}^2} + Z_{BO}\left[V'_{BO}(\tilde{R}) + \frac{6C_{BO}}{\tilde{R}^7}\right] + \right.\right.$$

$$\left.\left. + 2Z_{OO}\left[\frac{6C_{OO}}{\tilde{R}^7} - \frac{12D_{OO}}{\tilde{R}^{13}}\right]\right) + \frac{6C_{AO}}{\tilde{R}^7}\right\}$$

By identical algebra

$$\lambda_{BO} = \frac{\rho_{BO}\, e^{\sqrt{3}(u-1/4)\tilde{R}/\rho_{BO}}}{\sqrt{3}\,(u - 1/4)}\left\{\frac{1}{Z_{BO}}\left(\frac{\alpha_m \delta q^2}{\tilde{R}^2} + 2Z_{AO}\left[V'_{AO}(\tilde{R}) + \frac{6C_{AO}}{\tilde{R}^7}\right] + \right.\right. \qquad (5\text{-}2\text{-}30)$$

$$\left.\left. + 2Z_{OO}\left[\frac{6C_{OO}}{\tilde{R}^7} - \frac{12D_{OO}}{\tilde{R}^{13}}\right]\right) + \frac{6C_{BO}}{\tilde{R}^7}\right\}.$$

The Volume Dependence of the Bulk Modulus and the Pressure

The volume dependence of the bulk modulus is given by

$$K(R) = V\frac{\partial^2 W}{\partial V^2} = V\left[\frac{\partial^2 W}{\partial R^2}\left(\frac{\partial R}{\partial V}\right)^2 + \frac{\partial W}{\partial R}\,\frac{\partial^2 R}{\partial V^2}\right]. \qquad (5\text{-}2\text{-}31)$$

By using (5-2-19) for the V derivatives of R, and using (5-2-18) and (5-2-21) for the R derivatives of W, equation (5-2-31) may be written

$$K(R) = \frac{8}{9}\left\{ -\frac{40\alpha_m \Omega q^2}{R^4 v} + 2Z_{AO}\left[\frac{v_{AO}''}{R} - \frac{2v_{AO}'}{R^2} - \frac{54C_{AO}}{R^9}\right] + \right.$$

$$\left. + Z_{BO}\left[\frac{v_{BO}''}{R} - \frac{2v_{BO}'}{R^2} - \frac{54C_{BO}}{R^9}\right] + 2Z_{OO}\left[-\frac{54C_{OO}}{R^9} + \frac{180D_{OO}}{R^{15}}\right]\right\} \qquad (5\text{-}2\text{-}32)$$

where, according to (5-2-17)

$$v_{AO}' = -\frac{\lambda_{AO}}{R}\sqrt{\tfrac{43}{64} - \tfrac{11}{4}u + 3u^2}\left(\frac{R}{\rho_{AO}}\right) e^{-\sqrt{\frac{43}{64} - \frac{11}{4}u + 3u^2}\, R/\rho_{AO}}$$

$$v_{AO}'' = \frac{\lambda_{AO}}{R^2}\left(\tfrac{43}{64} - \tfrac{11}{4}u + 3u^2\right)\left(\frac{R}{\rho_{AO}}\right)^2 e^{-\sqrt{\frac{43}{64} - \frac{11}{4}u + 3u^2}\, R/\rho_{AO}}$$

$$v_{BO}' = -\frac{\lambda_{BO}}{R}\sqrt{3}\left(u - \tfrac{1}{4}\right)\left(\frac{R}{\rho_{BO}}\right) e^{-\sqrt{3}(u-1/4)R/\rho_{BO}}$$

$$v_{BO}'' = \frac{\lambda_{BO}}{R^2}\, 3\left(u - \tfrac{1}{4}\right)^2\left(\frac{R}{\rho_{BO}}\right)^2 e^{-\sqrt{3}(u-1/4)R/\rho_{BO}} .$$

The pressure-volume relation is given by

$$P = -\frac{\partial W}{\partial V} = -\frac{\partial W}{\partial R}\frac{\partial R}{\partial V} .$$

Using (5-2-18) and (5-2-19), gives

$$P = -\frac{8}{3}\left\{\frac{\alpha_m \Omega q^2}{R^4 v} + 2Z_{AO}\left[\frac{v_{AO}'}{R^2} + \frac{6C_{AO}}{R^9}\right] + Z_{BO}\left[\frac{v_{BO}'}{R^2} + \frac{6C_{BO}}{R^9}\right]\right.$$

$$\left. + 2Z_{OO}\left[\frac{6C_{OO}}{R^9} - \frac{12D_{OO}}{R^{15}}\right]\right\}. \qquad (5\text{-}2\text{-}33)$$

Equations (5-1-35) and (5-1-36) may be used to derive explicit expressions for the pressure derivatives of the elastic constants. However, because of the excessive algebra, these derivatives will be found by finite differencing on the computer.

Numerical Predictions for Al_2MgO_4 and Discussion

Linear extrapolation of V(T) and (K/V)(T) from the high temperature regime to T = 0°K gives the two input parameters $\tilde{R}$ = 8.001 Å and $\tilde{K}$ = 2140.6 kbar (see Figure 5-2-2). Since the ultrasonic data for MgO was best fit by an exponential cation-anion potential with $\delta \approx 0.7$; the parameters λ_{BO} and ρ_{BO} found for model G.7.E in the last section were used here. Equations (5-2-26), (5-2-28), and (5-2-29) were then used to find the other two parameters λ_{AO} and ρ_{AO} for the Al–O interaction.

Having thus obtained all the required parameters, equation (5-2-33) was used to compute P(R), equation (5-2-32) to compute K(R), and equations (5-2-12) to compute $C_{ij}(R)$. The results of these computations are summarized in Table 5-2-2 where they are compared with the ultrasonic data of O'Connell (1971). It should be pointed out that these data are for non-stoichiometric spinel of composition $MgO \cdot 2.61\, Al_2O_3$. Preliminary results of Lewis (personal communication) and O'Connell indicate that the elastic moduli are relatively insensitive to variations in stoichiometry, changing by less than 5%. The effect of non-stoichiometry on the pressure derivatives has yet to be measured.

An interesting result of these calculations is the distortion of the spinel structure from cubic close packing of the oxygen ions. If one assumes that the oxygens are close-packed and solves for λ_{AO} and ρ_{AO} using $u = .375$, one predicts elastic constants in poor agreement with experiment (Table 5-2-3). The largest disagreement is for C_{44} and is due to the large negative contribution from the internal strains. In

Figure (5-2-5) the cohesive energy (equation 5-2-15) is plotted as a function of u for P = 0. The energy has a minimum for $u = .392$. This says that if a spinel crystal having $u = .375$ and the repulsive parameters associated with that oxygen parameter were allowed to find its equilibrium configuration at P = 0, it would distort to $u = .392$ (expanding from R = 8.00 Å to R = 8.09 Å). The energy curve for P = 400 kb is also given, showing that the u parameter does not change with pressure for this model. The observed oxygen parameter is $u = .387$ (Wycoff, 1965). If λ_{AO} and ρ_{AO} are found for this u, the lattice will again distort to $u = .392$, but the associated expansion is only from R = 8.00 Å to R = 8.05 Å. The elastic constants in this case are in much better agreement with experiment (Table 5-2-2). Since the crystal is nearer its preferred distortion, the contributions to the elastic constants due to internal deformations are much smaller.

The distortion in this direction is due to the increase in the Madelung constant for larger u. This allows the crystal to distort and expand while still increasing the absolute value of the cohesive energy. The equilibrium u is also a function of the relative strengths of the Mg–O and Al–O bonds -- the fact that the model predicts a u close to that observed is confirmation of the consistent pair potential hypothesis. Conversely, the measured u parameter can be used to further refine the Mg–O potential, the readjustment being made in the ionicity factor, f, for MgO, which is not precisely determined by the elastic data for MgO. However, the discrepancy between calculated $u = .392$ and observed $u = .387$ may be due to a shortening of the

Mg–O bond due to a covalent contribution in the bonding -- and thus beyond the scope of this model. The inclusion of van der Waals and oxygen terms in the cohesive energy does not significantly change these results.

For spinel, as for NaCl and MgO, the predicted elastic constants and their pressure derivatives are not significantly changed by the inclusion of van der Waals and oxygen-oxygen second neighbor interactions. We shall therefore not include second neighbor effects in the next section on the rutile structure.

It is interesting that, experimentally, Al_2MgO_4 looks like a "Cauchy-solid" since $C_{12} \approx C_{44}$. One might be tempted to assume that this implied central forces. However, since spinel is not centrosymmetric, the central-force model predicts $C_{12} \neq C_{44}$. The difference between theory and experiment is presumably due to the same three-body forces responsible for the large deviation from Cauchy's relation observed for MgO.

In Table 5-2-2 the elastic constants and their pressure derivatives are given both with and without the round brackets. It can be seen that these contributions from the internal deformations have a large effect on the pressure derivatives — changing dC_{44}/dP and $d/dP\left[\frac{1}{2}(C_{11}-C_{12})\right]$ from positive to negative. This result will be seen to be also true for the silicate spinel, Mg_2SiO_4, investigated in the next chapter; it leads to the unsatisfactory result that dV_s/dP is negative. It is important to note that while the induced dipole moments do not contribute to the square brackets, they do make a contribution to the round

brackets (Cowley, 1962), and should be investigated in an attempt to remove this important discrepancy between the rigid-ion model and experimental data. Work in this direction is already in progress (Striefler and Barsch, 1971).

The geophysically interesting Mg_2SiO_4 spinel will be treated in Chapter VI, using the Mg–O bond parameters found for periclase in the previous section and the Si–O bond parameters found for stishovite in the next section.

TABLE 5-2-1

Neighbor Positions and Short-Range Sums for the Spinel Structure

For k = B, the k' sum is over the 4 nearest oxygen neighbors

$r_{BO} = \sqrt{3}\gamma$, $\gamma = (u - 1/4)R$, R = cell edge

Site Type 1

k	k'	$x_1(kk')$	$x_2(kk')$	$x_3(kk')$	x_1^2	$x_1^2 x_2^2$	x_1^4
1	14	$-\gamma$	$-\gamma$	γ	γ^2	γ^4	γ^4
1	13	$-\gamma$	γ	$-\gamma$	↓	↓	↓
1	10	γ	$-\gamma$	$-\gamma$	↓	↓	↓
1	9	γ	γ	γ	↓	↓	↓
				$\sum_{k'} \rightarrow$	$\frac{4}{3}r_{BO}^2$	$\frac{4}{9}r_{BO}^4$	$\frac{4}{9}r_{BO}^4$

Site Type 2

k	k'	$x_1(kk')$	$x_2(kk')$	$x_3(kk')$	x_1^2	$x_1^2 x_2^2$	x_1^4
2	7	$-\gamma$	$-\gamma$	$-\gamma$	γ^2	γ^4	γ^4
2	11	γ	γ	$-\gamma$	↓	↓	↓
2	12	γ	$-\gamma$	γ	↓	↓	↓
2	8	$-\gamma$	γ	γ	↓	↓	↓
				$\sum_{k'} \rightarrow$	$\frac{4}{3}r_{BO}^2$	$\frac{4}{9}r_{BO}^4$	$\frac{4}{9}r_{BO}^4$

(continued...)

TABLE 5-2-1 (continued)

For k = A, the k' sum is over the 6 nearest oxygen neighbors

$r_{AO} = \sqrt{\beta^2 + 2\delta^2}$, $\beta = (5/8 - u)R$, $\delta = (u - 3/8)R$

k	k'	$x_1(kk')$	$x_2(kk')$	$x_3(kk')$	x_1^2	$x_1^2 x_2^2$	x_1^4
3	8	β	δ	δ	β^2	$\beta^2\delta^2$	β^4
3	10	$-\beta$	$-\delta$	$-\delta$	β^2	$\beta^2\delta^2$	β^4
3	12	δ	β	δ	δ^2	$\beta^2\delta^2$	δ^4
3	13	$-\delta$	$-\beta$	$-\delta$	δ^2	$\beta^2\delta^2$	δ^4
3	11	δ	δ	β	δ^2	δ^4	δ^4
3	14	$-\delta$	$-\delta$	$-\beta$	δ^2	δ^4	δ^4
4	7	β	$-\delta$	$-\delta$	β^2	$\beta^2\delta^2$	β^4
4	9	$-\beta$	δ	δ	β^2	$\beta^2\delta^2$	β^4
4	14	$-\delta$	β	δ	δ^2	$\beta^2\delta^2$	δ^4
4	11	δ	$-\beta$	$-\delta$	δ^2	$\beta^2\delta^2$	δ^4
4	12	δ	$-\delta$	$-\beta$	δ^2	δ^4	δ^4
4	13	$-\delta$	δ	β	δ^2	δ^4	δ^4
5	14	β	$-\delta$	δ	β^2	$\beta^2\delta^2$	β^4
5	11	$-\beta$	δ	$-\delta$	β^2	$\beta^2\delta^2$	β^4
5	7	$-\delta$	β	$-\delta$	δ^2	$\beta^2\delta^2$	δ^4
5	9	δ	$-\beta$	δ	δ^2	$\beta^2\delta^2$	δ^4
5	8	$-\delta$	δ	$-\beta$	δ^2	δ^4	δ^4
5	10	δ	$-\delta$	β	δ^2	δ^4	δ^4
6	13	β	δ	$-\delta$	β^2	$\beta^2\delta^2$	β^4
6	12	$-\beta$	$-\delta$	δ	β^2	$\beta^2\delta^2$	β^4
6	10	δ	β	$-\delta$	δ^2	$\beta^2\delta^2$	δ^4
6	8	$-\delta$	$-\beta$	δ	δ^2	$\beta^2\delta^2$	δ^4
6	7	$-\delta$	$-\delta$	β	δ^2	δ^4	δ^4
6	9	δ	δ	$-\beta$	δ^2	δ^4	δ^4

(continued...)

TABLE 5-2-1 (continued)

For k = 0, the k' sum is over the 12 nearest oxygen neighbors (second neighbors). Only $x_i(kk')$ for $k > k'$ are tabulated since $x_i(k'k) = -x_i(kk')$.

$\delta = u - 3/8$ $\quad \xi = 2u - 1/2$ $\quad m = 2u - 1$

k	k'	$x_1(kk')$	$x_2(kk')$	$x_3(kk')$
7	8	0	ξ	ξ
	12	ξ	0	ξ
	13	$-1/4$	2δ	$-1/4$
	10	2δ	$-1/4$	$1/4$
	11	ξ	ξ	0
	11	m	m	0
	14	$-1/4$	$1/4$	2δ
	14	$1/4$	$-1/4$	2δ
	8	0	m	m
	12	m	0	m
	13	$1/4$	2δ	$-1/4$
	10	2δ	$1/4$	$-1/4$
8	12	ξ	$-\xi$	0
	12	m	$-m$	0
	13	$-1/4$	$-1/4$	-2δ
	13	$1/4$	$1/4$	-2δ
	11	ξ	0	$-\xi$
	14	$1/4$	-2δ	$1/4$
	9	2δ	$1/4$	$-1/4$
	11	m	0	$-m$
	14	$1/4$	-2δ	$1/4$
	9	2δ	$-1/4$	$1/4$

$$x_i(8, 7) = -x_i(7, 8)$$

(continued...)

TABLE 5-2-1 (continued)

k	k'	$x_1(kk')$	$x_2(kk')$	$x_3(kk')$
9	14	$-m$	$-m$	0
	14	$-s$	$-s$	0
	11	$1/4$	$-1/4$	-2δ
	11	$-1/4$	$1/4$	-2δ
	13	$-m$	0	$-m$
	10	0	$-m$	$-m$
	12	$-1/4$	-2δ	$1/4$
	13	$-s$	0	$-s$
	10	0	$-s$	$-s$
	12	$1/4$	-2δ	$-1/4$

$x_i(9, 8) = -x_i(8, 9)$

10	13	$-m$	m	0
	13	$-s$	s	0
	12	$-1/4$	$-1/4$	2δ
	12	$1/4$	$1/4$	2δ
	14	$-\psi$	0	ψ
	11	$-1/4$	2δ	$-1/4$
	14	$-s$	0	s
	11	$1/4$	2δ	$1/4$

$x_i(10, 9) = -x_i(9, 10)$ $\quad x_i(10, 7) = -x_i(7, 10)$

11	12	0	$-m$	m
	13	-2δ	$1/4$	$1/4$
	12	0	$-s$	s
	13	-2δ	$-1/4$	$-1/4$

$x_i(11, 7) = -x_i(7, 11)$; $x_i(11, 8) = -x_i(8, 11)$; $x_i(11, 9) = -x_i(9, 11)$; $x_i(11, 10) = -x_i(10, 11)$

(continued...)

TABLE 5-2-1 (continued)

k	k'	$x_1(kk')$	$x_2(kk')$	$x_3(kk')$
12	14	-28	-1/4	-1/4
	14	-28	1/4	1/4

$x_i(12, 7) = -x_i(7, 12)$; $x_i(12, 8) = -x_i(8, 12)$; $x_i(12, 9) = -x_i(9, 12)$;

$x_i(12, 10) = -x_i(10, 12)$; $x_i(12, 11) = -x_i(11, 12)$

13	14	0	-m	m
	14	0	-s	s

$x_i(13, 7) = -x_i(7, 13)$; $x_i(13, 8) = -x_i(8, 13)$; $x_i(13, 9) = -x_i(9, 13)$

$x_i(13, 10) = -x_i(10, 13)$; $x_i(13, 11) = -x_i(11, 13)$

$x_i(14, 7) = -x_i(7, 14)$; $x_i(14, 8) = -x_i(8, 14)$; $x_i(14, 9) = -x_i(9, 14)$;

$x_i(14, 10) = -x_i(10, 14)$; $x_i(14, 12) = -x_i(12, 14)$; $x_i(14, 13) = -x_i(13, 14)$

TABLE 5-2-2

Static Lattice Parameters for Al_2MgO_4 Spinel

Param.	Units	Ideal Structure No Multipoles $u = 0.375$	Al_2MgO_4 Structure No Multipoles $u = 0.387$	Al_2MgO_4 Incl. van der Waals O—O Interactions $u = 0.387$	Experimental Value	Experimental Source
$\tilde{R}$	Å	Input	Input	Input	8.001	Fig. 5-2-2
$\tilde{K}$	kbar	Input	Input	Input	2140.6	Fig. 5-2-2
$\tilde{C}_{11}$	kbar	2650	2916 (3402)	2934	3082	Fig. 5-2-3
$\tilde{C}_{12}$	kbar	1755	1709 (1509)	1714	1564	Fig. 5-2-3
$\tilde{C}_{44}$	kbar	249	1130 (1509)	1110	1617	Fig. 5-2-3
$\tilde{K}'$	--	3.8	3.7 (3.7)	3.6	3.9	Fig. 5-2-4
$\tilde{C}'_{11}$	--	4.6	3.1 (6.2)	3.0	4.4	Fig. 5-2-4
$\tilde{C}'_{12}$	--	3.5	3.9 (2.5)	3.8	3.6	Fig. 5-2-4
$\tilde{C}'_{44}$	--	-0.71	-0.30 (.45)	-0.39	0.8	Fig. 5-2-4

$\delta = 0.7$, Numbers in parentheses are the results when internal deformations are ignored.

TABLE 5-2-3

Contributions to the Theoretical Elastic Constants of Al_2MgO_4 Spinel

u	Elastic Constant	Sq. Bracket Contribution	Rnd. Bracket Contribution	Total	
.375	C_{11}	2781	-130.8	2650	No Multipoles
	C_{12}	1821	- 66.31	1755	
	C_{44}	1821	-1571.	248.9	
.387	C_{11}	3402	-486.	2916	No Multipoles
	C_{12}	1509	200.	1709	
	C_{44}	1509	-379.	1130	
.387	C_{11}	3324	-390.	2934	Including van der Waals and O–O Interactions
	C_{12}	1551	160.	1714	
	C_{44}	1551	-441.	1110	

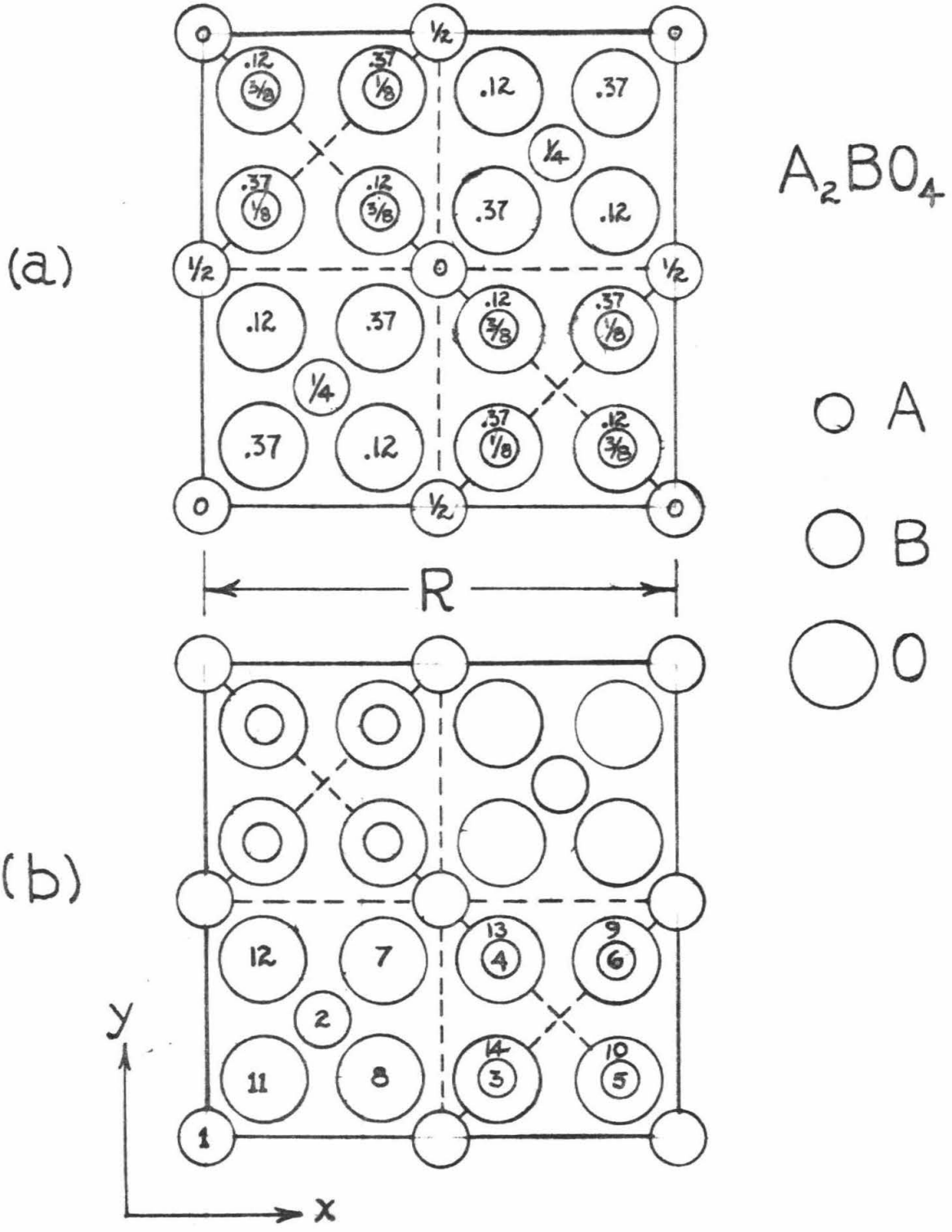

Figure 5-2-1. Spinel structure after Wyckoff (1965). (a) ion positions. (b) sublattice numbers.

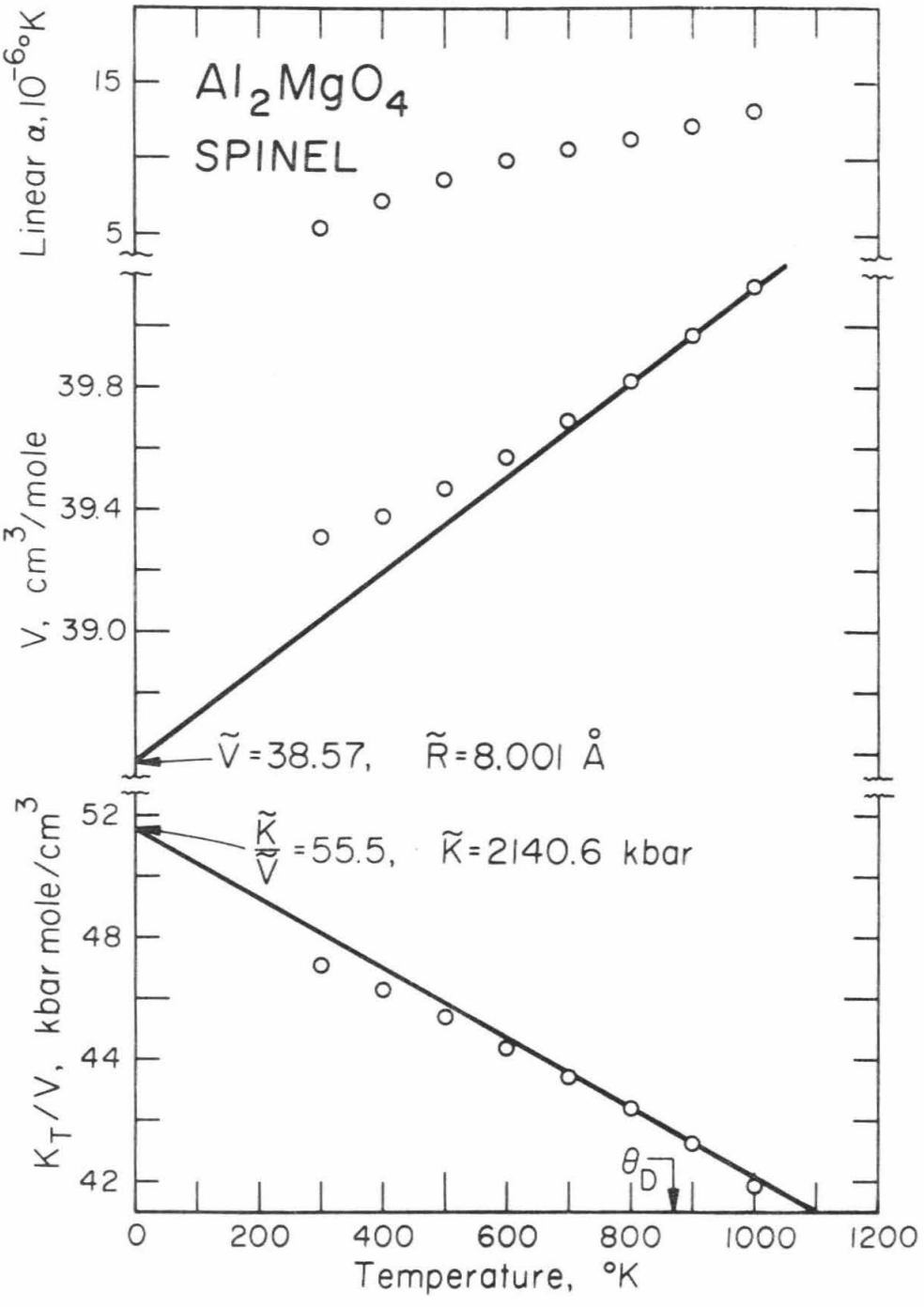

Figure 5-2-2. Static lattice parameters of Al_2MgO_4 spinel.

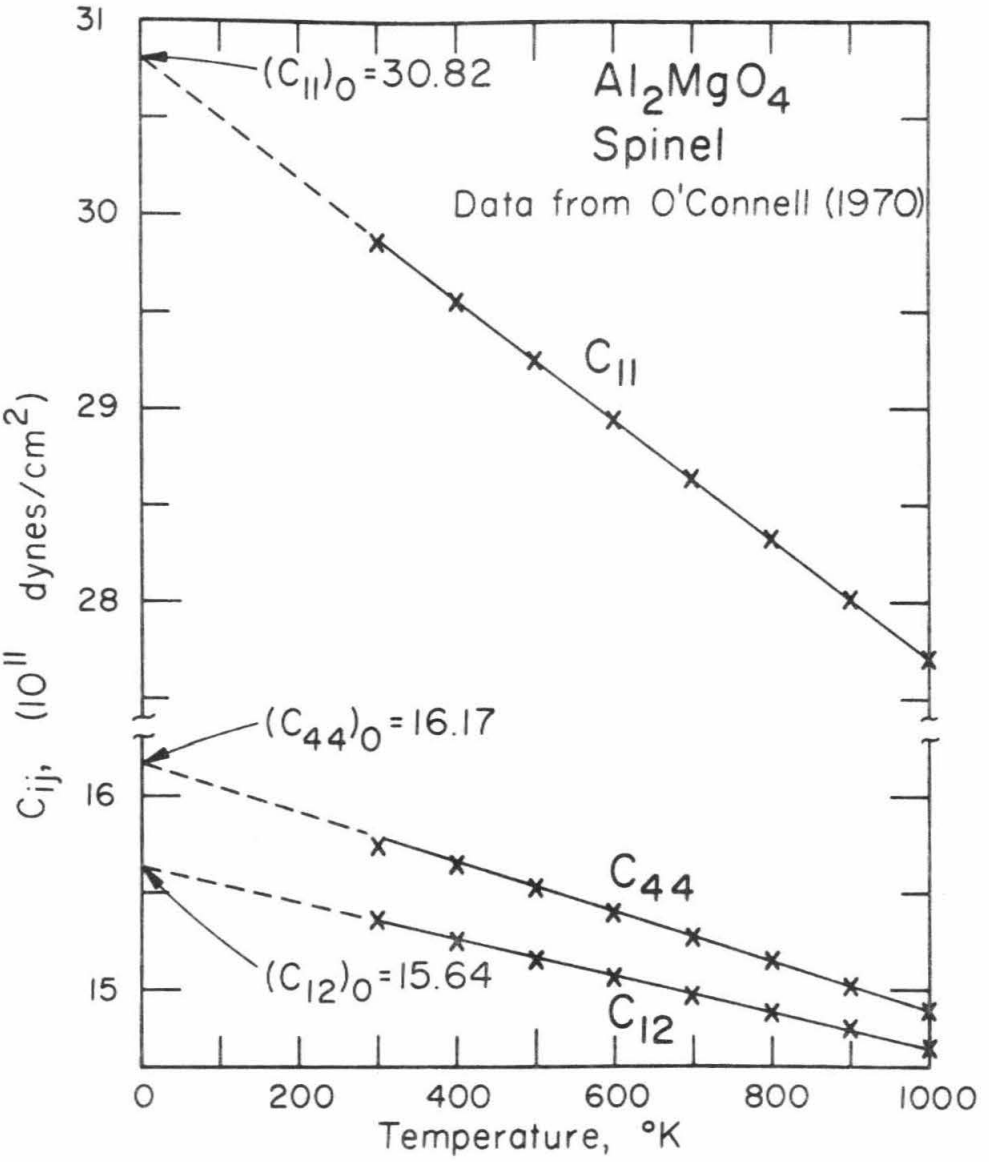

Figure 5-2-3. Temperature dependence of the C_{ij} for Al_2MgO_4.

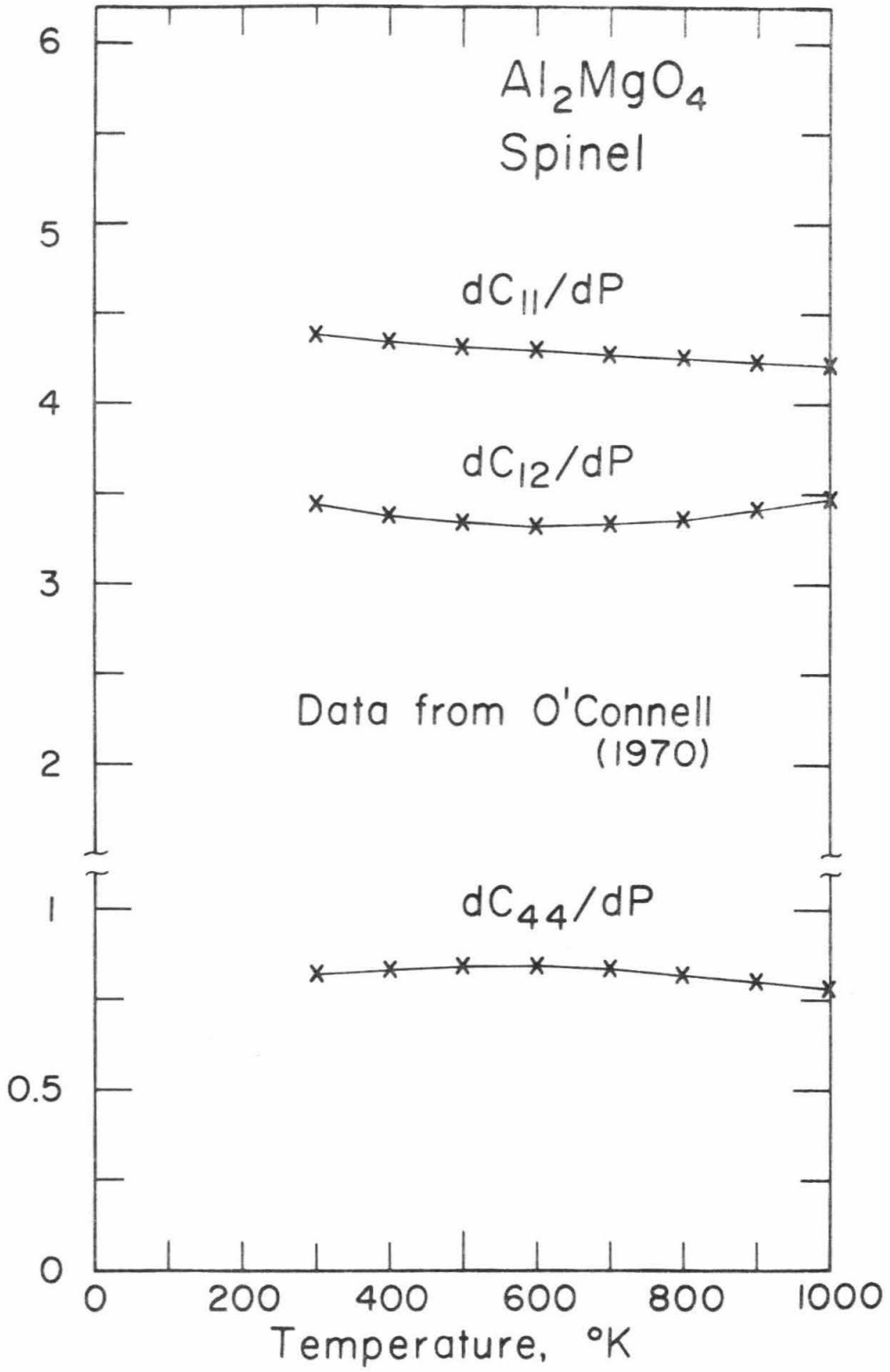

Figure 5-2-4. Temperature dependence of dC_{ij}/dP for Al_2MgO_4.

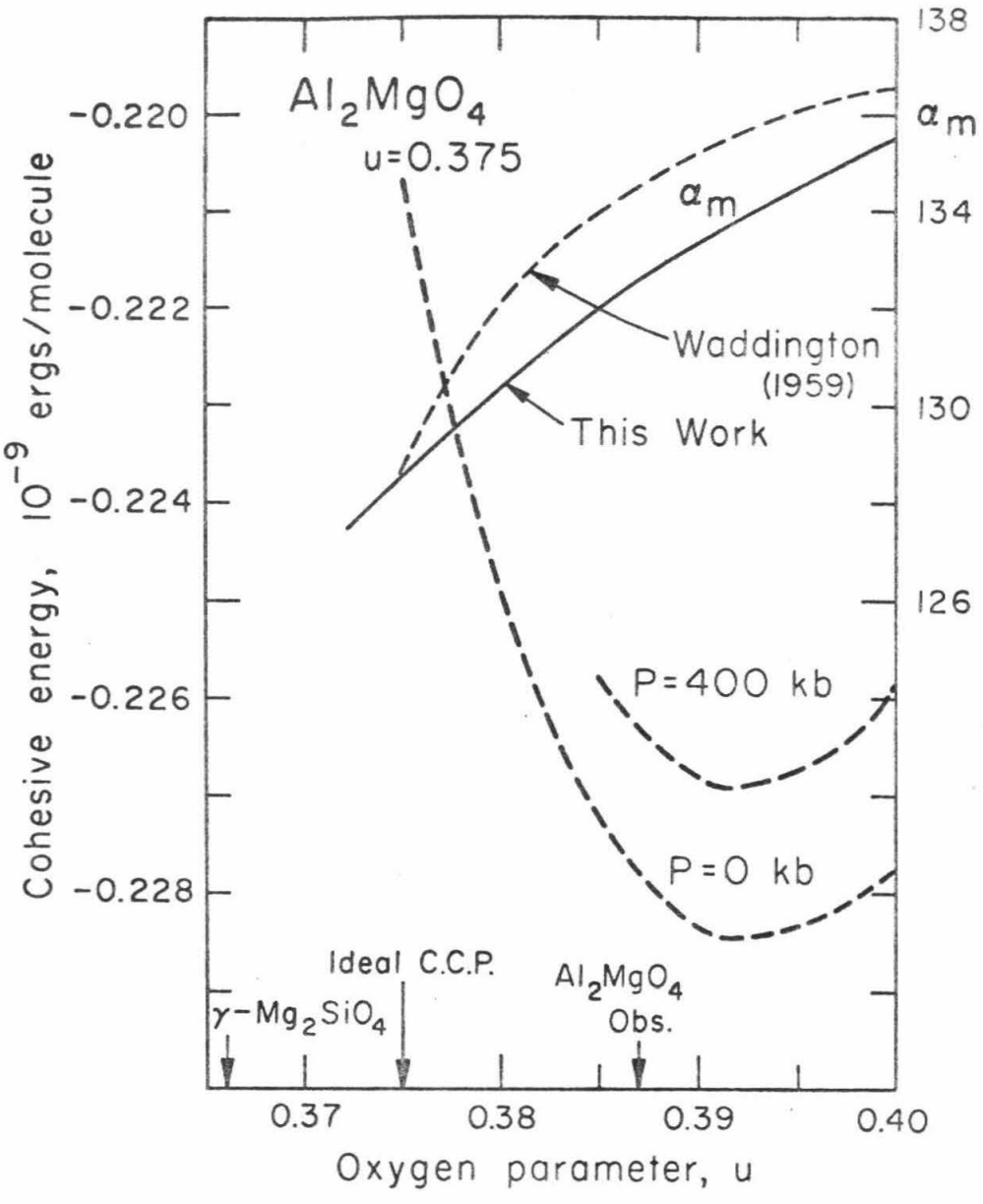

Figure 5-2-5. Cohesive energy versus oxygen parameter for Al_2MgO_4.

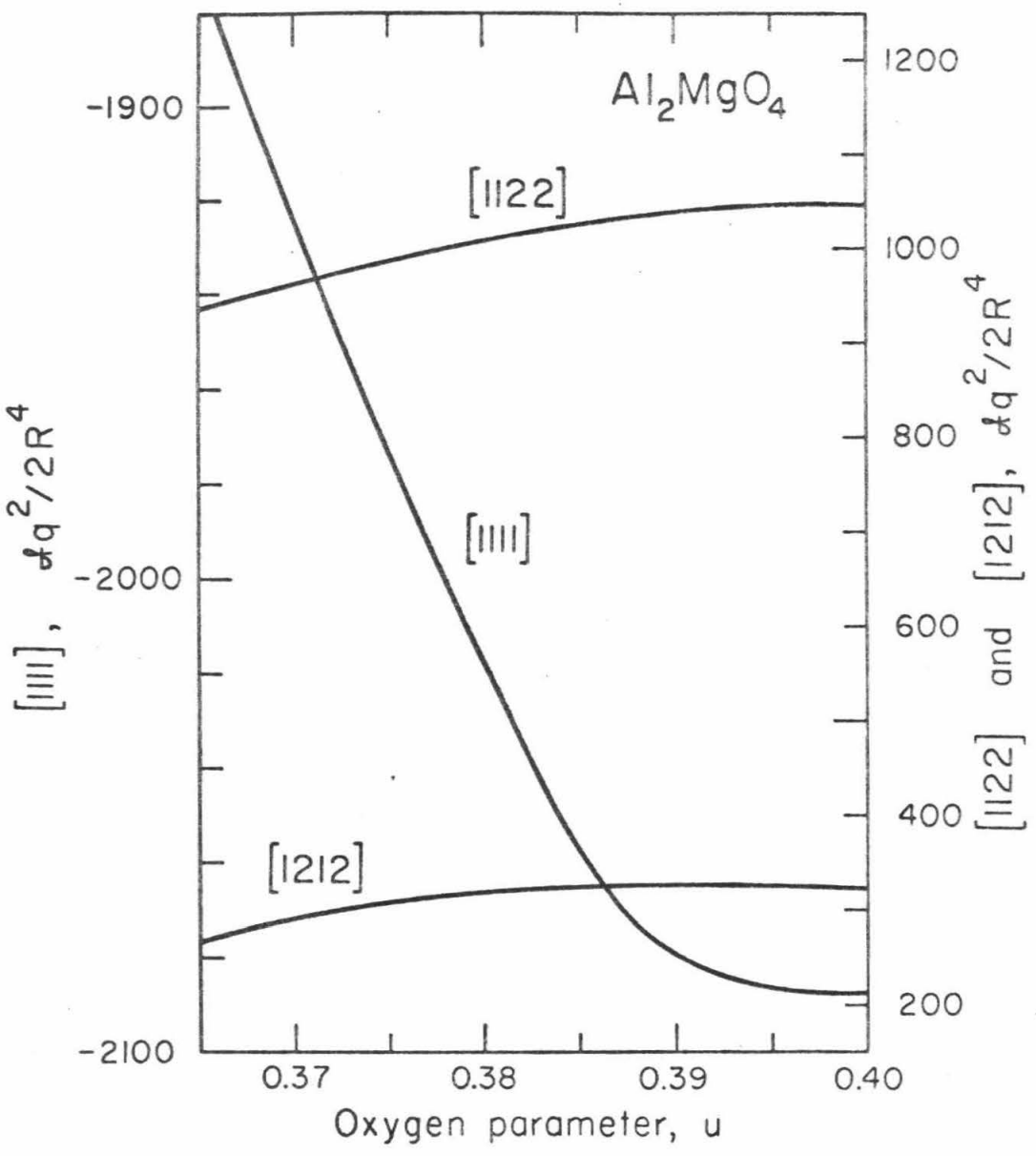

Figure 5-2-6. Electrostatic contribution to the elastic constants of Al_2MgO_4 as a function of the oxygen parameter.

5-3. The Rutile Structure

The rutile structure is of geophysical interest since it is the structure assumed by SiO_2 at pressures greater than 160 kbar. Originally synthesized by Stishov and Popova (1961), this high-pressure polymorph was identified by Chao, et al. (1962) in the shock-altered Coconino sandstone of Meteor Crater, Arizona, and named stishovite. The mixture of oxides SiO_2 (stishovite) + MgO (rock salt) is one of the candidate assemblages for the post-spinel region of the mantle and will be investigated in the next chapter.

The only relevant data which exist for stishovite are the lattice constants, the static x-ray and shock-wave compression curves (which yield the bulk modulus), and the coefficient of thermal expansion and Debye temperature. No ultrasonic measurements have been made, to date, on stishovite. Thus the only way to estimate individual elastic constants and their pressure derivatives for comparison with seismic data is through a lattice model. Since it seems technologically possible to make ultrasonic measurements on polycrystalline stishovite in the near future, the compressional and shear velocities predicted by this model can be checked. Measurement of the single-crystal elastic constants seems remote. High-precision ultrasonic data exist for single-crystal TiO_2 rutile (Manghnani, 1969) which will be compared with lattice-model predictions for that solid.

The importance of treating stishovite in the overall strategy of this thesis is that it yields the Si–O bond parameters which, under the

consistent pair-potential assumption, allow the elastic behavior of γ -Mg_2SiO_4 (spinel) to be predicted for comparison with the seismic profiles (Chapter VI). They are also the "least-ionic" of the solids investigated using the essentially ionic theory in this thesis. It is therefore of considerable interest to see to what extent the elastic behavior is effected by their non-ionic character.

In his review paper on the properties of rutile, Grant (1959) discusses the nature of the Ti—O bond on the basis of several criteria. First, the large static dielectric constant of rutile, 173, relative to the optical dielectric constant, 8.4, is typical of highly-ionic crystals and indicates a strong ionic character. However, based on the electronegativities, the Ti—O bond is only 43% ionic. Second, the observation of a feeble temperature independent paramagnetism has been taken to indicate a covalent contribution to the bonding. Third, the bond-length is somewhat shorter than that predicted for pure ionic bonding by Lennard-Jones and Dent (1927) indicating a covalent contribution. Fourth, the electron density, as determined by x-ray diffraction, does not have a node between the Ti and O ions (Baur, 1956). This is clear evidence for a covalent contribution to the bonding since not even the MgO map exhibits such a node. Fifth, the low solubility of rutile in polar solvents indicates a covalent contribution to the bonding, and, finally, the lower stability of the rutile structure predicted by Pauling's rules is probably compensated by a corresponding increase in the covalent contribution to the bonding.

These criteria, as outlined by Grant, are qualitative in nature, and more important, they do not even agree. The point is that some observables are more sensitive to the non-ionic character of the bond than others. For example, Baur (1961) concludes that the TiO_2 is largely covalent since an ionic model does not predict the equilibrium positions of the ions, while Wackman, et al. (1967) conclude, on the basis of energy calculations, that the bonding in rutile is predominantly ionic. In the hope that the elastic properties are not sensitive to a covalent contribution to the bond, we will proceed.

Specialization to the Rutile Structure

The unit cell of stoichiometric rutile is tetragonal and is diagrammed in Figure 5-3-1. The structure may be represented as six interpenetrating tetragonal Bravais lattices with origins (Wyckoff, Vol. I, 1965)

$$\begin{aligned} &\text{Ti: } 000 \;;\; \tfrac{1}{2}\,\tfrac{1}{2}\,\tfrac{1}{2} \\ &\text{O: } \pm\left(u\,u\,0 \;;\; u+\tfrac{1}{2}, \tfrac{1}{2}-u, \tfrac{1}{2}\right), \end{aligned} \qquad (5\text{-}3\text{-}1)$$

Any lattice site may be reached from one of the above six sublattice origins by a linear combination of the tetragonal basis vectors

$$\underline{a}_1 = (a, 0, 0), \qquad \underline{a}_2 = (0, a, 0), \qquad \underline{a}_3 = (0, 0, c). \qquad (5\text{-}3\text{-}2)$$

The u parameter is very near 0.30 for those rutile structures for which it has been measured. For TiO_2, Baur (1956) reports $u = 0.306 \pm .001$.

Because of the tetragonal symmetry, there are six independent elastic constants. In Voigt notation they are (see Nye, 1964, Table 9)

$$
\begin{aligned}
C_{11} = C_{22} &= \mathcal{S}_{1111} = [1111] + (1111) \\
C_{33} &= \mathcal{S}_{3333} = [3333] + (3333) \\
C_{44} = C_{55} &= \mathcal{S}_{2323} = [2233] + (2323) \\
C_{66} &= \mathcal{S}_{1212} = [1122] + (1212) \\
C_{12} &= \mathcal{S}_{1122} = 2[1212] - [1122] + (1122) \\
C_{13} = C_{23} &= \mathcal{S}_{1133} = 2[1313] - [1133] + (1133).
\end{aligned}
\tag{5-3-3}
$$

All other C_{ij} are zero.

The coulombic and non-coulombic contributions to the square brackets are again written separately

$$[\alpha\beta\gamma\lambda] = [\alpha\beta\gamma\lambda]^C + [\alpha\beta\gamma\lambda]^N .$$

Equation (3-3-54) was used to compute the coulombic sums. The sublattice indices in this case range from 1 to 6 with $\underline{x}(k)$ given by (5-3-1). The sum over the direct lattice was taken over the vectors $\underline{x}(\overset{\ell}{kk'}) = \underline{x}(k') - \underline{x}(k) + \ell_1\underline{a}_1 + \ell_2\underline{a}_2 + \ell_3\underline{a}_3$ where the basis vectors a_i are given by (5-3-2). The h' sum was taken over the reciprocal lattice vectors.

$$\underline{b}(h) = h_1\underline{b}_1 + h_2\underline{b}_2 + h_3\underline{b}_3 \tag{5-3-4}$$

where

$$\underline{b}_1 = (\tfrac{1}{a}, 0, 0), \qquad \underline{b}_2 = (0, \tfrac{1}{a}, 0), \qquad \underline{b}_3 = (0, 0, \tfrac{1}{c}) .$$

The results are

$u = 0.306$ (TiO_2), $c/a = .644$

Madelung constant $\alpha_M = 11.27$ (11.24) for $R = a = 4.594$ Å, $q = 2e$

Electrostatic Contribution to the Square Brackets	$[1111]^e$	$= 3.532$	(3.171)
	$[3333]^e$	$= -0.2691$	(2.400)
	$[2233]^e$	$= 0.1343$	(-1.198)
	$[1122]^e$	$= -1.886$	(-2.428)
	$[1212]^e$	$= -24.61$	(-25.86)
	$[1313]^e$	$= -24.38$	(-24.16)

$\Downarrow q^2/2R^4$ (5-3-5)

The numbers in parentheses are for $u = .3018$, the approximation for which all the Ti—O bond lengths are equal. The computer program was checked by comparing the Madelung constants with those computed by Baur (1961).

The expression for the elastic constants may be written in an analogous form to (5-1-4).

$$C_{11} = \frac{\alpha_{11}\Downarrow q^2}{2R^4} + \frac{1}{2Va}\sum_{kk'l}\left\{P^l_{kk'}\chi_1(\tfrac{l}{kk'})^2 + Q^l_{kk'}\chi_1(\tfrac{l}{kk'})^4\right\} + (1111)$$

$$C_{33} = \frac{\alpha_{33}\Downarrow q^2}{2R^4} + \frac{1}{2Va}\sum_{kk'l}\left\{P^l_{kk'}\chi_3(\tfrac{l}{kk'})^2 + Q^l_{kk'}\chi_3(\tfrac{l}{kk'})^4\right\} + (3333)$$

$$C_{44} = \frac{\alpha_{44}\Downarrow q^2}{2R^4} + \frac{1}{2Va}\sum_{kk'l}\left\{P^l_{kk'}\chi_3(\tfrac{l}{kk'})^2 + Q^l_{kk'}\chi_2(\tfrac{l}{kk'})^2\chi_3(\tfrac{l}{kk'})^2\right\} + (2323) \qquad (5\text{-}3\text{-}6)$$

$$C_{66} = \frac{\alpha_{66}\Downarrow q^2}{2R^4} + \frac{1}{2Va}\sum_{kk'l}\left\{P^l_{kk'}\chi_2(\tfrac{l}{kk'})^2 + Q^l_{kk'}\chi_1(\tfrac{l}{kk'})^2\chi_2(\tfrac{l}{kk'})^2\right\} + (1212)$$

$$C_{12} = \frac{\alpha_{12}\Downarrow q^2}{2R^4} + \frac{1}{2Va}\sum_{kk'l}\left\{-P^l_{kk'}\chi_2(\tfrac{l}{kk'})^2 + Q^l_{kk'}\chi_1(\tfrac{l}{kk'})^2\chi_2(\tfrac{l}{kk'})^2\right\} + (1122)$$

$$C_{13} = \frac{\alpha_{13}\Downarrow q^2}{2R^4} + \frac{1}{2Va}\sum_{kk'l}\left\{-P^l_{kk'}\chi_3(\tfrac{l}{kk'})^2 + Q^l_{kk'}\chi_2(\tfrac{l}{kk'})^2\chi_3(\tfrac{l}{kk'})^2\right\} + (2233)$$

In these equations:

$$\alpha_{11} = \left[1111\right]^C \frac{2R^4}{\Delta q^2} = 3.532 \qquad (3.171)$$

$$\alpha_{33} = \left[3333\right]^C \frac{2R^4}{\Delta q^2} = -0.2691 \qquad (2.400)$$

$$\alpha_{44} = \left[2323\right]^C \frac{2R^4}{\Delta q^2} = 0.1343 \qquad (-1.198) \qquad (5\text{-}3\text{-}7)$$

$$\alpha_{66} = \left[1122\right]^C \frac{2R^4}{\Delta q^2} = -1.886 \qquad (-2.428)$$

$$\alpha_{12} = \left\langle 2\left[1212\right]^C - \left[1122\right]^C \right\rangle \frac{2R^4}{\Delta q^2} = -47.33 \qquad (-49.29)$$

$$\alpha_{13} = \left\langle 2\left[1313\right]^C - \left[1133\right]^C \right\rangle \frac{2R^4}{\Delta q^2} = -48.89 \qquad (-47.12) \,.$$

The short-range sums in equations (5-3-6) may easily be done by hand with the help of Table 5-3-1 which gives the nearest neighbor positions for the two cation sites. Using this table, the elastic constants may be written in the form:

$$C_{11} = \frac{\alpha_{11}\Delta q^2}{2R^4} + \frac{1}{2V_a}\left\{4\left[2P_{B01}u^2a^2 + 4P_{B02}\psi^2a^2 + 2Q_{B01}u^4a^4 + 4Q_{B02}\psi^4a^4\right]\right\} + (1111)$$

$$C_{33} = \frac{\alpha_{33}\Delta q^2}{2R^4} + \frac{1}{2V_a}\left\{4\left[P_{B02}c^2 + Q_{B02}c^4/4\right]\right\} + (3333)$$

$$C_{44} = \frac{\alpha_{44}\Delta q^2}{2R^4} + \frac{1}{2V_a}\left\{4\left[P_{B02}c^2 + Q_{B02}\psi^2a^2c^2\right]\right\} + (2323) \qquad (5\text{-}3\text{-}8)$$

$$C_{66} = \frac{\alpha_{66}\Delta q^2}{2R^4} + \frac{1}{2V_a}\left\{4\left[2P_{B01}u^2a^2 + 4P_{B02}\psi^2a^2 + 2Q_{B01}u^4a^4 + 4Q_{B02}\psi^4a^4\right]\right\} + (1212)$$

$$C_{12} = \frac{\alpha_{12}\Delta q^2}{2R^4} + \frac{1}{2V_a}\left\{4\left[-2P_{B01}u^2a^2 - 4P_{B02}\psi^2a^2 + 2Q_{B01}u^4a^4 + 4Q_{B02}\psi^4a^4\right]\right\} + (1122)$$

$$C_{13} = \frac{\alpha_{13}\Delta q^2}{2R^4} + \frac{1}{2V_a}\left\{4\left[-P_{B02}c^2 + Q_{B02}\psi^2a^2c^2\right]\right\} + (2233) \,.$$

The parameter ψ is defined as $\psi \equiv 1/2 - \mathcal{U}$ (see Table 5-3-1). The derivatives of the potential are given by

$$P_{BOi} = \left[\frac{1}{r}\left(\frac{d\Phi_{BO}}{dr}\right)\right]_{r_{BOi}} = \left(\frac{V'_{BO}}{r}\right)_{r_{BOi}} \qquad (5\text{-}3\text{-}9)$$

$$Q_{BOi} = \left[\frac{1}{r}\frac{d}{dr}\left(\frac{1}{r}\frac{d\Phi_{BO}}{dr}\right)\right]_{r_{BOi}} = \left(-\frac{V'_{BO}}{r^3} + \frac{V''_{BO}}{r^2}\right)_{r_{BOi}} .$$

Note that the identical terms $P_{BO_i} = P_{OB_i}$ have been combined in equations (5-3-8).

Evaluation of the Empirical Parameters in V_{BO}

The energy density of the static lattice is given by

$$W = N_A\left\{-\frac{\alpha_m q^2}{a} + 2\lambda_{BO} e^{-\sqrt{2}\frac{\mathcal{U}a}{\rho_{BO}}} + 4\lambda_{BO} e^{-\sqrt{2\psi^2+(c/2a)^2}\frac{a}{\rho_{BO}}}\right\} . \qquad (5\text{-}3\text{-}10)$$

For the cubic crystals investigated in the previous two sections, it was possible to describe the hydrostatic compression by one variable -- the cube edge R. For tetragonal crystals like rutile, this is not always possible since the c/a ratio can change as a function of the hydrostatic pressure. Surprisingly, at the time of this writing, there is better data on the pressure dependence of c/a for stishovite than for rutile. For stishovite, Liu, et al. (1971) report that c/a increases with pressure according to the relation $\Delta c/c_o = (0.65 \pm 0.1)\,\Delta a/a_o$. For rutile, Clendenen and Drickamer (1966) find that c/a decreases with pressure according to $c/a \approx (c/a)_o\,(1 - 1.7P(10^{-4}))$ where P is in kbars. However, they express low confidence in their rutile data, and their

compression curve gives an anomalous bulk modulus. Liu, et al. (1971) show that Manghnani's (1969) ultrasonic data imply c/a increases with pressure as observed in stishovite.

Figure 5-3-2 shows that the cohesive energy (5-3-10) has a minimum at $u = .293$ at P = 0 and $u = .292$ at P = 369. Under the assumption that the two Ti—O bond lengths are equal, c/a can be written in terms of u as $c/a = \sqrt{8u - 2}$. Thus, according to the model, c/a should decrease with pressure according to the approximate relation $c/a \approx (c/a)_o (1 - .33 P(10^{-4}))$.

For the purpose of evaluating the empirical parameters in the potential, we will assume c/a = constant, independent of the pressure. In this approximation, the equilibrium condition is

$$\left.\frac{dW}{dV}\right|_v = \left[\frac{dW}{da}\frac{da}{dV}\right]_v = 0 \qquad (5\text{-}3\text{-}11)$$

and the bulk modulus is

$$K = V\frac{d^2W}{dV^2} = V\left\{\frac{dW}{da}\frac{d^2a}{dV^2} + \frac{d^2W}{da^2}\left(\frac{da}{dV}\right)^2\right\} \qquad (5\text{-}3\text{-}12)$$

where

$$V = \frac{N_A a^2 c}{2} = N_A a^3 (c/2a) \quad \text{volume/mole}. \qquad (5\text{-}3\text{-}13)$$

Differentiating equation (5-3-10) gives:

$$\frac{dW}{da} = \frac{\alpha m b q^2}{a^2} - \frac{2\sqrt{2}u\lambda_{BO}}{\rho_{BO}} e^{-\sqrt{2}ua/\rho_{BO}} - \frac{4\sqrt{2\psi^2 + (c/2a)^2}}{\rho_{BO}} \lambda_{BO} e^{-\sqrt{2\psi^2 + (c/2a)^2}\, a/\rho_{BO}}$$

$$\frac{d^2W}{da^2} = -\frac{2\alpha m b q^2}{a^3} + \frac{4u^2\lambda_{BO}}{\rho_{BO}^2} e^{-\sqrt{2}ua/\rho_{BO}} + \qquad (5\text{-}3\text{-}14)$$

$$+ 4\left[2\psi^2 + (c/2a)^2\right] \frac{\lambda_{BO}}{\rho_{BO}^2} e^{-\sqrt{2\psi^2 + (c/2a)^2}\, a/\rho_{BO}}$$

while the volume derivatives are, in the form of equation (5-2-19)

$$\frac{da}{dV} = \frac{C_1}{3}\left(\frac{1}{a}\right)^2 \qquad \frac{d^2a}{dV^2} = -\frac{2C_1^2}{9}\left(\frac{1}{a}\right)^5 \tag{5-3-15}$$

where $C_1 = (N_A\, c/2a)^{-1}$.

Exactly as in the previous two sections, the equilibrium condition (5-3-11) and the equilibrium bulk modulus

$$\tilde{K} = \tilde{V}\left[\frac{\partial^2 W}{\partial a^2}\left(\frac{da}{dV}\right)^2\right]\Bigg|_{\tilde{V}} \tag{5-3-16}$$

may be used to evaluate λ_{BO} and ρ_{BO}. However, because of the two distinct B—O bond lengths, the equations are not as trivial to solve. Using the equilibrium condition to eliminate λ from the expression for the equilibrium bulk modulus gives the following equation for ρ

$$\tilde{K} = \frac{2\alpha_m q^2}{9a^2 c}\left\{\frac{-2}{a} + \frac{1}{\rho_{BO}} \cdot \left[\frac{u^2 e^{-\frac{\sqrt{2}ua}{\rho_{BO}}} + (2\psi^2 + (c/2a)^2)\, e^{-\sqrt{2\psi^2+(c/2a)^2}\; a/\rho_{BO}}}{\frac{\sqrt{2}}{2}u e^{-\frac{\sqrt{2}a}{\rho_{BO}}} + \sqrt{2\psi^2+(c/2a)^2}\; e^{-\sqrt{2\psi^2+(c/2a)^2}\; a/\rho_{BO}}}\right]\right\}. \tag{5-3-17}$$

This equation was solved numerically by a method of successive approximations. The other parameter is given by

$$\lambda_{BO} = \frac{\alpha_m q^2}{a^2}\,\frac{\rho_{BO}}{4}\left[\frac{\sqrt{2}u}{2} e^{-\frac{\sqrt{2}ua}{\rho_{BO}}} + \sqrt{2\psi^2+(c/2a)^2}\; e^{-\sqrt{2\psi^2+(c/2a)^2}\; a/\rho_{BO}}\right]^{-1}. \tag{5-3-18}$$

The volume dependence of the pressure and bulk modulus are

$$P = -\frac{dW}{dV} = \frac{-1}{3(c/2a)}\left[\frac{\alpha_m q^2}{a^4} - \frac{4\lambda_{BO}}{\rho_{BO}a^2}\left\{\frac{\sqrt{2}u}{2} e^{-\sqrt{2}ua/\rho_{BO}} + \sqrt{2\psi^2+(c/2a)^2}\; e^{-\sqrt{2\psi^2+(c/2a)^2}\; a/\rho_{BO}}\right\}\right] \tag{5-3-19}$$

$$K = V\frac{\partial^2 W}{\partial V^2} = \frac{1}{9(c/2a)}\left\{-\frac{4\alpha m \phi q^2}{a^4} + \frac{4\lambda}{\rho_{00}}\left[\left(\frac{\sqrt{2}u}{a^2} + \frac{u^2}{a\rho_{00}}\right)e^{-\frac{\sqrt{2}ua}{\rho_{00}}} + \right.\right.$$

$$\left.\left. + \left(\frac{\sqrt{2\psi^2 + (c/2a)^2}}{a^2} + \frac{2\psi^2 + (c/2a)^2}{\rho a}\right)e^{-\sqrt{2\psi^2 - (c/2a)^2}}\right]\right\}. \qquad (5\text{-}3\text{-}20)$$

Computation Results and Discussion for Rutile and Stishovite

Linear extrapolation of $V(T)$ and $(K/V)(T)$ from the high-temperature regime yields the two rutile input parameters $\tilde{a}$ = 4.58 Å and $\tilde{K}$ = 2238 kbar (see Figure 5-3-3). The elastic constants were computed according to (5-3-8) for a range of ionicity factors $1.0 \leq \phi \leq 0.5$. Table 5-3-2 shows the mean deviation between the elastic constants as measured by Manghnani (1969) and the theoretical predictions. The best agreement is for $\phi = 0.5$. In Table 5-3-3, the theoretical elastic constants and their pressure derivatives ($\phi = 0.5$) are compared with Manghnani's (1969) measurements. While the elastic constants are in fair agreement, the pressure derivatives are all too small by a factor of ~ 2. However, these pressure derivatives were computed under the assumption that c/a and u are constant. If one allows c/a to vary as observed by Clendennen and Drickamer (1966), the pressure derivatives increase, as shown in Table 5-3-3, but not enough to be in agreement with the observations.

This large discrepancy between the theoretical and experimental pressure derivatives in rutile represents a significant failure of the Born model. It was hoped that the change in c/a with pressure would explain these large derivatives (relative to other oxides), but, if the measured

values are correct, the discrepancy must be due to either a non-exponential functional form for the repulsive potential or to the many-body, non-central forces neglected in the Born approximation.

Qualitatively, the pressure derivatives have the correct relative sizes, and the theoretical pressure derivative of the shear constant $1/2(C_{11} - C_{12})$ is negative as observed. Theoretically, the rutile lattice becomes elastically unstable ($1/2(C_{11} - C_{12}) = 0$) at P = 290 kbars. McQueen, et al. (1967) report that, under shock conditions, rutile transforms to a distorted fluorite structure at $P \approx 330$ kbar, while Linde and DeCarli (1968) report that the reaction commences between 150 and 200 kbars.

For stishovite, the input parameter a may be estimated from the room temperature lattice parameters given by Chao, et al. (1962) and coefficient of thermal expansion $\alpha = 18.62 \pm 0.35 \times 10^{-6}/°C$ (Weaver, 1971). By assuming α is proportional to C_V, $\tilde{a} = 4.164$ Å can be obtained as shown in Figure 5-3-4. Since there is no ultrasonic data, K must be estimated from compression data. Liu, et al. (1971) fit static x-ray diffraction data with a suit of K_o and K_o' ranging from $K_o' = 3$, $K_o = 3550$ kb to $K_o' = 8$, $K_o = 3190$ kb. Ahrens, et al. (1970) estimate $K_o = 3000$ kb, $K_o' = 7$.

Assuming $\tilde{K} = 3200$ kb, the elastic constants and their pressure derivatives were predicted for an exponential potential (Table 5-3-4). Note that this model gave K' = 3.3. In view of the poor results for rutile and the suggestion from compression data that K' should be larger for stishovite, it seems fruitless to proceed with this potential.

Taylor Series Potential

Since the Born model with an exponential potential could not explain the large pressure derivatives measured in rutile and suggested by compressional data for stishovite, we will drop the requirement that the repulsive potential be exponential in form, add one additional parameter to the potential, and use the measured value of K' as an input parameter.

The most straightforward way to do this is to write the cohesive energy W as a function of the cation-anion bond length r (assuming the two cation-anion bonds are the same length)

$$W(r) = N_A\left(-\frac{\alpha_m d q^2}{a(r)} + 6V_{Bo}(r)\right) \qquad \text{energy/mole} \qquad (5\text{-}3\text{-}21)$$

and then expand in a Taylor series about the energy minimum.

$$W(r) = \tilde{W} + B_2(r-\tilde{r})^2 + B_3(r-\tilde{r})^3 + \ldots \qquad (5\text{-}3\text{-}22)$$

where

$$B_2 = \frac{1}{2}\left(\frac{d^2W}{dr^2}\right)_{\tilde{r}} = \frac{9\tilde{r}\tilde{K}}{2C_1}$$

$$B_3 = \frac{2I}{6}\frac{\tilde{K}}{C_1}(1-\tilde{K}') \qquad (5\text{-}3\text{-}23)$$

$$C_1 = \frac{4\sqrt{2}\,u^3}{N_A(c/a)}\,.$$

Equations (5-3-21) and (5-3-22) may be used to write the repulsive cation-anion potential as

$$V_{BO}(r) = \frac{1}{6}\left[\frac{\tilde{U} + B_2(r-\tilde{r})^2 + B_3(r-\tilde{r})^3 + \ldots}{N_A} + \frac{\alpha_m \Delta q^2}{a}\right]$$

$$V'_{BO}(r) = \frac{1}{6}\left[\frac{2B_2(r-\tilde{r}) + 3B_3(r-\tilde{r})^2 + \cdots}{N_A} - \frac{\alpha_m \Delta q^2}{\sqrt{2}\,u a^2}\right] \qquad (5\text{-}3\text{-}24)$$

$$V''_{BO}(r) = \frac{1}{6}\left[\frac{2B_2 + 6B_3(r-\tilde{r}) + \ldots}{N_A} + \frac{\alpha_m \Delta q^2}{u^2 a^3}\right].$$

These equations may be used in (5-3-19) for the pressure, (5-3-20) for the bulk modulus, and (5-3-8) and (5-3-9) for the elastic constants.

The constants B_2 and B_3 are given in Tables 5-3-3 and 5-3-4 for rutile and stishovite, together with the predicted elastic constants and their pressure derivatives.

The deviation between measured and predicted elastic constants is given in Table 5-3-2 for both the exponential and Taylor series forms of the cation-anion repulsive potential. Note that when the potential is adjusted to give the larger K', the predicted elastic constants are also brought into closer agreement with the experimental values.

The lattice model predicts that, like rutile, stishovite will become unstable at high pressure. The pressure P^T at which $1/2(C_{11} - C_{12}) = 0$ is given for the three models in Table 5-3-4. It ranges between 475 and 760 kb. As for NaCl and MgO, the exact transition pressure is sensitive to the details of the model. The velocities and density will be computed for each of the three stishovite models developed in this chapter and compared with the seismic profiles in the next chapter.

The contribution of the internal deformations to the elastic constants and their pressure derivatives was found to be smaller for the rutile structure than for spinel. It is possible that the contribution to the round brackets from the polarization of the oxygen-ions may explain the large observed pressure derivatives. This could be tested using a modified rigid-ion model.

TABLE 5-3-1

Neighbor Positions and Short-Range Sums for the Rutile Structure

k	k'	$x_1(kk')$	$x_2(kk')$	$x_3(kk')$	$x_1^2(kk')$	$x_3^2(kk')$	$x_1^2 x_2^2$	$x_2^2 x_3^2$
		(a)	(a)	(c)	(a^2)	(c^2)	(a^4)	(a^2c^2)
1	3	$-u$	$-u$	0	u^2	0	u^4	0
	5	u	u	0	u^2	0	u^4	0
	4	$\frac{1}{2}-u$	$u-\frac{1}{2}$	$-\frac{1}{2}$	ψ^2	$\frac{1}{4}$	ψ^4	$\psi^4/4$
	4	$\frac{1}{2}-u$	$u-\frac{1}{2}$	$\frac{1}{2}$	ψ^2	$\frac{1}{4}$	ψ^4	$\psi^4/4$
	6	$u-\frac{1}{2}$	$\frac{1}{2}-u$	$-\frac{1}{2}$	ψ^2	$\frac{1}{4}$	ψ^4	$\psi^4/4$
	6	$u-\frac{1}{2}$	$\frac{1}{2}-u$	$\frac{1}{2}$	ψ^2	$\frac{1}{4}$	ψ^4	$\psi^4/4$
				$\sum_{k'} \rightarrow$	$2u^2+4\psi^2$	1	$2u^4+4\psi^4$	ψ^2
2	4	$-u$	u	0	u^2	0	u^4	0
	6	u	$-u$	0	u^2	0	u^4	0
	3	$\frac{1}{2}-u$	$\frac{1}{2}-u$	$\frac{1}{2}$	ψ^2	$\frac{1}{4}$	ψ^4	$\psi^4/4$
	3	$\frac{1}{2}-u$	$\frac{1}{2}-u$	$-\frac{1}{2}$	ψ^2	$\frac{1}{4}$	ψ^4	$\psi^4/4$
	5	$u-\frac{1}{2}$	$u-\frac{1}{2}$	$\frac{1}{2}$	ψ^2	$\frac{1}{4}$	ψ^4	$\psi^4/4$
	5	$u-\frac{1}{2}$	$u-\frac{1}{2}$	$-\frac{1}{2}$	ψ^2	$\frac{1}{4}$	ψ^4	$\psi^4/4$
				$\sum_{k'}$	$2u^2+4\psi^2$	1	$2u^4+4\psi^4$	ψ^4

$\psi = \frac{1}{2}-u$

TABLE 5-3-2

Comparison of model fit to the elastic constants for the exponential and Taylor series cation-anion repulsive potential.

	δ	Absolute Mean Deviation $\frac{1}{6}\sum_{1}^{6} \lvert C_{ij}(\text{theor.}) - C_{ij}(\text{exp.})\rvert$
Exponential Cation-Anion Repulsive Potential	.7	365 kb
	.6	283
	.5	253
Taylor Series Cation-Anion Repulsive Potential	.7	270
	.6	221
	.5	260

TABLE 5-3-3

Comparison of theoretical and experimental elastic constants and their pressure derivatives for TiO_2.

Exponential Cation-Anion Repulsive Potential (δ = 0.5)

	Theoretical c/a = const.	Theoretical c/a ≠ const.	Experimental (Manghnani, 1969)
C_{11}	2406 kb.	(c/a assumed to de-	2867 kb.
C_{33}	5102	crease with pressure	5239
C_{44}	1047	as measured by	1307
C_{66}	2128	Clendennen and	2241
C_{12}	1936	Drickamer, 1966)	1952
C_{13}	1060		1595
C'_{11}	2.8	3.6	6.5
C'_{33}	4.0	3.4	8.3
C'_{44}	-0.6	-1.8	1.1
C'_{66}	2.6	3.2	6.4
C'_{12}	4.4	4.6	9.1
C'_{13}	3.6	4.0	5.0
P^T $(C_{11}-C_{12})=0$	294 kb		352 kb.

Taylor Series Cation-Anion Repulsive Potential (δ = 0.6)

	Theoretical (c/a = const.)	Experimental (Manghnani, 1969)
C_{11}	2636 kb.	2867 kb.
C_{33}	5390	5239
C_{44}	1034	1307
C_{66}	2283	2241
C_{12}	2065	1952
C_{13}	1079	1592

(continued...)

TABLE 5-3-3 (continued)

	Theoretical (c/a = const.)	Experimental (Manghnani, 1969)
C'_{11}	5.9	6.5
C'_{33}	8.0	8.3
C'_{44}	0.1	1.1
C'_{66}	5.7	6.4
C'_{12}	7.4	9.1
C'_{13}	5.8	5.0
P^T $(C_{11}-C_{12}=0)$	381 kb.	352 kb

TABLE 5-3-4

Theoretical Elastic Constants and Pressure Derivatives for Stishovite

Inputs		Taylor Series Potentials				Exponential Potential
$\tilde{K}$	(kbar)	3200 kb.		3500 kb		3200 kb.
$\tilde{K}'$		7		4		(3.3) calc.
ν		.3008		.3008		.3008
$\tilde{a}$	(Å)	4.164		4.164		4.164
c/a		.6377		.6377		
ϕ		0.7	0.5	0.7	0.5	0.7
Calculated						
C_{11}	(kbar)	3869	3774	4224	4083	3871
C_{33}		8432	7137	8834	7467	8428
C_{44}		1470	1207	1552	1230	1469
C_{66}		3258	3312	3589	3624	3260
C_{12}		2805	3014	3160	3323	2808
C_{13}		1378	1733	1594	2006	1379
C'_{11}		6.6	5.7	3.2	2.9	2.7
C'_{33}		8.9	7.0	4.9	3.9	4.5
C'_{44}		0.88	-0.41	-0.06	-.69	0.03
C'_{66}		5.9	5.6	2.9	2.8	2.3
C'_{12}		8.0	7.3	4.7	4.5	4.2
C'_{13}		5.1	6.3	3.3	3.9	2.7
P^T	(kbar)	760	475	709	475	709
B_2	(10^{30} cgs)	.637233		.697527		$\lambda = .164738 \times 10^{-8}$
B_3	(10^{39} cgs)	-.215894		-.118667		$\rho = .305927 \times 10^{-8}$

Electrostatic constants for c/a = .6377, ν = .3008

α_m = 11.275 (units $\phi q^2/2a^4$) q = 2e

α_{11} = 3.547 α_{66} = - 2.467

α_{33} = 5.173 α_{12} = -50.63

α_{44} = -2.584 α_{13} = -47.72

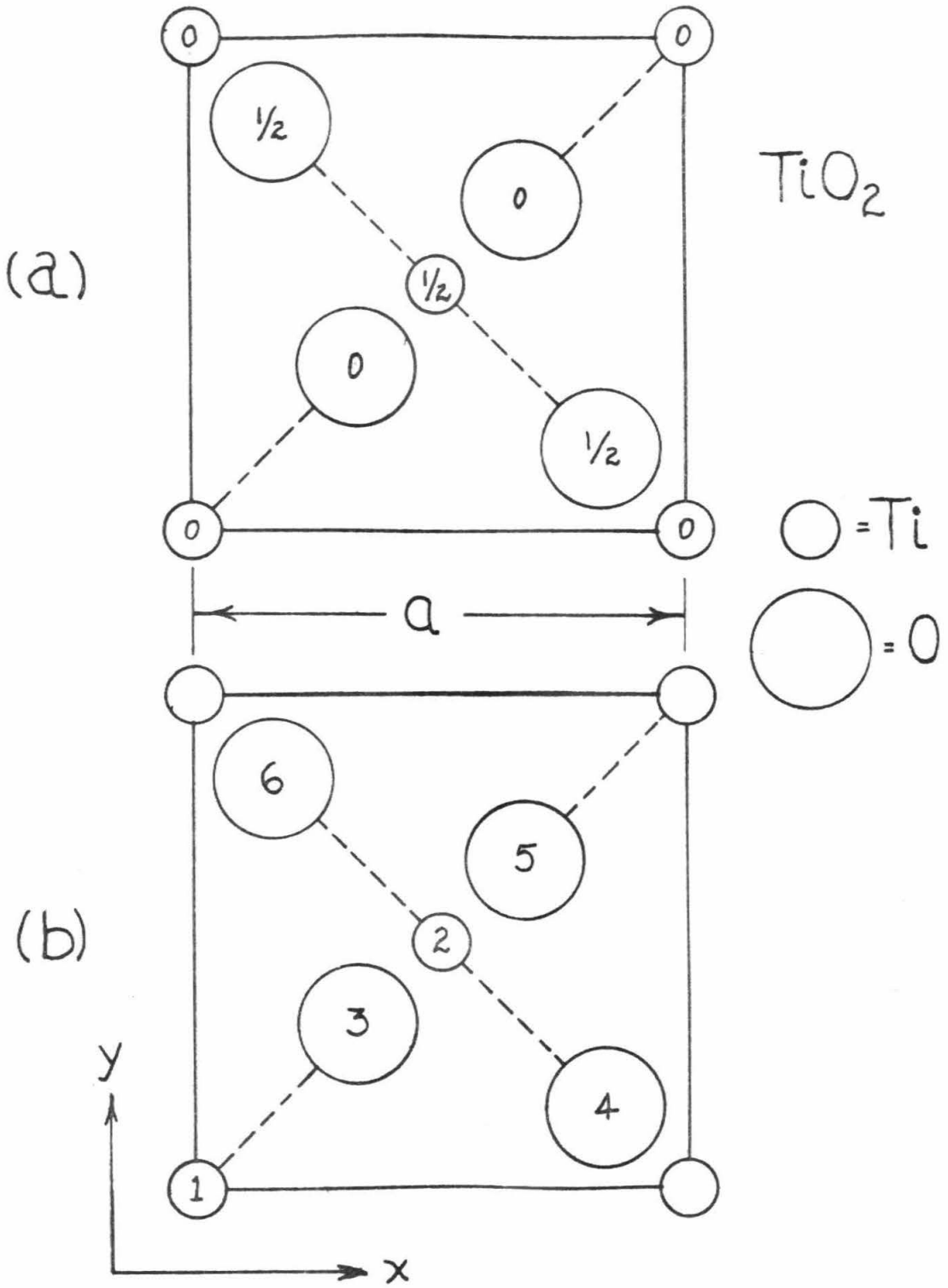

Figure 5-3-1. Rutile structure after Wyckoff (1965). (a) ion positions. (b) sublattice numbers.

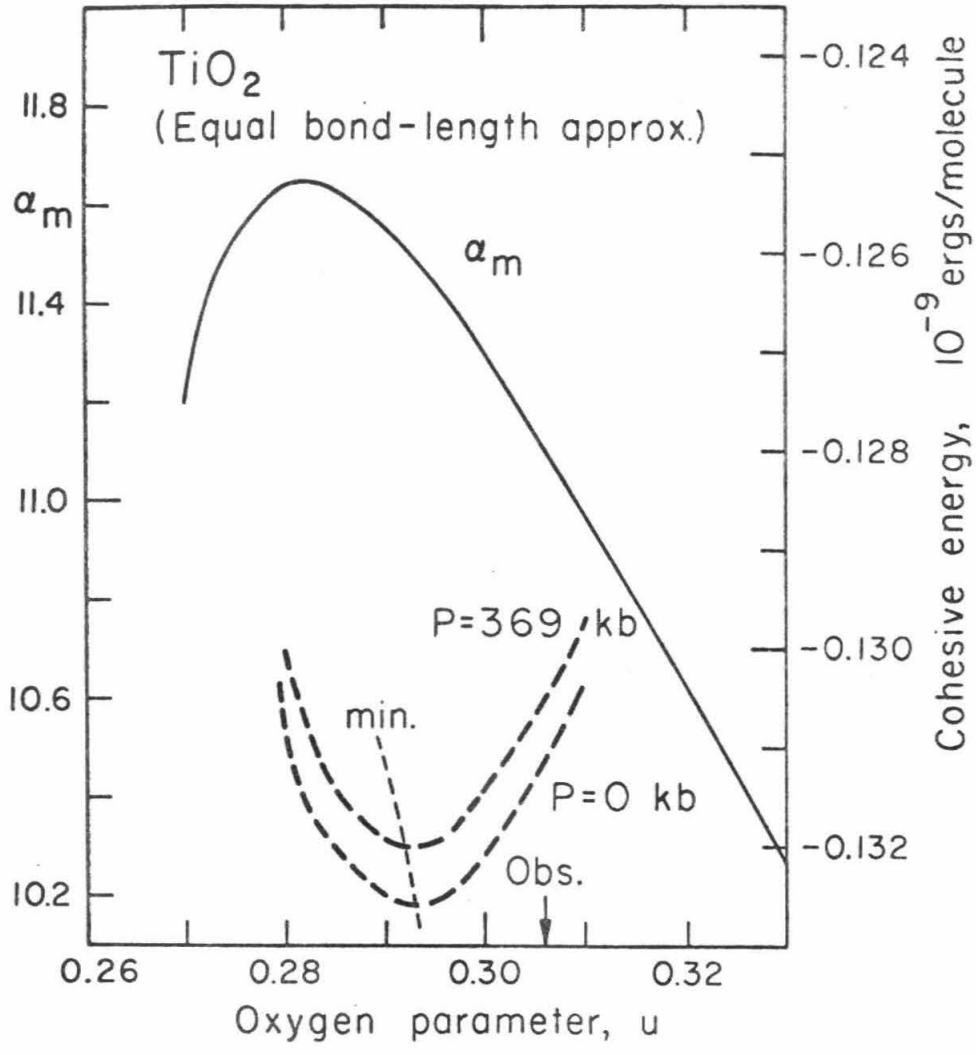

Figure 5-3-2. Cohesive energy versus oxygen parameter for TiO_2.

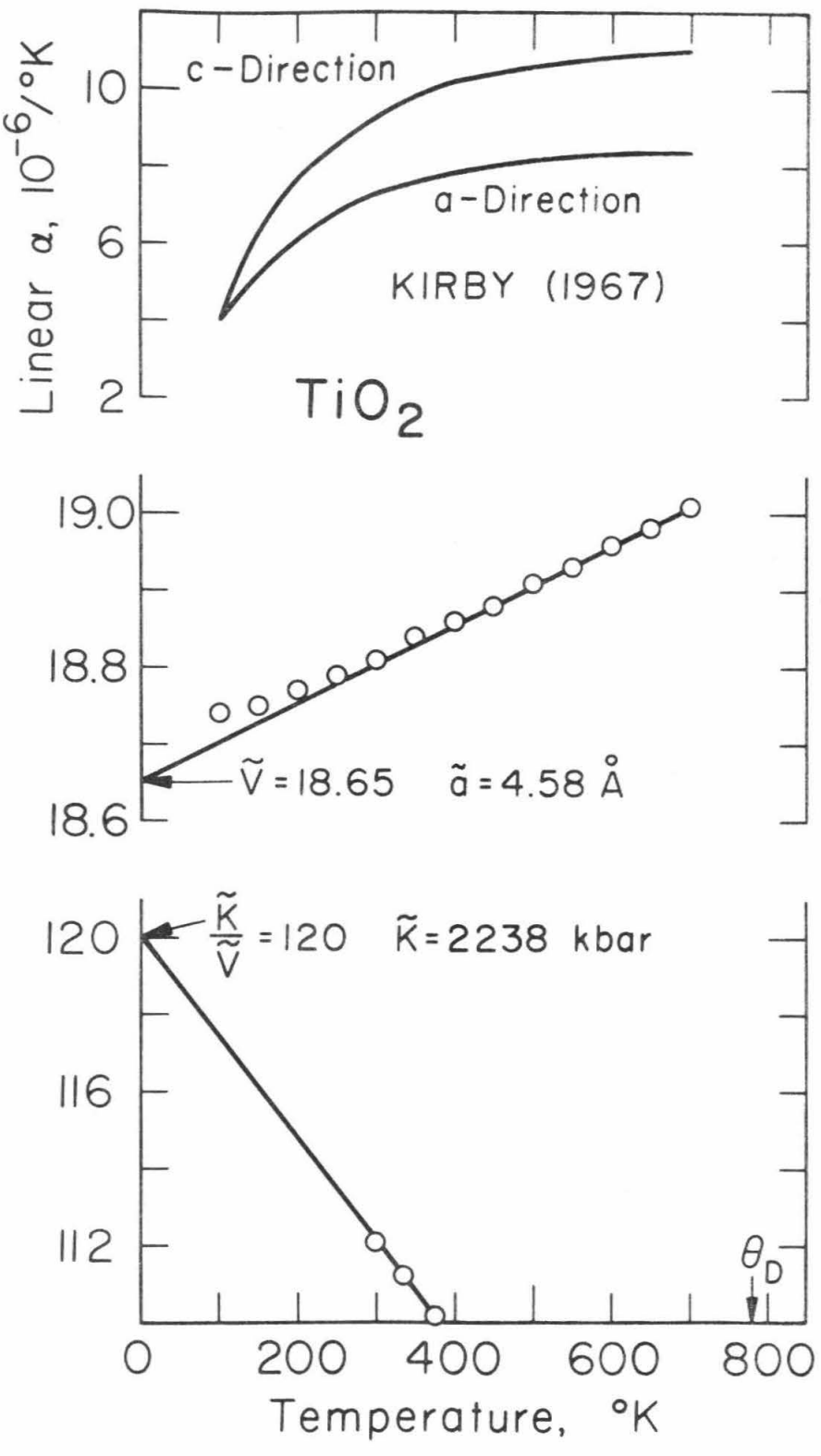

Figure 5-3-3. Static lattice parameters of TiO_2 rutile.

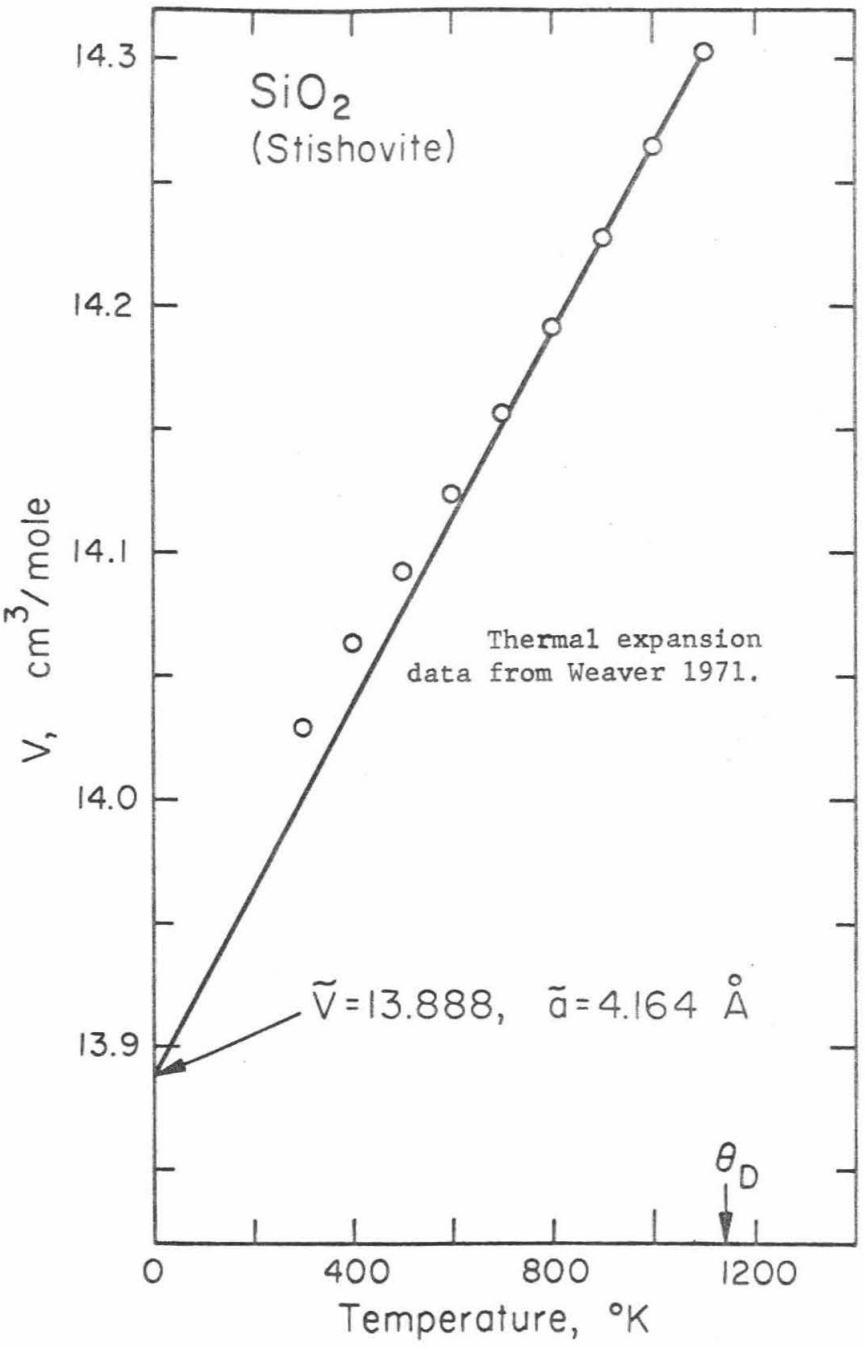

Figure 5-3-4. Volume of the static stishovite lattice.

VI. APPLICATIONS TO THE EARTH

In this chapter, the lattice models developed in Chapter V are used to predict the elastic behavior of several close-packed oxide and silicate mantle-candidate minerals at high pressures. The computed compressional and shear wave velocities are compared with seismically determined velocity-depth profiles in the earth. Two mineralogical models are investigated: (1) Mg_2SiO_4 (assumed to be in a normal spinel structure) in the pressure regime corresponding to the "spinel" region of the transition region of the mantle ($\sim$400-600 km) and (2) the combination of oxides $2MgO \quad SiO_2$ in the "post-spinel" region below $\sim$ 600 km.

There is no reason to believe that the mineralogy of the lower mantle is any less complex than the upper mantle or crust. The purpose of this chapter is not to propose and support a mineralogical model for the lower mantle, but rather to show how the lattice models may be used to predict elastic properties of unmeasured high-pressure phases.

6-1. Mg_2SiO_4 Spinel

Ringwood and Major (1966) demonstrated the existence of a distorted spinel polymorph of Mg_2SiO_4. The refined structure of this β-phase was given by Moore and Smith (1970). The β-phase differs from the normal γ-spinel in that the SiO_4 polyhedra, which are isolated in the γ-spinel, share one of their oxygen ions in the β-phase, resulting in a Si_2O_7 group (see Morimoto, et al., 1970, for a detailed diagram).

While both structures are based on a cubic close packing of the oxygens, the β-phase has orthorhombic symmetry.

Because of the work in the preceding chapter on the spinel structure, we will treat γ-Mg_2SiO_4, deferring a study of the β-phase for the present. Extrapolation of the lattice constant for members of the Mg_2SiO_4- Fe_2SiO_4 spinel solid solution series yields R = 8.07 Å for the magnesium end member (Ringwood and Major, 1970). Akimoto and Ida (1966) reported R = 8.07 ± .02 Å for Mg_2SiO_4, but it is not clear whether this was the β or γ phase. Kamb (1968) used this lattice constant to show that, under the assumption that the Si—O distance is the same as in the olivine phase, 1.625 Å, a Mg_2SiO_4 normal spinel would have the anomalously low oxygen parameter u = 0.366. This would correspond to an Mg—O bond length of 2.09 Å, close to that in MgO.

Under the consistent pair-potential hypothesis, we should be able to predict the properties of Mg_2SiO_4 spinel using only the bond parameters for Mg—O found for MgO and those for Si—O from stishovite. In Figure 6-1-1, the cohesive energy (equation (5-2-15)) is plotted as a function of u for P = 0 and for P = 200 kbars. The equilibrium lattice constant R varies along these curves as indicated. Although only the exponential Si—O potential is shown in Figure 6-1-1, the same calculation was made for the two Taylor series potentials found for stishovite in the last chapter. The oxygen parameter and lattice constant for each of these potentials are summarized below.

Si—O Potential	u	R (Å)
Exponential	.367	8.02
Taylor Series ($\tilde{K}$ = 3500, K' = 4)	.367	8.06
Taylor Series ($\tilde{K}$ = 3200, K' = 7)	.368	8.08

It is encouraging that the predicted lattice constant is close to the experimentally extrapolated 8.07 Å and that the equilibrium parameter has an abnormally low value close to .366 predicted by a bond-length argument (Kamb, 1968).

A comparison of Figure 6-1-1 with Figure 5-2-5 shows that the u parameter is controlled by the electrostatic part of the energy. For Al_2MgO_4, the Madelung constant (absolute value) increases for larger u, while for Mg_2SiO_4 it increases as u decreases. Thus, as noted in the previous chapter, an aluminate spinel with repulsive parameters determined assuming $u < .392$ will expand slightly and distort to find the energy minimum at constant pressure, while a silicate spinel has a tendency to have a smaller u.

Note that for Mg_2SiO_4, as for the aluminate spinel, u does not significantly change with pressure. Also, as was the case for Al_2MgO_4, the u-dependence of the Madelung constant found here using the Ewald method differs by less than 2% from that reported by Waddington (1959) based on an Evjen calculation. This gives a check on the lattice sum program.

Fyfe (1954) used Mulliken's (1951) semi-empirical relation between bond energies and overlap integrals to show that the short (1.6 Å) Si—O bond could be explained without invoking extensive π -bonding using "d" orbitals as suggested by Pauling (1952). The fact that the central-force, rigid-ion model used here was able to account for this effect lends support to Fyfe's argument.

The zero-pressure elastic constants, as well as the pressure dependence of V_p, V_s, and ρ predicted for each of the three Si—O potentials are given in Table 6-1-1. The velocities are compared with the seismic profiles in Figure 6-1-3. Note that these quantities have been tabulated both with and without the contributions from the internal deformations to clearly emphasize that it is the round bracket contributions which are responsible for the negative dV_s/dP.

A negative dV_s/dP is not impossible. Indeed, a small or negative $d\mu/dP$ appears characteristic of the spinel lattice. For Al_2MgO_4 $dV_s/dP = 0.43 \times 10^{-3} \frac{km}{sec\text{-}kb.}$, while for Fe_2NiO_4 $dV_s/dP = -0.03 \frac{km}{sec.\ kb.}$. However, before rejecting δ -Mg_2SiO_4 as a principal constituent of the mantle, we must be sure that the small predicted pressure derivatives are not the result of our neglect of the polarizability of the oxygen ion. The observation of a similar effect in Al_2MgO_4 spinel in § 5.2 suggests that this is the case.

Note that the bulk modulus predicted from systematics is in good agreement with the values given in Table 6-1-1. D. Anderson (1967b) predicted K_o = 1910, and D. Anderson (1969) predicted $K_o = 1980 \pm 210$ kb.

6-2. Post-Spinel Phases

Based on observed phase transformations in isostructural compounds, Ringwood (1970) suggested the following three phase changes in γ-Mg_2SiO_4 spinel

(1) Disproportionation into the mixed oxides

$$\underset{\text{(spinel)}}{\gamma\text{-}Mg_2SiO_4} \longrightarrow \underset{\text{(rock salt)}}{2MgO} + \underset{\text{(rutile)}}{SiO_2}$$

(2) Disproportionation into an ilmenite structure plus a rock salt oxide

$$\underset{\text{(spinel)}}{\gamma\text{-}Mg_2SiO_4} \longrightarrow \underset{\text{(ilmenite)}}{MgSiO_3} + \underset{\text{(rock salt)}}{MgO}$$

(3) Transformation to the Sr_2PbO_4 structure

$$\underset{\text{(spinel)}}{\gamma\text{-}Mg_2SiO_4} \longrightarrow \underset{\text{(strontium plumbate)}}{Mg_2SiO_4}$$

Ringwood (1970) argues that (3) is the most plausible post-spinel phase of Mg_2SiO_4 because

(a) All known $SrPbO_4$ isotypes are formed between end members possessing rock salt and rutile structures.

(b) All known Sr_2PbO_4 isotypes are characterized by molar volumes which are practically identical with the mixed oxides. $(MgFe)_2SiO_4$ transforms to a phase having a molar volume of the mixed oxides under shock conditions.

(c) Extrapolation of transformations in the solid solution Mg_2SiO_4-Mn_2GeO_4 suggest Mg_2SiO_4 would transform from

the beta structure to the strontium plumbate structure at pressures of 200-300 kb.

(d) The free energy ΔG_o of formation of Mg_2SiO_4 spinel from the constituent oxides is relatively high. Spinels with large ΔG_o are more likely to transform into a new single phase than to disproportionate into the oxides.

However, studies of $MgGeO_3$- $MgSiO_3$ indicate that an ilmenite form of Mg_2SiO_3 will become stable between 200 and 300 kb and this led Ringwood (1970) to conclude that (2) is a distinct possibility. He considers disproportionation into the mixed oxides as unlikley because of (d) above. Preliminary results of Bassett and Takahashi (1970) indicate that γ-Fe_2SiO_4 spinel disproportionates into the oxides.

It is interesting that each of these three transformations leads to similar densities and compression modulus Φ. A comparison of the shear properties of each of these "post-spinel" phases should be a next objective of the lattice model method developed in this thesis. However, because of the rather unsatisfactory results for the shear predictions in spinel, this study will be deferred until non-central forces and polarizable ions are incorporated into the models and better spinel agreement is obtained. Only the mixed oxide phases ((3) above) will be investigated at lower mantle pressures.

In Table 6-1-4, the elastic velocities and density of the MgO model developed in § 5.1 (δ = 0.7 and excluding second neighbors) are given as a function of depth. Table 6-1-3 gives this information

for each of the three stishovite models developed in § 5.3. These trajectories are compared with the seismic profiles in Figure 6-1-2.

Note that while the slope of the MgO trajectories for both V_p and V_s are parallel to the seismic profiles, they are too low in absolute value by 0.5-1.0 km/sec. These low values can be seen to be a consequence of the central force approximation. As shown in Figure - - , the central force model predicts C_{44} too low and C_{12} too high. The net result is that the shear modulus, μ , being a combination of C_{44} and $(C_{11} - C_{12})$ is predicted too low. Hence the theoretical predictions for both V_p and V_s are more than 0.5 km/sec lower than the measured values ($V_p = 9.66$, $V_s = 6.00$) even at P = 0. In order to remedy this situation, non-central forces would have to be introduced into the model.

For stishovite, note that the zero-pressure values of V_p and V_s are relatively insensitive to the model parameters. However, dV_p/dP and dV_s/dP are sensitive to the model. The effect of the internal deformation (round bracket) contributions is to lower the velocities, as was the case for γ-Mg_2SiO_4 spinel, but, unlike the spinel case, the profiles obtained by neglecting the round brackets are not satisfactory since the shear velocity still has a tendency to decrease with pressure. Hence, at this point a mechanical mixture of oxides does not look like a satisfactory post-spinel assemblage. Any stronger conclusion will have to await the inclusion of polarizable ions and non-central forces in the model. Once a more complete model has been formulated, it will be interesting to compare the three "post-spinel" phases outlined above.

TABLE 6-1-1

Predicted Elastic Behavior of Mg_2SiO_4 Spinel

Case 1 Exponential Si–O Potential

$\tilde{R}$ = 8.02 Å
u = .367
$\tilde{K}$ = 1754 (1998)*
$\tilde{C}_{11}$ = 2706 (3036)
$\tilde{C}_{12}$ = 1278 (1375)
$\tilde{C}_{44}$ = 995 (1461)

		Hashin-Strichtman†	
P (kb)	ρ (gm/cm)	V_p (km/sec)	V_s (km/sec)
0	3.62	9.35 (9.81)	4.91 (5.68)
140	3.84	9.58 (10.35)	4.55 (5.81)
308	4.09	9.58 (10.89)	3.67 (5.93)

Case 2 Taylor Series Si–O Potential (SiO_2, K_o = 3500, K_o' = 4)

$\tilde{R}$ = 8.06 Å
u = .367
$\tilde{K}$ = 1703 (1995)
$\tilde{C}_{11}$ = 2627 (2956)
$\tilde{C}_{12}$ = 1243 (1412)
$\tilde{C}_{44}$ = 990 (1509)

		Hashin-Strichtman	
P (kb)	ρ (gm/cm)	V_p (km/sec)	V_s (km/sec)
0	3.56	9.39 (9.87)	4.91 (5.69)
131	3.78	9.58 (10.33)	4.58 (5.79)
294	4.02	9.55 (10.77)	3.79 (5.86)

Case 3 Taylor Series Si–O Potential (SiO_2, K_o = 3200, K_o' = 7)

$\tilde{R}$ = 8.08 Å
u = .368
$\tilde{K}$ = 1829 (2364)
$\tilde{C}_{11}$ = 2654 (3277)
$\tilde{C}_{12}$ = 1416 (1806)
$\tilde{C}_{44}$ = 960 (1830)

		Hashin-Strichtman	
P (kb)	ρ (gm/cm)	V_p (km/sec)	V_s (km/sec)
35	3.56	9.82 (10.59)	4.76 (5.98)
193	3.78	9.96 (11.18)	4.10 (6.13)
390	4.02	10.2 (11.33)	3.43 (6.24)

* The numbers in parentheses are the results if internal deformations are neglected.

† Simmons (1967)

TABLE 6-1-2

Periclase Earth Model

(ϕ = 0.7, second neighbors included)

			Hashin-Stricktman*	
P (kbs)	Z† (km.)	ρ (gm/cm³)	V_p (km/sec.)	V_s (km/sec)
0	0	3.61	9.13	5.23
42	132	3.70	9.32	5.30
114	343	3.84	9.68	5.40
196	575	3.98	10.01	5.48
291	800	4.13	10.33	5.54
401	1075	4.29	10.64	5.56
526	1305	4.46	10.94	5.56
670	1590	4.63	11.23	5.53
835	1915	4.82	11.50	5.46

* Simmons (1967)

† Bullen A (1956)

TABLE 6-1-3

Stishovite Earth Models

Model 1: Exponential Potential K = 3200

P	Z	ρ	VRH. AVG. V_p	V_s
0	0	4.33	10.97	6.11
123.4 kb.	369 km.	4.49 gm/cm³	11.16 km/sec	5.96 km/sec
264.2	740	4.66	11.30	5.73
424.6	1095	4.83	11.40	5.39
607.0	1470	5.02	11.40	4.84

Model 2: Taylor Series Potential K = 3500, K' = 4

P	Z		VRH. AVG. V_p	V_s
0	0	4.33	11.39	6.25
136.1 kb	405 km	4.49 gm/cm³	11.63 km/sec	6.08 km/sec
293.3	805	4.66	11.80	5.79
473.0	1125	4.83	11.86	5.36
676.0	1605	5.02	11.75	4.56

Model 3: Taylor Series Potential K = 3200, K' = 7

P	Z		VRH. AVG. V_p	V_s
0	0	4.33	10.97	6.11
130.9 kb.	392 km.	4.49 gm/cm³	11.66 km/sec	6.10 km/sec
294.3	805	4.66	12.16	5.88
492.8	1233	4.83	12.48	5.44
728.7	1705	5.02	12.51	4.40

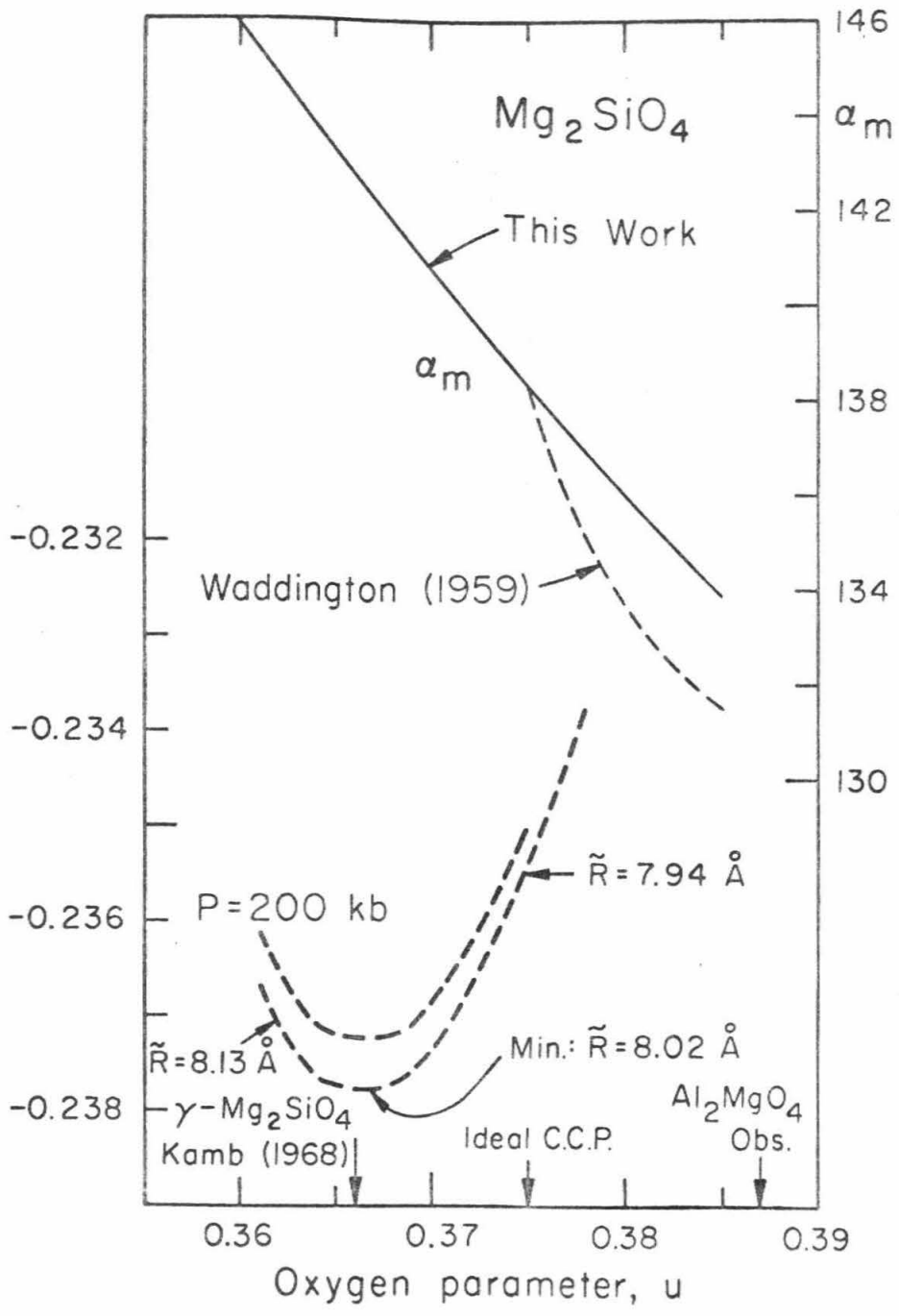

Figure 6-1-1. Cohesive energy versus oxygen parameter for γ-Mg_2SiO_4 spinel.

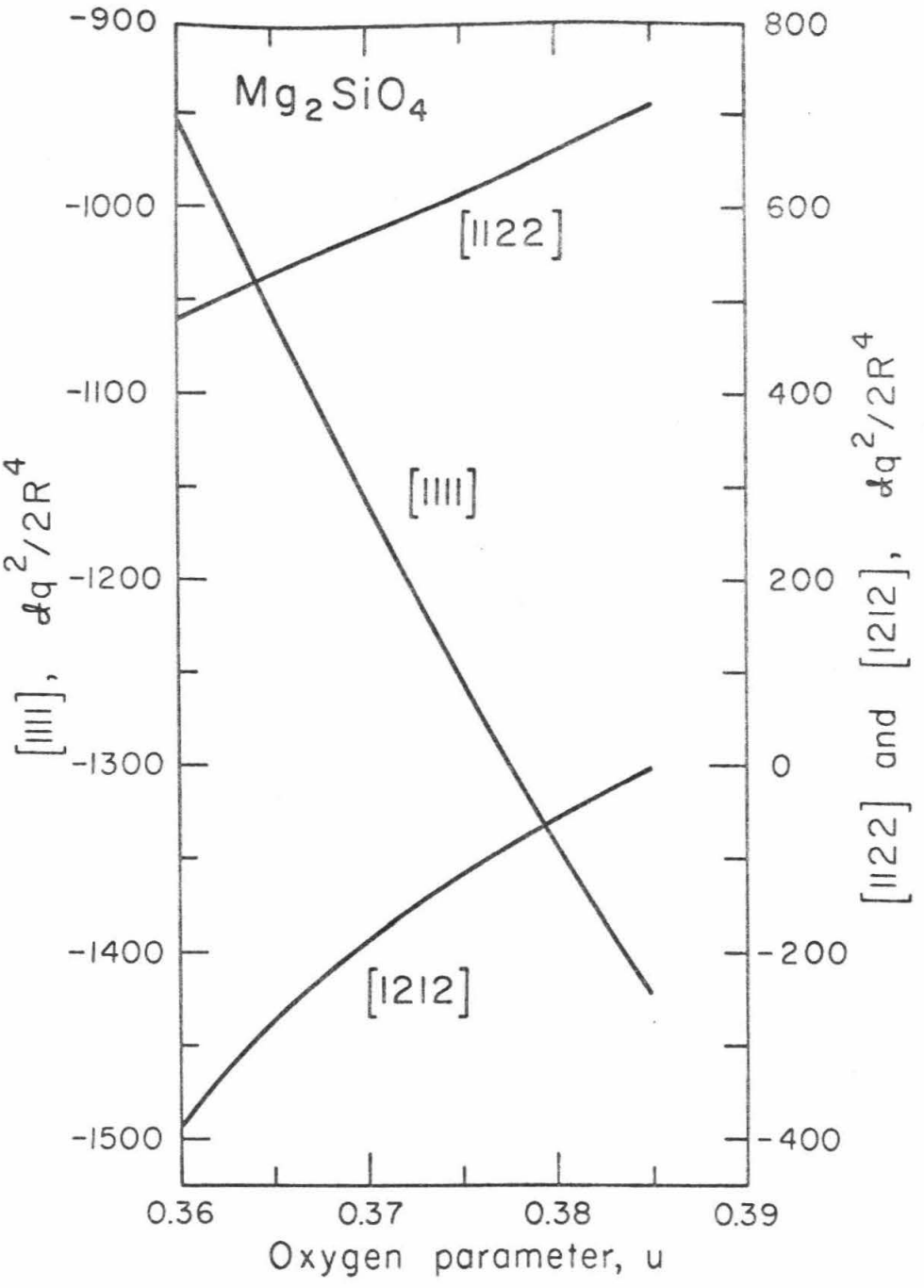

Fig. 6-1-2. Electrostatic contributions to the elastic constants as a function of the oxygen parameter for γ-Mg_2SiO_4 spinel.

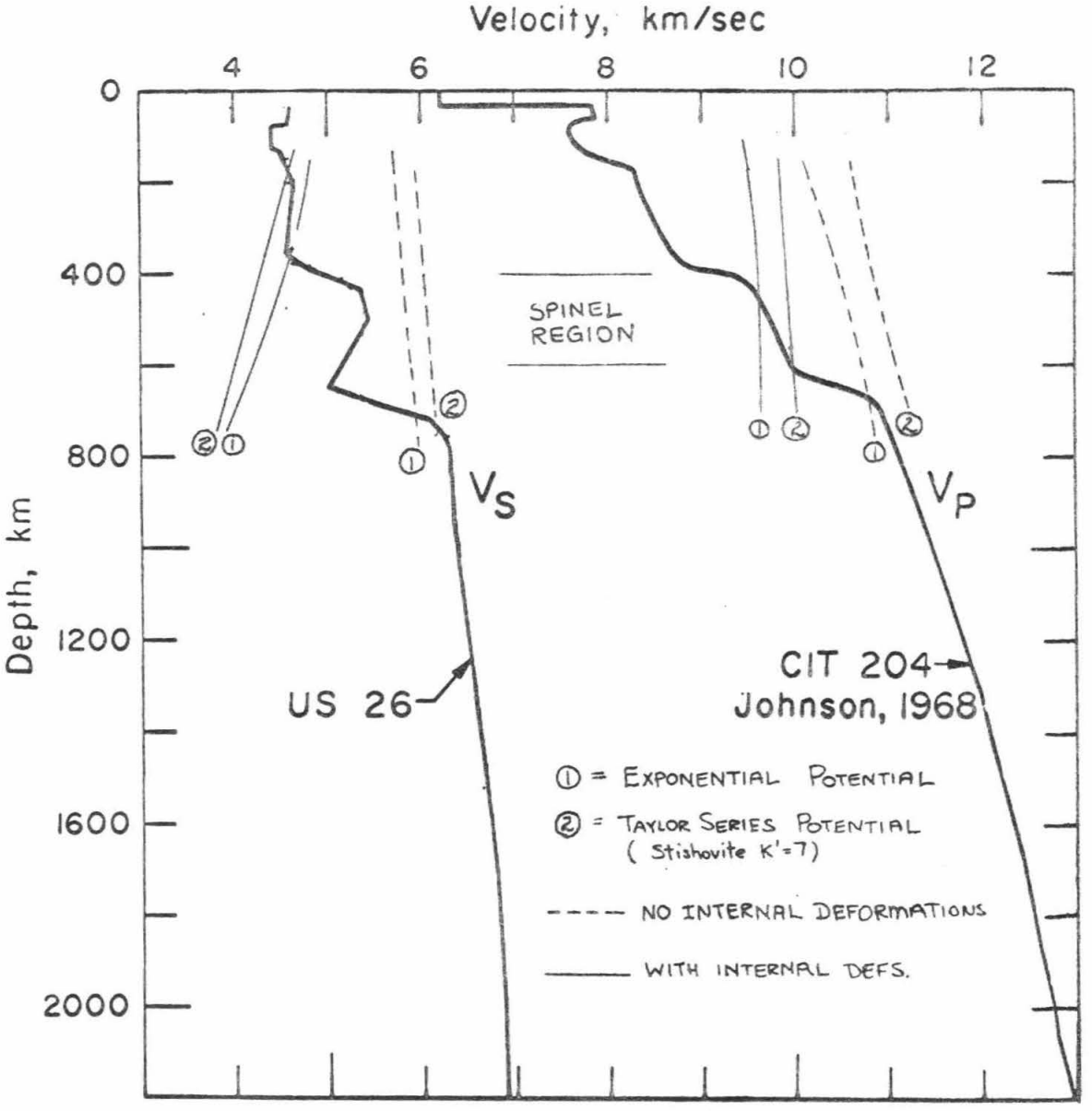

Figure 6-1-3. Predicted compressional and shear velocity as a function of depth for γ-Mg_2SiO_4 spinel. Seismic profiles after Anderson and Julian (1969).

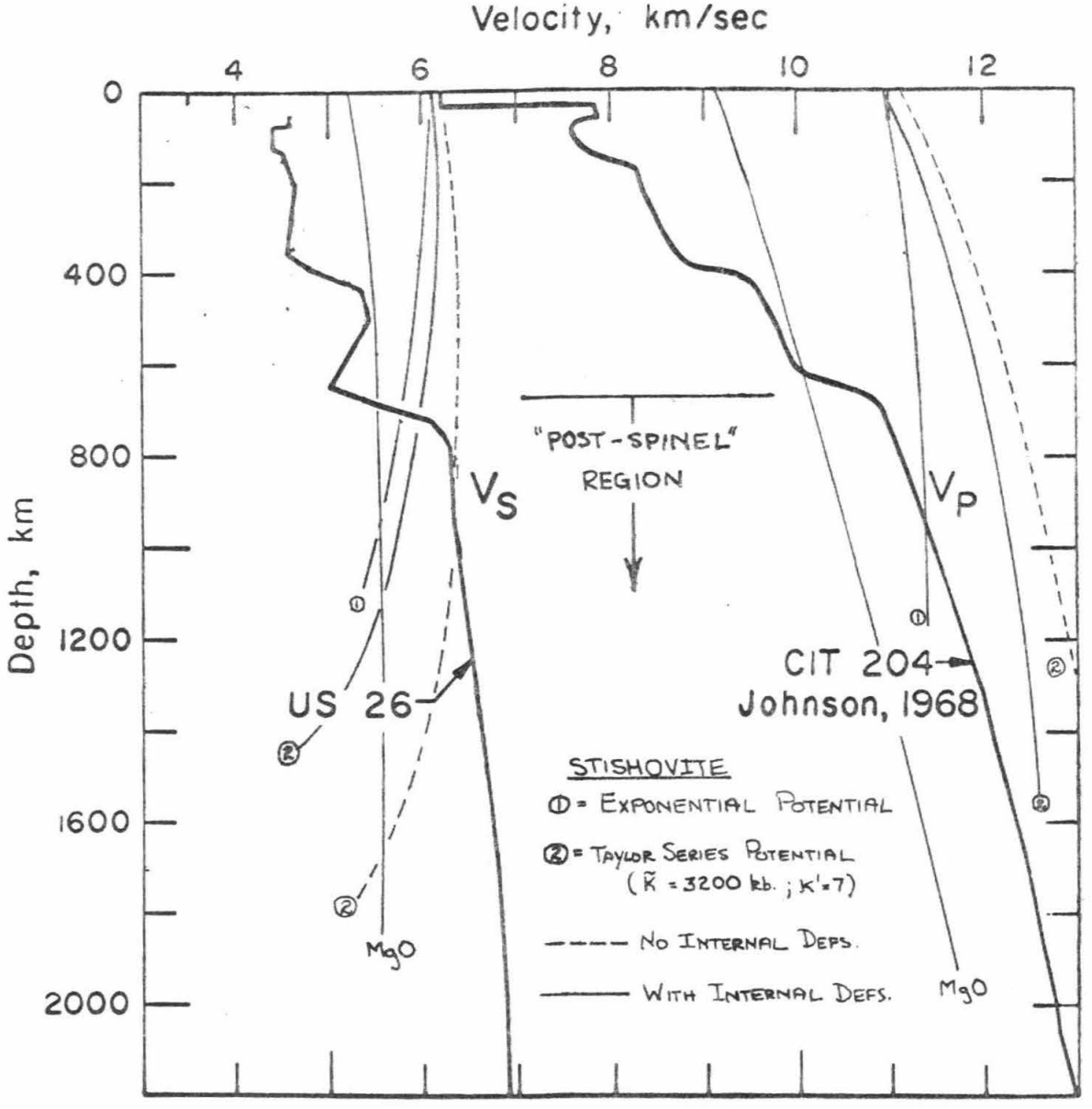

Figure 6-1-4. Predicted compressional and shear velocities for periclase and stishovite in the lower mantle. Seismic profiles after Anderson and Julian (1969).

VII. SUMMARY AND CONCLUSIONS

Chapter II summarizes previous work using elastic data to interpret seismic velocity and density profiles. Birch's early applications of isotropic finite strain theory to the lower mantle are reinvestigated with two improvements: (1) the velocity expressions are written to include terms neglected by Birch, and (2) these expressions are fit to recent inversion models which are free of the adiabatic homogeneous assumptions built into previous inversion techniques. The low density gradient in the lower mantle of these models leads to the conclusion that the lower mantle is not homogeneous and adiabatic. A rough calculation shows that observed inhomogeneities plus a small superadiabatic temperature gradient (0.2°C/km) can account for the worst case. In the review of systematics, it is shown that the assumption that pressure changes V_s in the same way as composition (along lines of constant $\overline{M}$) is not true for certain structures.

Chapter III reviews the various definitions of elastic constants, the distinction between thermodynamic and effective elastic constants, non-isotropic finite strain theory, and develops the method of long waves as formulated by Born and Huang. This chapter forms the theoretical basis of the remainder of the thesis.

Chapter IV discusses the various terms in the interatomic potential. Of particular interest is the concept of an effective ionic charge and the use of inert gas Lennard-Jones potentials to characterize the anion-anion interactions without necessitating additional empirical

parameters. It is also shown that a linear extrapolation of V(T) and (K/V)(T) from the high-temperature regime gives values appropriate to the static lattice. Although this has been pointed out by Leibfried and Ludwig (1961), the demonstration given here is a bit less complex. This is an important point in that the model is quite sensitive to the input parameters $\tilde{K}$ and $\tilde{\rho}$, and the extrapolation to the static lattice has been treated incorrectly in the recent geophysical literature (O. Anderson, 1970).

Chapter V applies the long wave interatomic potential model to three structures of geophysical interest; rock salt, spinel, and rutile. For NaCl it was found that (1) the experimental and theoretical elastic constants and their pressure derivatives were best fit by an exponential potential model with an ionicity factor, f, near 1.0. (2) The mixed derivatives $d^2C_{ij}/dP\,dT$ were important, in that the measured first pressure derivatives changed significantly between 300° and 0°K. (3) The anion-anion interaction does not significantly effect the predicted elastic constants or their pressure derivatives, but it does have a large effect on the predicted shear instability pressure ($C_{44} = 0$). For MgO, (1) the best agreement between experiment and theory was obtained for an exponential potential with an ionicity factor, f, between 0.6 and 0.7. (2) The large deviation from Cauchy's relation which is not treated by these models leads to a low prediction of the shear modulus. (3) The second neighbors do not significantly contribute to the elastic constants or their pressure derivatives. (4) The predicted shear instability pressure ($C_{44} = 0$) is sensitive to the details of the potential such as second

neighbors and the ionicity, ϕ . For Al_2MgO_4 spinel, the model successfully predicted the distortion from a cubic close packing of oxygen ions to $u > 0.375$. The internal deformations make a large contribution to the elastic constants and their pressure derivatives. They change dC_{44}/dP and $d/dP\left[\frac{1}{2}(C_{11}-C_{12})\right]$ from positive to negative, contrary to experiment, and lead to the unsatisfactory result that $d\mu/dP$ is negative. This discrepancy may be rectified by allowing the ions to be polarizable, since the deformation dipoles contribute to that part of the elastic constants associated with internal strains. For TiO_2 rutile, the model was quite successful in predicting the elastic constants, but unable to account for the large measured pressure derivative. Allowing c/a to change with pressure did not significantly increase the predicted derivatives. However, the large derivatives could be fit by changing the functional form of the cation-anion repulsive potential. This change also brought the theoretical and experimental elastic constants into better agreement, but does not constitute an "explanation" of the large derivatives. Since the compression data for stishovite also suggest a large K', it is important to understand whether this is a general characteristic of the rutile lattice or is dependent upon the nature of the cation-anion potential. Ultrasonic data on other solids in the rutile structure, like cassiterite, and a more flexible model containing non-central forces and polarizable ions will help answer this question.

In Chapter VI, the elastic properties of γ-Mg_2SiO_4 spinel are investigated using the Mg—O potential from periclase and the Si—O potential from stishovite. The resulting model has a very reasonable

equilibrium lattice constant, u-parameter, and bulk modulus. When the predicted velocities are compared with the seismic profiles in the "spinel" region of the mantle, both the values and gradients are too low. The cause can be traced to the large internal deformation contributions as was the case for Al_2MgO_4 spinel. Perhaps non-central forces and polarizable ions will reduce this discrepancy. The mechanical mixture of $2MgO + SiO_2$ is compared with the velocities. The predicted tendency of V_s for stishovite to decrease at high pressures does not appear to be due to the internal deformations. Although a firm conclusion must await a more thorough understanding of TiO_2 as explained above, it now appears that a mechanical mixture of oxides is not a good candidate for the post-spinel phase.

The next step is to include non-central forces and polarizable ions into the model in a way which will not significantly increase the number of empirical parameters. Besides the large pressure derivative problem in rutile, other interesting applications would be a comparison between the predicted elastic properties of β- and γ-Mg_2SiO_4 using the same potentials, and a comparison between the three possible post-spinel phases outlined in Chapter VI.

In a more complex model, optical data may be used to further refine the potential. Also, the observed transition pressure for those transitions due to an acoustic instability (i.e., NaCl $\longrightarrow$ CsCl) could be used as an input to help define the potentials. Also, suits of oxides containing the same cations should be measured to further test the "consistent pair-potential hypothesis". A natural next candidate is pyrope garnet

($Mg_3Al_2Si_3O_{12}$). Slow neutron diffraction as a function of pressure would provide data on the entire vibrational spectrum which could be utilized to further improve the models.

The point is that our best information about the constitution of the earth's interior is the seismic velocity and density profiles. Lattice models based upon interatomic potentials provide the most physically motivated framework through which laboratory data on the compressional, acoustical, and optical properties of oxides and silicates can be used to unravel the composition and crystal structure of the earth's mantle.

REFERENCES

Ahrens, T. J., D. L. Anderson, and A. E. Ringwood, Equations of state and crystal structures of high-pressure phases of shocked silicates and oxides, Rev. Geophys., 7, 667, 1969.

Ahrens, T. J., T. Takahashi, and G. F. Davies, A proposed equation of state of stishovite, J. Geophys. Res., 75, 310, 1970.

Akimoto, S. and Y. Ida, High-pressure synthesis of Mg_2SiO_4 spinel, Earth and Plan. Sci. Lett., 1, 358, 1966.

Anderson, Don L., A seismic equation of state, Geophys. J., 13, 9, 1967a.

Anderson, Don L., Phase changes in the upper mantle, Science, 157, 1165, 1967b.

Anderson, Don L., Bulk modulus-density systematics, J. Geophys. Res., 74, 3857, 1969.

Anderson, Don L., Velocity density relations, J. Geophys. Res., 75, 1623, 1970.

Anderson, Don L. and M. Smith, Mathematical and physical inversion of gross earth geophysical data (abst.), Trans. Am. Geophys. Union, 49, 283, 1968.

Anderson, Don L. and Orson L. Anderson, The bulk modulus-volume relationship for oxides, J. Geophys. Res., 75, 3494, 1970.

Anderson, Don L. and T. Jordan, The composition of the lower mantle, Phys. Earth Planet. Interiors, 3, 23, 1970.

Anderson, Don L. and B. Julian, Shear velocity and elastic parameters of the mantle, J. Geophys. Res., 74, 3281, 1969.

Anderson, Don L., C. G. Sammis, and T. Jordan, Composition and evolution of the mantle and core, Science, 171, 1103, 1971.

Anderson, Orson L., Elastic constants of the central force model for three cubic structures: Pressure derivatives and equations of state, J. Geophys. Res., 75, 2719, 1970.

Anderson, Orson L., E. Schreiber, R. C. Liebermann, and N. Soga, Some elastic constant data on minerals relevant to geophysics, Rev. Geophys., 6, 491, 1968.

Anderson, Orson L. and R. Liebermann, Equations for the elastic constants and their pressure derivatives for three cubic lattices and some geophysical applications, Phys. Earth Planet. Interiors, 3, 61, 1970.

Bartels, R. A. and D. E. Schuele, Pressure derivatives of the elastic constants of NaCl and KCl at 295°K and 195°K, J. Phys. Chem. Solids, 26, 537, 1965.

Bassett, W. A., T. Takahashi, H. Mao, and J. S. Weaver, Pressure-induced phase transformation in NaCl, J. Appl. Phys., 39, 319, 1968.

Baur, W. H., Über die Verfeinerung der Kristallstrukturbestimmung einiger Vertreter des Rutiltyps: TiO_2, SnO_2, GeO_2 und MgF_2, Acta Cryst., 9, 515, 1956.

Baur, W. H., Über die Verfeinerung der Kristallstrukturbestimmung einiger Vertreter des Rutiltyps. III. Zur Gittertheorie des Rutiltyps, Acta Cryst., 14, 209, 1961.

Begbie, G. H. and M. Born, Thermal scattering of X-rays by crystals,

I. Dynamical foundation, Proc. Roy. Soc. A, 188, 179, 1947.

Birch, F., The effect of pressure upon the elastic parameters of iostropic solids, according to Murnaghan's theory of finite strain, J. Appl. Phys., 9, 279-288, 1938.

Birch, F., The variation of seismic velocities within a simplified earth model in accordance with the theory of finite strain, Bull. Seism. Soc. Amer., 29, 463, 1939.

Birch, F., Elasticity and constitution of the earth's interior, J. Geophys. Res., 57, 227, 1952.

Birch, F., The velocity of compressional waves in rocks to 10 kilobars, Part 1, J. Geophys. Res., 65, 1083, 1960.

Birch, F., The velocity of compressional waves in rocks to 10 kilobars, Part 2, J. Geophys. Res., 66, 2199, 1961a.

Birch, F., Composition of the earth's mantle, Geophys. J., 4, 295, 1961b.

Birch, F., Density and composition of mantle and core, J. Geophys. Res., 69, 4377, 1964.

Birch, F., Thermal expansion at high pressures, J. Geophys. Res., 73, 817, 1968.

Born, M., Atomtheorie des Festen Zustandes, Teubner, Leipzig, 1923.

Born, M. and A. Landé, Kristallgitter und Bohrsches Atommodell, Verh. d. Deutsch. Phys. Ges., 20, 202, 1918a.

Born, M. and J. E. Mayer, Zur Gittertheorie der Ionenkristalle, Z. Phys., 75, 1, 1932.

Born, M. and K. Huang, Dynamic Theory of Crystal Lattices, Oxford Press, 1962.

Brück, H., Über die wellenmechanische Berechnung von Gitterkräften und die Bestimmung von Ionengrössen Kompressibilitäten und Gitterenergien bei einfachen Salzen, Z. Phys., 51, 707, 1928.

Bullen, K. E., Seismology and the broad structure of the earth's interior in Physics and Chemistry of the Earth, L. H. Ahrens, K. Rankama, S. K. Runcorn, eds., 1, pp. 68-93, McGraw-Hill, New York, 1956.

Chao, E. C. T., J. J. Fahey, J. Littler, and D. J. Milton, Stishovite, SiO_2, A very high-pressure new mineral from Meteor Crater, Arizona, J. Geophys. Res., 67, 419, 1962.

Clark, Jr., S. P. and A. E. Ringwood, Density distribution and constitution of the mantle, Rev. Geophys., 2, 35, 1964.

Clendennen, R. L. and H. G. Drickamer, Lattice parameters of nine oxides and sulfides as a function of pressure, J. Chem. Phys., 44, 4223, 1966.

Cowley, R. A., The elastic and dielectric properties of crystals with polarizable atoms, Proc. Roy. Soc. London, A-268, 121, 1962.

Enck, F. D. and J. G. Dommel, Behavior of the thermal expansion of NaCl at elevated temperatures, J. Appl. Phys., 36, 839, 1965.

Evjen, H. M., On the stability of certain heteropolar crystals, Phys. Rev., 39, 675, 1932.

Ewald, P. P., Die Berechnung optischer und electrostatischer Gitterpotentiale, Ann. Physik, 64, 253, 1921.

Fyfe, W. S., The problem of bond type, Am. Mineralogist, 39, 991, 1954.

Gaffney, E. S. and T. J. Ahrens, Heat of formation of O^{2-}, J. Chem. Phys., 51, 1088, 1969.

Ghafelehbashi, M. and K. M. Koliwad, Pressure dependence of the elastic constants of NaCl at low temperatures, J. Appl. Phys., 41, 4010, 1970.

Grant, F. A., Properties of rutile (titanium dioxide), Rev. Mod. Phys., 31, 646, 1959.

Hajj, F., Van der Waals coefficients for the alkali halides from optical data, J. Chem. Phys., 44, 4618, 1966.

Huang, K., Lattice theory of dielectric and piezoelectric constants in crystals, Phil. Mag., 40, 733, 1949.

Huang, K., On the atomic theory of elasticity, Proc. Roy. Soc. A, 203, 178, 1950.

Huggins, M. L. and Y. Sakamoto, Lattice energies and other properties of crystals of alkaline earth chalcogenides, J. Phys. Soc. Japan, 12, 241, 1957.

Hughes, D. S. and J. L. Kelly, Second-order elastic deformation of solids, Phys. Rev., 92, 1145, 1953.

Jeffreys, H., On the materials and density of the earth's crust, Mon. Nat. Roy. Astron. Soc., Geophysics Suppl., 4, 50, 1937.

Johnson, L. R., Array measurements of P velocities in the lower mantle, Bull. Seism. Soc. Amer., 59, 973, 1969.

Jordan, T. and Don L. Anderson, Manuscript in preparation, 1971.

Jordan, T., C. Sammis, and Don L. Anderson, The interpretation of inversion models using finite strain theory, manuscript in preparation, 1971.

Kalinin, V. A., Deformation of filled electron shells of atoms and ions at high confining pressures, Izv. Geophys. Ser., 2, 333, 1960.

Kamb, Barclay, Structural basis of the olivine-spinel stability relation, Am. Mineralogist, 53, 1439, 1968.

Kirby, R. K., Thermal expansion of rutile from 100 to 700°K, J. Res. NBS, A, Phys. Chem., 71A, 363, 1967.

Kittel, C., Introduction to Solid State Physics, John Wiley and Sons, New York, 1966.

Kumazawa, M. and Orson L. Anderson, Elastic moduli, pressure derivatives, and temperature derivatives of single-crystal olivine and single-crystal forsterite, J. Geophys. Res., 74, 5961, 1969.

La, S. Y. and G. R. Barsch, Pressure derivatives of second-order elastic constants of MgO, Phys. Rev., 172, 957, 1968.

Landshoff, R., Quantenmechanische Berechnung des Verlaufes der Gitterenergie des Na-Cl-Gitters in Abhängigkeit vom Gitterabstand, Z. Phys., 102, 201, 1936.

Landshoff, R., Quantum mechanical calculation of the lattice energy of NaCl (abst.), Phys. Rev., 52, 246, 1937.

Liebermann, R. C., Effect of iron content upon the elastic properties of oxides and some applications to geophysics, Ph.D. thesis, Columbia University, New York, 1969.

Liebfreid, G. and W. Ludwig, Theory of anharmonic effects in crystals, Solid State Phys., 12, 275, 1961.

Lennard-Jones, J. E. and B. M. Dent, Some theoretical determinations of crystal parameters, Phil. Mag., 3, 1204, 1927.

Linde, R. K. and P. S. DeCarli, Polymorphic behavior of titania under dynamic loading, J. Chem. Phys., 50, 319, 1969

Liu, L. G., W. A. Bassett, and T. Takahashi, Effect of pressure on the lattice parameters of stishovite, J. Geophys. Res., in press, 1971.

Love, A. E. H., A Treatise on the Mathematical Theory of Elasticity, 4th Ed., Dover Publications, New York, 1944.

Löwdin, P. O., A quantum mechanical calculation of the cohesive energy, the interionic distance, and the elastic constants of some ionic crystals I., Ark. mat. astr. fys., 35A, 1, 1947.

Löwdin, P. O., A theoretical investigation into some properties of ionic crystals, Ph.D. thesis, Univ. of Uppsala, 1948.

Löwdin, P. O., Quantum theory of the cohesive properties of solids, Adv. Phys., 5, 1, 1956.

Lundqvist, S. O., On the limiting vibrational frequencies of a cubic ionic lattice, Arkiv Fysik, 9, 435, 1955.

Lyddane, R. H., R. G. Sachs, and E. Teller, On the polar vibrations of alkali halides, Phys. Rev., 59, 673, 1941.

McQueen, R. G., J. C. Jamieson, and S. P. Marsh, Shock-wave compression and X-ray studies of titanium dioxide, Science, 155, 1, 1967.

Manghnani, M. H., Elastic constants of single-crystal rutile, J. Geophys. Res., 74, 4317, 1969.

Margenau, H., Van der Waals forces, Revs. Mod. Phys., 11, 1, 1939.

Mayer, J. E., Dispersion and polarizability and the van der Waals Potential in alkali halides, J. Chem. Phys., 1, 270, 1933.

Meincke, P. P. M. and G. M. Graham, The thermal expansion of alkali halides, Canad. J. Phys., 43, 1853, 1965.

Moiseiwitsch, B. L., Variational Principles, J. Wiley, New York, 1966.

Moore, P. B. and J. V. Smith, Crystal structure of β-Mg_2SiO_4: Crystal-chemical and geophysical implications, Phys. Earth Planet. Interiors, 3, 166, 1970.

Morimoto, N., S. Akimoto, K. Koto, and M. Tokonami, Crystal Structures of high-pressure modifications of Mn_2GeO_4 and Co_2SiO_4, Phys. Earth Planet. Interiors, 3, 161, 1970

Mulliken, R. S., Overlap and bonding power of 2s, 2p hybrid orbitals, J. Chem. Phys., 19, 900, 1951.

Murnaghan, F. D., Finite deformations of an elastic solid, Am. Jour. Math., 39, 235, 1937.

Murnaghan, F. D., Finite Deformation of an Elastic Solid, J. Wiley and Sons, New York, 1951.

Nye, J. F., Physical Properties of Crystals, Their Representation by Tensors and Matrices, University Press, Oxford, 1964.

O'Connell, R. J., Equation of state of spinel to 10 kb and 800°K (abst.), Trans. Am. Geophys. Union, 51, 419, 1970.

Pauling, L., The sizes of ions and their influence on the properties of salt-like compounds, Z. Krist, 67, 377, 1928.

Pauling, L., Interatomic distances and bond character in oxygen acids and related substances, J. Phys. Chem., 19, 900, 1952.

Pitzer, K. S., Inter- and intra-molecular forces and molecular polarizability, Adv. Chem. Phys., 2, 59, 1959.

Ringwood, A. E., Phase transformations and the constitution of the mantle, Phys. Earth Planet. Interiors, 3, 109, 1970.

Ringwood, A. E. and A. Major, Synthesis of Mg_2SiO_4-Fe_2SiO_4 spinel solid solutions, Earth and Planet. Sci. Lett., 1, 241, 1966.

Ringwood, A. E. and A. Major, The system Mg_2SiO_4-Fe_2SiO_4 at high pressures and temperatures, Phys. Earth Planet. Interiors, 3, 89-108, 1970.

Sammis, C. G., Don L. Anderson, and T. Jordan, Application of isotropic finite strain theory to ultrasonic and seismological data, J. Geophys. Res., 75, 4478, 1970.

Simmons, G., Velocity of compressional waves in various minerals at pressures to 10 kilobars, J. Geophys. Res., 69, 1117, 1964a.

Simmons, G., Velocity of shear waves in rocks to 10 kilobars, J. Geophys. Res., 69, 1123, 1964b.

Simmons, G., Hashin bounds for aggregates of cubic crystals, J. Grad. Res. Center, S.M.U., 36, 1, 1967.

Slagle, O. D. and H. A. McKinstry, Temperature dependence of the elastic constants of the alkali halides. I. NaCl, KCl, and KBr, J. Appl. Phys., 38, 437, 1967.

Slater, J. C., Insulators, semiconductors, and metals, Quantum Theory of Molecules and Solids, 3, chapt. 9, McGraw-Hill, 1967.

Spetzler, H., Effect of temperature and pressure on elastic properties of polycrystalline and single-crystal MgO. Part II, Ph.D. thesis, California Institute of Technology, Pasadena, 1969.

Spetzler, H., Equation of state of polycrystalline and single-crystal MgO to 8 kilobars and 800°K, J. Geophys. Res., 75, 2073, 1970.

Spetzler, H., C. G. Sammis, and R. O'Connell, The elastic properties of NaCl to 8 kilobars and 800°K, manuscript in preparation, 1971.

Striefler, M. E. and G. R. Barsch, Pressure dependence of the elastic constants and infrared optical frequencies of spinel (abst.), Trans. Am. Geophys. Union, 52, 359, 1971.

Stishov, S. M. and S. V. Popova, New dense polymorphic modification of silica, Geokhimiya, 10, 837, 1961.

Swenson, C. A., Equation of state of cubic solids; Some generalizations, J. Phys. Chem. Solid, 29, 1337, 1968.

Szigeti, B., Polarizability and dielectric constant of ionic crystals, Trans. Faraday Soc., 45, 155, 1949.

Thomsen, L., On the fourth-order anharmonic equation of state of solids, J. Phys. Chem. Solids, 31, 2003, 1970a.

Thomsen, L., The fourth-order anharmonic theory -- elasticity and stability, submitted to J. Chem. Phys. Solids, 1970b.

Thurston, R. N., Wave propagation in fluids and in normal solids, in Physical Acoustics, 1A, W. P. Mason, ed., Academic Press, Inc., New York, 1964.

Thurston, R. N., Effective elastic coefficients for wave propagation in crystals under stress, J. Acoust. Soc. Amer., 37, 348, 1965.

Thurston, R. N. and K. Brugger, Third-order elastic constants and the velocity of small amplitude elastic waves in homogeneously stressed media, Phys. Rev., 133, A1604, 1964.

Tosi, M. P., A comment on the Born model treatment of the polymorphic transitions of the alkali halides, J. Phys. Chem. Solids, 24, 1067, 1963.

Tosi, M. P., Cohesion of ionic solids in the Born model, Solid State Phys., 16, 1, 1964.

Truesdell, C. and R. A. Toupin, The classical field theories, in Handbuch der Physik, III/I, S. Flügge, 226, Springer Berlin, 1960.

Unsöld, A., Quantentheorie des Wasserstoffmolekülions und der Born Landéschen Abstossungskräfte, Z. Phys., 43, 563, 1927.

Wackman, P. H., W. M. Hirthe, and R. E. Frounfelker, The cohesive energy of TiO_2 (rutile), J. Phys. Chem. Solids, 28, 1525, 1967.

Waddington, T. C., Lattice energies and their significance in inorganic chemistry, Advan. Inorg. Chem. Radiochem., 1, 157, 1959.

Wallace, Duane C., Lattice dynamics and elasticity of stressed crystals, Rev. Mod. Phys., 37, 57, 1965.

Wallace, Duane C., Thermoelasticity of stressed materials and comparison of various elastic constants, Phys. Rev., 162, 776, 1967.

Weaver, J. S., T. Takahashi, and W. A. Bassett, Paper presented at Symp. on the Accurate Characterization of the High-Pressure Environment, Gaithersburg, Maryland, 1968.

Weaver, J. S., Equation of state of NaCl, MgO, and Stishovite, Ph.D. thesis, University of Rochester, New York, 1971.

Wyckoff, R. W. G., Crystal Structures, 3 vols., 2nd ed., J. Wiley and Sons, New York, 1965.

APPENDIX 1

Derivation of the Relations Between Various Elastic Constants

Relation between the Huang Coefficients and the Thermodynamic Elastic Constants

The following proof of equation (3-1-9) follows that in Wallace (1967). Consider the expansion given in equation (3-1-7).

$$\bar{\rho}E(S_{ij},S) = \bar{\rho}E(0,S) + \bar{T}_{ij}S_{ij} + \tfrac{1}{2}C_{ijkl}S_{ij}S_{kl} + \dots$$

Expressing this in terms of the displacement gradients

$$\bar{\rho}E(S_{ij},S) = \bar{\rho}E(0,S) + \tfrac{1}{2}\bar{T}_{ij}\left[U_{ij}+U_{ji}+U_{si}U_{sj}\right] + \\ + \tfrac{1}{8}C_{ijkl}\left[U_{ij}+U_{ji}+U_{si}U_{sj}\right]\left[U_{kl}+U_{lk}+U_{sk}U_{sl}\right]$$

Regrouping like powers of U_{ij} through the quadratic terms

$$\bar{\rho}E(S_{ij},S) = \bar{\rho}E(0,S) + \tfrac{1}{2}\bar{T}_{ij}\left[U_{ij}+U_{ji}\right] + \\ + \tfrac{1}{2}\bar{T}_{jl}U_{sj}U_{sl} + \tfrac{1}{8}C_{ijkl}\left[U_{ij}U_{kl}\right]$$

$$\bar{\rho}E(S_{ij},S) = \bar{\rho}E(0,S) + \bar{T}_{ij}U_{ij} + \tfrac{1}{2}\left(\bar{T}_{jl}\delta_{ik}+C_{ijkl}\right)U_{ij}U_{kl}$$

Comparing this term by term with the Huang expansion (equation 3-1-8)

$$\bar{\rho}E(\mathbf{x},U_{ij},S) = \bar{\rho}(\mathbf{x},0,S) + S_{ij}U_{ij} + \tfrac{1}{2}S_{ijkl}U_{ij}U_{kl} + \dots$$

one gets the desired relation

$$S_{ijkl} = \bar{T}_{jl}\delta_{ik} + C_{ijkl}$$

Relation Between the Birch Coefficients and the Thermodynamic Elastic Constants

Equation (3-1-14) in the text relates the Birch coefficients to the thermodynamic elastic constants as

$$B_{ijkl} = \tfrac{1}{2}\left(\bar{T}_{ik}\delta_{jl} + \bar{T}_{il}\delta_{jk} + \bar{T}_{jk}\delta_{il} + \bar{T}_{jl}\delta_{ik} - 2\bar{T}_{ij}\delta_{kl}\right) + C_{ijkl}$$

The first step in the derivation of the above relation is to express the stress in the present state in terms of the stress in the initial state

$$\frac{T_{ij}}{\rho} = F_{ik}\frac{\bar{T}_{kl}}{\bar{\rho}}F_{lj}^{T} \qquad \text{where} \quad F_{ij} = \partial x_i/\partial X_j$$

or

$$T_{ij} = \frac{1}{J}F_{ik}F_{jl}\bar{T}_{kl} \qquad J = \bar{\rho}/\rho \tag{A-1-1}$$

We can thus compute the Birch coefficients according to their definition

$$B_{ijkl} \equiv \left(\partial T_{ij}/\partial \epsilon_{kl}\right)\Big|_{X}$$

using the chain rule

$$\frac{\partial T_{ij}}{\partial \epsilon_{kl}} = \frac{\partial T_{ij}}{\partial F_{rs}}\frac{\partial F_{rs}}{\partial \epsilon_{kl}} \tag{A-1-2}$$

Differentiating (A-1-1) gives the first factor on the r.h.s. of (A-1-2)

$$\frac{\partial T_{ij}}{\partial F_{rs}} = -\frac{1}{J^2}\frac{\partial J}{\partial F_{rs}}\left[F_{ik}F_{jl}\bar{T}_{kl}\right] + \frac{1}{J}\frac{\partial F_{ik}}{\partial F_{rs}}F_{jl}\bar{T}_{kl} + \frac{1}{J}\frac{\partial F_{jl}}{\partial F_{rs}}F_{ik}\bar{T}_{kl} + \frac{1}{J}F_{ik}F_{jl}\frac{\partial \bar{T}_{kl}}{\partial F_{rs}} \tag{A-1-3}$$

Since,

$$\frac{\partial J}{\partial F_{rs}}\Big|_{X} = -\delta_{rs}J\Big|_{X} = -\delta_{rs} \qquad \frac{\partial F_{ik}}{\partial F_{rs}} = \delta_{ir}\delta_{ks}$$

$$\left.\frac{\partial \bar{\bar{T}}_{ij}}{\partial F_{rs}}\right|_X = \left.\frac{1}{2}\left[C_{klmn}\frac{\partial F_{pm}}{\partial F_{rs}}F_{pn} + C_{klmn}\frac{\partial F_{pn}}{\partial F_{rs}}F_{pm}\right]\right|_X$$

$$= \left.\frac{1}{2}\left[C_{klmn}\delta_{pr}\delta_{ms}\delta_{pn} + C_{klmn}\delta_{pr}\delta_{ns}\delta_{pm}\right]\right|_X$$

$$= \left. C_{klrs}\right|_X$$

equation (A-1-3) may be written (at x = X)

$$\left.\frac{\partial \bar{\bar{T}}_{ij}}{\partial F_{rs}}\right|_X = -\delta_{rs}\delta_{ik}\delta_{jl}\bar{\bar{T}}_{kl} + \delta_{ir}\delta_{ks}\delta_{jl}\bar{\bar{T}}_{kl} + \delta_{jr}\delta_{is}\delta_{ik}\bar{\bar{T}}_{kl} + \delta_{ik}\delta_{jl}C_{klrs}$$

$$= -\bar{\bar{T}}_{ij}\delta_{rs} + \bar{\bar{T}}_{sj}\delta_{ir} + \bar{\bar{T}}_{is}\delta_{jr} + C_{ijrs}$$

Solving equations (3-1-12) for F_{ij} gives

$$F_{ij} = \frac{1}{2}(\epsilon_{ij} + \epsilon_{ji} + \omega_{ij}\bar{\bar{\cdot}}\,\omega_{ji} + 2\delta_{ij})$$

which may be differentiated to yield the second factor on the r.h.s. of equation (A-1-2).

$$\frac{\partial F_{rs}}{\partial \epsilon_{kl}} = \frac{1}{2}\left(\delta_{rk}\delta_{sl} + \delta_{rl}\delta_{sk}\right)$$

So equation (A-1-12) becomes

$$B_{ijkl} \equiv \left.\frac{\partial \bar{\bar{T}}_{ij}}{\partial \epsilon_{kl}}\right|_X = \frac{1}{2}(\delta_{rk}\delta_{sl} + \delta_{rl}\delta_{sk})\left[-\bar{\bar{T}}_{ij}\delta_{rs} + \bar{\bar{T}}_{sj}\delta_{ir} + \bar{\bar{T}}_{is}\delta_{jr} + C_{ijrs}\right]$$

$$= \frac{1}{2}\left[-\bar{\bar{T}}_{ij}\delta_{ke} + \bar{\bar{T}}_{ej}\delta_{ik} + \bar{\bar{T}}_{il}\delta_{jk} + C_{ijkl} - \right.$$

$$\left. - \bar{\bar{T}}_{ij}\delta_{el} + \bar{\bar{T}}_{kj}\delta_{il} + \bar{\bar{T}}_{ik}\delta_{jl} + C_{ijlk}\right]$$

$$= \frac{1}{2}\left[\bar{\bar{T}}_{ik}\delta_{jl} + \bar{\bar{T}}_{il}\delta_{jk} + \bar{\bar{T}}_{jk}\delta_{il} + \bar{\bar{T}}_{jl}\delta_{ik} - 2\bar{\bar{T}}_{ij}\delta_{kl}\right] + C_{ijkl}$$

which is the desired result.

APPENDIX 2

Details of the Coulombic Sums

Electrostatic Contributions to the Square Brackets

In section 3-3, Ewald's theta-function transformation was used to write the Coulombic contribution to the square brackets as (equation 3-3-82)

$$[\alpha\beta\gamma\lambda]^C = \frac{1}{8\pi^2 V_a} \sum_{kk'} (m_k m_{k'})^{1/2} \bar{C}^{(2)C}_{\alpha\beta\gamma\lambda}(kk')$$

where (equation 3-3-54)

$$\begin{aligned}
\bar{C}^{(2)C}_{\alpha\beta\gamma\lambda}(kk') = &- \frac{4\pi^3 e_k e_{k'}}{R^2 V_a \sqrt{m_k m_{k'}}} (\delta_{\alpha\gamma}\delta_{\beta\lambda} + \delta_{\alpha\lambda}\delta_{\beta\gamma}) + \\
&+ \frac{4\pi^2 R^3 e_k e_{k'}}{\sqrt{m_k m_{k'}}} \sum_{l'} H_{\alpha\beta}(R\,\underline{x}(^{l'}_{kk'})) \, X_\gamma(^{l'}_{k'k}) X_\lambda(^{l'}_{k'k}) + \\
&+ \frac{4\pi^3 e_k e_{k'}}{R^2 V_a \sqrt{m_k m_{k'}}} \sum_h{}' \Big\{ (\delta_{\alpha\gamma}\delta_{\beta\lambda} + \delta_{\alpha\lambda}\delta_{\beta\gamma}) G(\pi^2 |\underline{y}(h)|^2/R^2) + \\
&+ \frac{4\pi^4}{R^4} y_\alpha(h) y_\beta(h) y_\gamma(h) y_\lambda(h) \, G''(\pi^2 |\underline{y}(h)|^2/R^2) + \\
&+ \frac{2\pi^2}{R^2} \Big\langle y_\alpha(h) y_\beta(h) \delta_{\gamma\lambda} + y_\alpha(h) y_\gamma(h) \delta_{\beta\lambda} + y_\alpha(h) y_\lambda(h) \delta_{\beta\gamma} + y_\beta(h) y_\gamma(h) \delta_{\alpha\lambda} + \\
&\qquad + y_\beta(h) y_\lambda(h) \delta_{\alpha\gamma} \Big\rangle G'(\pi^2 |\underline{y}(h)|^2/R^2) \Big\} \cdot \\
&\cdot e^{2\pi i \underline{y}(h)\cdot(\underline{x}(k) - \underline{x}(k'))}
\end{aligned}$$

where

$$G(X) \equiv e^{-X}/X$$

$$G'(X) \equiv dG/dX = -\frac{e^{-X}}{X}\left(1 + \frac{1}{X}\right)$$

$$G''(X) \equiv d^2G/dX^2 = \frac{e^{-X}}{X}\left(1 + \frac{2}{X} + \frac{2}{X^2}\right)$$

$$H_{\alpha\beta}(Z_1) = \frac{\partial^2}{\partial Z_{1\alpha}\partial Z_{1\beta}} H(Z_1) \qquad \text{(A-2-1)}$$

$$H(Z_1) = \frac{2}{\sqrt{\pi}} \frac{1}{Z_1} \int_{Z_1}^{\infty} e^{-\xi^2} d\xi = \frac{1 - \mathrm{erf}(Z_1)}{Z_1}$$

$$\mathrm{erf}(Z_1) = \frac{2}{\sqrt{\pi}} \int_0^{Z_1} e^{-\xi^2} d\xi$$

It is understood that for the case k = k', $H_{\alpha\beta}(Z)$ is to be replaced by $H^{o}_{\alpha\beta}(Z)$ in the $\ell = 0$ term where (equation 3-3-42)

$$H^{(0)}(Z_1) = \frac{-2}{Z_1\sqrt{\pi}} \int_0^{Z_1} e^{-\xi^2} d\xi = \frac{\mathrm{erf}(Z_1)}{Z_1}$$

Since the evaluation of equation (3-3-54) for specific structures may not be obvious, it will now be worked out in detail.

Consider first the term $H_{\alpha\beta}(R\underset{\sim}{X}(\ell'_{k'k}))$. In this case $Z_1 = R\chi(\ell_{rk})$ is the dimensionless argument. Using the chain rule, the differentiation (A-2-1) may be carried out as follows:

$$H_{\alpha\beta}(Z_1) = \frac{\partial}{\partial Z_{1\alpha}} \left\{ \frac{\partial H(Z_1)}{\partial Z_1} \frac{\partial Z_1}{\partial Z_{1\beta}} \right\}$$

$$\frac{\partial H(Z_1)}{\partial Z} = \frac{\partial}{\partial Z_1} \left[\frac{1 - \frac{2}{\sqrt{\pi}} \int_0^{Z} e^{-\xi^2} d\xi}{Z_1} \right]$$

$$= \frac{-1}{Z_1} \left[H(Z_1) + \frac{2}{\sqrt{\pi}} e^{-Z^2} \right]$$

$$\frac{\partial Z_1}{\partial Z_{1\beta}} = \frac{\partial(R|\underset{\sim}{X}|)}{\partial(RX_\beta)} = \frac{X_\beta}{|\underset{\sim}{X}|} = \frac{RX_\beta}{Z_1}$$

$$H_{\alpha\beta}(Z_1) = \frac{\partial}{\partial Z_{1\alpha}} \left\{ - \frac{RX_\beta}{Z_1^2} \left[H(Z_1) + \frac{2}{\sqrt{\pi}} e^{-Z_1^2} \right] \right.$$

Carrying out the final differentiation gives:

$$H_{\alpha\beta}(Z_i) = -\delta_{\alpha\beta}\frac{1}{Z^2}\left[H(Z_i) + \frac{2}{\sqrt{\pi}}e^{-Z_i^2}\right]$$
$$+ RX_\beta \frac{2}{\partial Z_i}\left\{-\frac{1}{Z^2}\left[H(Z_i)+\frac{2}{\sqrt{\pi}}e^{-Z_i^2}\right]\right\}\frac{\partial Z_i}{\partial Z_{i\alpha}}$$

Differentiating the second term on the r.h.s.

$$RX_\beta\left\{\frac{3}{Z_i^3}\left[H(Z_i) + \frac{2}{\sqrt{\pi}}e^{-Z_i^2}\right] + \frac{4}{\sqrt{\pi}Z_i}e^{-Z_i^2}\right\}\frac{RX_\alpha}{Z_i}$$

So:

$$H_{\alpha\beta}(Z_i) = -\delta_{\alpha\beta}\frac{1}{Z^2}\left[H(Z_i) + \frac{2}{\sqrt{\pi}}e^{-Z_i^2}\right]$$
$$+ R^2X_\alpha X_\beta\left\{\frac{3}{Z_i^4}\left[H(Z_i) + \frac{2}{\sqrt{\pi}}e^{-Z_i^2}\right] + \frac{4}{\sqrt{\pi}Z_i^2}e^{-Z_i^2}\right\}$$

For the $H^{(o)}_{\alpha\beta}$ case, replace H(Z) with $H^{(o)}(Z)$ in the expression above. Of course, this is only important in the $\bar{C}^{(o)}_{\alpha\beta}$ term of the round brackets because of the x $(^{l'}_{kk'})$ factors in $\bar{C}^{(1)}_{\alpha\beta\delta}$ and $\bar{C}^{(2)}_{\alpha\beta\delta\lambda}$ terms. The FORTRAN program used to compute the square brackets is given, with notes, at the end of this appendix. It was checked by reproducing Cowley's (1962) numbers for the NaCl structure. For the more complex structures, a direct check was not possible since the electrostatic contributions to the square brackets have not been previously calculated. However, the Madelung constant was checked against previous calculations -- since this was calculated in parallel with the square brackets, they are presumably also correct.

The Madelung Constant

The Madelung constant was computed according to the equation (II.12) in Born and Huang (1962)

$$\frac{\alpha_m q_0^2}{r} = \frac{R}{2}\sum_{k'k}{}' e_k e_{k'} H(R|\underline{x}(k'k)|) + \frac{\pi}{2V_a R^2}\sum_{kk'} e_k e_{k'} \cdot$$
$$\cdot \sum_h{}' G(\pi^2|\underline{y}(h)|^2/R^2)\, e^{2\pi i\, \underline{x}(h)\cdot(\underline{x}(k)-\underline{x}(k'))} -$$
$$- \frac{R}{\sqrt{\pi}}\sum_k e_k^2$$

where r is the reference dimension of the lattice (not to be confused with the theta-function break-point R). Note that, as in the $\overline{C}^{(2)}_{\alpha\beta 0\lambda}$ case, the reciprocal lattice term is symmetric in $\underline{y}$ so the complex phase exponential can be written as a cosine.

The insensitivity to the theta-function break-point R can be seen for the case of rutile below. For any new structure, a curve like this should be computed to choose a suitable R before the square brackets are computed.

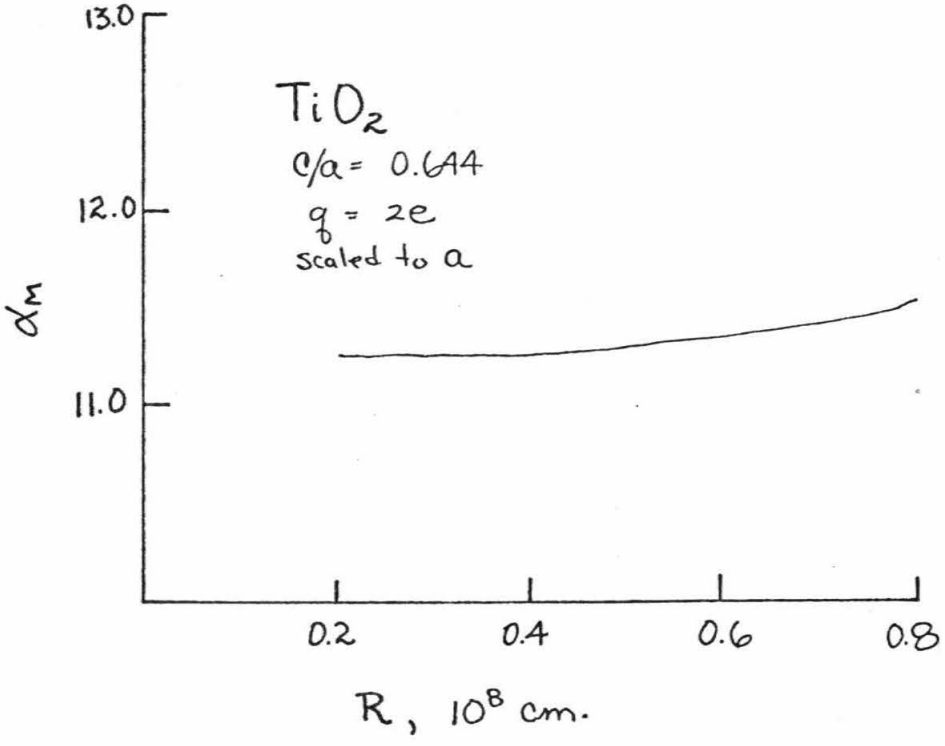

The Round Brackets

As stated in the text, it is not generally possible to separate the round brackets into coulombic and non-coulombic parts. However, the electrostatic contributions to $\bar{C}^{(o)}_{\alpha\beta}$ and $\bar{C}^{(1)}_{\alpha\beta\gamma}$ must be computed. These were computed according to equations (3-3-52) and (3-3-53) using the methods given in this appendix. The basic program was checked by recalculating Cowley's (1962) numbers for the ZnS structure.

```
      DIMENSION X(3),Y(3),XX(20),YY(20),ZK(20),OK(20)
C     NCASE TELLS THE NUMBER OF INPUT CASES BEING RUN.
C     EACH CASE (ICASE=1,NCASE) REQUIRES A COMPLETE INPUT DECK.
      READ(5,100) NCASE
  100 FORMAT(I3)
      DO 1 ICASE=1,NCASE
      READ(5,101) NRBKT,NSUB,MAX,IBUG
  101 FORMAT(4I3)
      READ(5,99) RMAX
   99 FORMAT(F5.3)
C     RMAX IS THE MAGNITUDE OF THE LARGEST L VECTOR ALLOWED.
C     NRBKT TELLS THE NUMBER OF SQUARE BRACKETS BEING COMPUTED.
C     NSUB IS THE NUMBER OF SUBLATTICES.
C     MAX IS THE LARGEST L AND H VECTOR CONSIDERED.
C     IBUG=0 FOR NO DEBUG OUTPUT
      PI=3.14159
      SQRPI=SQRT(PI)
      READ(5,102) R,THETA,Q
  102 FORMAT(3F15.6)
C     R IS THE REFERENCE DIMENSION OF THE LATTICE IN CM. UNITS.
C     THETA IS THE BREAK-POINT OF THE THETA-FUNCTION TRANSFORMATION IN
C     INVERSE CM. UNITS.
C     Q IS THE REFERENCE CHARGE TO WHICH THE ALPHA(I,J) ARE SCALED.(ESU)
      READ(5,103) A1X,A1Y,A1Z,A2X,A2Y,A2Z,A3X,A3Y,A3Z
      READ(5,103) B1X,B1Y,B1Z,B2X,B2Y,B2Z,B3X,B3Y,B3Z
  103 FORMAT(9F5.2)
C     A1X,A1Y.....A3Y,A3Z ARE THE COMPONENTS OF THE LATTICE BASIS
C     VECTORS A1,A2,A3.  B1X,B2X.....B3Y,B3Z ARE THE COMPONENTS OF THE
C     RECIPROCAL LATTICE BASIS VECTORS B1,B2,B3.  BOTH ARE DIMENSIONLESS
C     BEING SCALED TO R AND 1/2R RESPECTIVELY.
      CPX=A2Y*A3Z-A2Z*A3Y
      CPY=A2Z*A3X-A2X*A3Z
      CPZ=A2X*A3Y-A2Y*A3X
      VA=R*R*R*(CPX*A1X+CPY*A1Y+CPZ*A1Z)
      WRITE(6,200)
  200 FORMAT(1H1//,10X,'BASIS VECTORS, DIRECT LATTICE',19X,'BASIS VECTOR
     1S,RECIPROCAL LATTICE')
      WRITE(6,201) A1X,A1Y,A1Z,B1X,B1Y,B1Z
      WRITE(6,201) A2X,A2Y,A2Z,B2X,B2Y,B2Z
      WRITE(6,201) A3X,A3Y,A3Z,B3X,B3Y,B3Z
  201 FORMAT(1HO,10X,3F6.3,41X,3F6.3)
      WRITE(6,202) R
  202 FORMAT(1HO,10X,'REFERENCE DIMENSION',20X,'R=',F15.6)
      WRITE(6,203) Q
  203 FORMAT(1HO,10X,'REFERENCE CHARGE',23X,'Q=',F15.6)
      WRITE(6,204) THETA
  204 FORMAT(1HO,10X,'THETA-FUNCTION BREAK POINT',9X,'THETA=',F15.6)
      WRITE(6,205) NSUB
  205 FORMAT(1HO,10X,'NUMBER OF SUBLATTICES',15X,'NSUB=',I3)
      WRITE(6,206) MAX
  206 FORMAT(1HO,10X,'MAX. VECTOR COMPONENT',16X,'MAX=',I3)
      WRITE(6,98) RMAX
   98 FORMAT(1HO,10X,'RMAX=',F5.3)
      WRITE(6,207) VA
  207 FORMAT(1HO,10X,'CELL VOLUME',27X,'VA=',F15.6)
      WRITE(6,208)
  208 FORMAT(1HO,10X,'* * * * * * * * * *')
```

Do loop on ICASE Brackets whole program.

THETA Corresponds to R in the text. Not to be confused with the use of R for the reference dimension of the lattice.

Cell Volume $V_a = \underset{\sim}{a}_1 \cdot \underset{\sim}{a}_2 \times \underset{\sim}{a}_3$

```
      DO 80 KSUB=1,NSUB
      READ(5,310) XK(KSUB),YK(KSUB),ZK(KSUB),QK(KSUB)
  310 FORMAT(4F10.3)
      QK(KSUB)=QK(KSUB)*4.80294 E-10
   80 CONTINUE
C     XK,YK,ZK ARE THE COMPONENTS OF VECTOR TO THE K SUBLATTICE.
C     THEY ARE SCALED TO R AND ARE DIMENSIONLESS.
C     QK IS THE CHARGE ON THE K SUBLATTICE.  IT IS SCALED TO E.
C     AND IS DIMENSIONLESS
      DO 2 IBRKT=1,NBRKT
      READ(5,101) I,J,K,L
C     INTEGERS I,J,K,L DEFINE THE SQUARE BRACKET BEING COMPUTED (IJ,KL)
      WRITE(6,209) I,J,K,L
  209 FORMAT(1H0,10X,'SQUARE BRACKET BEING COMPUTED      (IJKL)=',4I3)
      CSUM=0.0
      SAMAD=0.0
      SKMAD=0.0
      DO 3 KSUB=1,NSUB
      SAMAD=SAMAD+THETA*R*QK(KSUB)*QK(KSUB)/SQRPI
      DO 4 KPSUB=1,NSUB
      QKQKP=QK(KSUB)*QK(KPSUB)
      XKKP1=XK(KSUB)-XK(KPSUB)
      XKKP2=YK(KSUB)-YK(KPSUB)
      XKKP3=ZK(KSUB)-ZK(KPSUB)
      WRITE(6,210) KSUB,KPSUB
  210 FORMAT(1H0,20X,'K=',I3,5X,'KP=',I3)
      WRITE(6,211) XKKP1,XKKP2,XKKP3
  211 FORMAT(1H0,20X,'COMPONENTS OF VECTOR JOINING K AND KP =',3F5.2)
      IF(IBUG.EQ.0) GO TO 81
      WRITE(6,212)
  212 FORMAT(1H0,20X,'DIRECT LATTICE SUM')
      WRITE(6,213)
  213 FORMAT(1H0,2*X,'X1',8X,'X2',8X,'X3',13X,'X(1)',9X,'X(2)',12X,
     1'X(3)',8X,'HIJ')
   81 MAX2=2*MAX+1
      HSUM=0.0
      SLMAD=0.0
      DO 5 L1=1,MAX2
      DO 6 L2=1,MAX2
      DO 7 L3=1,MAX2
      X1=FLOAT(MAX+1-L1)*A1X+FLOAT(MAX+1-L2)*A2X+FLOAT(MAX+1-L3)*A3X
      X2=FLOAT(MAX+1-L1)*A1Y+FLOAT(MAX+1-L2)*A2Y+FLOAT(MAX+1-L3)*A3Y
      X3=FLOAT(MAX+1-L1)*A1Z+FLOAT(MAX+1-L2)*A2Z+FLOAT(MAX+1-L3)*A3Z
      CHECK=SQRT(X1*X1+X2*X2+X3*X3)
      IF(CHECK.GT.RMAX) GO TO 7
      X(1)=(X1+XKKP1)*R
      X(2)=(X2+XKKP2)*R
      X(3)=(X3+XKKP3)*R
      XVECT=SQRT(X(1)*X(1)+X(2)*X(2)+X(3)*X(3))
      ZARG=THETA*XVECT
      IF(ZARG.GE.12.0) GO TO 7
      IF(KSUB.EQ.KPSUB) GO TO 20
      GO TO 11
   20 IF(X1.EQ.X2) GO TO 12
      GO TO 11
   12 IF(X2.EQ.X3) GO TO 14
      GO TO 11
   14 IF(X1.EQ.0.0) GO TO 7
   11 HZ=EXP(ZARG)/ZARG
      SLMAD=SLMAD+THETA*R*QKQKP*HZ/2.
   15 HEACT=HZ*2.*EXP(-ZARG*ZARG)/SQRPI
```

Do loop on IBRKT brackets the remainder of the program.

Sum over k

Sum over k'

$X_1(kk')$, $X_2(kk')$, $X_3(kk')$

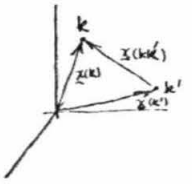

Sum over lattice vectors ℓ^1, ℓ^2, ℓ^3

Lattice translation vectors $\underset{\sim}{X}(\ell) = \ell^1\underset{\sim}{a}_1 + \ell^2\underset{\sim}{a}_2 + \ell^3\underset{\sim}{a}_3$

If $|\underset{\sim}{X}(\ell)|$ is longer than r_{max} it is not included in the sum to follow. The region of summation is thus roughly spherical

$XVECT = \underset{\sim}{X}(\ell_{kk'}) = \underset{\sim}{X}(kk') + \underset{\sim}{X}(\ell)$

$ZARG = R\underset{\sim}{X}(\ell_{kk'})$ in the text) It is the arguement of $H_{\alpha\beta}$

If $k=k'$ and $\ell=0$, no contribution to HSUM below is computed.

Contribution to the Madelung constant from the term with primed sum

$$H_{ij}(\underset{\sim}{z}) = -\frac{\delta_{ij}}{z^3}\left[H(z)+\frac{2e^{-z^2}}{\sqrt{\pi}}\right] + R^2 x_i x_j\left\{\frac{3}{z^4}\left[H(z)+\frac{2e^{-z^2}}{\sqrt{\pi}}\right]+\frac{4}{\sqrt{\pi}z^2}e^{-z^2}\right\}$$

```
      HIJ=(-DEL(I,J)*HFACT/(ZARG*ZARG)+THETA*THETA*X(I)*X(J)*
     1(3.*HFACT/(ZARG*ZARG*ZARG)+4./(ARG*ZARG)+4./EXP(-ZARG*ZARG)/
     2(SQRPI*ZARG*ZARG)))*X(K)*X(L)
      HSUM=HSUM+HIJ
```

Note: this is a primed sum over $\underset{\sim}{l}$ since the $k=k'$, $l=0$ term has be excluded above

```
      IF (IBUG.EQ.0) GO TO 7
      WRITE(6,214) X1,X2,X3,X(1),X(2),X(3),HIJ
  214 FORMAT(1H ,2F8X,3F10.3,5X,4E15.6)
    7 CONTINUE
    6 CONTINUE
    5 CONTINUE
      IF(IBUG.EQ.0) GO TO 82
      WRITE(6,215) HSUM
  215 FORMAT(1H0,20X,'HSUM=',E15.6)
      WRITE(6,216)
  216 FORMAT(1H0,20X,'RECIPROCAL LATTICE SUM')
      WRITE(6,217)
  217 FORMAT(1H0,25X,'Y(1)',12X,'Y(2)',12X,'Y(3)',15X,'EG')
   82 GSUM=0.0
      SHMAD=0.0
```

Sum over reciprocal lattice

```
      DO 8 M1=1,MAX2
      DO 9 M2=1,MAX2
      DO10 M3=1,MAX2
```

Reciprocal lattice vectors

$$\underset{\sim}{\chi}(h) = h_1\underset{\sim}{b}^1 + h_2\underset{\sim}{b}^2 + h_3\underset{\sim}{b}^3$$

```
      Y(1)=(.5/R)*(FLOAT(MAX+1-M1)*R1X+FLOAT(MAX+1-M2)*R2X+
     1FLOAT(MAX+1-M3)*R3X)
      Y(2)=(.5/R)*(FLOAT(MAX+1-M1)*R1Y+FLOAT(MAX+1-M2)*R2Y+
     1FLOAT(MAX+1-M3)*R3Y)
      Y(3)=(.5/R)*(FLOAT(MAX+1-M1)*R1Z+FLOAT(MAX+1-M2)*R2Z+
     1FLOAT(MAX+1-M3)*R3Z)
      YVECT=SQRT(Y(1)*Y(1)+Y(2)*Y(2)+Y(3)*Y(3))
```

If $\underset{\sim}{\chi}=0$, no contribution to Gsum is computed below

```
      IF(YVECT.EQ.0.0) GO TO 10
      CHECK=YVECT*2.*R
```

If $|\underset{\sim}{\chi}(h)|$ is longer than RMAX it is not included in the sum

```
      IF(CHECK.GT.RMAX) GO TO 10
      GARG=PI*PI*YVECT*YVECT/(THETA*THETA)
      IF (GARG.GE.170.) GO TO 10
      G=EXP(-GARG)/GARG
```

Contribution to the Madelung Constant from the primed $\underset{\sim}{h}$ sum:

$$\sum_{\underset{\sim}{h}}{}'\Big\{(\delta_{\gamma\beta}\delta_{\alpha\lambda}+\delta_{\alpha\gamma}\delta_{\alpha\beta})G(\underset{\sim}{\chi}) + \frac{4\pi^4}{R^4}\chi_\alpha\chi_\beta\chi_\gamma\chi_\gamma G''(\underset{\sim}{\chi}) + \frac{2\pi^2}{R^2}\Big\}\chi_\alpha\chi_\beta\,\delta_{\alpha\lambda} + \chi_\gamma\chi_\beta\delta_{\beta\lambda}\chi_\alpha\chi_\gamma\delta_{\beta\alpha} + \chi_\beta\chi_\gamma\delta_{\alpha\lambda} + \chi_\beta\chi_\gamma\delta_{\alpha\beta}\}G'(\underset{\sim}{\chi})e^{2\pi i\underset{\sim}{\gamma}\cdot(\underset{\sim}{x}(k)-\underset{\sim}{x}(k'))}$$

```
      GP=-G*(1.+1./GARG)
      GPP=G*(1.+2./GARG+2./(GARG*GARG))
      COSKK=COS(2.*PI*(Y(1)*R*XKKP1+Y(2)*R*XKKP2+Y(3)*R*XKKP3))
      SHMAD=SHMAD+(PI*PI*OKOKP*G/(2.*VA*THETA*THETA))*COSKK
      EG=((DEL(I,K)*DEL(J,L)+DEL(I,L)*DEL(J,K))*G+ 4.*(PI/THETA)**4*
     1Y(I)*Y(J)*Y(K)*Y(L)*GPP+2.*PI*PI/(THETA*THETA)*(Y(I)*Y(J)*DEL(K,L)
     2+Y(I)*Y(K)*DEL(J,L)+Y(I)*Y(L)*DEL(J,K)+Y(J)*Y(K)*DEL(I,L)+
     3Y(J)*Y(L)*DEL(I,K))*GP)*COSKK
      GSUM=GSUM+EG
      IF (IBUG.EQ.0) GO TO 10
      WRITE(6,218) Y(1),Y(2),Y(3),EG
  218 FORMAT(1H ,20X,4E15.6)
   10 CONTINUE
    9 CONTINUE
    8 CONTINUE
```

$\bar{C}^{(2)c}_{ijkl}(kk')$

```
      C2BAR=-(4.*PI*PI*PI*OKOKP/(THETA*THETA*VA))*(DEL(I,K)*DEL(J,L)+
     1DEL(I,L)*DEL(J,K))+4.*PI*PI*THETA*THETA*(THETA*OKOKP*HSUM+4.*PI*
     2PI*PI*OKOKP*GSUM/(THETA*THETA*VA)
      CSUM=CSUM+(1./(R*PI*PI*VA))*C2BAR
```

$$[ijkl]^c = \frac{1}{8\pi^2 V_k}\sum_{kk'}\bar{C}^{(2)c}_{ijkl}(kk')$$

Madelung Constant kk' sum.

```
      SKMAD=SKMAD+SUMAD+SHMAD
      IF(IBUG.EQ.0) GO TO 4
      WRITE(6,221) GSUM
  221 FORMAT(1H0,20X,'GSUM=',E15.6)
      WRITE(6,219) C2BAR
  219 FORMAT(1H0,20X,'C2BAR=',E15.6)
    4 CONTINUE
```

Scaling $[ijkl]^c$ to $q^2/2R^*$. (R = reference dimension)

Madelung Constant Scaled to q^2

```
      3 CONTINUE
        ALFA=2.*R*R*R*CSUM/(0*0)
        WRITE(6,220) ALFA
  220 FORMAT(1HO,'ALFA=',F15.6)
        RMAD=(SRMAD-SAMAD)/(0*0)
        WRITE(6,230)RMAD
  230 FORMAT(1HO,10X,'MADELUNG CONSTANT = ',F15.6)
      2 CONTINUE
      1 CONTINUE
        STOP
        END
```

Function S_{ij} used in main program above →

```
        FUNCTION DEL(I,J)
        IF(I.EQ.J)GO TO 1
        DEL=0.0
        GO TO 2
      1 DEL=1.0
      2 RETURN
        END
```

Sample Data Deck for γ-Mg_2SiO_4 spinel

$\hat{R}$ = 8.07 Å

θ = 0.2 $\times 10^8$

ν = 0.385

```
//DATA   DD   *
   1
  3 14  5  0
  5.0
 8.07       E-08  0.2        E 08  4.80294  E-10
 0.0  0.5  0.5  0.5  0.0  0.5  0.5  0.5  0.0
-2.0  2.0  2.0  2.0 -2.0  2.0  2.0  2.0 -2.0
 0.0        0.0        0.0        4.
 .250       .250       .250       4.
 .625       .625       .625       2.
 .625       .975       .875       2.
 .875       .625       .875       2.
 .875       .875       .625       2.
  .385       .385       .385      -2.0
  .385      -.385      -.385      -2.0
 -.135      -.135      -.135      -2.0
 -.135       .635       .635      -2.0
 -.385      -.385       .385      -2.0
 -.385       .385      -.385      -2.0
  .635      -.135       .635      -2.0
  .635       .635      -.135      -2.0
  1  1  1  1
  1  1  2  2
  1  2  1  2
//
```

APPENDIX 3

The Born Haber Cycle for MgO

It was noted in Chapter V that although the lowering of the ionicity gave better agreement between the theoretical and experimental elastic constants for MgO, it significantly reduced the cohesive energy. For $f = 0.7$, the cohesive energy is (using the parameters given in Table 5-1-9)

$$W = N_A\left(-\frac{\alpha_m f q_0^2}{R} + 6\lambda e^{-R/\rho}\right) = -668.18 \text{ kcal/mole}$$

which is to be compared with W = -905.53 kcal/mole computed from essentially the same data by Gaffney and Ahrens (1969).

In principle the cohesive energy can be obtained experimentally through the Born Haber thermochemical cycle diagrammed in Figure A-3-1. In practice this is not possible since the heat of formation of O^{2-} has not been measured. By solving for this missing link, Gaffney and Ahrens (1969) calculated

$$H_f^o(O^{2-}) = -W_L + 5RT - H_f^o(\text{cation}) + H_f^o(\text{oxide})$$

$$(907.?) - (561.8) - (143.8) = 202.3 \text{ kcal/mole}$$

Using the lower value of W corresponding to $f = 0.7$ above, one calculates $\Delta H_f^o(O^{2-}) = -35.2$ kcal/mole. Hence the lowered ionicity must be compensated by a covalent contribution to the cohesive energy not treated in this development.

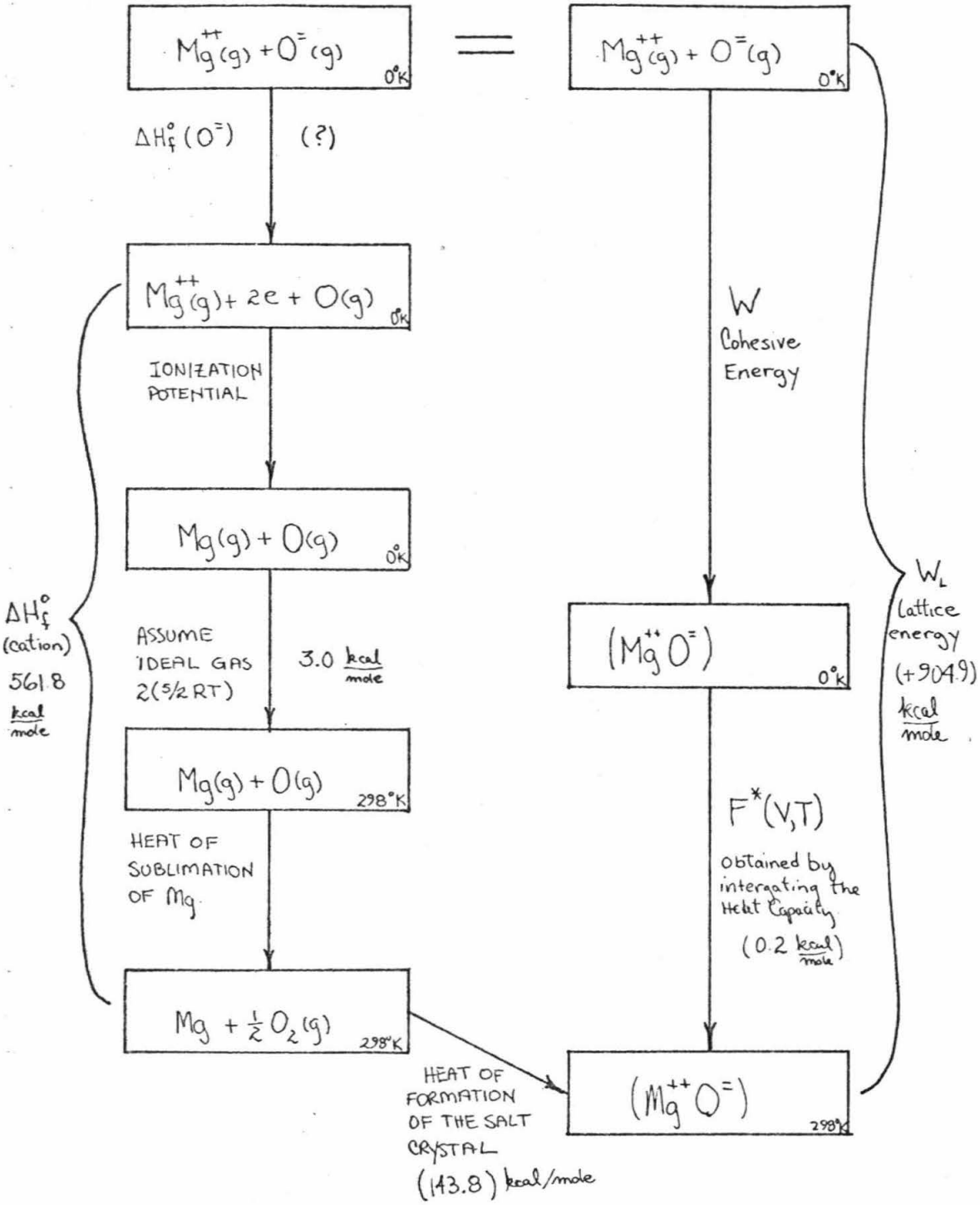

Figure A-3-1. Born Haber cycle for MgO.

APPENDIX 4

The Consistent Pair-Potential Hypothesis

Below the repulsive parameters found from MgO and Al_2MgO_4 are given as a function of the ionicity. The static lattice parameters of Al_2O_3 found in Figure A-4-1 were used to compute λ_{AlO} and ρ_{AlO} for direct comparison with those in Al_2MgO_4.

MgO (nearest neighbor only)			Al_2O_3 (nearest neighbor only)		
f	λ (10^{-11}) ergs	ρ Å		λ (10^{-11}) ergs	ρ Å
1.0	62.79	.373	1.0	93.05	.360
.9	78.80	.348	.9	125.2	.337
.8	106.8	.321	.8	182.6	.312
.7	162.2	.292	.7	299.0	.285
.6			.6	583.1	.255

Al_2MgO_4 (nearest neighbor only)

	Al–O Bond		
f	λ (10^{-11}) ergs	ρ (Å)	u
0.7	262.4	.275	.375
	196.6	.287	.387

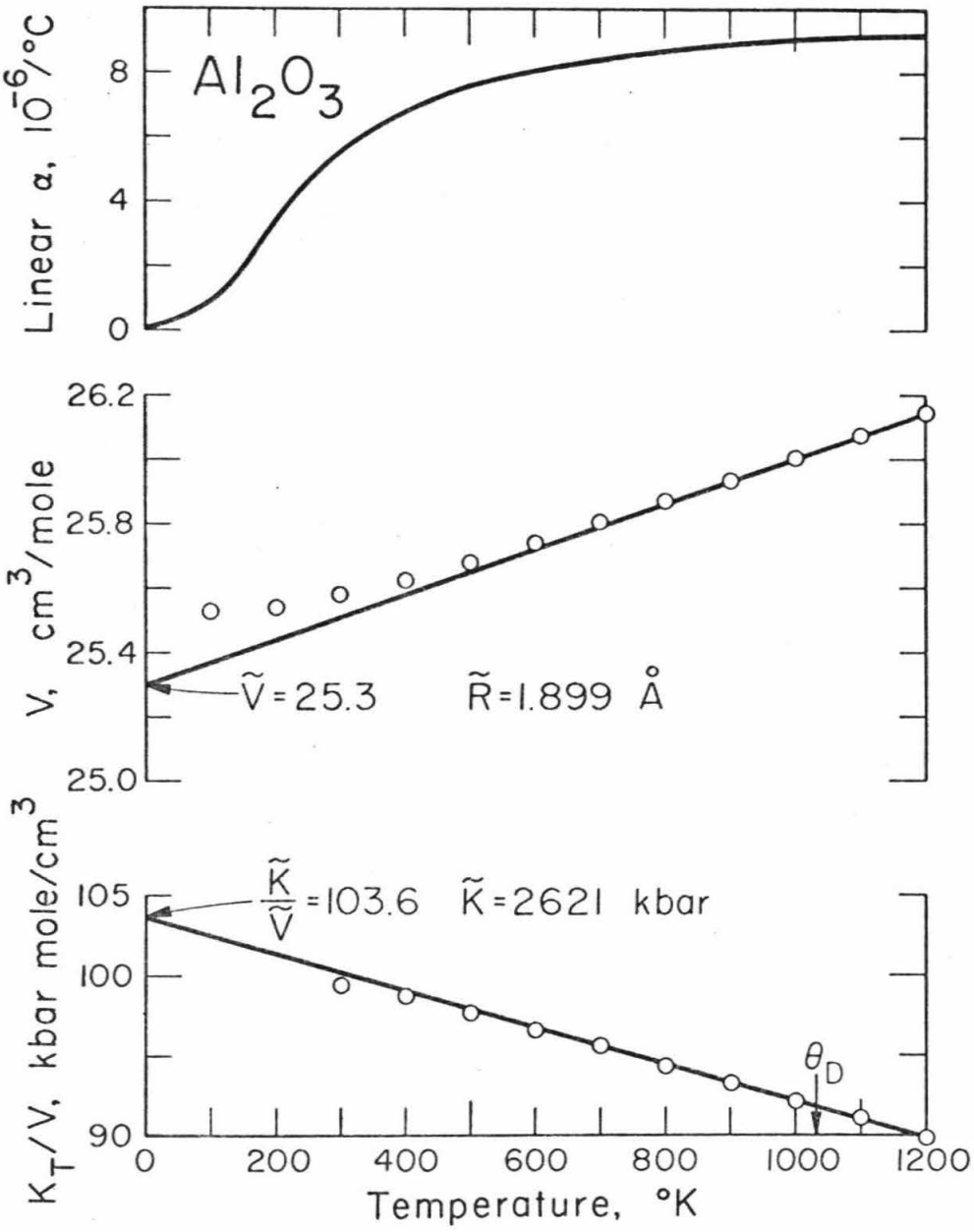

Figure A-4-1. Static lattice parameters of Al_2O_3.